# IDENTIFICATION OF PRRSV NONSTRUCTURAL PROTEINS AND THEIR FUNCTION IN HOST INNATE IMMUNITY

by

YANHUA LI

B.S., Soochow University, 2007
M.S., Chinese Academy of Agricultural Sciences, 2010

AN ABSTRACT OF A DISSERTATION

submitted in partial fulfillment of the requirements for the degree

DOCTOR OF PHILOSOPHY

Department of Diagnostic Medicine / Pathobiology
College of Veterinary Science

KANSAS STATE UNIVERSITY
Manhattan, Kansas

2014

# Abstract

Porcine reproductive and respiratory syndrome virus (PRRSV) employs multiple functions to modulate host's innate immune response, and several viral nonstructural proteins (nsps) are major players. In this dissertation, the research was mainly focused on identification and functional dissection of ORF1a-encoded nsps.

PRRSV replicase polyproteins encoded by ORF1a region are predicted to be processed into at least ten nonstructural proteins. In chapter 2, these predictions were verified by using a panel of newly established antibodies specific to ORF1a-encoded nsps. Most predicted nsps (nsp1β, nsp2, nsp4, nsp7α, nsp7β and nsp8) were identified, and observed to be co-localized with *de novo*-synthesized viral RNA in the perinuclear region of the cell.

Among all PRRSV proteins screened, nsp1β is the strongest type I interferon antagonist. In chapter 3, mutagenesis analysis of nsp1β was performed to knock down nsp1β's IFN antagonist function. A highly conserved motif, GKYLQRRLQ, was determined to be critical for nsp1β's ability to suppress IFN-β and reporter gene expression. Double mutations introduced in this motif, K130A/R134A (type 1 PRRSV) or K124A/R128A (type 2 PRRSV), improved PRRSV's ability to stimulate the expression of IFN-α, IFN-β and ISG15. In addition to its critical roles involving in modulating host innate immune response, in the studies of Chapter 4, we demonstrated that PRRSV nsp1β functions as a transactivator to induce the -2/-1 ribosomal frameshifting in nsp2, which results in expression of two novel PRRSV proteins, nsp2TF and nsp2N. The conserved motif GKYLQRRLQ is also determined to be critical for the transactivation function of nsp1β.

In chapter 5, the interferon antagonist, de-Ub and de-ISGylation activity of newly identified nsp2TF and nsp2N were evaluated. *In vitro* and *in vivo* characterization of three nsp2TF-deficient recombinant viruses indicated that all mutant viruses have improved ability to stimulate the innate immune response and provide improved protection in mutant virus-vaccinated animals.

In summary, this study verified the previously predicted PRRSV pp1a processing products, further evaluated the function of nsp1β and nsp2-related proteins. These data obtained here will provide basic knowledge for future development of vaccines and control measurements.

# IDENTIFICATION OF PRRSV NONSTRUCTURAL PROTEINS AND THEIR FUNCTION IN HOST INNATE IMMUNITY

by

YANHUA LI

B.S., Soochow University, 2007
M.S., Chinese Academy of Agricultural Sciences, 2010

A DISSERTATION

submitted in partial fulfillment of the requirements for the degree

DOCTOR OF PHILOSOPHY

Department of Diagnostic Medicine / Pathobiology
College of Veterinary Science

KANSAS STATE UNIVERSITY
Manhattan, Kansas

2014

Approved by:

Major Professor
Ying Fang

# Abstract

Porcine reproductive and respiratory syndrome virus (PRRSV) employs multiple functions to modulate host's innate immune response, and several viral nonstructural proteins (nsps) are major players. In this dissertation, the research was mainly focused on identification and functional dissection of ORF1a-encoded nsps.

PRRSV replicase polyproteins encoded by ORF1a region are predicted to be processed into at least ten nonstructural proteins. In chapter 2, these predictions were verified by using a panel of newly established antibodies specific to ORF1a-encoded nsps. Most predicted nsps (nsp1β, nsp2, nsp4, nsp7α, nsp7β and nsp8) were identified, and observed to be co-localized with *de novo*-synthesized viral RNA in the perinuclear region of the cell.

Among all PRRSV proteins screened, nsp1β is the strongest type I interferon antagonist. In chapter 3, mutagenesis analysis of nsp1β was performed to knock down nsp1β's IFN antagonist function. A highly conserved motif, GKYLQRRLQ, was determined to be critical for nsp1β's ability to suppress IFN-β and reporter gene expression. Double mutations introduced in this motif, K130A/R134A (type 1 PRRSV) or K124A/R128A (type 2 PRRSV), improved PRRSV's ability to stimulate the expression of IFN-α, IFN-β and ISG15. In addition to its critical roles involving in modulating host innate immune response, in the studies of Chapter 4, we demonstrated that PRRSV nsp1β functions as a transactivator to induce the -2/-1 ribosomal frameshifting in nsp2, which results in expression of two novel PRRSV proteins, nsp2TF and nsp2N. The conserved motif GKYLQRRLQ is also determined to be critical for the transactivation function of nsp1β.

In chapter 5, the interferon antagonist, de-Ub and de-ISGylation activity of newly identified nsp2TF and nsp2N were evaluated. *In vitro* and *in vivo* characterization of three nsp2TF-deficient recombinant viruses indicated that all mutant viruses have improved ability to stimulate the innate immune response and provide improved protection in mutant virus-vaccinated animals.

In summary, this study verified the previously predicted PRRSV pp1a processing products, further evaluated the function of nsp1β and nsp2-related proteins. These data obtained here will provide basic knowledge for future development of vaccines and control measurements.

# Table of Contents

# List of Figures

**Figures in chapter 1:**



**Figures in chapter 2:**



**Figures in chapter 3:**

**Figures in chapter 4:**



**Figures in chapter 5:**

# List of Tables

# Acknowledgements

I really appreciate my major advisor, Dr. Ying Fang for her mentoring during the past 4.5 years. She gave me tremendous freedom and trust in conducting my research projects, provided me opportunities to attend various professional conferences which would greatly enhanced my career development, and always encouraged me to think independently and to work smart.

I'd like to acknowledge my committee members, Dr. Raymond R.R. Rowland, Dr. Stephen Higgs, and Dr. Stefan Rothenburg, for their precious suggestions on my research. My thanks also are given to my previous committee members in South Dakota State University, Dr. David Zeman, Dr. Michael Hildreth, Dr. Alan Erickson and Dr. Adam D. Hoppe, for all their time and helpful guidance.

Special thanks to Dr. M.M. Chengappa, Dr. T.G. Nagaraja, and other faculties and staffs in the department of Diagnostic Medicine / Pathobiology, who helped me in fulfilling the requirements of my Ph.D degree.

I express my thanks to all of the lab members in Dr. Ying Fang's laboratory, including Dr. Zhi Sun, Dr. Steve Lawson, Robert Langenhorst, Russel Ransburgh, Zhiyong Jiang, Longchao Zhu, Pengcheng Shang, Rui Guo and Yin Wang. Additionally, thanks go out to all my friends who have given me tremendous help in my life.

I would especially like to thank my girlfriend, Qiuwen Kou, for her support. Finally, I give my deepest gratitude to my families in China, my father, Enyang Li, my sister, Suyan Li, and my brother, Yanping Li, for their unlimited support to me during my studying in USA.

# Chapter 1 - Literature review

## 1.1 Porcine Reproductive and Respiratory Syndrome and the etiological agent

Porcine reproductive and respiratory syndrome (PRRS) is one of the most economically significant viral diseases to swine industry worldwide for over two decades. It causes an estimated loss of 664 million to the United States annually alone (Miller, 2011). This disease was first reported in North America in 1987 (Keffaber, 1989) and almost simultaneously in Central Europe (Wensvoort *et al.*, 1991). Initially, PRRS was referred to as "mystery swine disease" and "mystery reproductive syndrome", and characterized as blue-ear pig disease. Reproductive failure in sows and respiratory distress in young pigs are typical clinical signs of this disease. Since its emergence, several highly pathogenic PRRSV strains, which have caused PRRS disease outbreaks, were reported in different countries. In 2006, highly pathogenic (HP) PRRSV strains were isolated in China and South East Asia (Feng *et al.*, 2008; Tian *et al.*, 2007). Another highly pathogenic East European subtype 3 PRRSV, Lena, was reported in Eastern Europe (Karniychuk *et al.*, 2010). Infection with HP-PRRSV strains is associated with severe clinical signs, pulmonary lesions and aberrant host immune responses (Hu *et al.*, 2013; Lv *et al.*, 2008; Xiao *et al.*, 2010).

The etiological agent, porcine reproductive and respiratory syndrome virus (PRRSV), is a small, enveloped virus with positive sense RNA genome. It belongs to the order *Nidovirales*, family *Arteriviridae*, which also includes equine arteritis virus (EAV), lactate dehydrogenase-elevating virus (LDV) and simian hemorrhagic fever virus (SHFV) (Snijder *et al.*, 2013; Snijder & Meulenberg, 1998). PRRSV can be further divided into two distinct genotypes, type 1 (European genotype) and type 2 (North American genotype), which share about 63% nucleotide identity (Allende *et al.*, 1999; Nelsen *et al.*, 1999; Ropp *et al.*, 2004). Lelystad virus (Wensvoort *et al.*, 1991) and VR-2332 (Benfield *et al.*, 1992; Collins *et al.*,

1992), first isolated in Europe and Northern America, represent prototypic strains of European and North American genotypes.

To date, PRRSV virion structure has been analyzed by employing several techniques, including negative stain electron microscopy (EM), cryo-EM and Cryo-electron tomography (Dea *et al.*, 1995; Mardassi *et al.*, 1994; Spilman *et al.*, 2009). By cryo-EM, PRRSV virions appear as round or egg-shaped particles with a diameter from 50 nm to 74 nm (Spilman *et al.*, 2009). Unlike the structure of club-shaped protrusions on coronaviruses, PRRSV particles display a smooth and mostly featureless surface with few protruding features (Dea *et al.*, 1995; Mardassi *et al.*, 1994). The virions contain an internal core with an average diameter of 39 nm, and a lipid bilayer envelope about 4.5 nm in thickness, which are separated from each other by a 2-3 nm gap. In addition to the two-dimensional structure revealed by electron micrographs, cryo-electron tomography shows the pleiomorphic morphology of the PRRSV virions in greater detail and in three dimensions (Spilman *et al.*, 2009).

Swine are the only known natural host of PRRSV. PRRSV also has a very restricted cell tropism for cells of the monocytic lineage. The fully differentiated porcine alveolar macrophage (PAM) serves as a primary cell target for PRRSV infection (Duan *et al.*, 1997a; b). Among many different cell lines tested, only the African green monkey kidney cell line MA-104 and derivatives such as MARC-145 are fully permissive to PRRSV replication (Kim *et al.*, 1993). PRRSV enters PAM through standard clathrin-mediated endocytosis. The viral nucleocapsid is released into the cytosol following endosome acidification and membrane fusion (Nauwynck *et al.*, 1999). The host factors mediating viral entry have been extensively studied for PRRSV (Van Breedam *et al.*, 2010a; Welch & Calvert, 2010). To date, CD163 is believed to be major receptor which mediates viral internalization and disassembly. Van Breedam et al. (2010b) suggested that sialoadhesin (CD169) mediates viral internalization by the interaction with the ectodomains of GP5/M heterodimer (Van Breedam *et al.*, 2010b). However, Prather *et al.* (2013) demonstrated that an intact sialoadhesin (CD169) is not required for attachment/internalization of the porcine reproductive and respiratory syndrome

virus using a CD169 gene knockout pig (Prather *et al.*, 2013). By screening a PAM cDNA library for receptor function, CD163, a member of the scavenger receptor cysteine-rich family, was identified as a key factor in the initiation of PRRSV infection (Calvert *et al.*, 2007). Overexpression of CD163 renders a variety of non-permissive cell lines susceptible to PRRSV infection. Two minor structural proteins, GP2a and GP4, were determined as viral attachment proteins which mediate virus entry into susceptible host cell by interacting with CD163 (Das *et al.*, 2010). In addition, EAV minor structural proteins (GP2a, GP3, GP4 and E) swapped into a chimeric PRRSV extended PRRSV cell tropism (Tian *et al.*, 2012), which further provides genetic evidence to support that the minor GPs are the prime determinants of host cell binding and possibly also fusion and entry.

After release of viral genomic RNA, PRRSV encodes replicase subunits through polyprotein processing in cytoplasm. Like all + RNA viruses, PRRSV replicase subunits appear to co-localize in the perinuclear region and assemble into replication and transcription complexes (RTC) for viral RNA synthesis. However, it is noteworthy that the majority of PRRSV nsp1β localizes to nuclear region at the late stage of virus infection, and nsp2TF seems to co-localize with Golgi (Chen *et al.*, 2010; Fang *et al.*, 2012). In EAV, large numbers of "double membrane vesicles" (DMV) are formed during virus infection, and the viral RTC is likely anchored on these DMVs (Pedersen *et al.*, 1999; van Hemert *et al.*, 2008). ORF1a-encoded putative membrane-spanning proteins nsp2, nsp3 and nsp5 are major proteins involved in the formation of this membranous structure for the RTC (Snijder *et al.*, 2001). Based on the evolutionary relationship, PRRSV infection is also supposed to induce DMV for viral RNA synthesis. Clearly, additional research is needed to further address the questions about PRRSV replicative cycle.

During PRRSV replication, viral structural proteins are translated from 3'-co-terminal nested set of subgenomic (sg) mRNAs, which serves as a hallmark of arteriviruses and other nidoviruses. All sg mRNAs share a common 5' "leader sequence" which is identical to the 5'-proximal part of viral genome (Yu *et al.*, 2009). The synthesis of sg mRNA

is considered to rely on discontinuous negative-strand RNA synthesis – a mechanism that similar to copy – choice RNA recombination (Pasternak *et al.*, 2001; Sola *et al.*, 2011). In brief, discontinuous negative strand RNA synthesis is considered to generate a nested set of negative-stranded sg RNAs, which subsequently serve as templates for sg mRNA synthesis. In this model, base pairing between leader transcriptional regulatory sequence (TRS) and body TRSs plays a key role in regulating viral transcription (Zheng *et al.*, 2014). In addition, Sg mRNAs are supposed to be functionally monocistronic, with the exception of sg mRNA2 and sg mRNA5, which encode two partial overlapped genes, E/GP2 and ORF5a/GP5, respectively.

## 1.2 PRRSV genome organization and gene expression

PRRSV contains a ~15-kb plus-strand genomic RNA. The viral genome consists of a 5' - untranslated region (UTR) with 5' cap structure, at least ten open reading frames (ORF1a, ORF1b, ORF2a, ORF2b, ORF3, ORF4, ORF5a, ORF5, ORF6 and ORF7), followed by a 3' - untranslated region and a poly-A tail. The viral nonstructural proteins (nsp), major components of viral replication-transcription complex, are encoded in ORF1a and ORF1b which are located in 5' proximal end of the genome and occupy about 75% of genome. Once the genome is released into the cytoplasm, two polyproteins, pp1a and pp1ab, are translated with the expression of the latter depending on a -1 ribosomal frameshift signal in the ORF1a/ORF1b overlap region. These polyproteins are processed by four viral proteases (PLP1α (nsp1α), PLP1β (nsp1β), PLP2 (nsp2) and SP (nsp4)) to yield at least 14 functional nonstructural proteins. The 3'-terminal quarter of viral genome encodes structural proteins, including four envelope glycoproteins (GP2a, GP3, GP4 and GP5), three non-glycosylated membrane proteins [2b, ORF5a and matrix (M)] and the nucleocapsid protein (N) (Bautista *et al.*, 1996; Firth *et al.*, 2011; Johnson *et al.*, 2011; Mardassi *et al.*, 1996; Meng *et al.*, 1996; Meulenberg & Petersen-den Besten, 1996; Meulenberg *et al.*, 1995; Mounir *et al.*, 1995;

Snijder *et al.*, 1999; Wu *et al.*, 2001) (Table 1.1). All these structural proteins are translated from a nested set of 3'-coterminal subgenomic RNA, which is a unique replication strategy to viruses in the order *Nidovirales*. In addition, a TF ORF overlapping with the nsp2 coding region was discovered recently, which generated two novel viral proteins, nsp2TF and nsp2N. nsp2TF, which is translated through a programmed -2 ribosomal frame shifting (PRF) mechanism, is a tranframe protein sharing the N-terminal region with nsp2. At the same position of -2 PRF, a programmed -1 ribosomal frameshifting seems also occur to express nsp2N, a C-terminal truncated form of nsp2, named as nsp2N (Fang *et al.*, 2012).

The translation of pp1a and pp1ab replicase polyproteins initiates viral replication in PRRSV-infected host cells. Through serial proteolytic cleavages of pp1a and pp1ab polyproteins, individual PRRSV nonstructural proteins (nsps) are generated. Instead of polyprotein precursor, the functional nonstructural proteins play a key role in both viral genomic RNA synthesis and subgenomic RNA transcription. Currently, the proteolytic cleavages of PRRSV polyproteins are still not much known.

In EAV, the prototypic virus of Arterivirus family, the processing of pp1a and pp1ab is well-understood by using bioinformatics, nsp-specific antisera, and various experimental systems (Snijder & Meulenberg, 1998; van Aken *et al.*, 2006; Ziebuhr *et al.*, 2000). Thus, most of our current knowledge about PRRSV nsps and their function are predicted by comparative sequence alignment between PRRSV and EAV. According to the processing scheme of pp1a and pp1ab developed in EAV, nsp1 and nsp2 are rapidly released from pp1a and pp1ab by co and posttranslational proteolytic cleavages of viral autoproteases, which contain papain-like cysteine proteases (PLP1 and PLP2) respectively. The remaining polyproteins from nsp3 to nsp12 are further processed into individual nonstructural proteins by a serine protease (SP) located in nsp4. Nsp7 is further processed into nsp7α and nsp7β by an internal cleavage. In addition, many intermediate cleavage products of unknown functions have been detected (Snijder *et al.*, 1994; van Dinten *et al.*, 1996). Wassenaar *et al.* (1997) proposed a processing model for EAV nsp3-8 region, including alternative major and minor

processing pathways. In the major processing pathway, cleaved nsp2 interacts with nsp3 and acts as a co-factor of SP, for cleavage of the nsp4/5 site in the nsp3–8 processing intermediate. Alternatively, when nsp2 does not associate with nsp3–8, a minor pathway can be followed in which the nsp5/6 and nsp6/7 sites are processed instead of the cleavage of nsp4/5 site (Wassenaar *et al.*, 1997) (Fig. 1.1).

Based on comparative sequence analysis (Ziebuhr *et al.*, 2000), many features of replicase polyproteins appear to be conserved in other arteriviruses, there are still a number of striking differences. Firstly, PRRSV and EAV are only distantly related. For instance, the overall sequence identity in the pp1ab replicase polyproteins of EAV and PRRSV is about 30–45 %, depending on the genome region and specific strains used for alignment (Nelsen *et al.*, 1999). Secondly, there are considerable size differences, in particular in nsp2 of ORF1a. EAV nsp2 is about 571 aa, whereas the PRRSV counterpart can be up to ~1196 aa. Finally, an additional protease domain (papain-like protease α, PLPα) residing in nsp1 region was determined to be functional in PRRSV, which has lost its enzymatic activity in EAV (den Boon *et al.*, 1995). Thus, the PRRSV polyproteins are assumed to be cleaved by three papain-like proteases (PLPα, PLPβ and PLP2) located in the nsp1–nsp2 region, and the viral main protease, SP, residing in nsp4. According to the polyprotein processing scheme in EAV, PRRSV replicase polyproteins are being cleaved into at least 14 nsps, specifically nsp1 to nsp12, with nsp1 and nsp7 being subject to an internal cleavage. The nsp1 is auto-cleaved by PLPα yielding two subunits, nsp1α and nsp1β (Chen *et al.*, 2010), and the nsp7 is processed by main protease (nsp4) into nsp7α and nsp7β.

Recently, the authentic cleavage sites of nsp1α/nsp1β and nsp1β/2 were determined by crystal structure analysis and N-terminal protein sequencing (Chen *et al.*, 2010; Sun *et al.*, 2009). In type 2 PRRSV, M180 and A181, 14 amino acids downstream of a previously proposed candidate site (166Q↓R167), was identified as the nsp1α/nsp1β cleavage site. Based on sequence alignment of nsp1 from type 1 and type 2 PRRSV, 180H ↓ S181 is predicted to be nsp1α/nsp1β site in type 1 PRRSV. Also, consistent with a previous prediction (Ziebuhr *et*

*al.*, 2000), 383G ↓ A384 was confirmed as nsp1β/2 cleavage site in Type II PRRSV (Fang & Snijder, 2010).

PRRSV nsp2 contains a papain-like cysteine protease domain (PLP) in its N-terminal domain, which rapidly releases nsp2 from pp1a/pp1ab by cleaving nsp2/3 and has *cis*- and *trans*-cleavage activities (Han *et al.*, 2009; Snijder *et al.*, 1995). Through sequence alignment analysis, two possible nsp2/3 cleavage sites were predicted (Ziebuhr *et al.*, 2000). Also, the candidate of nsp2/nsp3 cleavage site (1445GG ↓ A1447 in type 2 PRRSV), one amino acid downstream from the previously predication, close to the highly conserved nsp3 subunit was believed to be authentic site most likely (Fang & Snijder, 2010).

PRRSV nsp4, the main protease involved in polyprotein processing, is a 3C-like serine protease belonging to a subgroup of chymotrypsin-like enzymes named after the picornavirus 3C proteases. The crystal structure of PRRSV nsp4 has been resolved, which reveals that the protein is composed of three domains, with the C-terminal domain III dispensable for proteolytic activity (Tian et al., 2009). Based on a comparison with EAV, the PRRSV nsp4 mediates nine cleavages in nsp3-nsp12 region. In addition, the previously predicted cleavage sites of nsp3/4, nsp4/5, and nsp11/12 (Ziebuhr *et al.*, 2000) were confirmed as cleavable peptides (Tian et al., 2009).

## 1.3 Non-canonical translation and PRRSV replicase expression

Whilst a majority of cellular mRNAs are monocistronic, many viruses have evolved a profusion of non-canonical mechanisms which allow them to translate multiple viral proteins from a single RNA transcript. Non-canonical translational strategies comprise internal ribosome entry, leaky scanning, non-AUG initiation, ribosome shunting, reinitiation, ribosomal frameshifting and stop-codon readthrough. Particularly in RNA viruses, some individual viruses employ several different strategies to translate viral proteins. As a positive-stranded RNA virus, PRRSV has a relatviely compact genome which is ~15.0 kb in length.

To optimize the usage of the availability of sequence space, PRRSV uses multiple strategies to translate non-structural or structural proteins. Meulenberg *et al.* (1993) identified a heptanucleotide slippery sequence (UUUAAAC) and a putative pseudoknot structure in the overlapping region of ORF1a and ORF1b of type 1 PRRSV, which are required for efficient -1 ribosomal frameshifting. Recently, an efficient -2 programmed ribosomal frameshifting (PRF) was reported in PRRSV to be utilized for the expression of nsp2N and nsp2TF, although the detailed mechanism is still elusive (Fang *et al.*, 2012). Here, it is the first -2 PRF reported in eukaryotic systems including the potential shift sites and stimulatory elements. PRRSV GP2 and E (2b) protein appear to be encoded by a single subgenomic mRNA2, with the translation of E protein dependent on a leaking ribosomal scanning (Wu *et al.*, 2001). They identified a 10-kDa structural protein of PRRSV encoded by ORF2b, whose start codon is only 6 nucleotides downstream of the adenine of the ORF2a start codon. Another case of leaking ribosomal scanning in PRRSV was studies by Johnson *et al.* (2011). In this study, they screened highly purified virions of strain VR2332 for additional structural proteins. Based on the analysis of proteins incorporated into virions by mass spectrometry, ORF5a protein (a 51 amino acids polypeptide) was discovered that is encoded by an alternative ORF of the subgenomic mRNA5 encoding the major envelope glycoprotein, GP5. These results suggested that GP5 and ORF5a protein are encoded by the same subgenomic mRNA via a translation initiation mechanism involving leaky ribosomal scanning. The study of Sun *et al.* (2013) further confirmed that ORF5a protein is essential for virus viability by inactivating its expression in both type 1 and type 2 PRRSV.

*-1 programmed ribosomal frameshifting and the expression of PRRSV pp1ab*

Programmed -1 ribosomal frameshifting was first reported as a mechanism utilized by Rous sarcoma alpharetrovirus to express the Gag-Pol polyprotein from overlapping gag and pol ORFs (Jacks & Varmus, 1985; Jacks *et al.*, 1988). -1 frameshifting has since been documented in many other viruses, including HIV, coronaviruses and arteriviruses. -1 frameshifting has also been identified in conventional cellular genes of both prokaryotes and

eukaryotes, as well as in other replicating elements (reviewed by Giedroc & Cornish, 2009; Brierley *et al.*, 2010). In eukaryotic systems, the -1 frameshifting signal consists of two elements: a slippery sequence with consensus X_XXY_YYZ (underlines separate zero-frame codons; XXX represents anythree identical nucleotides, YYY represents AAA or UUU, and Z represents A, C or U) where the ribosome changes frame, and a downstream stimulatory RNA structure (Firth and Brierley, 2012). A requirement of appropriate spacing (typically 5-9 nt) between these two elements for efficient frameshifting is important. Although extensive investigations have been conducted to dissect the mechanism using different systems, it is still uncertain how the stimulatory RNAs function to promote frameshifting. As reviewed in (Ahlquist, 2006), the utilization of frameshifting as an expression strategy has numerous potential advantages. For instance, in retroviruses, frameshifting allows the virus to express Gag:Gag-Pol at a defined ratio that is likely to be optimized for virion assembly, as down-regulation of this ratio inhibits retrovirus assembly, release and infectivity (Karacostas *et al.*, 1993; Shehu-Xhilaga *et al.*, 2001). Similarly, in many other positive-sense RNA viruses, frameshifting is used to downregulate polymerase expression. By this strategy, like coronaviruses, they may produce the polymerase at a fixed ratio relative to other components of the replication complex. In addition, manipulating the frameshifting efficiency is able to attenuate RNA viruses, like HIV and severe acute respiratory syndrome (SARS) coronaviruses (Dulude *et al.*, 2006; Plant *et al.*, 2010), although a modest stimulation of frameshifting can actually increase HIV infectivity (Miyauchi *et al.*, 2006). Recently, the possibility of ribosomal frameshifting targeted for antiviral therapy was tested in SARS coronavirus (Ahn *et al.*, 2011). Their data showed that SARS replication was suppressed by antisense peptide nucleic acids through interference of ribosomal frameshifting.

In PRRSV, programmed -1 frameshifting is utilized to express pp1ab dependent on the frameshifting elements within the overlapping region between ORF1a and ORF1b, including a heptanucleotide slippery sequence (U_UUA_AAC) and a putative pseudoknot RNA structure (Meulenberg et al., 1993). The estimated frameshifting efficiency is about 15-

20% in a reporter system (den Boon *et al.*, 1991; Firth & Brierley, 2012). There is almost a knowledge gap of -1 ribosomal frameshifting in PRRSV, although it has been extensively characterized in many RNA viruses. Based on the biological significance of -1 ribosomal frameshifting in other RNA viruses, -1 PRF may play critical roles in viral replication and the host-virus interaction. On one hand, through low efficiency of -1 PRF, PRRSV may produce replicase proteins in ORF1a and ORF1b at a preferred ratio to assemble viral replication and transcription complexes. On the other hand, PRRSV may produce more ORF1a-encoded nonstructural proteins to arrest host systems for its own benefits, since several ORF1a-encoded nonstructural proteins were identified as antagonist to the host innate system.

*-2 programmed ribosomal frameshifting and the expression of PRRSV nsp2N and nsp2TF*

Recently, additional -2/-1 PRF was described to express two nsp2 variants (nsp2TF/nsp2N) in all arteriviruses except EAV (Fang *et al.*, 2012). It is the first case of -2 PRF described for eukaryotes. On the basis of bioinformatics prediction, this -2/-1 PRF was identified by identifying specific peptide covering the frameshifting site by mass spectrometry analysis. The estimated efficiencies of -2 and -1 PRF in PRRSV-infected cells are 16-20% and 7%, respectively. By using reverse genetics, two critical elements of -2 PRF were demonstrated, including a slippery sequence (G_GUU_UUU) and a conserved downstream RNA sequence (CCCANCUCC). However, unlike -1 PRF in RNA viruses reported previously, no particular RNA structure was predicted to function as frameshifting stimulatory element. It is also noteworthy that PRRSV nsp2TF and nsp2N share the N-terminus of nsp2 containing an OTU domain (Ovarian Tumor domain) which inhibits Ub- and ISG15-dependent antiviral pathways (Frias-Staheli *et al.*, 2007; Sun *et al.*, 2010a; Sun *et al.*, 2012). In addition, viable recombinant viruses with -2/-1 PRF inactivated were recovered in both PRRSV genotypes, and showed attenuated viral growth *in vitro,* which implied a possible application of -2/-1 PRF in PRRSV vaccine development.

## 1.4 PRRSV Reverse genetics and their application

For RNA viruses, reverse genetics is an approach utilizing recombinant DNA technology to reverse transcribe virus genome into cDNA and generate viruses from the cloned DNA. Since establishing the first reverse genetics system of polio virus, a positive-strand RNA virus (Racaniello & Baltimore, 1981), reverse genetics systems have been constructed for many groups of RNA viruses, which has accelerated investigation in many aspects of virologic research, including characterization of viral replication and viral pathogenesis determinants, virus-host interactions, and vaccine development. The first PRRSV infectious cDNA clone was constructed for Lelystad virus strain, the prototype of European type PRRSV (Meulenberg *et al.*, 1998). In this system, a copy of viral genome length cDNA was assembled and cloned into a low copy number plasmid under the bacteriophage T7 RNA polymerase promoter. The linearized plasmid created by digestion immediately downstream of the viral polyA tail was used as a template for in vitro transcription utilizing T7 RNA polymerase in the presence of a cap analog. The RNA transcripts were transfected into baby hamster kidney (BHK-21) cells which provided high transfection efficiency. At 24 h after transfection, the culture supernatant from transfected BHK-21 cells was harvested and transferred to porcine alveolar lung macrophages or CL2621 cells to rescue infectious virus. In addition, a genetic marker was introduced into the cDNA clone to differentiate the recombinant virus from parental virus by creating a new restriction enzyme site immediately downstream of ORF7. A few years later, an infectious clone of VR-2332, the prototype North American PRRSV, was generated (Nielsen *et al.*, 2003). Based on the P129 infectious clone containing a highly virulent PRRSV isolated in 1995 under the T7 promoter, Lee *et al.* (2005) established a DNA-launched reverse genetics system for PRRSV (Lee *et al.*, 2005). The T7 promoter in the infectious clone was switched with the human cytomegalovirus (hCMV) immediate early promoter. PRRSV was rescued by direct transfection of DNA plasmid into Marc-145 cells, and cytopathic effects were observed at 3 days post-transfection. To date, several reverse genetics systems have been developed for

various PRRSV isolates, including classic PRRSV (Choi *et al.*, 2006; Fang *et al.*, 2006; Li *et al.*, 2013; Ran *et al.*, 2008) and highly pathogenic PRRSV (Lv *et al.*, 2008; Truong *et al.*, 2004; Zhang *et al.*, 2011; Zhou *et al.*, 2009), and they are widely employed in many aspects of PRRSV investigation. Among numerous applications of PRRSV infectious clone, in this section, we will mainly summarize the investigations employing infectious clone in identification of virulence determinant and vaccine development.

*Reverse genetics in identification of virulence determinants*

To date, multiple research groups have employed infectious clone to search for genetic markers for virulence. The results from (Wang *et al.*, 2008) suggested that the replicase gene is a critical player in viral virulence and attenuation. Herein, they established infectious clones for two genetically distinct PRRSV stains, Ingelvac® PRRS MLV (vaccine) and MN184 (virulent strain). Through exchanging the genomic regions between two PRRSV strains, two reciprocal chimeric clones (pMLVORF1/MN184 and pMN184ORF1/MLV) were created. The pathogenesis of parental and chimeric viruses was evaluated in a nursery pig model, which showed that introduction of the 5' four-fifths of the vaccine virus into virulent virus disrupted the acute pathogenicity of MN184. At the same, another study of (Kwon *et al.*, 2008) provided a more detailed analysis of virulence factors embedded in the PRRSV replicase gene. In this study, a highly virulent PRRSV infectious clone (pFL12) was used as backbone to construct a series of chimeric viruses with specific genomic regions swapped from an attenuated vaccine strain (Prime Pac). The *in vivo* pathogenicity of parental and chimeric viruses was evaluated in a sow reproductive failure model. Nsp3-8-coding region in the replicase gene appeared to be key player in PRRSV virulence, since the sows inoculated with the chimeric virus carrying nsp3-8 region from the vaccine strain exhibited a significantly improved piglet survival rate in comparison to that of parental virus group. In addition, the nsp1-3 and nsp10-12 regions may also contain potential virulence determinants. Although above results suggest that the genomic region of nsp3-8 from the vaccine strain attenuates highly virulent PRRSV, it is still unknown whether the same region from the

highly virulent PRRSV could elevate the virulence of PRRSV vaccine. Recently, Li *et al.* (2014) further dissected PRRSV virulence determinant using infectious clones constructed from two genetically distinct PRRSV strains isolated in China, HB-1/3.9 (low pathogenic strain) and JXwn (highly pathogenic strain) (Li *et al.*, 2014). A series of recombinant viruses with swapped coding regions between the highly pathogenic and low pathogenic PRRSV were generated, and were characterized both *in vitro* and *in vivo.* Their data showed that both HP-PRRSV nsp9- and nsp10-coding regions increased the replication efficiency of low pathogenic PRRSV *in vitro* and *in vivo* and were related to the increased pathogenicity and fatal virulence for piglets. Consistently, the corresponding regions of low pathogenic PRRSV swapped into highly pathogenic PRRSV backbone attenuated HP-PRRSV *in vitro* and *in vivo.*

*PRRSV infectious clones in vaccine development*

To date, modified-live attenuated vaccines (MLV) against PRRSV are most efficient in in combating clinical disease. However, the animals vaccinated with current commercial MLV can't be differentiated from naturally infected animals. Reverse genetics system opens the possibility for designing and generating the vaccine candidates with genetic markers which allow the differentiation of naturally infected and vaccinated animals (DIVA). There are two types of genetic markers utilized in designing marker vaccines for various animal RNA and DNA viruses, positive markers created by insertion of foreign antigens and negative markers created by deletion of epitopes or nonessential genomic sequences. Thus, the complementary assays can be performed to differentiate vaccinated animals from naturally infected animals by detecting the antibody response to genetic markers or modified genomic sequences (Castillo-Olivares *et al.*, 2003; van Oirschot *et al.*, 1996; Walsh *et al.*, 2000a; Walsh *et al.*, 2000b).

Several research groups have designed and generated marker vaccine candidates for PRRSV. Taking advantage of type I PRRSV infectious clone (pSD 01-08), Fang, *et al.* (2006) generated a recombinant PRRSV with eGFP gene expressed in the central region of the nsp2-coding sequence (Fang *et al.*, 2006). In a following study (Fang *et al.*, 2008), using this GFP-

tagged PRRSV as a backbone, a recombinant virus with both positive and negative marker virus were constructed by deletion of the B-cell epitope ES4 of nsp2, located downstream of the GFP insertion. The recovered virus (GFP/ΔES4 marker virus) was characterized in a nursery piglet disease model. Additionally, GFP- and ES4 epitope-based ELISA assays were developed as accompanying tests. The results showed that marker virus-vaccinated pigs could be recognized by GFP-positive and ES4-negative ELISA results, whereas wild type virus-infected pigs could be identified by GFP-negative and ES4-positive ELISA results. Similarly, several type 2 PRRSV infectious clones were used as a backbone to construct marker vaccine candidates by manipulating the PRRSV nsp2 region. A VR2332 infectious clone was used as a backbone to express GFP gene as a nsp2 fusion protein by insertion of GFP into a nsp2 deletion (V7-nsp2Δ324-434) (Han *et al.*, 2007). Although the recombinant virus was viable, the GFP insertion was unstable after being passaged on permissive cells. Also, a similar strategy was used to express GFP gene in the pCMV-129 infectious clone by replacing 131-aa in the C-terminal region of nsp2. To date, many other foreign sequences were inserted into the nsp2 high-variable region to create marker viruses (de Lima *et al.*, 2008; Lin *et al.*, 2012; Sang *et al.*, 2012; Xu *et al.*, 2013; Xu *et al.*, 2012). Nevertheless, the stability of the marker viruses is still a problem for its application in field. Pei, *et al.* (2009) described an additional strategy to express GFP and porcine circovirus type 2 capsid protein from a dedicated subgenomic RNA (Pei *et al.*, 2009). In this strategy, using an infectious clone of type 2 PRRSV strain P129 as backbone, the foreign genes were inserted between ORF1b and ORF2a followed by a copy of TRS6 to drive ORF2a/b transcription. The data of serial *in vitro* passage showed that the marker viruses are phenotypically stable for at least 37 passages. To evaluate the immunogenicity of the recombinant viruses, piglets were immunized with wild type virus and marker viruses. Specific antibody response to GFP or PCV2 capsid were elicited in the animals inoculated with marker viruses, but not in the wild type virus-infected animals.

During the past decade, multiple PRRSV proteins were identified to be responsible for the delayed host innate immune response and neutralizing antibody response. By using available PRRSV infectious clones, several recombinant PRRSV with improved ability to elicit host immune response were generated by introducing specific mutations into the viral genome. By using reverse genetics, the effect of three putative N-linked glycosylation sites located on PRRSV GP5 ectodomain on the neutralizing antibody response was evaluated (Ansari *et al.*, 2006). By incorporating targeted mutations into a full-length cDNA clone, three recombinant viruses with glycosylation sites disrupted were rescued and characterized *in vitro* and *in vivo.* Neutralizing antibody profiles in pig serum showed that the mutant viruses induced significantly higher levels of neutralizing antibodies against the mutant and wild type PRRSV. By using a type 1 PRRSV infectious cDNA clone (pCMV-SD 01-08), Sun and coworkers knocked down the inhibitory effect of PRRSV on the host innate immune response by introducing mutations/deletions to impair the deubiquitination activity of OTU domain embedded in nsp2 (Sun *et al.*, 2012; Sun *et al.*, 2010b). In their investigations, the cysteine protease domain embedded in PRRSV nsp2 was identified as an innate immune antagonist, which was facilitated by two major mechanisms, deubiquitination and deISGylation. The recombinant viruses with reduced deubiquitination and deISGylation activity were generated by modifying nsp2 PLP2 domain with mutations or deletions. Thus, all the investigations summarized above demonstrate that improved vaccine candidates with increased ability to elicit the host immune response may be designed and generated by utilizing reverse genetics.

## 1.5 Host innate immunity and immune evasion by PRRSV nonstructural proteins

*Host antiviral innate immunity*

Host innate immune response function as the first line of defense against viral infection, which also provide a time interval for establishing specific adaptive immunity.

Interferons (IFNs) are a group of multifunctional cytokines which play significant roles in initial innate immune defense and modulating adaptive immunity. IFNs comprise two types, type I and type II IFNs. Recently, three novel IFNs, IFN-λ1 to λ3 have been classified into type III IFNs whose role in antiviral immunity remains to be evaluated (Randall & Goodbourn, 2008). Type I IFNs are believed to be the main players for innate immunity against viral infections and consist of various subtypes depending on the mammal species. In pigs, type I IFNs comprise multiple porcine IFN-α, IFN-ω, and IFN-δ like molecules, such as porcine IFN-α which are encoded by up to fifteen functional genes (Cheng *et al.*, 2006; Sang *et al.*, 2011). Additionally, porcine IFN-β, IFN-ε and IFN-κ are encoded by single gene loci in pigs (Artursson *et al.*, 1992; Sang *et al.*, 2011). Up on viral infection, pathogen associated molecular patterns (PAMP) stimulate IFNα/β expression through Toll-like receptors (TLR) and Retinoic acid inducible gene I-like receptors (RLR) in infected cells (Fig. 1.2A). After being recognized by host PAMP receptors, viral PAMPs activate serial protein signaling cascades, which results in the activation of transcription factors, including interferon regulatory factor 3 (IRF3), NF-κB, and ATF-2/c JUN. The coordinated activation of these transcription factors leads to the formation of transcriptionally competent enhanceosomes in the cell nucleus to induce the expression of type I interferons. Local production of type I IFNs establishes a major antiviral defense to inactivate and restrict virus spreading to adjacent cells. Many viruses, including Hepatitis C virus, HIV and severe acute respiratory syndrome (SARS) coronavirus, are very sensitive to type I IFNs, which has led to the development of several IFN-based antiviral therapies (Deutsch *et al.*, 2007; Haagmans & Osterhaus, 2006; Loomba & Liang, 2007; Sulkowski & Benhamou, 2007; Yu *et al.*, 2007). Besides direct antiviral activity, type I IFNs induce antiviral response through a receptor containing two subunits, IFNAR-1 and IFNAR-2. After being secreted, the interaction between type I IFNs and their receptors on adjacent cell surfaces activates the so-called JAK-STAT signaling pathway (Fig. 1.2B). Briefly, the receptor binding activates JAKs (Janus activated kinases) and Tyk2, which phosphorylate signal transducers and activators of

transcription (STATs). The phosphorylated STAT1 and STAT2, in association with IRF9, form the heterotrimeric complex ISGF3 (interferon-stimulated gene factor 3), which is imported into the nucleus where it binds to IFN stimulated response elements (ISRE) in the promoter and induces the transcription of IFN-stimulated genes (ISGs). Activation of these genes enables the cell to establish an antiviral state to fight the infection and inhibit virus replication.

Multiple studies have described that PRRSV infection elicits poor innate immune response, which may in turn result in a weak adaptive immune response. Miller *et al.* (2014) showed that PRRSV infection significantly suppressed the activation of type I interferon in Marc-145 cells, while stimulation by exogenous double-stranded RNA induced a significant production of type I interferon mRNA (Miller *et al.*, 2004). Consistent with that, results from (Luo *et al.*, 2008) indicated that the induction of IFN-β production is significantly inhibited by PRRSV infection. Recently, the luciferase gene based reporter assays have been employed to investigate the function of PRRSV nonstructural proteins in modulating host innate immune response. By using these tools, several PRRSV nonstructural proteins appear to possess the ability to modulate type I IFN synthesis and / or signaling in *in vitro* expression systems. The results from previous investigations (Beura *et al.*, 2010; Chen *et al.*, 2010; Kim *et al.*, 2010; Sun *et al.*, 2010a) suggested that PRRSV nsp1α/β and nsp2 strongly antagonize IFN-β promoter activation, although the detailed mechanisms are still not well-understood. The antagonism function of PRRSV nsp4 on IFN-β promoter activation has also been documented (Huang *et al.*, 2014), although it induces apoptosis dependent on its serine protease activity (Ma *et al.*, 2013). In addition, nsp11 was reported to have an inhibitory effect on IFN-β promoter activation (Beura *et al.*, 2010). However, this observation may need detailed follow-up studies to rule out the possibility that the inhibitory effect may be due to toxicity to host cells when these potentially toxic viral enzymes are expressed *in vitro.* The inhibitory effect of PRRSV nsp2 PLP2 domain on IFN-β production and signaling was evaluated in HEK-293T cells. The results also confirmed that PRRSV nsp2 PLP2 domain is

able to de-conjugate both ubiquitin and interferon stimulated gene 15 (ISG15) from cellular proteins, which exerts inhibitory effect on ubiquitin- and ISG15- dependent innate immune response(Sun *et al.*, 2010a; Sun *et al.*, 2012).

*Suppression of Type I interferon synthesis and signaling by PRRSV nsp1α and nsp1β*

PRRSV nsp1α and nsp1β are the first two viral proteins synthesized after viral infection, and show predominantly nucleus localization at the later stages of infection (Chen *et al.*, 2010). They appear to exert inhibitory effects on type I IFN production and signaling through different mechanisms. Expressed individually in cell culture systems, nsp1α shows stronge suppression on IFN synthesis, while nsp1β has the ability to inhibit both IFN synthesis and signaling (Beura *et al.*, 2010; Chen *et al.*, 2010; Kim *et al.*, 2010). When testing the IFN antagonist mechanism *in vitro* using luciferase gene based immune assays, the regulatory factor 3 (IRF3)- dependent gene induction pathway for IFN-β synthesis appeared to be significantly arrested by nsp1β expression (Beura *et al.*, 2010; Chen *et al.*, 2010). The results from (Beura *et al.*, 2010) showed that nsp1β inhibited Sendai virus-mediated activation of porcine IFN-β promoter activity in a porcine myelomonocytic cell line. At the same time, Chen *et al*. (2010) screened each molecule that could be targeted by nsp1α/β in the IRF3 induction pathway. However, none of the cytoplasmic components were identified, indicating PRRSV nsp1α/β may act downstream of IRF3 activation, which may have a direct effect on the formation of the transcription enhanceosome on the IFN-β promoter in the nucleus. The study of (Kim *et al.*, 2010) suggested that nsp1α/β may interfere with IFN-β production through degradation of transcription factor CREB-binding protein (CBP300) in the cell nucleus. Their data indicated that nsp1α/β did not block IRF3 phosphorylation or its nuclear translocation, but inhibited IRF3 association with CBP300 to form the transcription enhanceosome in the nucleus, when expressed in HeLa or MARC-145 cells. Han *et al.* (2013) showed that the N-terminal zinc finger motif (ZF1) is the essential element of nsp1α for IFN suppression. In their study, the IFN antagonism of nsp1α was impaired by inactivating the

ZF1 motif by site-directed mutations, which indicated that the CBP degradation is likely the key mechanism for IFN suppression mediated by the nsp1α (Han *et al.*, 2013).

Besides its role in suppression of IFN production, PRRSV nsp1β showed strong ability to suppress the IFN-dependent signaling pathway leading to ISG expression (Beura *et al.*, 2010). In another study, reporter gene expression from an IFN-stimulated response element (ISRE) promoter was significantly inhibited after IFN-β stimulation (Chen *et al.*, 2010). The results indicated that the phosphorylation and nuclear translocation of the transcription factor STAT1 was blocked by nsp1β expression. Song *et al.* (2009) identified a protein inhibitor of activated STAT1 (PIAS1) as a specific cellular interaction partner for nsp1α and nsp1β. In addition(Song *et al.*, 2009), Wang *et al.* (2013) suggested that nsp1β inhibited interferon-activated JAK/STAT signal transduction by inducing karyopherin-α1 degradation. Nsp1β induced the degradation of karyopherin-α1 (KPNA1, also called importin-α5), which is known to mediate the nuclear import of ISGF3, heterodimers comprising phosphorylated STAT1, STAT2 and IRF9 (Wang *et al.*, 2013).

*PRRSV nsp2 antagonisms the host innate immunity through multiple mechanisms*

In PRRSV, nsp2 is the largest (mature) viral protein and contains at least four distinct domains: the N-terminal PLP2/OTU domain, a central hypervariable region, a putative transmembrane domain, and a C-terminal region of unknown function that is rich in conserved Cys residues (Snijder *et al.*, 1995). Based on comparative sequence analysis, the PRRSV nsp2 PLP2 domain appears to be a member of the OTU family of deubiquitinating enzymes (Makarova *et al.*, 2000). The deubiquitinating activity of nsp2 PLP2 domain for arteriviruses was further confirmed both *in vitro* and cell-based assays, and the protease activity of PLP2 is considered to be essential for its deubiquitinase function (Frias-Staheli *et al.*, 2007; Sun *et al.*, 2010a; van Kasteren *et al.*, 2012). Frias-Staheli *et al.* (2007) also reported the deISGylation function of the nsp2 PLP2 domain, which deconjugates ISG15, an interferon-induced ubiquitin-like molecule, from host cellular proteins to exhibit antiviral activity (Frias-Staheli *et al.*, 2007). The biological significance of this activity was supported

by its capacity to inhibit NF-κB dependent signaling and antagonize the antiviral effects of ISG15 when expressed in combination with a Sindbis virus infection *in vivo*. The investigation of (Sun *et al.*, 2010a) showed that PRRSV nsp2 inhibited the IFN-β promoter dependent luciferase reporter expression in response to Sendai virus-medicated stimulation, when expressed in human HEK-293T cells. The results indicated that PRRSV nsp2 PLP2 domain antagonizes the type I IFN induction by interfering with the NF-κB signaling pathway. This domain interfered with the polyubiquitination process of IκBα, which subsequently prevents IκBα degradation to inhibit NF-κB activation. ISG15 overexpression inhibited PRRSV replication in cell culture, while PRRSV replication antagonized ISG15 production and conjugation (Sun *et al.*, 2012). When overexpressed in human HEK-293T cells, nsp2, especially PLP2 domain, showed a strong inhibitory effect on ISG15 production and ISG15 conjugation of cellular proteins. By engineering a panel of mutants with deletions and/or mutations at the N-terminal border of the nsp2 PLP2 domain of type 1 PRRSV, a 19-amino-acid deletion, in combination with a single mutation of S465A, partially relieved the ISG15 antagonist function.

*Inhibition of type I interferon production by PRRSV nsp4*

PRRSV nsp4, the main protease responsible for replicase polyprotein processing, has been identified as a type I IFN antagonist. Beura *et al.* (2010) showed that nsp4, together with nsp1α/β, nsp2 and nsp11, suppressed IFN-β promoter activation. Recently, two more studies have been performed to dissect the antagonist function of nsp4 on type I IFN production (Chen *et al.*, 2014; Huang *et al.*, 2014). The results (Chen *et al.*, 2014) suggests that nsp4 inhibited IFN synthesis mainly through suppressing NF-κB-dependent signaling pathway without interfering with NF-κB phosphorylation and nuclear translocation. The nuclear localization property of nsp4 was found to be responsible for inhibiting IFN-β activation. In addition, the IFN antagonism ability of nsp4 from different PRRSV strains with different pathogenesis was compared, which indicated that the nsp4 from Asian highly pathogenic (HP)-PRRSV exhibited a stronger inhibitory effect. Huang *et al.* (2014) also

studied the mechanism of nsp4's immune antagonism function on IFN-β promoter, and suggested that nsp4 targeted the NF-κB essential modulator (NEMO) at the E349-S350 site to mediate its cleavage. The serine protease (SP) of nsp4 appears to mediate the cleavage of NEMO, since mutated nsp4 with inactivated SP domain lost its ability to cleave NEMO and inhibit IFN-β production. Interestingly, these two studies contradict with each other, because different steps of NF-κB signaling pathway were considered to be targeted by PRRSV nsp4. Also, PRRSV nsp4 was found to induce apoptosis dependent on its 3C-Like serine protease activity (Ma *et al.*, 2013). Thus, more detailed investigations are needed to further dissect the mechanism of nsp4's inhibitory effect on IFN-promoter activation, ruling out whether the observed effects may be (partially) due to its ability to induce apoptosis.

## 1.6 Purpose of this research

Since its emergence, PRRSV became the most devastating and economically important pathogen to challenge the global swine industry. During the past two decades, a great amount of information has been obtained on PRRSV structural proteins. However, the structure and function of PRRSV nsps is largely undetermined. Therefore, the overall goal of this research is to identify PRRSV nonstructural proteins in infected cells and determine their functions in host innate immunity. Based on the current knowledge on PRRSV nsps, four specific aims will be fulfilled in this investigation, including: a) to identify PRRSV ORF1a-encoded non-structural proteins in virus-infected cells; b) to determine the role of PRRSV nsp1β protein in host innate immune response; c) to elucidate the function of nsp1β in trans-activating the expression of nsp2-related products; d) to attenuate PRRSV by inactivating expression of -2/-1 ribosomal frameshifting products: implication for the rational design of vaccines.

## 1.7 References


**Ahlquist, P. (2006).** Parallels among positive-strand RNA viruses, reverse-transcribing viruses and double-stranded RNA viruses. *Nat Rev Microbiol* **4**, 371-382.

**Ahn, D. G., Lee, W., Choi, J. K., Kim, S. J., Plant, E. P., Almazan, F., Taylor, D. R., Enjuanes, L. & Oh, J. W. (2011).** Interference of ribosomal frameshifting by antisense peptide nucleic acids suppresses SARS coronavirus replication. *Antiviral Res* **91**, 1-10.

**Allende, R., Lewis, T. L., Lu, Z., Rock, D. L., Kutish, G. F., Ali, A., Doster, A. R. & Osorio, F. A. (1999).** North American and European porcine reproductive and respiratory syndrome viruses differ in non-structural protein coding regions. *J Gen Virol* **80 ( Pt 2)**, 307-315.

**Ansari, I. H., Kwon, B., Osorio, F. A. & Pattnaik, A. K. (2006).** Influence of N-linked glycosylation of porcine reproductive and respiratory syndrome virus GP5 on virus infectivity, antigenicity, and ability to induce neutralizing antibodies. *J Virol* **80**, 3994-4004.

**Artursson, K., Gobl, A., Lindersson, M., Johansson, M. & Alm, G. (1992).** Molecular cloning of a gene encoding porcine interferon-beta. *J Interferon Res* **12**, 153-160.

**Bautista, E. M., Meulenberg, J. J., Choi, C. S. & Molitor, T. W. (1996).** Structural polypeptides of the American (VR-2332) strain of porcine reproductive and respiratory syndrome virus. *Arch Virol* **141**, 1357-1365.

**Benfield, D. A., Nelson, E., Collins, J. E., Harris, L., Goyal, S. M., Robison, D., Christianson, W. T., Morrison, R. B., Gorcyca, D. & Chladek, D. (1992).** Characterization of swine infertility and respiratory syndrome (SIRS) virus (isolate ATCC VR-2332). *J Vet Diagn Invest* **4**, 127-133.

**Beura, L. K., Sarkar, S. N., Kwon, B., Subramaniam, S., Jones, C., Pattnaik, A. K. & Osorio, F. A. (2010).** Porcine reproductive and respiratory syndrome virus nonstructural protein 1beta modulates host innate immune response by antagonizing IRF3 activation. *J Virol* **84**, 1574-1584.

**Calvert, J. G., Slade, D. E., Shields, S. L., Jolie, R., Mannan, R. M., Ankenbauer, R. G. & Welch, S. K. (2007).** CD163 expression confers susceptibility to porcine reproductive and respiratory syndrome viruses. *J Virol* **81**, 7371-7379.

**Castillo-Olivares, J., Wieringa, R., Bakonyi, T., de Vries, A. A., Davis-Poynter, N. J. & Rottier, P. J. (2003).** Generation of a candidate live marker vaccine for equine arteritis virus by deletion of the major virus neutralization domain. *J Virol* **77**, 8470-8480.

**Chen, Z., Lawson, S., Sun, Z., Zhou, X., Guan, X., Christopher-Hennings, J., Nelson, E. A. & Fang, Y. (2010).** Identification of two auto-cleavage products of nonstructural protein 1 (nsp1) in porcine reproductive and respiratory syndrome virus infected cells: nsp1 function as interferon antagonist. *Virology* **398**, 87-97.

**Chen, Z., Li, M., He, Q., Du, J., Zhou, L., Ge, X., Guo, X. & Yang, H. (2014).** The amino acid at residue 155 in nonstructural protein 4 of porcine reproductive and respiratory syndrome virus contributes to its inhibitory effect for interferon-beta transcription in vitro. *Virus Res* **189**, 226-234.

**Cheng, G., Chen, W., Li, Z., Yan, W., Zhao, X., Xie, J., Liu, M., Zhang, H., Zhong, Y. & Zheng, Z. (2006).** Characterization of the porcine alpha interferon multigene family. *Gene* **382**, 28-38.

**Choi, Y. J., Yun, S. I., Kang, S. Y. & Lee, Y. M. (2006).** Identification of 5' and 3' cis-acting elements of the porcine reproductive and respiratory syndrome virus: acquisition of novel 5' AU-rich sequences restored replication of a 5'-proximal 7-nucleotide deletion mutant. *J Virol* **80**, 723-736.

**Collins, J. E., Benfield, D. A., Christianson, W. T., Harris, L., Hennings, J. C., Shaw, D. P., Goyal, S. M., McCullough, S., Morrison, R. B., Joo, H. S. & et al. (1992).** Isolation of swine infertility and respiratory syndrome virus (isolate ATCC VR-2332) in North America and experimental reproduction of the disease in gnotobiotic pigs. *J Vet Diagn Invest* **4**, 117-126.

**Das, P. B., Dinh, P. X., Ansari, I. H., de Lima, M., Osorio, F. A. & Pattnaik, A. K. (2010).** The minor envelope glycoproteins GP2a and GP4 of porcine reproductive and respiratory syndrome virus interact with the receptor CD163. *J Virol* **84**, 1731-1740.

**de Lima, M., Kwon, B., Ansari, I. H., Pattnaik, A. K., Flores, E. F. & Osorio, F. A. (2008).** Development of a porcine reproductive and respiratory syndrome virus differentiable (DIVA) strain through deletion of specific immunodominant epitopes. *Vaccine* **26**, 3594-3600.

**Dea, S., Sawyer, N., Alain, R. & Athanassious, R. (1995).** Ultrastructural characteristics and morphogenesis of porcine reproductive and respiratory syndrome virus propagated in the highly permissive MARC-145 cell clone. *Adv Exp Med Biol* **380**, 95-98.

**den Boon, J. A., Faaberg, K. S., Meulenberg, J. J., Wassenaar, A. L., Plagemann, P. G., Gorbalenya, A. E. & Snijder, E. J. (1995).** Processing and evolution of the N-terminal region of the arterivirus replicase ORF1a protein: identification of two papainlike cysteine proteases. *J Virol* **69**, 4500-4505.

**den Boon, J. A., Snijder, E. J., Chirnside, E. D., de Vries, A. A., Horzinek, M. C. & Spaan, W. J. (1991).** Equine arteritis virus is not a togavirus but belongs to the coronaviruslike superfamily. *J Virol* **65**, 2910-2920.

**Deutsch, M., Manesis, E. K., Hadziyannis, E., Vassilopoulos, D. & Archimandritis, A. J. (2007).** Thrombotic thrombocytopenic purpura with fatal outcome in a patient with chronic hepatitis C treated with pegylated interferon-a/2b. *Scand J Gastroenterol* **42**, 408-409.

**Duan, X., Nauwynck, H. J. & Pensaert, M. B. (1997a).** Effects of origin and state of differentiation and activation of monocytes/macrophages on their susceptibility to

porcine reproductive and respiratory syndrome virus (PRRSV). *Arch Virol* **142**, 2483-2497.

**Duan, X., Nauwynck, H. J. & Pensaert, M. B. (1997b).** Virus quantification and identification of cellular targets in the lungs and lymphoid tissues of pigs at different time intervals after inoculation with porcine reproductive and respiratory syndrome virus (PRRSV). *Vet Microbiol* **56**, 9-19.

**Dulude, D., Berchiche, Y. A., Gendron, K., Brakier-Gingras, L. & Heveker, N. (2006).** Decreasing the frameshift efficiency translates into an equivalent reduction of the replication of the human immunodeficiency virus type 1. *Virology* **345**, 127-136.

**Fang, Y., Christopher-Hennings, J., Brown, E., Liu, H., Chen, Z., Lawson, S. R., Breen, R., Clement, T., Gao, X., Bao, J., Knudsen, D., Daly, R. & Nelson, E. (2008).** Development of genetic markers in the non-structural protein 2 region of a US type 1 porcine reproductive and respiratory syndrome virus: implications for future recombinant marker vaccine development. *J Gen Virol* **89**, 3086-3096.

**Fang, Y., Rowland, R. R., Roof, M., Lunney, J. K., Christopher-Hennings, J. & Nelson, E. A. (2006).** A full-length cDNA infectious clone of North American type 1 porcine reproductive and respiratory syndrome virus: expression of green fluorescent protein in the Nsp2 region. *J Virol* **80**, 11447-11455.

**Fang, Y. & Snijder, E. J. (2010).** The PRRSV replicase: exploring the multifunctionality of an intriguing set of nonstructural proteins. *Virus Res* **154**, 61-76.

**Fang, Y., Treffers, E. E., Li, Y., Tas, A., Sun, Z., van der Meer, Y., de Ru, A. H., van Veelen, P. A., Atkins, J. F., Snijder, E. J. & Firth, A. E. (2012).** Efficient -2 frameshifting by mammalian ribosomes to synthesize an additional arterivirus protein. *Proc Natl Acad Sci U S A* **109**, E2920-2928.

**Feng, Y., Zhao, T., Nguyen, T., Inui, K., Ma, Y., Nguyen, T. H., Nguyen, V. C., Liu, D., Bui, Q. A., To, L. T., Wang, C., Tian, K. & Gao, G. F. (2008).** Porcine respiratory and reproductive syndrome virus variants, Vietnam and China, 2007. *Emerg Infect Dis* **14**, 1774-1776.

**Firth, A. E. & Brierley, I. (2012).** Non-canonical translation in RNA viruses. *J Gen Virol* **93**, 1385-1409.

**Firth, A. E., Zevenhoven-Dobbe, J. C., Wills, N. M., Go, Y. Y., Balasuriya, U. B., Atkins, J. F., Snijder, E. J. & Posthuma, C. C. (2011).** Discovery of a small arterivirus gene that overlaps the GP5 coding sequence and is important for virus production. *J Gen Virol* **92**, 1097-1106.

**Frias-Staheli, N., Giannakopoulos, N. V., Kikkert, M., Taylor, S. L., Bridgen, A., Paragas, J., Richt, J. A., Rowland, R. R., Schmaljohn, C. S., Lenschow, D. J., Snijder, E. J., Garcia-Sastre, A. & Virgin, H. W. t. (2007).** Ovarian tumor domain-containing viral proteases evade ubiquitin- and ISG15-dependent innate immune responses. *Cell Host Microbe* **2**, 404-416.

**Haagmans, B. L. & Osterhaus, A. D. (2006).** Coronaviruses and their therapy. *Antiviral Res* **71**, 397-403.

**Han, J., Liu, G., Wang, Y. & Faaberg, K. S. (2007).** Identification of nonessential regions of the nsp2 replicase protein of porcine reproductive and respiratory syndrome virus strain VR-2332 for replication in cell culture. *J Virol* **81**, 9878-9890.

**Han, J., Rutherford, M. S. & Faaberg, K. S. (2009).** The porcine reproductive and respiratory syndrome virus nsp2 cysteine protease domain possesses both trans- and cis-cleavage activities. *J Virol* **83**, 9449-9463.

**Han, M., Du, Y., Song, C. & Yoo, D. (2013).** Degradation of CREB-binding protein and modulation of type I interferon induction by the zinc finger motif of the porcine reproductive and respiratory syndrome virus nsp1alpha subunit. *Virus Res* **172**, 54-65.

**Hu, S. P., Zhang, Z., Liu, Y. G., Tian, Z. J., Wu, D. L., Cai, X. H. & He, X. J. (2013).** Pathogenicity and distribution of highly pathogenic porcine reproductive and respiratory syndrome virus in pigs. *Transbound Emerg Dis* **60**, 351-359.

**Huang, C., Zhang, Q., Guo, X. K., Yu, Z. B., Xu, A. T., Tang, J. & Feng, W. H. (2014).** Porcine Reproductive and Respiratory Syndrome Virus Nonstructural Protein 4 Antagonizes Beta Interferon Expression by Targeting the NF-kappaB Essential Modulator. *J Virol* **88**, 10934-10945.

**Johnson, C. R., Griggs, T. F., Gnanandarajah, J. & Murtaugh, M. P. (2011).** Novel structural protein in porcine reproductive and respiratory syndrome virus encoded by an alternative ORF5 present in all arteriviruses. *J Gen Virol* **92**, 1107-1116.

**Karacostas, V., Wolffe, E. J., Nagashima, K., Gonda, M. A. & Moss, B. (1993).** Overexpression of the HIV-1 gag-pol polyprotein results in intracellular activation of HIV-1 protease and inhibition of assembly and budding of virus-like particles. *Virology* **193**, 661-671.

**Karniychuk, U. U., Geldhof, M., Vanhee, M., Van Doorsselaere, J., Saveleva, T. A. & Nauwynck, H. J. (2010).** Pathogenesis and antigenic characterization of a new East European subtype 3 porcine reproductive and respiratory syndrome virus isolate. *BMC Vet Res* **6**, 30.

**Keffaber, K. K. (1989).** Reproductive failure of unknown etiology. *Am Assoc Swine Pract Newsl* **1**, 1-9.

**Kim, H. S., Kwang, J., Yoon, I. J., Joo, H. S. & Frey, M. L. (1993).** Enhanced replication of porcine reproductive and respiratory syndrome (PRRS) virus in a homogeneous subpopulation of MA-104 cell line. *Arch Virol* **133**, 477-483.

**Kim, O., Sun, Y., Lai, F. W., Song, C. & Yoo, D. (2010).** Modulation of type I interferon induction by porcine reproductive and respiratory syndrome virus and degradation of CREB-binding protein by non-structural protein 1 in MARC-145 and HeLa cells. *Virology* **402**, 315-326.

**Kwon, B., Ansari, I. H., Pattnaik, A. K. & Osorio, F. A. (2008).** Identification of virulence determinants of porcine reproductive and respiratory syndrome virus through construction of chimeric clones. *Virology* **380**, 371-378.

**Lee, C., Calvert, J. G., Welch, S. K. & Yoo, D. (2005).** A DNA-launched reverse genetics system for porcine reproductive and respiratory syndrome virus reveals that homodimerization of the nucleocapsid protein is essential for virus infectivity. *Virology* **331**, 47-62.

**Li, Y., Zhou, L., Zhang, J., Ge, X., Zhou, R., Zheng, H., Geng, G., Guo, X. & Yang, H. (2014).** Nsp9 and Nsp10 contribute to the fatal virulence of highly pathogenic porcine reproductive and respiratory syndrome virus emerging in China. *PLoS Pathog* **10**, e1004216.

**Li, Y., Zhu, L., Lawson, S. R. & Fang, Y. (2013).** Targeted mutations in a highly conserved motif of the nsp1beta protein impair the interferon antagonizing activity of porcine reproductive and respiratory syndrome virus. *J Gen Virol* **94**, 1972-1983.

**Lin, T., Li, X., Yao, H., Wei, Z., Tan, F., Liu, R., Sun, L., Zhang, R., Li, W., Lu, J., Tong, G. & Yuan, S. (2012).** Use of reverse genetics to develop a novel marker porcine reproductive and respiratory syndrome virus. *Virus Genes* **45**, 548-555.

**Loomba, R. & Liang, T. J. (2007).** Treatment of chronic hepatitis B. *Antivir Ther* **12 Suppl 3**, H33-41.

**Luo, R., Xiao, S., Jiang, Y., Jin, H., Wang, D., Liu, M., Chen, H. & Fang, L. (2008).** Porcine reproductive and respiratory syndrome virus (PRRSV) suppresses interferon-beta production by interfering with the RIG-I signaling pathway. *Mol Immunol* **45**, 2839-2846.

**Lv, J., Zhang, J., Sun, Z., Liu, W. & Yuan, S. (2008).** An infectious cDNA clone of a highly pathogenic porcine reproductive and respiratory syndrome virus variant associated with porcine high fever syndrome. *J Gen Virol* **89**, 2075-2079.

**Ma, Z., Wang, Y., Zhao, H., Xu, A. T., Tang, J. & Feng, W. H. (2013).** Porcine reproductive and respiratory syndrome virus nonstructural protein 4 induces apoptosis dependent on its 3C-like serine protease activity. *PLoS One* **8**, e69387.

**Makarova, K. S., Aravind, L. & Koonin, E. V. (2000).** A novel superfamily of predicted cysteine proteases from eukaryotes, viruses and Chlamydia pneumoniae. *Trends Biochem Sci* **25**, 50-52.

**Mardassi, H., Athanassious, R., Mounir, S. & Dea, S. (1994).** Porcine reproductive and respiratory syndrome virus: morphological, biochemical and serological characteristics of Quebec isolates associated with acute and chronic outbreaks of porcine reproductive and respiratory syndrome. *Can J Vet Res* **58**, 55-64.

**Mardassi, H., Massie, B. & Dea, S. (1996).** Intracellular synthesis, processing, and transport of proteins encoded by ORFs 5 to 7 of porcine reproductive and respiratory syndrome virus. *Virology* **221**, 98-112.

**Meng, X. J., Paul, P. S., Morozov, I. & Halbur, P. G. (1996).** A nested set of six or seven subgenomic mRNAs is formed in cells infected with different isolates of porcine reproductive and respiratory syndrome virus. *J Gen Virol* **77 ( Pt 6)**, 1265-1270.

**Meulenberg, J. J., Bos-de Ruijter, J. N., van de Graaf, R., Wensvoort, G. & Moormann, R. J. (1998).** Infectious transcripts from cloned genome-length cDNA of porcine reproductive and respiratory syndrome virus. *J Virol* **72**, 380-387.

**Meulenberg, J. J. & Petersen-den Besten, A. (1996).** Identification and characterization of a sixth structural protein of Lelystad virus: the glycoprotein GP2 encoded by ORF2 is incorporated in virus particles. *Virology* **225**, 44-51.

**Meulenberg, J. J., Petersen-den Besten, A., De Kluyver, E. P., Moormann, R. J., Schaaper, W. M. & Wensvoort, G. (1995).** Characterization of proteins encoded by ORFs 2 to 7 of Lelystad virus. *Virology* **206**, 155-163.

**Miller, L. C., Laegreid, W. W., Bono, J. L., Chitko-McKown, C. G. & Fox, J. M. (2004).** Interferon type I response in porcine reproductive and respiratory syndrome virus-infected MARC-145 cells. *Arch Virol* **149**, 2453-2463.

**Miller, M. (2011).** PRRS price tag, $664 million. *Porknetwork http://wwwporknetworkcom/pork-news/127963843html*.

**Miyauchi, K., Komano, J., Myint, L., Futahashi, Y., Urano, E., Matsuda, Z., Chiba, T., Miura, H., Sugiura, W. & Yamamoto, N. (2006).** Rapid propagation of low-fitness drug-resistant mutants of human immunodeficiency virus type 1 by a streptococcal metabolite sparsomycin. *Antivir Chem Chemother* **17**, 167-174.

**Mounir, S., Mardassi, H. & Dea, S. (1995).** Identification and characterization of the porcine reproductive and respiratory virus ORFs 7, 5 and 4 products. *Adv Exp Med Biol* **380**, 317-320.

**Nauwynck, H. J., Duan, X., Favoreel, H. W., Van Oostveldt, P. & Pensaert, M. B. (1999).** Entry of porcine reproductive and respiratory syndrome virus into porcine alveolar macrophages via receptor-mediated endocytosis. *J Gen Virol* **80 ( Pt 2)**, 297-305.

**Nelsen, C. J., Murtaugh, M. P. & Faaberg, K. S. (1999).** Porcine reproductive and respiratory syndrome virus comparison: divergent evolution on two continents. *J Virol* **73**, 270-280.

**Nielsen, H. S., Liu, G., Nielsen, J., Oleksiewicz, M. B., Botner, A., Storgaard, T. & Faaberg, K. S. (2003).** Generation of an infectious clone of VR-2332, a highly virulent North American-type isolate of porcine reproductive and respiratory syndrome virus. *J Virol* **77**, 3702-3711.

**Pasternak, A. O., van den Born, E., Spaan, W. J. & Snijder, E. J. (2001).** Sequence requirements for RNA strand transfer during nidovirus discontinuous subgenomic RNA synthesis. *EMBO J* **20**, 7220-7228.

**Pedersen, K. W., van der Meer, Y., Roos, N. & Snijder, E. J. (1999).** Open reading frame 1a-encoded subunits of the arterivirus replicase induce endoplasmic reticulum-derived

double-membrane vesicles which carry the viral replication complex. *J Virol* **73**, 2016-2026.

**Pei, Y., Hodgins, D. C., Wu, J., Welch, S. K., Calvert, J. G., Li, G., Du, Y., Song, C. & Yoo, D. (2009).** Porcine reproductive and respiratory syndrome virus as a vector: immunogenicity of green fluorescent protein and porcine circovirus type 2 capsid expressed from dedicated subgenomic RNAs. *Virology* **389**, 91-99.

**Plant, E. P., Rakauskaite, R., Taylor, D. R. & Dinman, J. D. (2010).** Achieving a golden mean: mechanisms by which coronaviruses ensure synthesis of the correct stoichiometric ratios of viral proteins. *J Virol* **84**, 4330-4340.

**Prather, R. S., Rowland, R. R., Ewen, C., Trible, B., Kerrigan, M., Bawa, B., Teson, J. M., Mao, J., Lee, K., Samuel, M. S., Whitworth, K. M., Murphy, C. N., Egen, T. & Green, J. A. (2013).** An intact sialoadhesin (Sn/SIGLEC1/CD169) is not required for attachment/internalization of the porcine reproductive and respiratory syndrome virus. *J Virol* **87**, 9538-9546.

**Racaniello, V. R. & Baltimore, D. (1981).** Cloned poliovirus complementary DNA is infectious in mammalian cells. *Science* **214**, 916-919.

**Ran, Z. G., Chen, X. Y., Guo, X., Ge, X. N., Yoon, K. J. & Yang, H. C. (2008).** Recovery of viable porcine reproductive and respiratory syndrome virus from an infectious clone containing a partial deletion within the Nsp2-encoding region. *Arch Virol* **153**, 899-907.

**Randall, R. E. & Goodbourn, S. (2008).** Interferons and viruses: an interplay between induction, signalling, antiviral responses and virus countermeasures. *J Gen Virol* **89**, 1-47.

**Ropp, S. L., Wees, C. E., Fang, Y., Nelson, E. A., Rossow, K. D., Bien, M., Arndt, B., Preszler, S., Steen, P., Christopher-Hennings, J., Collins, J. E., Benfield, D. A. & Faaberg, K. S. (2004).** Characterization of emerging European-like porcine reproductive and respiratory syndrome virus isolates in the United States. *J Virol* **78**, 3684-3703.

**Sang, Y., Rowland, R. R. & Blecha, F. (2011).** Porcine type I interferons: polymorphic sequences and activity against PRRSV. *BMC Proc* **5 Suppl 4**, S8.

**Sang, Y., Shi, J., Sang, W., Rowland, R. R. & Blecha, F. (2012).** Replication-competent recombinant porcine reproductive and respiratory syndrome (PRRS) viruses expressing indicator proteins and antiviral cytokines. *Viruses* **4**, 102-116.

**Shehu-Xhilaga, M., Crowe, S. M. & Mak, J. (2001).** Maintenance of the Gag/Gag-Pol ratio is important for human immunodeficiency virus type 1 RNA dimerization and viral infectivity. *J Virol* **75**, 1834-1841.

**Snijder, E. J., Kikkert, M. & Fang, Y. (2013).** Arterivirus molecular biology and pathogenesis. *J Gen Virol* **94**, 2141-2163.

**Snijder, E. J. & Meulenberg, J. J. (1998).** The molecular biology of arteriviruses. *J Gen Virol* **79 ( Pt 5)**, 961-979.

**Snijder, E. J., van Tol, H., Pedersen, K. W., Raamsman, M. J. & de Vries, A. A. (1999).** Identification of a novel structural protein of arteriviruses. *J Virol* **73**, 6335-6345.

**Snijder, E. J., van Tol, H., Roos, N. & Pedersen, K. W. (2001).** Non-structural proteins 2 and 3 interact to modify host cell membranes during the formation of the arterivirus replication complex. *J Gen Virol* **82**, 985-994.

**Snijder, E. J., Wassenaar, A. L. & Spaan, W. J. (1994).** Proteolytic processing of the replicase ORF1a protein of equine arteritis virus. *J Virol* **68**, 5755-5764.

**Snijder, E. J., Wassenaar, A. L., Spaan, W. J. & Gorbalenya, A. E. (1995).** The arterivirus Nsp2 protease. An unusual cysteine protease with primary structure similarities to both papain-like and chymotrypsin-like proteases. *J Biol Chem* **270**, 16671-16676.

**Sola, I., Mateos-Gomez, P. A., Almazan, F., Zuniga, S. & Enjuanes, L. (2011).** RNA-RNA and RNA-protein interactions in coronavirus replication and transcription. *RNA Biol* **8**, 237-248.

**Song, C., Lu, R., Bienzle, D., Liu, H. C. & Yoo, D. (2009).** Interaction of the porcine reproductive and respiratory syndrome virus nucleocapsid protein with the inhibitor of MyoD family-a domain-containing protein. *Biol Chem* **390**, 215-223.

**Spilman, M. S., Welbon, C., Nelson, E. & Dokland, T. (2009).** Cryo-electron tomography of porcine reproductive and respiratory syndrome virus: organization of the nucleocapsid. *J Gen Virol* **90**, 527-535.

**Sulkowski, M. S. & Benhamou, Y. (2007).** Therapeutic issues in HIV/HCV-coinfected patients. *J Viral Hepat* **14**, 371-386.

**Sun, Y., Xue, F., Guo, Y., Ma, M., Hao, N., Zhang, X. C., Lou, Z., Li, X. & Rao, Z. (2009).** Crystal structure of porcine reproductive and respiratory syndrome virus leader protease Nsp1alpha. *J Virol* **83**, 10931-10940.

**Sun, Z., Chen, Z., Lawson, S. R. & Fang, Y. (2010a).** The cysteine protease domain of porcine reproductive and respiratory syndrome virus nonstructural protein 2 possesses deubiquitinating and interferon antagonism functions. *J Virol* **84**, 7832-7846.

**Sun, Z., Li, Y., Ransburgh, R., Snijder, E. J. & Fang, Y. (2012).** Nonstructural protein 2 of porcine reproductive and respiratory syndrome virus inhibits the antiviral function of interferon-stimulated gene 15. *J Virol* **86**, 3839-3850.

**Sun, Z., Liu, C., Tan, F., Gao, F., Liu, P., Qin, A. & Yuan, S. (2010b).** Identification of dispensable nucleotide sequence in 3' untranslated region of porcine reproductive and respiratory syndrome virus. *Virus Res* **154**, 38-47.

**Tian, D., Wei, Z., Zevenhoven-Dobbe, J. C., Liu, R., Tong, G., Snijder, E. J. & Yuan, S. (2012).** Arterivirus minor envelope proteins are a major determinant of viral tropism in cell culture. *J Virol* **86**, 3701-3712.

**Tian, K., Yu, X., Zhao, T., Feng, Y., Cao, Z., Wang, C., Hu, Y., Chen, X., Hu, D., Tian, X., Liu, D., Zhang, S., Deng, X., Ding, Y., Yang, L., Zhang, Y., Xiao, H., Qiao, M., Wang, B., Hou, L., Wang, X., Yang, X., Kang, L., Sun, M., Jin, P., Wang, S.,**

**Kitamura, Y., Yan, J. & Gao, G. F. (2007).** Emergence of fatal PRRSV variants: unparalleled outbreaks of atypical PRRS in China and molecular dissection of the unique hallmark. *PLoS One* **2**, e526.

**Tian, X., Lu, G., Gao, F., Peng, H., Feng, Y., Ma, G., Bartlam, M., Tian, K., Yan, J., Hilgenfeld, R. & Gao, G. F. (2009).** Structure and cleavage specificity of the chymotrypsin-like serine protease (3CLSP/nsp4) of Porcine Reproductive and Respiratory Syndrome Virus (PRRSV). *J Mol Biol* **392**, 977-993.

**Truong, H. M., Lu, Z., Kutish, G. F., Galeota, J., Osorio, F. A. & Pattnaik, A. K. (2004).** A highly pathogenic porcine reproductive and respiratory syndrome virus generated from an infectious cDNA clone retains the in vivo virulence and transmissibility properties of the parental virus. *Virology* **325**, 308-319.

**van Aken, D., Zevenhoven-Dobbe, J., Gorbalenya, A. E. & Snijder, E. J. (2006).** Proteolytic maturation of replicase polyprotein pp1a by the nsp4 main proteinase is essential for equine arteritis virus replication and includes internal cleavage of nsp7. *J Gen Virol* **87**, 3473-3482.

**Van Breedam, W., Delputte, P. L., Van Gorp, H., Misinzo, G., Vanderheijden, N., Duan, X. & Nauwynck, H. J. (2010a).** Porcine reproductive and respiratory syndrome virus entry into the porcine macrophage. *J Gen Virol* **91**, 1659-1667.

**Van Breedam, W., Van Gorp, H., Zhang, J. Q., Crocker, P. R., Delputte, P. L. & Nauwynck, H. J. (2010b).** The M/GP(5) glycoprotein complex of porcine reproductive and respiratory syndrome virus binds the sialoadhesin receptor in a sialic acid-dependent manner. *PLoS Pathog* **6**, e1000730.

**van Dinten, L. C., Wassenaar, A. L., Gorbalenya, A. E., Spaan, W. J. & Snijder, E. J. (1996).** Processing of the equine arteritis virus replicase ORF1b protein: identification of cleavage products containing the putative viral polymerase and helicase domains. *J Virol* **70**, 6625-6633.

**van Hemert, M. J., de Wilde, A. H., Gorbalenya, A. E. & Snijder, E. J. (2008).** The in vitro RNA synthesizing activity of the isolated arterivirus replication/transcription complex is dependent on a host factor. *J Biol Chem* **283**, 16525-16536.

**van Kasteren, P. B., Beugeling, C., Ninaber, D. K., Frias-Staheli, N., van Boheemen, S., Garcia-Sastre, A., Snijder, E. J. & Kikkert, M. (2012).** Arterivirus and nairovirus ovarian tumor domain-containing Deubiquitinases target activated RIG-I to control innate immune signaling. *J Virol* **86**, 773-785.

**van Oirschot, J. T., Kaashoek, M. J., Rijsewijk, F. A. & Stegeman, J. A. (1996).** The use of marker vaccines in eradication of herpesviruses. *J Biotechnol* **44**, 75-81.

**Walsh, E. P., Baron, M. D., Anderson, J. & Barrett, T. (2000a).** Development of a genetically marked recombinant rinderpest vaccine expressing green fluorescent protein. *J Gen Virol* **81**, 709-718.

**Walsh, E. P., Baron, M. D., Rennie, L. F., Monaghan, P., Anderson, J. & Barrett, T. (2000b).** Recombinant rinderpest vaccines expressing membrane-anchored proteins as

genetic markers: evidence of exclusion of marker protein from the virus envelope. *J Virol* **74**, 10165-10175.

**Wang, R., Nan, Y., Yu, Y. & Zhang, Y. J. (2013).** Porcine reproductive and respiratory syndrome virus Nsp1beta inhibits interferon-activated JAK/STAT signal transduction by inducing karyopherin-alpha1 degradation. *J Virol* **87**, 5219-5228.

**Wang, Y., Liang, Y., Han, J., Burkhart, K. M., Vaughn, E. M., Roof, M. B. & Faaberg, K. S. (2008).** Attenuation of porcine reproductive and respiratory syndrome virus strain MN184 using chimeric construction with vaccine sequence. *Virology* **371**, 418-429.

**Wassenaar, A. L., Spaan, W. J., Gorbalenya, A. E. & Snijder, E. J. (1997).** Alternative proteolytic processing of the arterivirus replicase ORF1a polyprotein: evidence that NSP2 acts as a cofactor for the NSP4 serine protease. *J Virol* **71**, 9313-9322.

**Welch, S. K. & Calvert, J. G. (2010).** A brief review of CD163 and its role in PRRSV infection. *Virus Res* **154**, 98-103.

**Wensvoort, G., Terpstra, C., Pol, J. M., ter Laak, E. A., Bloemraad, M., de Kluyver, E. P., Kragten, C., van Buiten, L., den Besten, A., Wagenaar, F. & et al. (1991).** Mystery swine disease in The Netherlands: the isolation of Lelystad virus. *Vet Q* **13**, 121-130.

**Wu, W. H., Fang, Y., Farwell, R., Steffen-Bien, M., Rowland, R. R., Christopher-Hennings, J. & Nelson, E. A. (2001).** A 10-kDa structural protein of porcine reproductive and respiratory syndrome virus encoded by ORF2b. *Virology* **287**, 183-191.

**Xiao, S., Mo, D., Wang, Q., Jia, J., Qin, L., Yu, X., Niu, Y., Zhao, X., Liu, X. & Chen, Y. (2010).** Aberrant host immune response induced by highly virulent PRRSV identified by digital gene expression tag profiling. *BMC Genomics* **11**, 544.

**Xu, Y. Z., Zhou, Y. J., Tong, W., Li, L., Jiang, Y. F. & Tong, G. Z. (2013).** [Study on using NSP2 protein of porcine reproductive and respiratory syndrome virus (HuN4-F112) to express E2 neutralizing epitope of classical swine fever virus]. *Bing Du Xue Bao* **29**, 17-25.

**Xu, Y. Z., Zhou, Y. J., Zhang, S. R., Jiang, Y. F., Tong, W., Yu, H. & Tong, G. Z. (2012).** Stable expression of foreign gene in nonessential region of nonstructural protein 2 (nsp2) of porcine reproductive and respiratory syndrome virus: applications for marker vaccine design. *Vet Microbiol* **159**, 1-10.

**Yu, D., Lv, J., Sun, Z., Zheng, H., Lu, J. & Yuan, S. (2009).** Reverse genetic manipulation of the overlapping coding regions for structural proteins of the type II porcine reproductive and respiratory syndrome virus. *Virology* **383**, 22-31.

**Yu, M. L., Huang, C. F., Dai, C. Y., Huang, J. F. & Chuang, W. L. (2007).** Long-term effects of interferon-based therapy for chronic hepatitis C. *Oncology* **72 Suppl 1**, 16-23.

**Zhang, S., Zhou, Y., Jiang, Y., Li, G., Yan, L., Yu, H. & Tong, G. (2011).** Generation of an infectious clone of HuN4-F112, an attenuated live vaccine strain of porcine reproductive and respiratory syndrome virus. *Virol J* **8**, 410.

**Zheng, H., Zhang, K., Zhu, X. Q., Liu, C., Lu, J., Gao, F., Zhou, Y., Lin, T., Li, L., Tong, G., Wei, Z. & Yuan, S. (2014).** Genetic manipulation of a transcription-regulating sequence of porcine reproductive and respiratory syndrome virus reveals key nucleotides determining its activity. *Arch Virol* **159**, 1927-1940.

**Zhou, L., Zhang, J., Zeng, J., Yin, S., Li, Y., Zheng, L., Guo, X., Ge, X. & Yang, H. (2009).** The 30-amino-acid deletion in the Nsp2 of highly pathogenic porcine reproductive and respiratory syndrome virus emerging in China is not related to its virulence. *J Virol* **83**, 5156-5167.

**Ziebuhr, J., Snijder, E. J. & Gorbalenya, A. E. (2000).** Virus-encoded proteinases and proteolytic processing in the Nidovirales. *J Gen Virol* **81**, 853-879.

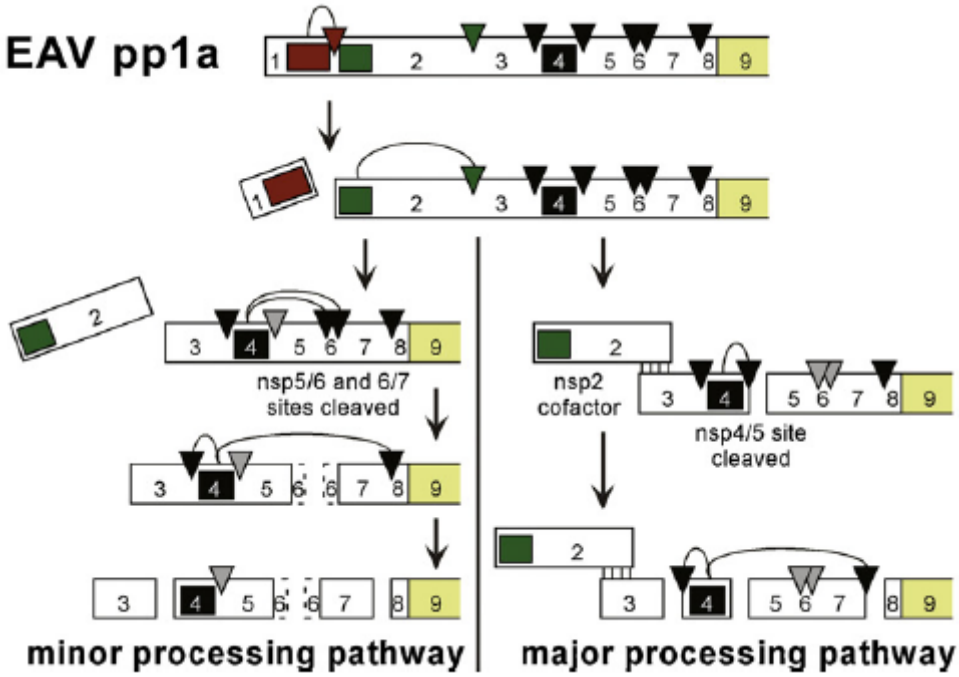


**Figure 1. 1 Model for alternative processing of the EAV nsp3–8 region in pp1a.** The interaction between cleaved nsp2 and nsp3-8 directs cleavage of the nsp4/5 site by the nsp4 SP (major pathway). Alternatively, instead of processing the nsp4/5 site, the nsp5/6 and 6/7 sites are cleaved in the absence of nsp2. Figure adapted from Fang & Snijder (2010).

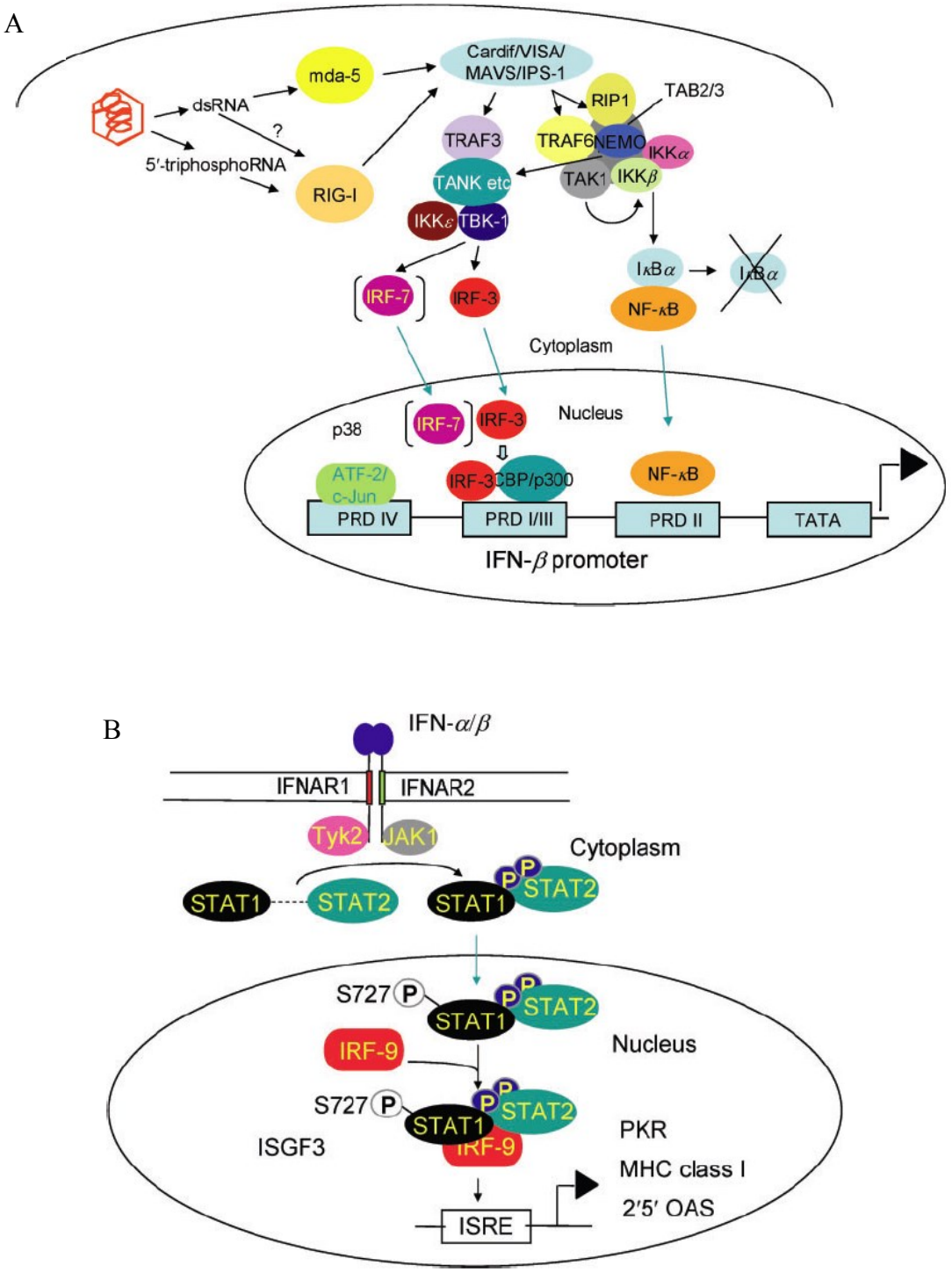


**Figure 1. 2 Type I interferon production and signaling pathways.** (A) mda-5- and RIG-I-dependent signalling. (B) Signalling pathway activated by IFN-α/β. Figures adapted from Randall & Goodbourn (2008).

**Table 1. 1** PRRSV proteins and their (potential) functions.

| name | Coding region | | Known or predicted functions[2] |
|---|---|---|---|
| | Type 1 PRRSV | Type 2 PRRSV | |
| Nonstructural proteins encoded by ORF1a and ORF1b[1] | | | |
| nsp1α | 1-? | 1-180 | zinc finger-protein; accessory protease PCPα; regulator of sg mRNA synthesis; potential IFN antagonist |
| nsp1β | ?-385 | 181-383 | accessory protease PCPβ; potential IFN antagonist |
| nsp2 | 386-1446 | 384-1579 | accessory protease CP; deubiquitinating (DUB) enzyme (OTU class); potential IFN antagonist; transmembrane protein, involved in membrane modification |
| nsp3 | 1447-1677 | 1580-1809 | transmembrane protein, involved in membrane modification |
| nsp4 | 1678-1879 | 1810-2013 | main protease SP; induce apoptosis; potential IFN antagonist |
| nsp5 | 1880-2049 | 2014-2183 | transmembrane protein, possibly involved in membrane modification |
| nsp6 | 2050-2065 | 2184-2199 | Unknown |
| nsp7α | 2066-2214 | 2200-2348 | Unknown |
| nsp7β | 2215-2334 | 2349-2458 | Unknown |
| nsp8 | 2335-2379 | 2459-2503 | Unknown |
| nsp9 | 2335-3019 | 2459-3143 | RNA-dependent RNA polymerase |
| nsp10 | 3020-3461 | 3144-3584 | NTPase; RNA helicase; contains putative zinc-binding domain |
| nsp11 | 3462-3685 | 3585-3807 | endoribonuclease (NendoU); arrest cell cycle |
| nsp12 | 3686-3837 | 3808-3960 | Unknown |
| Newly identified viral proteins[3] | | | |
| nsp2TF | 1371-3518, 3517-4023 | 1340-3889, 3888-4394 | Potential deubiquitinating (DUB) enzyme (OTU class); potential IFN antagonist |
| nsp2N | 1371-3518 | 1340-3889 | Potential deubiquitinating (DUB) enzyme (OTU class); potential IFN antagonist |

| Structural proteins[3] | | | |
|---|---|---|---|
| GP2 | 11745-12494 | 12074-12844 | Form GP2/GP3/GP4 complex; virus entry |
| E | 11750-11962 | 12079-12300 | Ion channel; play a role in processing of GP2/3/4 |
| GP3 | 12353-13150 | 12697-13461 | Form GP2/GP3/GP4 complex; virus entry |
| GP4 | 12895-13446 | 13242-13778 | Form GP2/GP3/GP4 complex; induce neutralizing antibody; virus entry |
| GP5 | 13443-14048 | 13789-14391 | Major structural protein; form GP5/M dimer; induce neutralizing antibody; reduce the capacity of antibodies to neutralize PRRSV by "glycan shielding"; drive force for virus assembly and budding |
| ORF5a | 13448-13579 | 13779-13934 | unknown |
| M | 14036-14557 | 14376-14900 | Major structural protein; form GP5/M dimer; drive force for virus assembly and budding |
| N | 14547-14933 | 14890-15261 | Genome package; potential IFN antagonist |

[1] Amino acid numbers refer to the pp1ab sequence of Type I PRRSV strain SD01-08 (GenBank accession # DQ489311) or Type II PRRSV strain SD95-21 (GenBank accession # KC469618).

[2] PCP: Papain-like cysteine proteine protease; CP: cysteine protease; SP: serine protease.

[3] Nucleotide numbers refer to the genomic sequence of Type I PRRSV strain SD01-08 (GenBank accession # DQ489311) or Type II PRRSV strain SD95-21 (GenBank accession # KC469618).

# Chapter 2 - Identification of Porcine Reproductive and Respiratory Syndrome Virus ORF1a-Encoded Nonstructural Proteins in Virus-Infected Cells

**Abstract:** The porcine reproductive and respiratory syndrome virus (PRRSV) replicase gene consists of two large open reading frames, ORF1a and ORF1b, of which the latter is expressed by ribosomal frameshifting. The ORF1a-encoded part of the resulting replicase polyproteins (pp1a and pp1ab) is predicted to be proteolytically processed into ten nonstructural proteins (nsps), known as nsp1 to nsp8, with both the nsp1 and nsp7 regions being cleaved internally (yielding nsp1α plus nsp1β, and nsp7α plus nsp7β). The experimental verification of these predictions strongly depends on the ability to identify individual cleavage products with specific antibodies. In this study, a panel of monoclonal and polyclonal antibodies was generated, which together can recognize eight ORF1a-encoded PRRSV nsps. Using these reagents, replicase cleavage products were detected in PRRSV-infected MARC-145 cells using a variety of immunoassays. By immunofluorescence microscopy, most nsps could be detected as early as 7 hours post-infection. During the early stages of infection, nsp1β, nsp2, nsp4, nsp7α, nsp7β and nsp8 co-localized in distinct punctate foci in the perinuclear region of the cell, which were determined to be the site of viral RNA synthesis by *in situ* labeling. Western blot and immunoprecipitation analysis identified most individual nsps and several long-lived processing intermediates (nsp3-4, nsp5-7, nsp5-8, nsp3-8). The identification and subcellular localization of PRRSV nsps in virus-infected cells documented here provides a basis for the further structure-function studies. Thus, our PRRSV antibody panel will be an important tool for future studies on the replication and pathogenesis of this major swine pathogen.

## 2.1 Introduction

PRRS, a disease first described in the US in 1987 (Keffaber, 1989) and in Europe in 1991 (Wensvoort *et al*., 1991), has caused tremendous economic losses to the swine industry since its appearance, with recent annual costs estimated to be at least $600 million in the US alone (Neumann *et al*., 2005). Hallmark symptoms of PRRS are mild to severe respiratory disease in infected newborn and growing pigs, and reproductive failure in pregnant sows. The etiological agent, PRRSV, was first identified in the Netherlands in 1991, and is represented by the European prototypic strain, Lelystad virus (LV) (Wensvoort *et al*., 1991). In the US, PRRSV was first isolated in 1992, and the North American prototypic strain was designated as VR-2332 (Benfield *et al*., 1992; Collins *et al*., 1992). At the genome level, these two genotypes, European (Type I) and North American (Type II), share about 60% sequence identity (Allende *et al*., 1999; Nelsen *et al*., 1999). PRRSV is classified in the family *Arteriviridae*, which also includes equine arteritis virus (EAV), lactate dehydrogenase-elevating virus (LDV), and simian hemorrhagic fever virus (SHFV) (Snijder & Meulenberg, 1998).

PRRSV is a small, enveloped virus containing a single positive-stranded RNA genome. The genome is about 15 kb in length and contains at least ten open reading frames. The 3'– terminal quarter of the genome encodes structural proteins, including four envelope glycoproteins (GP2a, GP3, GP4, and GP5), three nonglycosylated membrane proteins (2b, ORF5a and M) and the nucleocapsid protein (N) (Meulenberg *et al*., 1995a; Meulenberg *et al*., 1995b; Mounir *et al*., 1995; Bautista *et al*., 1996; Mardassi *et al*., 1996; Meng *et al*., 1996; Meulenberg & Petersen-den Besten, 1996; Snijder *et al*., 1999; Wu *et al*., 2001; Firth *et al*., 2011; Johnson *et al*., 2011). The PRRSV replicase gene consists of open reading frames (ORFs) 1a and 1b, which occupy the 5'-proximal three quarters of the genome. Both these ORFs are expressed from the viral genome, with expression of ORF1b depending on a conserved ribosomal frameshifting mechanism. Subsequently, extensive proteolytic processing of the resulting pp1a and pp1ab polyproteins yields the functional nonstructural

proteins (nsps), most of which assemble into a membrane-associated replication and transcription complex. This enzyme complex not only mediates genome replication but also controls the synthesis of a nested set of subgenomic (sg) mRNAs for expression of the structural protein genes (Snijder *et al*., 1994; van Dinten *et al*., 1996; van der Meer *et al*., 1998; Ziebuhr *et al*., 2000; Fang & Snijder, 2011).

The proteolytic maturation of the arterivirus pp1a and pp1ab replicase polyproteins has been studied in detail only for EAV, the family prototype. A complex proteolytic cascade was uncovered, involving three of ORF1a-encoded proteases, at least 11 cleavage events (Snijder *et al*., 1992; Snijder *et al*., 1995; Ziebuhr *et al*., 2000), and alternative processing pathways (Wassenaar *et al*., 1997). Although, based on sequence comparison, many of these features appear to be conserved in other arteriviruses, a number of striking differences complicate a straightforward comparison (Fig. 2.1). First of all, the currently known arteriviruses are only distantly related. For example, the overall sequence identity in the pp1ab replicase polyproteins of EAV and PRRSV is about 30-45% amino acids (aa) identity, depending on the genome region and specific strains analyzed (Nelsen *et al*., 1999). Secondly, there are considerable size differences, in particular in the N-terminal region of ORF1a, leading to a pp1a of only 1727 aa in EAV, whereas the PRRSV counterpart can be up to ~2500 aa long. Finally, an additional protease domain is known to be functional in the case of PRRSV, and likely all other arteriviruses, which has lost its proteolytic activity in the case of EAV (den Boon *et al*., 1995). Thus, the PRRSV polyproteins are assumed to be cleaved by three papain-like proteases (PLPα, PLPβ, and PLP2) located in the nsp1-nsp2 region, and the viral main protease, a serine protease (SP) residing in the nsp4. A comparison with the EAV sequence and data would suggest that the PRRSV replicase polyproteins are being cleaved into at least 14 nsps, specifically nsp1 to nsp12, with both the nsp1 and nsp7 parts being subject to an internal cleavage (yielding nsp1α plus nsp1β, and nsp7α plus nsp7β). Although nsp1α and nsp1β were previously detected in PRRSV-infected cells (Chen *et al*., 2010), a comprehensive analysis of the processing steps and products in PRRSV replicase maturation

clearly depends on the availability of specific antibodies that can recognize individual cleavage products in a variety of immunoassays. Since the identification of PRRSV more than 20 years ago, and despite the importance of the virus as a veterinary pathogen, such a panel of reagents has not been described so far. Therefore, as a first and essential step toward understanding the structure and function of PRRSV nsps, we have now generated a panel of antibodies against the PRRSV ORF1a-encoded nsps, and have used it to detect the expression of these proteins and analyze their subcellular localization in virus-infected cells.

## 2.2 Materials and methods

**Cells and Viruses:** Embryonic monkey kidney cells (MARC-145) were maintained in appropriate medium and incubation conditions as previously described (Kim et al., 1993). The Type 1 PRRSV strain SD01-08 (GenBank Accession #DQ489311; Fang *et al*., 2006a) was propagated in MARC-145 cells.

**Antigen expression:** Recombinant proteins, including nsp1 (α plus β together), nsp2, nsp4, nsp7 and nsp8, were generated based on the sequence of the PRRSV SD01-08 strain. For nsp2 antigen expression, the conserved PLP2 domain region was expressed as a recombinant protein. The antigens for production of antibodies to nsp1, nsp4, nsp7, and nsp8 were expressed as recombinant proteins based on the predicted cleavage sites (Table 1). These nsp-coding regions were amplified by RT-PCR, and the PCR products were cloned into the pET-28a (+) vector (Novagen). Recombinant proteins were expressed and purified as described previously (Johnson et al., 2007; Brown et al., 2009). Sequence analysis (Hopp-Wood hydrophilicity) showed that nsp3 and nsp5 contain mostly hydrophobic regions, but include several predicted B-cell linear epitopes. Therefore, instead of expressing the entire nsp3 and nsp5 regions as recombinant proteins, predicted B-cell linear epitope regions were synthesized as synthetic peptides for mouse immunization. The predicted nsp6 subunit, consisting of only 11 amino acids, was also synthesized. A rabbit antiserum recognizing both nsp2 and nsp3 was raised previously (Kroeze *et al*., 2008) using synthetic peptides. These

were based on the sequences of the PRRSV type-I Lelystad isolate, with the N-terminal nsp2 peptide containing four point mutations compared to SD01-08 and the nsp3 C-terminal peptide being identical for both isolates.

**Antibody production**: Monoclonal antibodies (mAb) were produced by immunizing BALB/c mice with 50 ug of antigen mixed with Freund's incomplete adjuvant at two-week intervals for eight weeks. Mouse splenocytes were fused with NS-1 myeloma cells. Specific anti-PRRSV mAbs were screened by enzyme-linked immunosorbent assay (ELISA) and indirect immunofluorescent assays (IFA) as described previously (Fang *et al*., 2006a). Hybridomas secreting PRRSV-specific mAbs were sub-cloned. The mAbs were produced by intraperitoneal injection of pristine-primed mice with hybridoma cells ($5x10^4$ cells), and the mAb-containing mouse ascites fluids were collected about 2 weeks after injection. MAbs were isotyped using an IsoStrip Kit (Serotech, Inc.) following the manufacture's instruction. Polyclonal antibodies (pAb) were raised in New Zealand white rabbits. For primary immunizations, 100 ug of antigen was mixed with an equal volume of Freund's incomplete adjuvant, and injected subcutaneously at six different locations. Rabbits were boosted twice at two-week intervals. The immune response was monitored using IFA and ELISA.

**Expression plasmids and transfection**: The nsp4-, nsp7-, nsp7α-, and nsp7β-coding regions of the SD01-08 virus were RT-PCR amplified from genomic RNA, and PCR products were cloned into eukaryotic expression vector, pCAGGS (a generous gift from Dr. AdolfoGarcia-Sastre), designated as pCAGGS-nsp4, pCAGGS-nsp7, pCAGGS-nsp7α, and pCAGGS-nsp7β. HEK293T cells were seeded in 24-well plates and were co-transfected with pCAGGS-nsp4 and pCAGGS-nsp7 DNA, or transfected with individual pCAGGS-nsp4, pCAGGS-nsp7, pCAGGS-nsp7α, or pCAGGS-nsp7β expression plasmids. Transfection was performed using HD-FuGENE 6 transfection reagent following the manufacturer's instruction (Roche Molecular Biochemicals). At 24 hours post-transfection, cells were fixed with 80% acetone for immunofluorescence microscopy. For Western blot detection of nsp expression, transfected cells were harvested and lysed in Laemmli sample buffer (Laemmli, 1970).

**Immunofluorescence microscopy**: For detection of nsp expression, MARC-145 cells were infected with 0.1 MOI of PRRSV, and cells were fixed with 3.7% formaldehyde in PBS (pH 7.4) at 6, 7, 8, 10, and 12 h post-infection. Following permeabilization with 0.1% - 0.2% Triton X-100 in PBS for 15 min at room temperature, cells were incubated with nsp-specific mAbs or polyclonal rabbit antisera at dilutions of 1:1000 or 1:200, respectively for 1h. Subsequently, FITC-conjugated goat anti-mouse IgG (ICN Biomedicals) or FITC-conjugated goat anti-rabbit IgG (Invitrogen) were used as secondary antibody. For nsp co-localization studies, polyclonal rabbit antiserum pAb Eu-nsp2 was used to stain nsp2, and DyLight 549-labeled goat anti-rabbit IgG (H+L) (KPL, red fluorescent) was used as the secondary antibody. The same infected cell was dual stained with mAbs against nsp1β, nsp4, nsp7α, nsp7β, or nsp8 as indicated in Figure 2.2, and FITC-conjugated goat anti-mouse antibody (ICN Biomedicals) was added as the secondary antibody. Nuclear staining with DAPI (4', 6'-diamino-2-phenylindole 2HCl) was performed as recommended by the manufacturer (Molecular Probes). Specimens were imaged using a Zeiss LSM510 confocal microscope with a 63x objective, and images were processed with NIH Image/J and Adobe Photoshop 6.0 software.

**BrUTP labeling of viral RNA synthesis:** Metabolic labeling of viral RNA synthesis with 5-bromouridine 5'-triphosphate (BrUTP, Sigma) was performed as described previously (van der Meer *et al*., 1998). Briefly, the newly synthesized viral RNA in PRRSV-infected MARC-145 cell was labeled at 9 h post-infection and 30 min before labeling cells were given 10 ug/ml of actinomycin D (Sigma) to block host cell transcription. BrUTP was introduced into the cells by liposome-mediated transfection using X-tremeGENE 9 (Roche) following the manufacturer's instructions. Viral RNA synthesis was labeled for 1 h, after which cells were fixed with 3.7% formaldehyde for 15 min at room temperature and blocked with 0.1% - 0.2% Triton X-100 and 3% BSA in PBS for 15 min at room temperature. BrUTP-labeled viral RNA was visualized using anti-BrdU mAb clone BU-33 (Sigma) and DyLight 549 labeled goat anti-rabbit IgG (H+L) (KPL) as secondary antibody. Cells were also stained for nsp2

using the polyclonal rabbit antiserum and a goat anti-rabbit FITC-conjugate (ICN Biomedicals, Inc).

**Western Blotting**: PRRSV-infected MARC-145 cell lysates were heated in Laemmli sample buffer for 10 min and proteins were separated by SDS-PAGE. Protein bands were blotted onto a nitrocellulose membrane as described previously (Wu *et al*., 2001). After blotting, membranes were blocked with PBST and 5% nonfat dry milk. The membranes were then incubated with nsp-specific antibodies (1:500 dilution of mAbs and 1:50 dilution of rabbit antisera) for 1h at RT. After washing with PBST, HRP-conjugated goat anti-mouse or HRP-conjugated goat anti-rabbit antibodies were added and samples were incubated for 45 minutes. Protein bands were visualized using a chemiluminescence detection kit (Pierce) following the manufacturer's instructions.

**Radioimmunoprecipitation and SDS-PAGE:** MARC-145 cells were infected with MOI 5 of PRRSV SD01-08 for 24 hours in DMEM containing 2% fetal calf serum. Cells were washed with PBS, followed by starvation for 30 minutes in methione- and cysteine-free medium. Subsequently, protein synthesis in the infected cells was metabolically labeled for 6 hours in methionine- and cysteine-free medium containing 200 µCi/ml of a [$^{35}$S] methionine/cysteine mixture. After labeling, cells were harvested in lysis buffer (20mM Tris-HCl pH 7.6, 150 mM NaCl, 1% NP-40, 0.1% DOC, 0.1%SDS) and nuclei were removed by centrifugation. Routinely, 5 µl of mouse ascites or rabbit antiserum was used for the immunoprecipitation analysis of a 200-µl aliquot of cell lysate, the equivalent of 4x10$^5$ cells. Binding was carried out overnight at 4°C in lysis buffer containing 0.1-0.5 % SDS, depending on the antibody used. Subsequently, immune complexes were pulled down using a 1:1 mixture of protein A- and protein G-sepharose beads (GE Healthcare). Beads were washed three times in NET buffer (50 mM Tris-HCL, 150 mM NaCl, 5mM EDTA, 0.5% NP-40) before complexes were dissolved in Laemmli sample buffer. Prior to loading onto 12% polyacrylamide gels, samples were heated at 96°C for 6 min. Gels were exposed to phosphor imager screens, which were subsequently scanned using a Typhoon Variable Mode Imager

(GE Healthcare). Image analysis and quantification of band intensities were performed with the ImageQuant TL software (GE Healthcare).

## 2.3 Results

**Generation of antibodies to ORF1a-encoded replicase subunits**

Based on comparative sequence analysis and the established EAV replicase cleavage sites, the predicted cleavage sites for PRRSV replicase polyprotein processing had been inferred previously (Ziebuhr *et al*., 2000; Fang & Snijder, 2011). In this study, these putative cleavage sites were used as borders for cloning and expression in *E. coli* of sequences representing individual PRRSV replicase subunits (nsp1, nsp2, nsp4, nsp7, and nsp8) or synthesis of peptide antigens (nsp2, nsp3, nsp5, and nsp6) for production of nsp-specific antibodies (Table 1). Previous studies had identified the nsp1α/1β and nsp1β/2 cleavage sites of type II PRRSV (Chen *et al*., 2010; Sun *et al*., 2010). Based on sequence comparison, amino acids 1-180 of pp1a of type 1 PRRSV SD01-08 was expressed as recombinant protein for production of an nsp1α-specific antibody. Mice were immunized with individual recombinant proteins or synthetic peptides. After mouse splenocytes had been fused with NS-1 myeloma cells, the supernatants of the resulting hybridoma cell lines were initially screened by Enzyme-linked immunosorbent assay (ELISA) and immunofluorescence assay (IFA), and further analyzed by Western blot as described in the following paragraph.

Mice immunized with nsp1 produced a strong antibody response to nsp1β. All of the mAbs obtained from the mice immunized with nsp1 recognized nsp1β. Additionally, we obtained mAbs against nsp2, nsp4, nsp7, and nsp8, but not for nsp1α, nsp3, nsp5, and nsp6. The isotypes of the various mAbs are listed in Table 1. To facilitate dual labeling experiments, we immunized rabbits with recombinant proteins representing nsp1α or nsp2, or a combination of synthetic peptides derived from the nsp2 N-terminus and the nsp3 C-terminus (Table 1), and obtained a set of rabbit polyclonal antisera (pAb).

Immunofluorescence microscopy was performed on cells infected with either strain SD01-08 (genotype I virus) or strain VR2332 (genotype II virus), which revealed that this panel of mAbs is highly genotype-specific since cross-reactivity between our type I-specific mAbs and type II virus-infected cells was not observed. The pAb against nsp1α was also genotype specific, but the Eu-nsp2 and nsp2+3 pAbs generated with type I-specific antigens also reacted with type II virus (data not shown).

**Monoclonal antibody reactivity to nsp7α and nsp7β**

In EAV, the nsp7 subunit was previously found to contain an internal cleavage site (van Aken *et al*., 2006), which is used with a relatively low efficiency by the nsp4 SP to generate nsp7α and nsp7β subunits. Sequence alignment showed that this cleavage site is conserved in PRRSV nsp7 ($E_{2214}/N_{2215}$). To determine which part of nsp7 was recognized by the anti-nsp7 mAbs that we obtained (Table1: mAb Eu9-31/Eu24-40), nsp7, nsp7α, and nsp7β were expressed from CMV promoter constructs (vector pCAGGS) and a similar construct was used to co-express nsp4. Initially, HEK 293T cells were transfected with pCAGGS-nsp7α or pCAGGS-nsp7β, and IFA was performed using mAb Eu9-31 or Eu24-40. The result showed that mAb Eu9-31 recognized nsp7α, while mAb Eu24-40 recognized nsp7β (Figure 2A). To further confirm that PRRSV nsp7 can actually be cleaved into α and β subunits, nsp7 and nsp4 were co-expressed in HEK 293T cells and the nsp7 processing was analyzed by Western blot. As shown in Figure 2B, nsp7 was detected as a single ~30 kDa protein in lysates from cells transfected with pCAGGS-nsp7 only. In contrast, in cells co-transfected with pCAGGS-nsp7 and pCAGGS-nsp4 the level of nsp7 was much lower than in cells transfected with pCAGGS-nsp7 only, and both nsp7 and nsp7α were detected by mAb Eu9-31, demonstrating that nsp7 was indeed cleaved by nsp4. In three independent experiments, mAb Eu24-40 appeared not to react with nsp7β in the Western blot, but it did recognize the full length nsp7 (Fig. 2.2B). In our previous studies (Brown et al., 2009; Langenhorst et al., 2012), we noted that recombinant nsp7β was sensitive to degradation after purification from E. *coli*. This observation may relate to the result of the current study, as

most of the cleaved nsp7β could be rapidly degraded during sample preparation for Western blot analysis, and/or our detection method may not have been sensitive enough to detect the remaining part of nsp7β if it were present.

**Identification of ORF1a-encoded replicase proteins in virus-infected cells by Western blot and radioimmunoprecipitation**

To investigate the expression and processing of the 2379 amino acids encoded by PRRSV SD01-08 ORF1a, we used the panel of antibodies raised against nsps 1-8 of the SD01-08 virus in Western blot and radioimmunoprecipitation (RIP) analysis. Rabbit preimmunization sera, mouse ascites containing non-PRRSV specific mAb, and uninfected cell lysates were used as negative controls.

In Western blot, the pAb Eu-nsp1α detected a single protein band just below the 22-kDa molecular marker, which corresponded to the predicted size of nsp1α (18.9 kDa, Fig. 2.3A), while mAb Eu22-28 detected a strong protein band above the 22 kDa molecular marker, corresponding to the predicted size of nsp1β (25.1 kDa, Fig. 2.3B). These two proteins, nsp1α and nsp1β were also consistently detected in radioimmunoprecipitation (RIP) experiments (Fig. 2.4A and 2.4B).

The mAb against nsp2 (EU36-19) generated a strong background signal in the Western blot analysis (data not shown), but in RIP this mAb brought down a specific protein band migrating substantially slower than the 98-kDa molecular weight marker (Fig. 2.4C). Several additional weak protein bands were detected in the nsp2 RIP, but it remains to be established whether these represent nsp2-related processing or degradation products.

Rabbit antiserum pAb-nsp2+3 was raised using a combination of nsp2 and nsp3 epitopes (Table 1) and in Western blot analysis indeed both a specific protein of about 22 kDa (nsp3) and a large protein in the size range predicted for nsp2 were detected (Fig. 2.3C). However, in immunoprecipitation analysis of infected cell lysates pAb-nsp2+3 mainly recognized nsp3 (Fig. 2.4D). The apparent size of the presumed nsp2 subunit detected in both

Western blot and RIP appeared to be larger than the predicted size (114 kDa), but this may be due to aberrant migration of this product, which contains a sizeable hydrophobic domain. MAb Eu54-19 against nsp4, the viral main protease, detected a distinct protein band around 24 kDa in both Western blot (Fig. 2.3D) and RIP (Fig. 2.4E). In the case of EAV, nsp3-4 and nsp3-8 were observed as relatively long-lived intermediate cleavage products (Snijder *et al*., 1994). The predicted sizes of the PRRSV counterparts of these products are 46 kDa (nsp3-4) and 100 kDa (nsp3-8), and in RIP analysis, products nicely matching these sizes were specifically recognized by mAb Eu54-19 (Fig. 2.4E). This observation suggests important parallels between the two arteriviruses with regard to the sequence and timing of replicase processing events.

In virus-infected cell lysates, the nsp7α-specific mAb Eu9-31 recognized a doublet just above the 46-kDa size marker (Fig. 2.3E), which appeared to match the calculated sizes of the prominent nsp5-7 (49.7 kDa) and nsp5-8 (54.7 kDa) processing intermediates observed in the EAV system (Snijder *et al*., 1994; Wassenaar *et al*., 1997). In addition, a ~15-kDa product was observed that likely corresponded to nsp7α (see also Fig. 2.2B). The identification of nsp5-7 and nsp5-8 was further supported by the fact that only the upper of the two bands was recognized by the nsp8-specific antibody Eu12-40 (Figure 3F). Nsp8 is the last subunit upstream of the ribosomal frameshift site and is identical to the N-terminal domain of the RdRp-containing nsp9 subunit, of which the N-terminus is released by cleavage of the nsp7/8 site. On Western blot, we noticed a weak protein band around 85 kDa, which is the predicted size of nsp9 (Fig. 2.3F), but further studies are needed to confirm the identity of this product.

The antibody against nsp7β (mAb Eu24-40) did not specifically recognize any PRRSV proteins in Western blot (data not shown), which was consistent with the result obtained in the eukaryotic expression system (Fig. 2.2B). However, upon its use in RIP, this antibody did bring down the presumed nsp5-7 and nsp5-8 bands (Fig. 2.4F). Also the nsp8-specific mAb Eu24-40 brought down the same doublet (Fig. 2.4G), which must be explained

by co-immunoprecipitation of the two products under these conditions, since nsp5-7 should not be recognized by this antibody and only the nsp5-8 band was recognized in Western blot (Fig. 2.3F). The nsp8-specific RIP also revealed a very small product that may correspond to fully cleaved nsp8 (predicted size about 5 kDa). Finally, the RIP experiments targeting nsp4, nsp7, and nsp8 revealed a number of larger precursors, including nsp3-8 (Fig. 2.4E-G).

**Intracellular localization of PRRSV ORF1a replicase proteins**

Previous immunofluorescence microscopy studies of EAV- infected cells showed that replicase processing products assemble in the perinuclear region where they form a membrane-associated complex that is thought to direct viral replication and transcription (van der Meer *et al*., 1998). We now employed our newly obtained antibody panel to study whether PRRSV nsps behave similarly and to visualize the site of viral RNA synthesis.

To investigate the intracellular localization of PRRSV ORF1a-encoded replicase subunits, the panel of antibodies was used in immunofluorescence microscopy of infected cells. To assess the timing of replicase expression, PRRSV-infected MARC-145 cells were fixed at 6, 7, 8, 10, and 12 hours post infection (hpi) and stained with various antibodies. No nsp-specific labeling was detected at 6 hpi, but by 7 hpi all PRRSV-infected MARC-145 cells could be stained with anti-nsp1β, anti-nsp2, anti-nsp4, anti-nsp7α, nsp7β, and anti-nsp8 antibody, revealing small but bright fluorescent foci that were mostly concentrated on one side of the nucleus. By 12 hpi, a more intense and diffuse labeling pattern was observed. For nsp1β, a predominantly nuclear and perinuclear staining pattern was observed in about 80% of the cells, both at 10 and 12 hpi (Fig. 2.5). The pAb directed against nsp1α (Eu-nsp1α) could not be used in IFA since it produced a high background signal. To verify colocalization of the different nsps, PRRSV-infected MARC-145 cells were double stained with anti-nsp mAbs and a rabbit antiserum to nsp2. At 7 hpi, the labeling for nsp1β, nsp4, nsp7α, nsp7β and nsp8 was largely co-localized with nsp2 in punctate and perinuclear spots (Fig. 2.6), although some additional nsp2 labeling was commonly found in the periphery of the cell. Furthermore, as described previously, part of nsp1β localized to the nucleus.

In EAV- infected cells viral RNA synthesis was previously found to be associated with the nsp-containing membrane structures in the perinuclear region (van der Meer *et al*., 1998; Pedersen *et al*., 1999). To determine if the perinuclear foci that labeled for PRRSV nsps were indeed the site of viral RNA synthesis, we treated infected cells with actinomycin D to block host cell mRNA synthesis, and transfected them with BrUTP to label the newly synthesized viral RNA for 1 hour. Transfected cells were double stained with antibodies that recognize BrU-labeled RNA and PRRSV nsp2. The result showed co-localization of PRRSV nsp2 with *de novo*-synthesized viral RNA (Fig. 2.7). Overall, these data supported the findings of previous studies on EAV (van der Meer *et al*., 1998), and suggested that also PRRSV nsps assemble into a membrane-bound replication and transcription complex.

## 2.4 Discussion

Since the first isolation of PRRSV, a wealth of information has been obtained on the structural proteins of this pathogen. However, little is known about the structure and function of PRRSV nsps, whose coding sequence occupies ~ 75% of the viral genome (Snijder & Meulenberg, 1998; Fang & Snijder, 2010). Thus far, the existence of individual PRRSV nsps and their involvement in genome replication and expression were mainly deduced from studies of EAV. As underlined by these EAV studies, specific antisera are key reagents in studies on nsp structure and function. Although previous PRRSV studies yielded a large panel of mAbs against structural proteins (Nelson *et al*., 1993; Drew *et al*., 1995; Yoon *et al*., 1995; Dea *et al*., 1996; Magar *et al*., 1997; Yang *et al*., 1999; Yang *et al*., 2000), few mAbs were raised against nsps. This study is the first to describe the development of a panel of antibodies against PRRSV ORF1a-encoded-nsps and its use to detect these proteins in PRRSV-infected cells.

For nsp1, we detected two products, nsp1α and 1β, in PRRSV-infected cells, in contrast to one mature nsp1 product from EAV. PRRSV nsp1β showed two different intracellular localization patterns, an early punctate perinuclear localization and a

predominantly nuclear labeling late in infection. Since our anti-nsp1α antiserum did not specifically recognize nsp1α of Type I PRRSV in IFA, its intracellular localization could not be determined. However, our previous study using Type II PRRSV demonstrated that nsp1α also localizes to the nucleus during the course of infection (Chen *et al*., 2010), and similar observations were made for EAV nsp1. This protein was also found to interact with the host protein p100, a transcriptional co-activator, suggesting that nsp1 might modulate transcription in the infected cell (Tijms & Snijder, 2003). Recent studies demonstrated that PRRSV nsp1α and nsp1β are likely involved in modulating the interferon response; in particular, the nuclear localization of PRRSV nsp1 was determined to be associated with the degradation of interferon transcription factor CREB-binding protein (Kim *et al*., 2010). These studies suggest that arterivirus nsp1 proteins not only function in viral replication, but also play an important role in host metabolism and immune modulation.

Comparative sequence analysis showed that the PRRSV nsp2 was predicted to be cleaved at $_{385}$G/A$_{386}$ of SD01-08 at its N-terminus. The C-terminal cleavage site is most likely located at $_{1446}$G/A$_{1447,}$ one amino acid downstream from the previously predicted site at $_{1445}$G/G$_{1446}$ (Ziebuhr *et al*., 2000), since the nsp2-encoded cysteine protease is now known to have a preference to cleave after GG instead of between GG (Frias-Staheli *et al*., 2007). The predicted size for nsp2 (replicase residues 386-1446 of SD01-08) is 114 kDa. However, in our analysis, the nsp2-specific antibody recognized a product with a considerably larger apparent molecular weight. Whether this is caused by aberrant migration or post-translational modifications could not be resolved in this study. In addition, several smaller and less abundant products were also detected by nsp2-specific antibodies in terms of RIP experiments. A similar phenomenon was also observed in nsp2 immunoprecipitation experiments using Type II PRRSV, VR2332 (Han *et al*., 2010). At this time, we cannot exclude the possibility of the existence of other nsp2-related processing or degradation products. Furthermore, we also cannot exclude the involvement of host cell proteases that could generate smaller nsp2-related products. In EAV, the 61-kDa nsp2 was found to be

cleaved internally by a host cell-specific protease, yielding 18 kDa and 44 kDa cleavage products in Vero cells, but not in BHK-21 and RK-13 cells (Snijder *et al*., 2001). Identification of other smaller protein products is in progress in our laboratories.

Protein sequence analysis showed that nsp3 and nsp5 are largely composed of hydrophobic domains as in other arteriviruses. The generally hydrophobic nature of these proteins is a likely explanation for our failure to generate specific mAbs against these replicase subunits. Nsp6 is predicted to consist of only 11 amino acids, but this peptide seemed to be poorly immunogenic and we could not generate the antibodies by immunizing mice with an nsp6 synthetic peptide.

Based on the EAV replicase processing model of major versus minor proteolytic processing pathways (Wassenaar *et al*., 1997), nsp5 and nsp5-6 may not be produced at all since cleavage of the nsp4/5 site seems to prevent cleavage of the nsp5/6 and nsp6/7 sites and vice versa. Consequently, nsp5 and nsp6 were only detected in the form of processing intermediates with other nsps. Using the PRRSV nsp7- and nsp8-specific antibodies, we specifically detected a protein doublet with a molecular weight around 50 kDa. Based on their size estimates, we assume that this protein doublet is formed by the processing intermediates nsp5-7 and nsp5-8 (predicted sizes of about 50 and 55 kDa). Further studies, in particular mutagenesis of specific cleavage sites, are needed to determine the actual protein components of these products. Unlike the N-terminal portion of the pp1a/pp1ab, no functional assignments have been made for the C-terminal portion, nsp6 to nsp8 region. We believe that antibodies generated from this study will prove to be valuable tools for future studies on the structure and function of these proteins.

In immunofluorescence assays, PRRSV ORF1a-encoded nsps could be detected by 7 hpi. This implies that nsp-specific mAbs can also be useful tools for the early detection of PRRSV infection. Furthermore, since replicase proteins contain both highly variable domains and regions that are conserved within/between genotypes, it would be useful to identify a

panel of nsp-specific mAbs that is both broadly reactive to various field strains and able to differentiate between certain specific strains or (sub) genotypes.

In conclusion, we developed a panel of antibodies against PRRSV ORF1a-encoded nsps, and confirmed the existence of individual mature nsps in virus-infected cells. This study provides a basis for both applied and basic research on the role of PRRSV nsps in viral replication and pathogenesis.

## 2.5 References


**Allende, R., Lewis, T.L., Lu, Z., Rock, D.L., Kutish, G.F., Ali, A., Doster, A.R. & Osorio, F.A. (1999).** North American and European porcine reproductive and respiratory syndrome viruses differ in non-structural protein coding regions. *J Gen Virol* **80,** 307-315.

**Bautista, E.M., Meulenberg, J.J., Choi, C.S. & Molitor, T.W. (1996).** Structural polypeptides of the American (VR-2332) strain of porcine reproductive and respiratory syndrome virus. *Arch Virol* **141(7),** 1357-1365.

**Benfield, D.A., Nelson, E., Collins, J.E., Harris, L., Goyal, S.M., Robison, D., Christianson, W.T., Morrison, R.B., Gorcyca, D. & Chladek, D. (1992).** Characterization of swine infertility and respiratory syndrome (SIRS) virus (isolate ATCC VR-2332). *J Vet Diagn Invest* **4,** 127-133.

**Brown, E., Lawson, S., Welbon, C., Gnanandarajah, J., Li, J., Murtaugh, M.P., Nelson, E.A., Molina, R.M., Zimmerman, J.J., Rowland, R.R. & Fang, Y. (2009).** Antibody response to porcine reproductive and respiratory syndrome virus (PRRSV) nonstructural proteins and implications for diagnostic detection and differentiation of PRRSV types I and II. *Clin Vaccine Immunol* **16(5),** 628-635.

**Chen, Z., Lawson, S., Sun, Z., Zhou, X., Guan, X., Christopher-Hennings, J., Nelson, E.A. & Fang, Y. (2010).** Identification of two auto-cleavage products of nonstructural protein 1 (nsp1) in porcine reproductive and respiratory syndrome virus infected cells: nsp1 function as interferon antagonist. *Virology* **398(1),** 87-97.

**Collins, J.E., Benfield, D.A., Christianson, W.T., Harris, L., Hennings, J.C., Shaw, D.P., Goyal, S.M., McCullough, S., Morrison, R.B. & Joo, H.S. & other authors (1992).** Isolation of swine infertility and respiratory syndrome virus (isolate ATCC VR-2332) in North America and experimental reproduction of the disease in gnotobiotic pigs. *J Vet Diagn Invest* **4(2),** 117-126.

**Dea, S., Gagnon, C.A., Mardassi, H. & Milane, G. (1996).** Antigenic variability among North American and European strains of porcine reproductive and respiratory

syndrome virus as defined by monoclonal antibodies to the matrix protein. *J Clin Microbiol* **34(6),** 1488-1493.

**den Boon, J.A., Snijder, E.J., Chirnside, E.D., de Vries, A.A., Horzinek, M.C. & Spaan, W.J. (1991).** Equine arteritis virus is not a togavirus but belongs to the coronaviruslike superfamily. *J Virol* **65(6),** 2910-2920.

**den Boon, J.A., Faaberg, K.S., Meulenberg, J.J., Wassenaar, A.L., Plagemann, P.G., Gorbalenya, A.E. & Snijder, E.J. (1995).** Processing and evolution of the N-terminal region of the arterivirus replicase ORF1a protein: identification of two papainlike cysteine proteases. *J Virol* **69(7),** 4500-4505.

**Drew, T.W., Meulenberg, J.J., Sands, J.J. & Paton, D.J. (1995).** Production, characterization and reactivity of monoclonal antibodies to porcine reproductive and respiratory syndrome virus. *J Gen Virol* **76 ( Pt 6),** 1361-1369.

**Fang, Y., Rowland, R.R., Roof, M., Lunney, J.K., Christopher-Hennings, J. & Nelson, E.A. (2006a).** A full-length cDNA infectious clone of North American type 1 porcine reproductive and respiratory syndrome virus: expression of green fluorescent protein in the Nsp2 region. *J Virol* **80(23),** 11447-11455.

**Fang, Y., Pekosz, A., Haynes, L., Nelson, E.A. & Rowland, R.R. (2006b).** Production and characterization of monoclonal antibodies against the nucleocapsid protein of SARS-CoV. *Adv Exp Med Biol* **581,** 153-156.

**Fang, Y. & Snijder, E. (2011).** The PRRSV replicase: Exploring the multifunctionality of an intriguing set of nonstructural proteins. *Virus Research* **154,** 61-76.

**Firth, A.E., Zevenhoven-Dobbe, J.C., Wills, N.M., Go, Y.Y., Balasuriya, U.B., Atkins, J.F., Snijder, E.J. & Posthuma, C.C. (2011).** Discovery of a small arterivirus gene that overlaps the GP5 coding sequence and is important for virus production. *J Gen Virol* **92(Pt 5),** 1097-1106.

**Frias-Staheli, N., Giannakopoulos, N.V., Kikkert, M., Taylor, S.L., Bridgen, A., Paragas, J., Richt, J.A., Rowland, R.R., Schmaljohn, C.S., Lenschow, D.J., Snijder, E.J., Garcia-Sastre, A. & Virgin, H.W.T. (2007).** Ovarian tumor domain-containing viral proteases evade ubiquitin- and ISG15-dependent innate immune responses. *Cell Host Microbe* **2(6),** 404-416.

**Han, J., Rutherford, M.S., Faaberg, K.S. (2010).** Proteolytic products of the porcine reproductive and respiratory syndrome virus nsp2 replicase protein. *J Virol* **84(19),** 10102-10112.

**Johnson, C.R., Griggs, T.F., Gnanandarajah, J. & Murtaugh, M.P. (2011).** Novel structural protein in porcine reproductive and respiratory syndrome virus encoded by an alternative ORF5 present in all arteriviruses. *J Gen Virol* **92(Pt 5),** 1107-1116.

**Johnson, C.R., Yu, W. & Murtaugh, M.P. (2007).** Cross-reactive antibody responses to nsp1 and nsp2 of Porcine reproductive and respiratory syndrome virus. *J Gen Virol* **88(Pt 4),** 1184-1195.

**Keffaber, K.K. (1989).** Reproductive failure of unknown etiology. *Am. Assoc. Swine Pract. Newsl.* **1,** 1-9.

**Kim, H.S., Kwang, J., Yoon, I.J., Joo, H.S. & Frey, M.L. (1993).** Enhanced replication of porcine reproductive and respiratory syndrome (PRRS) virus in a homogeneous subpopulation of MA-104 cell line. *Arch Virol* **133(3-4),** 477-483.

**Kim, O., Sun, Y., Lai, F.W., Song, C. & Yoo, D. (2010).** Modulation of type I interferon induction by porcine reproductive and respiratory syndrome virus and degradation of CREB-binding protein by non-structural protein 1 in MARC-145 and HeLa cells. *Virology* **402(2),** 315-326.

**Kroese, M.V., Zevenhoven-Dobbe, J.C., Bos-de Ruijter, J.N., Peeters, B.P., Meulenberg, J.J., Cornelissen, L.A. & Snijder, E.J. (2008).** The nsp1alpha and nsp1 papain-like autoproteinases are essential for porcine reproductive and respiratory syndrome virus RNA synthesis. *J Gen Virol* **89(2),** 494-499.

**Laemmli, U.K. (1970).** Cleavage of structural proteins during the assembly of the head of bacteriophage T4. *Nature* **227(5259),** 680-685.

**Langenhorst, R. J., Lawson, S., Kittawornrat, A., Zimmerman, J. J., Sun, Z., Li, Y., Christopher-Hennings, J., Nelson, E. A. & Fang, Y. (2012).** Development of a fluorescent microsphere immunoassay for detection of antibodies against porcine reproductive and respiratory syndrome virus using oral fluid samples as an alternative to serum-based assays. Clin Vaccine Immunol 19, 180-189.

**Magar, R., Larochelle, R., Nelson, E.A. & Charreyre, C. (1997).** Differential reactivity of a monoclonal antibody directed to the membrane protein of porcine reproductive and respiratory syndrome virus. *Can J Vet Res* **61(1),** 69-71.

**Mardassi, H., Massie, B. & Dea, S. (1996).** Intracellular synthesis, processing, and transport of proteins encoded by ORFs 5 to 7 of porcine reproductive and respiratory syndrome virus. *Virology* **221(1),** 98-112.

**Meng, X.J., Paul, P.S., Morozov, I. & Halbur, P.G. (1996).** A nested set of six or seven subgenomic mRNAs is formed in cells infected with different isolates of porcine reproductive and respiratory syndrome virus. *J Gen Virol* **77 ( Pt 6),** 1265-1270.

**Meulenberg, J.J., Bende, R.J., Pol, J.M., Wensvoort, G. & Moormann, R.J. (1995a).** Nucleocapsid protein N of Lelystad virus: expression by recombinant baculovirus, immunological properties, and suitability for detection of serum antibodies. *Clin Diagn Lab Immunol* **2(6),** 652-656.

**Meulenberg, J.J. & Petersen-den Besten, A. (1996).** Identification and characterization of a sixth structural protein of Lelystad virus: the glycoprotein GP2 encoded by ORF2 is incorporated in virus particles. *Virology* **225(1),** 44-51.

**Meulenberg, J.J., Petersen-den Besten, A., De Kluyver, E.P., Moormann, R.J., Schaaper, W.M. & Wensvoort, G. (1995b).** Characterization of proteins encoded by ORFs 2 to 7 of Lelystad virus. *Virology* **206(1),** 155-163.

**Mounir, S., Mardassi, H. & Dea, S. (1995).** Identification and characterization of the porcine reproductive and respiratory virus ORFs 7, 5 and 4 products. *Adv Exp Med Biol* **380,** 317-320.

**Nedialkova, D.D., Gorbalenya, A.E. & Snijder, E.J. (2010).** Arterivirus Nsp1 modulates the accumulation of minus-strand templates to control the relative abundance of viral mRNAs. *PLoS Pathog.* **6(2):**e1000772.

**Nelsen, C.J., Murtaugh, M.P. & Faaberg, K.S. (1999).** Porcine reproductive and respiratory syndrome virus comparison: divergent evolution on two continents. *J Virol* **73(1),** 270-280.

**Nelson, E.A., Christopher-Hennings, J., Drew, T., Wensvoort, G., Collins, J.E. & Benfield, D.A. (1993).** Differentiation of U.S. and European isolates of porcine reproductive and respiratory syndrome virus by monoclonal antibodies. *J Clin Microbiol* **31(12),** 3184-3189.

**Neumann, E.J., Kliebenstein, J.B., Johnson, C.D., Mabry, J.W., Bush, E.J., Seitzinger, A.H., Green, A.L. & Zimmerman, J.J. (2005).** Assessment of the economic impact of porcine reproductive and respiratory syndrome on swine production in the United States. *J Am Vet Med Assoc* **227(3),** 385-392.

**Pedersen, K. W., van der Meer, Y., Roos, N. & Snijder, E. J. (1999).** Open reading frame 1a-encoded subunits of the arterivirus replicase induce endoplasmic reticulum-derived double-membrane vesicles which carry the viral replication complex. *J Virol* **73**, 2016-2026.

**Snijder, E.J., Wassenaar, A.L. & Spaan, W.J. (1992).** The 5' end of the equine arteritis virus replicase gene encodes a papainlike cysteine protease. *J Virol* **66(12),** 7040-7048.

**Snijder, E.J., Wassenaar, A.L. & Spaan, W.J. (1994).** Proteolytic processing of the replicase ORF1a protein of equine arteritis virus. *J Virol* **68(9),** 5755-5764.

**Snijder, E.J., Wassenaar, A.L., Spaan, W.J. & Gorbalenya, A.E. (1995).** The arterivirus Nsp2 protease. An unusual cysteine protease with primary structure similarities to both papain-like and chymotrypsin-like proteases. *J Biol Chem* **270(28),** 16671-16676.

**Snijder, E.J. & Meulenberg, J.J. (1998).** The molecular biology of arteriviruses. *J Gen Virol* **79 ( Pt 5),** 961-979.

**Snijder, E.J., van Tol, H., Pedersen, K.W., Raamsman, M.J. & de Vries, A.A. (1999).** Identification of a novel structural protein of arteriviruses. *J Virol* **73(8),** 6335-6345.

**Snijder, E.J., van Tol, H., Roos, N. & Pedersen, K.W. (2001).** Non-structural proteins 2 and 3 interact to modify host cell membranes during the formation of the arterivirus replication complex. *J Gen Virol* **82(Pt 5),** 985-994.

**Sun, Z., Chen, Z., Lawson, S.R. & Fang, Y. (2010).** The cysteine protease domain of porcine reproductive and respiratory syndrome virus nonstructural protein 2 possesses deubiquitinating and interferon antagonism functions. *J Virol* **84(15),** 7832-7846.

**Tijms, M.A. & Snijder, E.J. (2003).** Equine arteritis virus non-structural protein 1, an essential factor for viral subgenomic mRNA synthesis, interacts with the cellular transcription co-factor p100. *J Gen Virol* **84(Pt 9),** 2317-2322.

**van Aken, D., Zevenhoven-Dobbe, J., Gorbalenya, A.E. & Snijder, E.J. (2006).** Proteolytic maturation of replicase polyprotein pp1a by the nsp4 main proteinase is essential for equine arteritis virus replication and includes internal cleavage of nsp7. *J Gen Virol* **87(Pt 12),** 3473-3482.

**van der Meer, Y., van Tol, H., Locker, J.K. & Snijder, E.J. (1998).** ORF1a-encoded replicase subunits are involved in the membrane association of the arterivirus replication complex. *J Virol* **72(8),** 6689-6698.

**van Dinten, L. C., Wassenaar, A. L., Gorbalenya, A. E., Spaan, W. J. & Snijder, E. J. (1996).** Processing of the equine arteritis virus replicase ORF1b protein: identification of cleavage products containing the putative viral polymerase and helicase domains. *J Virol* **70**, 6625-6633.

**Wassenaar, A. L., Spaan, W. J., Gorbalenya, A. E. & Snijder, E. J. (1997).** Alternative proteolytic processing of the arterivirus replicase ORF1a polyprotein: evidence that NSP2 acts as a cofactor for the NSP4 serine protease. *J Virol* **71**, 9313-9322.

**Wensvoort, G., Terpstra, C., Pol, J.M., ter Laak, E.A., Bloemraad, M., de Kluyver, E.P., Kragten, C., van Buiten, L., den Besten, A., Wagenaar, F. & other authors (1991).** Mystery swine disease in The Netherlands: the isolation of Lelystad virus. *Vet Q* **13(3),** 121-130.

**Wu, W.H., Fang, Y., Farwell, R., Steffen-Bien, M., Rowland, R.R., Christopher - Hennings, J. & Nelson, E.A. (2001).** A 10-kDa structural protein of porcine reproductive and respiratory syndrome virus encoded by ORF2b. *Virology* **287(1),** 183-191.

**Yang, L., Frey, M.L., Yoon, K.J., Zimmerman, J.J. & Platt, K.B. (2000).** Categorization of North American porcine reproductive and respiratory syndrome viruses: epitopic profiles of the N, M, GP5 and GP3 proteins and susceptibility to neutralization. *Arch Virol* **145(8),** 1599-1619.

**Yang, L., Yoon, K.J., Li, Y., Lee, J.H., Zimmerman, J.J., Frey, M.L., Harmon, K.M. & Platt, K.B. (1999).** Antigenic and genetic variations of the 15 kD nucleocapsid protein of porcine reproductive and respiratory syndrome virus isolates. *Arch Virol* **144(3),** 525-546.

**Yoon, K.J., Zimmerman, J.J., Swenson, S.L., McGinley, M.J., Eernisse, K.A., Brevik, A., Rhinehart, L.L., Frey, M.L., Hill, H.T. & Platt, K.B. (1995).** Characterization of the humoral immune response to porcine reproductive and respiratory syndrome (PRRS) virus infection. *J Vet Diagn Invest* **7(3),** 305-312.

**Ziebuhr, J., Snijder, E.J. & Gorbalenya, A.E. (2000).** Virus-encoded proteinases and proteolytic processing in the Nidovirales. *J Gen Virol* **81(Pt 4),** 853-879.

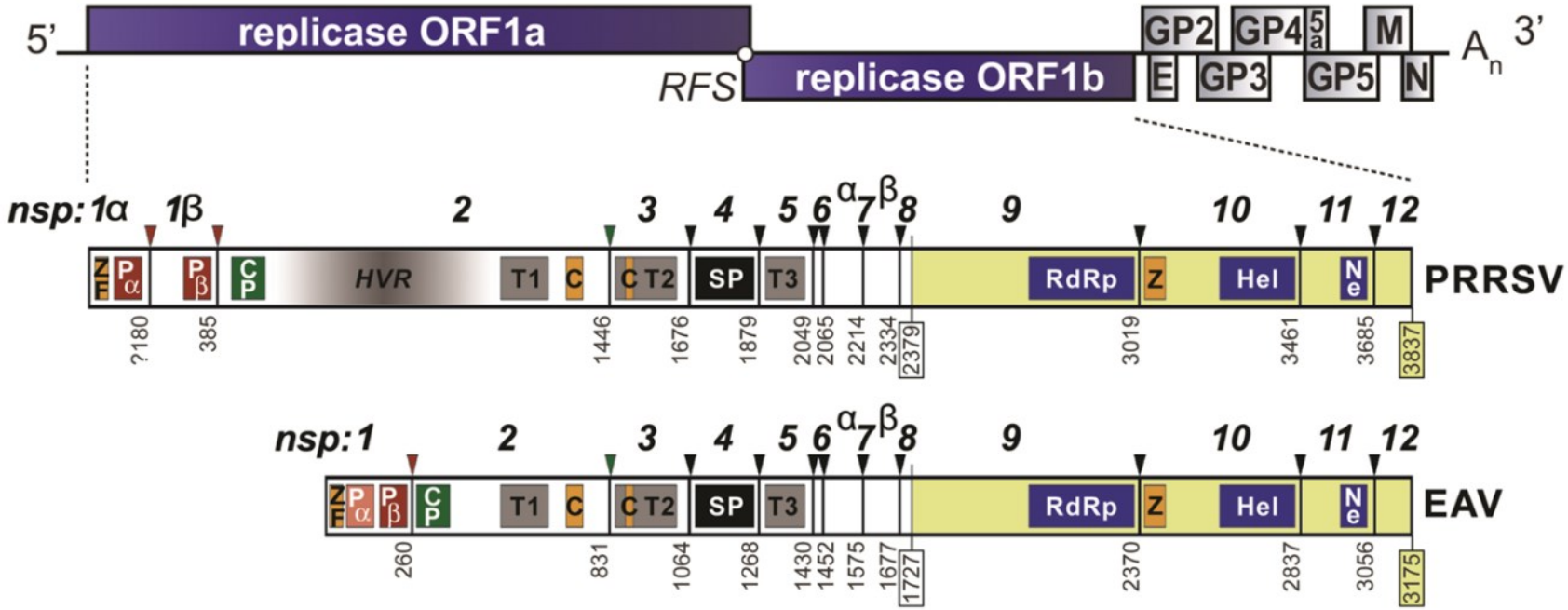
5'
replicase ORF1a
RFS
replicase ORF1b
GP2
GP4
5a
M
E
GP3
GP5
N
An
3'
nsp: 1α 1β 2 3 4 5 6 α 7 β 8 9 10 11 12
ZF
Pα
Pβ
CP
HVR
T1
C
C T2
SP
T3
RdRp
Z
Hel
Ne
PRRSV
?180
385
1446
1676
1879
2049
2065
2214
2334
2379
3019
3461
3685
3837
nsp: 1 2 3 4 5 6 α 7 β 8 9 10 11 12
EAV
260
831
1064
1268
1430
1452
1575
1677
1727
2370
2837
3056
3175

**Figure 2. 1 Comparison of EAV and PRRSV replicase polyprotein size, domain organization, and (tentative) proteolytic processing schemes.** *Top:* PRRSV genome organization, showing the 5'-proximal replicase open reading frames (ORFs) 1a and 1b, as well as the downstream ORFs encoding the viral structural proteins envelope (E), membrane (M), nucleocapsid (N), ORF5a (5a), glycoproteins (GP) 2 - 5 and the 3' poly(A) tail (An). *Bottom:* overview of the PRRSV and EAV pp1ab replicase polyproteins that derive from genome translation when ORF1a/1b ribosomal frameshifting (RFS) occurs. Arrowheads represent the sites cleaved by the three or four virus-encoded proteases [the cysteine proteases PLPα (Pα), PLPß (Pß), PLP2 (CP), and the 'main protease', the nsp4 serine protease (SP)]. The numbering/nomenclature of the resulting nonstructural proteins (nsp) is indicated. In addition, to the protease domains, three ORF1b-encoded enzymatic domains are depicted: the nsp9 RNA-dependent RNA polymerase (RdRp), the nsp10 helicase (Hel), and the nsp11 endoribonuclease (Ne). Domains labeled T are putative transmembrane regions that are thought to be involved in membrane anchoring of the viral replicase complex. Note the presence of an uncleaved nsp1 in EAV and nsp1α and nsp1ß subunits in PRRSV, and the remarkable size difference between the nsp2 subunits of both viruses. Amino acid numbering is based on PRRSV strain SD01-08 (Fang *et al*., 2006a) and EAV strain Bucyrus (den Boon *et al*., 1991) ZF: zinc finger; HVR: hypervariable region; C: cluster of conserved Cys residues; Z: predicted zinc-binding domain; RFS: -1 ORF1a/1b ribosomal frameshift site. Figures adapted from Nedialkova *et al*., 2010 and Fang & Snijder, 2010.

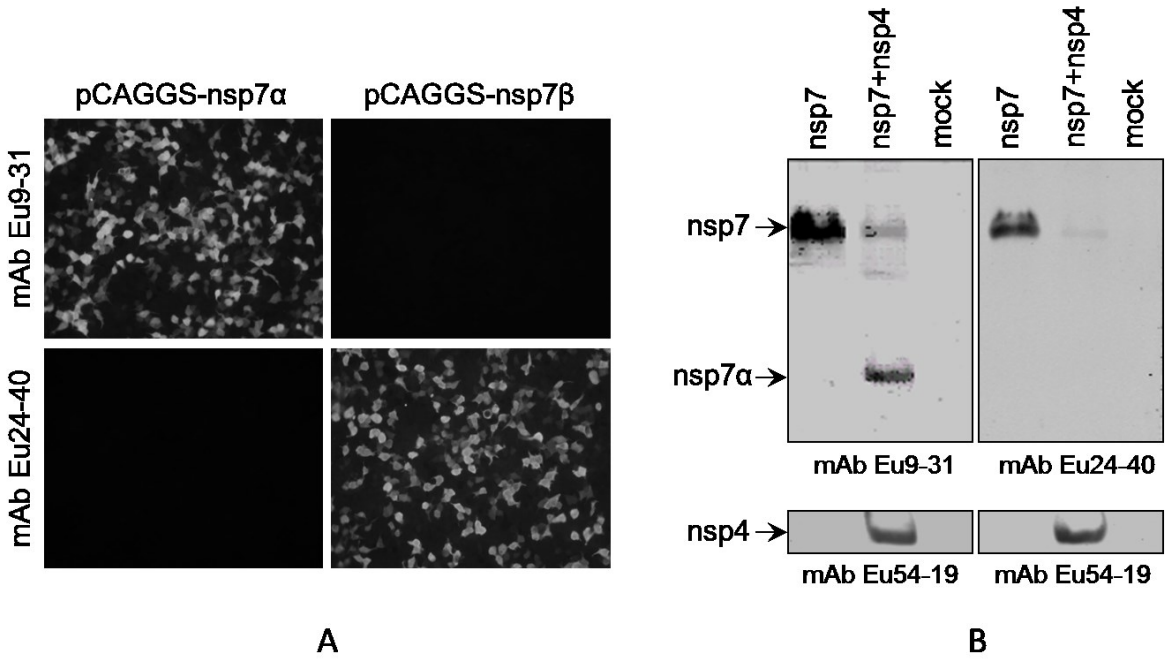


**Figure 2. 2 Reactivity of monoclonal antibodies to PRRSV nsp7α and nsp7β.** A). HEK293T cells were transfected with plasmids expressing PRRSV nsp7α or nsp7β proteins and analyzed by immunofluorescence microscopy following staining with the specific antibodies indicated at the left side of the panel. Images were taken by fluorescence microscopy; B). HEK293T cells were transfected with a plasmid expressing PRRSV nsp7 or co-transfected with plasmids expressing nsp7 and nsp4. At 24 h posttransfection, cells were harvested and Western blot analysis was performed using nsp7- or nsp4-specific antibodies as indicated at the bottom of each panel. Arrows point to specific PRRSV proteins detected by Western blot.

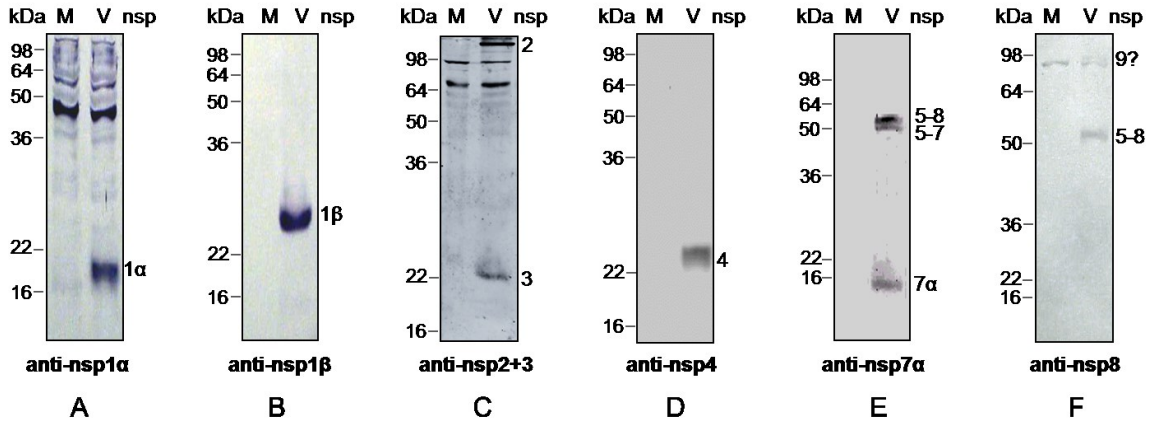


**Figure 2. 3 Western blot detection of ORF1a-encoded nsps in PRRSV-infected cell lysates using a panel of ORF1a protein-specific antibodies.** Cell lysates from PRRSV SD01-08-infected or mock-infected cells were separated by SDS-PAGE, and transferred to a nitrocellulose membrane. Each membrane was probed with an nsp-specific mAb or pAb as indicated on the bottom of each panel. M, Mock-infected cell lysate; V, PRRSV-infected cell lysate.

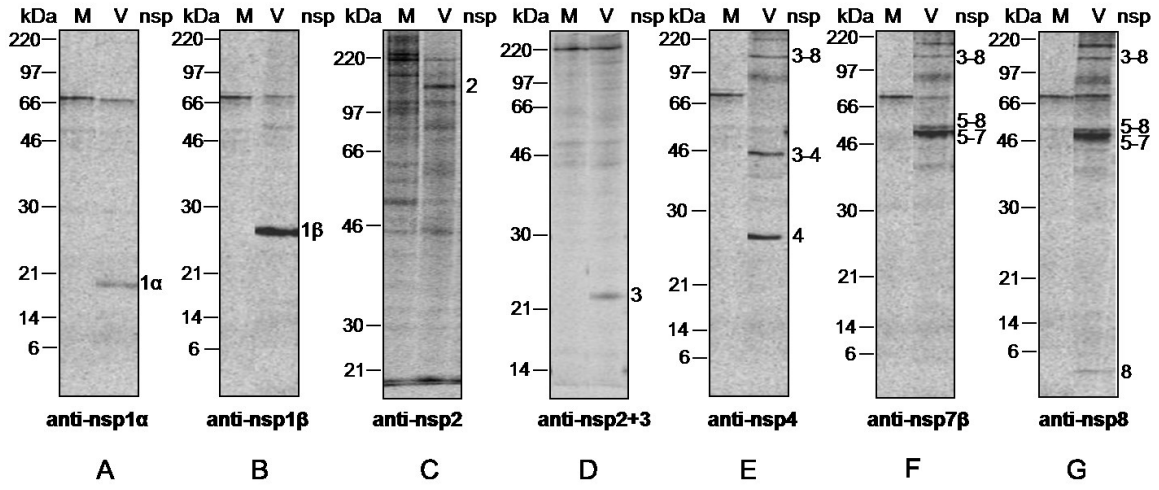


**Figure 2. 4 Radioimmunoprecipitation analysis of PRRSV-infected or mock-infected MARC-145 cell lysates with ORF1a protein-specific antibodies.** For each antibody (indicated at the bottom of each panel), a set of two lanes is shown: M, immunoprecipitation with mock-infected cell lysate; V, immunoprecipitation with PRRSV-infected cell lysate. The position of the molecular weight marker and various PRRSV nonstructural proteins are indicated. Cells were infected with MOI 5 and $^{35}$S-labeled from 24 to 30 hours post-infection.

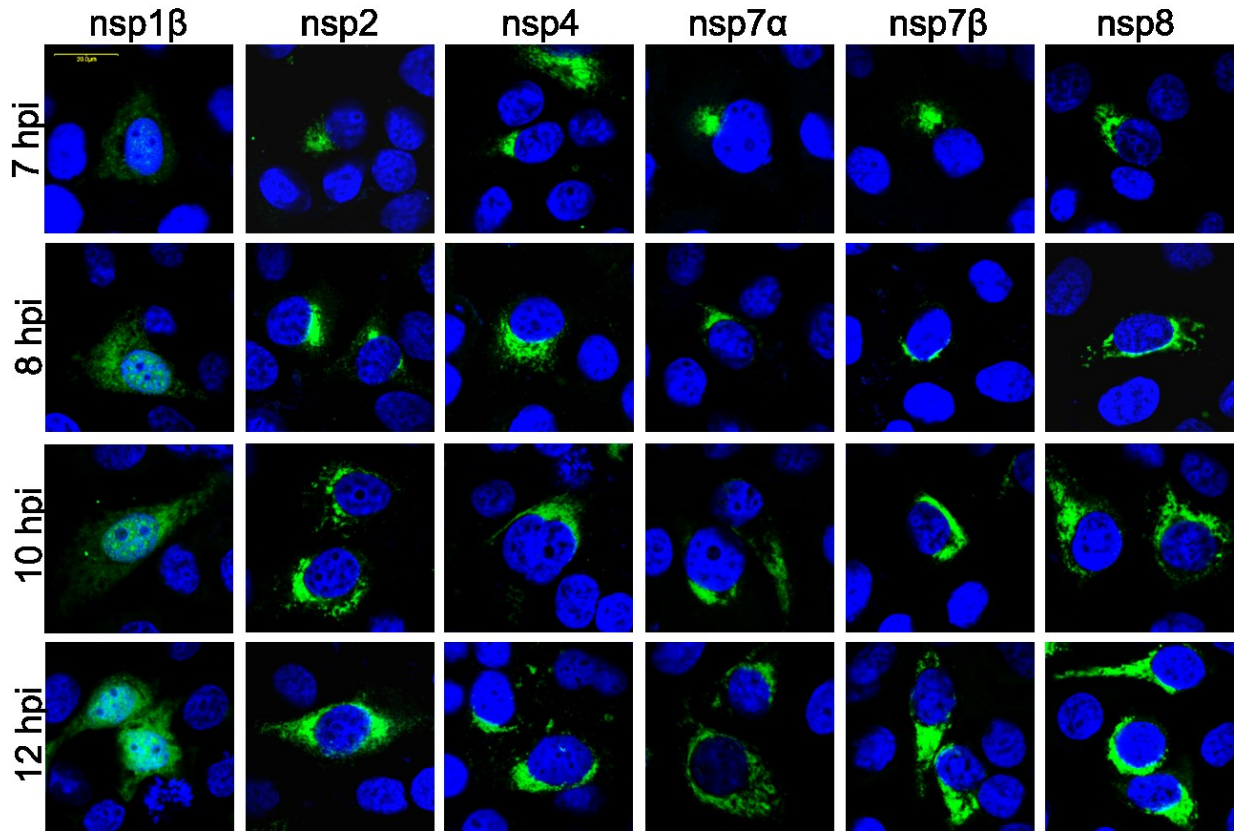


**Figure 2. 5 Detection of PRRSV ORF1a-encoded nsp expression in infected cells by immunofluorescence microscopy.** MARC-145 cells were infected with PRRSV SD01-08 and fixed at 7, 8, 10, or 12 hpi. Cells were stained with the nsp-specific antibodies listed in Table 2.1. Specimens were imaged on a Zeiss LSM510 confocal microscope. A 0.8-μm slice through the nucleus is shown in each image.

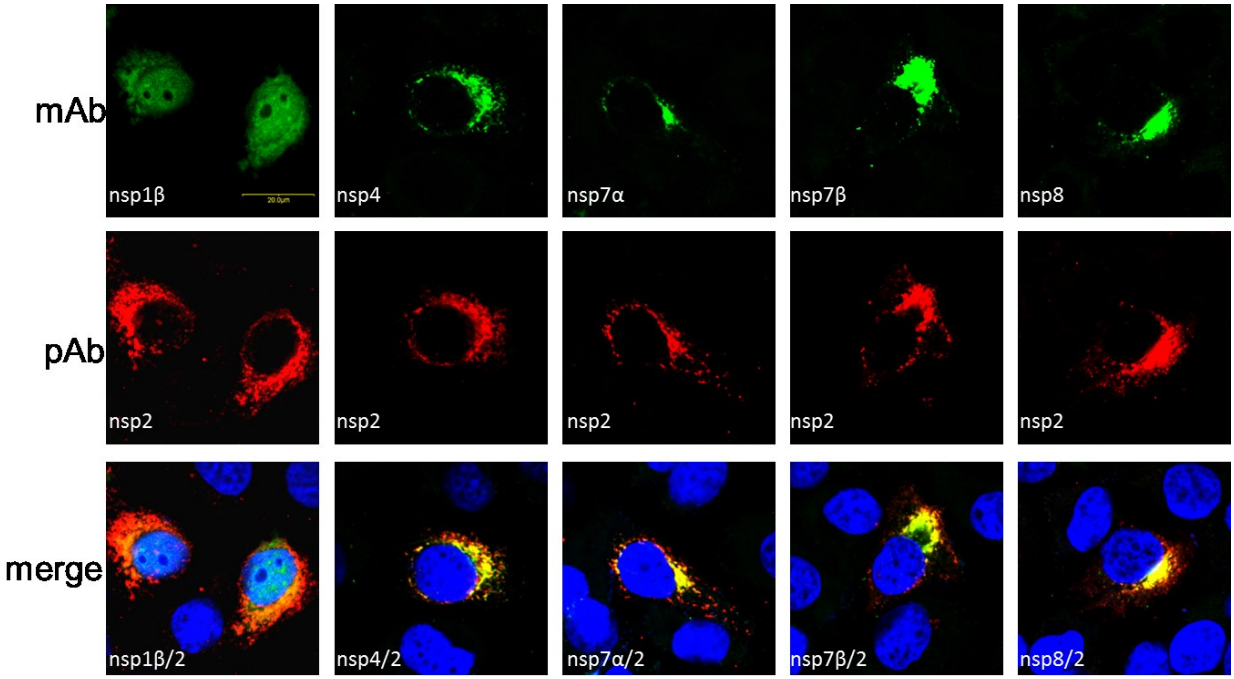


**Figure 2. 6 Colocalization of PRRSV replicase proteins.** MARC-145 cells were fixed at 8 h post infection, and were double stained with an nsp2-specific rabbit antiserum and a panel of mAbs recognizing other nsps. Note that each individual nsp localizes to the perinuclear region.

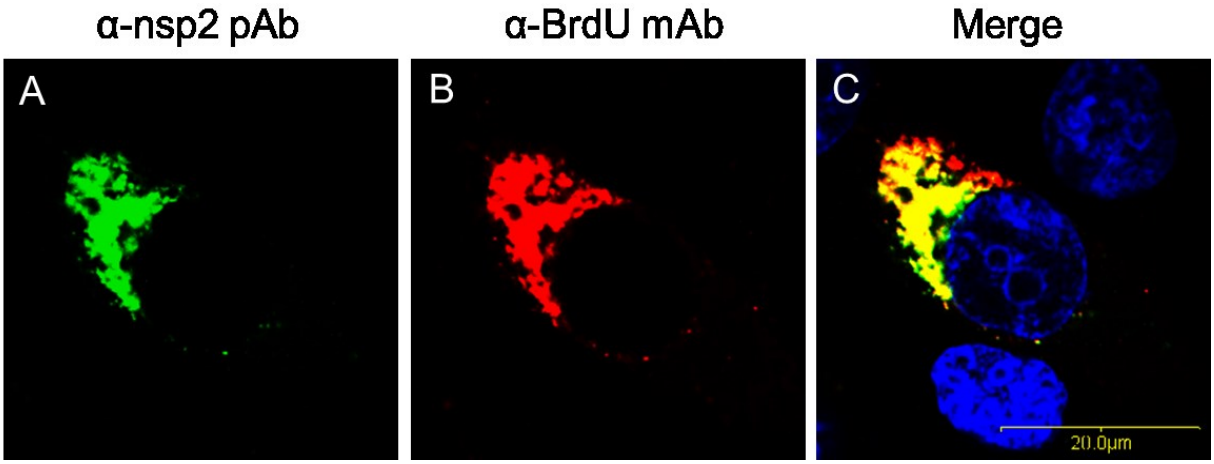


**Figure 2. 7 Colocalization of PRRSV nsp2 with de novo-synthesized viral RNA.** PRRSV-infected MARC-145 cells were transfected with BrUTP in the presence of actinomycin D, incubated for 60 min, fixed and double stained with a rabbit antiserum against nsp2 (A) and an anti-BrdU mAb to detect newly synthesized RNA (B); (C). Overlay image of A and B. Specimens were imaged on a Zeiss LSM510 confocal microscope.

**Table 2. 1 Generation of antibodies to PRRSV SD01-08 ORF1a-encoded replicase protein**

| Nonstructural protein | Predicted MW (kDa) | *Antigen (replicase pp1a residues) | Antiserum/antibody name | mAb isotype | Detection assays# |
|---|---|---|---|---|---|
| nsp1 (nsp1α + nsp1β) | 44.0 | 1 - 385 | pAb Eu-nsp1 (nsp1α)<br>mAb Eu22-28 (nsp1β) | IgG1 | pAb: RIP<br>mAb: IFA, WB, RIP |
| nsp2 | 114.1 | 427 - 505 | pAb Eu-nsp2<br>mAb Eu36-19 | IgG1 | pAb: IFA, RIP<br>mAb: IFA, RIP |
| nsp2+3 | 24.6 | 385-408 (nsp2)<br>1658-1676 (nsp3) | pAb Eu-nsp2+3 | N/A | IFA, WB, RIP |
| nsp4 | 21.1 | 1677 - 1879 | mAb Eu54-19 | IgG1 | IFA, WB, RIP |
| nsp7α | 15.7 | 2066 - 2214 | mAb Eu9-31 | IgG1 | IFA, WB, RIP |
| nsp7β | 13.8 | 2215 - 2334 | mAb Eu24-40 | IgG1 | IFA, RIP |
| nsp8 | 4.8 | 2335 – 2379 | mAb Eu12-40 | IgG1 | IFA, WB, RIP |

* The nsp2+3 antigen was made from PRRSV Lelystad isolate (GenBank accession number M96262), and the rest of the antigens were made from PRRSV SD01-08 isolate (GenBank accession number DQ489311).

# IFA: immunofluorescence microscopy assay; WB: Western Blot; RIP: radio immunoprecipitation.

# Chapter 3 - Attenuation of interferon antagonizing function of PRRSV by targeted mutations in a highly conserved motif of nsp1β protein

**Abstract:** Nonstructural protein 1β (nsp1β) of porcine reproductive and respiratory syndrome virus (PRRSV) contains a papain-like cysteine protease (PCPβ) domain, and was determined to be the main viral protein antagonizing host innate immune response. In this study, nsp1β was determined to suppress the expression of reporter genes as well as suppress "self-expression" in transfected cells, and this activity appeared to associate with its interferon (IFN) antagonist function. To knock down the effect of nsp1β on IFN activity, a panel of site-specific mutations in nsp1β was analyzed. Double mutations K130A/R134A (type 1 PRRSV) or K124A/R128A (type 2 PRRSV), targeting on a highly conserved motif of nsp1β, G**K**YLQ**R**RLQ, impaired the nsp1β's ability to suppress IFN-β and reporter gene expression, as well as to suppress "self-expression" *in vitro.* Subsequently, viable recombinant viruses, vSD01-08-K130A/R134A and vSD95-21-K124A/R128A, containing double mutations in G**K**YLQ**R**RLQ motif were generated using reverse genetics. In comparison to wild-type viruses, these nsp1β mutants showed impaired growth ability in infected cells, but the PCPβ cleavage function was not directly affected. The expression of selected innate immune genes was determined in vSD95-21-K124A/R128A mutant-infected cells. The results consistently showed that gene expression levels of IFN-α, IFN-β and ISG15 were up-regulated in cells that were infected with the vSD95-21-K124A/R128A compared with that of wild-type virus. These data suggest that PRRSV nsp1β may selectively suppress cellular gene expression, including those involved in host innate immune function. Modifying the key residues on the conserved G**K**YLQ**R**RLQ motif could attenuate the virus growth and improve cellular innate immune responses.

## 3.1 Introduction

Porcine reproductive and respiratory syndrome (PRRS) continues to be a major problem in the swine industry worldwide. It causes late term reproductive failure in sows and severe pneumonia in neonatal pigs. Since its emergence, PRRS has been estimated to cost the US swine industry at least $600 million annually (Miller, 2011). The etiological agent is a small, enveloped, positive-stranded RNA virus, which belongs to the order *Nidovirales,* family *Arteriviridae,* including equine arteritis virus (EAV), lactate dehydrogenase-elevating

virus (LDV), and simian hemorrhagic fever virus (SHFV) (Snijder & Meulenberg, 1998). PRRSV can be divided into distinct European (type 1) and North American (type 2) genotypes, sharing about 63% nucleotide identity (Allende *et al.*, 1999; Nelsen *et al.*, 1999; Ropp *et al.*, 2004).

The PRRSV genome is about 15kb in length and contains at least ten open reading frames. The replicase-associated genes, ORF1a and ORF1ab encode two long nonstructural polyproteins, pp1a and pp1ab, with expression of the latter depending on a -1 ribosomal frame shift signal in the ORF1a/ORF1ab overlap region. Following their synthesis from the genomic mRNA template, the pp1a and pp1ab replicase polyproteins are processed into 14 nonstructural proteins by a complex proteolytic cascade that is directed by four proteinase domains encoded in ORF1a, which includes two papain-like cysteine proteases (PLPα and PLPβ) located in the nsp1α and nsp1β, a papain-like protease (PLP2) domain located at the N-terminal of nsp2, and a serine protease (SP) located in nsp4. The PLPα autocleaves between nsp1α/1β, PLPβ autocleaves between nsp1β/2, and PLP2 cleaves between nsp2/3, which mediate nsp1α, nsp1β and nsp2 rapid releasing from the polyprotein. The SP of nsp4 mediates 9 cleavages in the nsp3-12 region to generate the other individual nsps (Fang & Snijder, 2010). In addition, a new ORF (TF) was recently discovered in the central region of ORF1a, which expresses a transframe protein, nsp2TF, through a novel -2 ribosomal frame shifting mechanism (Fang *et al.*, 2012).

Viruses depend on host cellular machinery for survival and replication. Most viral infections are efficiently resolved by the host innate and adaptive immune system. The innate immune response provides an important first line of defense against pathogen intruders. It is essential for the initial control of infection and allows time for the establishment of an adaptive immune response. A key aspect of the antiviral innate immune response is the synthesis and secretion of type I interferon (IFN), such as IFN-α and IFN-β. After being secreted, type I IFNs bind to their receptors on adjacent cell surfaces to activate the so-called JAK–STAT signaling pathway. Activation of this pathway induces the activation of IFN-stimulated response elements (ISRE) in the promoter, results the transcription of IFN-stimulated genes (ISGs). Expression of this group of ISGs enables the cell to fight the infection and inhibit virus replication (Weber *et al.*, 2004). As a counteraction to host innate antiviral responses, viruses have evolved strategies to actively suppress and/or evade the innate immune responses. Some viruses encode proteins that selectively interfere with certain components of the IFN system, while some others have evolved to target the general host gene expression machinery resulting in blocking the innate immune responses (Basler *et al.*,

2000; Chen *et al.*, 1999; Foy *et al.*, 2003; Kamitani *et al.*, 2009; Kamitani *et al.*, 2006; Komatsu *et al.*, 2004; Le May *et al.*, 2004; Lokugamage *et al.*, 2012; Wang *et al.*, 2000). Various PRRSV nonstructural proteins (nsp1α, nsp1β, nsp2, nsp11) appear to be able to suppress the host innate antiviral function (Fang & Snijder, 2010; Yoo *et al.*, 2010). Previous studies from our laboratory and others demonstrated that individually expressed PRRSV nsp1β showed strong inhibitory effects on IFN-β promoter activation (Beura *et al.*, 2010; Chen *et al.*, 2010; Kim *et al.*, 2010). The nsp1β was also determined to be able to inhibit the IFN-dependent signaling pathway leading to ISGs expression (Beura *et al.*, 2010; Chen *et al.*, 2010). As an effort to attenuate the IFN antagonist function of PRRSV nsp1β, in this study, we analyzed a panel of site-specific mutations in nsp1β region using both expression system and reverse genetics. A highly conserved G**K**YLQ**R**RLQ motif of nsp1β was identified and mutations in this motif were further characterized to determine their effect on nsp1β's function in viral replication and cellular immune responses.

## 3.2 Materials and methods

**Cells and viruses.** HEK-293T cells, BHK-21 cells and MARC-145 cells were maintained in Eagle's minimum essential medium (Invitrogen) supplemented with 10% fetal bovine serum and antibiotics at $37^0$C with 5% $CO_2$. Porcine alveolar macrophages were obtained by lung lavage of 6-week-old PRRSV-naive piglets using a method described previously (Zeman et al., 1993).The Sendai virus (SeV) Cantell strain was grown in embryonated chicken eggs and used for Type I IFN stimulation. The US Type 1 PRRSV isolate SD01-08 (Fang *et al.*, 2006), type 2 PRRSV isolate SD95-21 (GenBank accession: KC469618), and their nsp1β mutants were used to infect macrophages or MARC-145 cells for subsequent experiments.

**Plasmids.** The nsp1α or nsp1β expressing plasmids were constructed by RT-PCR amplification of the nsp1α or nsp1β region from the genomic RNA of SD01-08 (EU) or SD95-21 (NA) virus. The PCR product was cloned into a eukaryotic expression vector, p3xFLAG-CMV-24 (sigma), designated as p3xFLAG-EU-nsp1α (222 nt to 761 nt of SD01-08 genome), p3xFLAG-EU-nsp1β (762 nt to 1376 nt of SD01-08 genome) and p3xFLAG-NA-nsp1β (731 nt to 1339 nt of SD95-21 genome). Specific mutations in nsp1β were constructed by site-directed mutagenesis using QuickChange$^{TM}$ site-directed mutagenesis kit (Stratagene) following the manufacturer's instruction. Table 1 lists each construct and corresponding mutations introduced into nsp1β. Four reporter plasmids were used in this study. The p125-Luc plasmid expresses the firefly luciferase under the control of the IFN-β

promoter (Yoneyama *et al.*, 1996); The pISRE-Luc plasmid expresses the firefly luciferase under the control of the interferon-stimulated response element (ISRE) promoter (Stratagene); The pRL-SV40 plasmid expresses a *Renilla* luciferase under the control of a simian virus (SV) 40 promoter (Promega), and pEGFP-N1 plasmid expresses the enhanced green fluorescence protein (EGFP) under the control of CMV promoter (Clone Tech). For expression of nsp1β-2 in a vaccinia-T7 polymerase system, the nsp1β-2 region was RT-PCR amplified from genomic RNA of PRRSV SD01-08 (EU) or SD95-21 (NA). The PCR product of nsp1β-2 was cloned into the pL1a plasmid (Snijder *et al.*, 1994), designated as pL-EU-nsp1β-2 (763 nt to 4559 nt of SD01-08 genome) or pL-NA-nsp1β-2 (731 nt to 4927 nt of SD95-21 genome). The K130A and R134A mutations were introduced into the nsp1β region of pL-EU-nsp1β-2 to construct plasmid pL-EU-nsp1β-2-mt, while K124A and R128A mutations were introduced into the nsp1β region of pL-NA-nsp1β-2 to construct plasmid pL-NA-nsp1β-2-mt. In addition, C96S mutation was introduced into PCPβ catalytic site of pL-EU-nsp1β-2 to construct the plasmid EU-nsp1β-2-C96S. These plasmids containing the nsp1β-2 (or its nsp1β mutant) gene are under the control of a T7 RNA polymerase promoter and an encephalomyocarditis virus internal ribosomal entry site, followed by a downstream T7 terminator sequence.

**Cell transfection and luciferase reporter assay.** HEK-293T cells were seeded at $0.5\times10^5$ cells/ml in 24-well plates one day prior to the transfection. Cells were transfected with p3xFLAG-EU-nsp1β or p3xFLAG-NA-nsp1β (or their mutants) plasmid DNA (0.5 μg) mixed with luciferase reporter plasmid p125-Luc, pISRE-Luc (0.4 μg) or pRL-SV40 (0.02 μg). Transfection was performed using FuGENE HD transfection reagent followed the manufacturer's instruction (Roche Molecular Biochemicals). At 24 h post-transfection, cells were infected with Sendai virus at 100 HA unit/ml/well for 12–16 h, or treated with IFN-β at 2000 IU/ml/well for 16 h. Cells were harvested and subjected to reporter gene assay using the luciferase reporter system (Promega) according to manufacturer's instruction. Firefly or *Renilla* luciferase activity was measured in a luminometer (Bethold). Cell lysates were also subjected to SDS-PAGE and western blot analysis for protein expression.

**Quantitative analysis of mRNA.** To measure the IFN-β mRNA expression level, HEK-293T cells were transfected with a plasmid expressing nsp1β or its mutant using FuGENE HD transfection reagent (Roche Molecular Biochemicals) followed the manufacturer's instruction. The empty plasmid was also used to transfect cells as a control. At 24 h post-transfection, cells were infected with 100 HA unit/ml of SeV or mock infected. At 16 h post-infection (hpi), total intracellular RNAs were extracted using the TRIzol® RNA Isolation Reagents

(Invitrogen, Carlsbad, CA). The contaminating genomic DNA was digested with DNase I (Invitrogen, Carlsbad, CA). Total RNA (1ug) was used to synthesize first strand cDNA using high capacity RNA- to -cDNA kit (Invitrogen, Carlsbad, CA). Subsequently, real-time PCR was performed to quantify the expression of IFN-β mRNA and 18S rRNA (as endogenous control) using a TaqMan gene expression master mix reagent kit (Applied Biosystems). A total of 40 cycles was performed on an ABI PRISM 7900 real-time thermocycler (Applied Biosystems, Foster City, CA). The amount of IFN-β mRNA was normalized to the endogenous 18S rRNA. For quantitative analysis of reporter gene mRNA expression, HEK-293T cells were co-transfected with the plasmid expressing nsp1β (or its mutant) and pRL-SV40 expressing *Renilla* luciferase. At 24h post-transfection, total intracellular RNAs were extracted, and the expression level of *Renilla* luciferase mRNA was measured by real-time PCR using a TaqMan gene expression master mix reagent kit (Applied Biosystems).

**Western Blot Analysis.** Virus-infected or plasmid DNA-transfected cells were harvested and lysed in lyses buffer (10 mM Tris, 150 mM NaCl, 1% NP-40, 0.5% deoxycholate, 0.1% sodium dodecyl sulfate [SDS], 1 mM EDTA, PH7.4) supplemented with protease inhibitor cocktail (Roche). Cell lysates were frozen at -80°C, thawed, and centrifuged to remove the insoluble pellet. Protein concentration in the supernatant was determined by a Bradford assay (Bio-Rad). Equal amounts of protein samples from different treatments were separated by sodium dodecyl sulfate-polyacrylamide gel electrophoresis (SDS-PAGE). The separated proteins were blotted onto a nitrocellulose membrane, and the membrane was blocked with 5% non-fat dry milk in PBST (0.05% Tween 20 in 1×PBS). The membrane was then incubated with primary antibodies for 1 h at room temperature. For detection of the PRRSV nsp1β and nsp2 expression, mouse monoclonal antibodies (mAbs) against nsp1β and nsp2 were used as described previously (Li *et al.*, 2012). For detection of FLAG-tagged proteins, the anti-FLAG mAb (sigma) was used. In addition, mAb to EGFP (sigma) or ISG15 (Santa Cruz Biotechnology) was used as a primary antibody. The anti-β-tubulin mAb (Lamda Biotech) was used as a control. After incubation with the primary antibody, the membrane was washed three times with PBST. DyLight 680-labeled goat anti-rabbit antibody or DyLight 800-labeled goat anti-mouse antibody (LI-COR Biosciences, Lincoln, NE) was added and the membrane was incubated for additional 1 h at room temperature. Image of the membrane was obtained by scanning under an appropriate excitation wavelength using a digital image system (Odyssey infrared imaging system; LI-COR Biosciences, Lincoln, NE). Quantification of protein expression levels was performed by using Adobe Photoshop,

following the method described at *http://rsbweb.nih.gov/ij/*. For each protein lane on the Western blot, the target protein level was normalized to that of β-tubulin.

**Recovery recombinant virus from infectious cDNA clones.** The PRRSV full-length cDNA infectious clones, pCMV-SD01-08 (type 1 PRRSV) and pCMV-SD95-21 (type 2 PRRSV) and their nsp1β-mutated plasmids were used to transfect BHK-21 cells. Transfection was performed using Lipofectamine® LTX with Plus™ Reagent followed the manufacturer's instruction (Life technology). To rescue the virus, cell culture supernatant obtained at 24 - 48 h post-transfection was passaged on MARC-145 cells. Cells were stained with the mAb specific to nsp1β (Li *et al.*, 2012) and FITC-conjugated SDOW17 to nucleocapsid (N) protein for monitoring genome replication and subgenomic transcription as we described previously (Fang *et al.*, 2006). The passage 3 viruses from the MARC-145 cells were used for further analysis.

**Sequencing of nsp1β mutation regions.** To determine the stability of each mutation, cell lysate from recombinant virus-infected cells was harvested and RNA was extracted using a QiaAmp viral RNA kit (Qiagen) following the manufacturer's instruction. The corresponding mutations were amplified by RT-PCR, and PCR products were sequenced at the Iowa State University DNA sequencing facility (Ames, IA).

**Virus titration and plaque assay.** MARC-145 cells were infected with nsp1β mutants and wild-type virus at an MOI of 0.1. Infected cells were harvested at 48 hpi, and virus titers were determined by fluorescent focus assay as described previously (Sun *et al.*, 2012). Plaque morphology between the nsp1β mutant and wild-type virus was compared by plaque assay using the method we described previously (Fang *et al.*, 2006).

**Nsp1β-2 expression in recombinant vaccinia virus/T7 polymerase system.** The pL-EU-nsp1β-2-C96S, pL-EU-nsp1β-2, pL-EU-nsp1β-2-mt, pL-NA-nsp1β-2, or pL-NA-nsp1β-2-mt plasmid was transiently expressed in HEK-293T cells using the recombinant vaccinia virus-T7 polymerase expression system (Fuerst *et al.*, 1986) as described previously (Snijder *et al.*, 1994). Cells were harvested at 24 h post transfection and subjected to western blot analysis using the mAbs specific to nsp1β and nsp2 PLP2 domain (Li *et al.*, 2012; Fang *et al.,* 2012).

**Swine cytokine fluorescence microsphere immunoassay (FMIA).** Porcine alveolar macrophages were infected with 1 MOI of wild-type or recombinant viruses. At 24 hpi, culture supernatant was harvested for analyzing the IFN-α expression using a FMIA as described previously (Lawson et al., 2010). The quantity of IFN-α was determined using mean fluorescent intensity (MFI) values, and the result was compared with the mean values from Mock-infected control cells.

## 3.3 Results

**Generation of PRRSV nsp1β mutants with reduced ability to suppress type I interferon production and signaling**

Since PRRSV nsp1β was determined to be one of the main interferon antagonists, in an effort to knock down its interferon antagonist function, a panel of site-specific nsp1β mutations was constructed (Table 1). They were designed based on the protein surface accessibility prediction (Emini *et al.*, 1985), hydrophilicity analysis (Hopp & Woods, 1981) and crystal structure of nsp1β (Xue *et al.*, 2010). The conserved hydrophilic amino acids predicted to be exposed on the protein surface were targeted for mutation (Fig. 3.1). Each of the nsp1β genes carrying double mutations was cloned into the plasmid, p3xFLAG-CMV-24, in which the gene expression is under the control of CMV promoter and expressed as FLAG-tagged protein. Initially, the panel of nsp1β mutants generated from a type 1 PRRSV strain, SD01-08 (Table 1.1) was analyzed in an IFN-β promoter driven-luciferase reporter assay. The HEK-293T cells were cotransfected with a plasmid expressing wild-type or mutated nsp1β and a reporter plasmid (p125-Luc) that expresses luciferase reporter gene under the control of IFN-β promoter. As controls, the PCPβ catalytic site mutant C96S and empty plasmid p3xFLAG-CMV-24 were included in the analysis. At 24 hour (h) post transfection, cells were mock-infected or infected with Sendai virus (SeV). Cells were harvested to test the luciferase activities at 16 h post-infection (hpi). As shown in Fig. 3.2A, SeV infection induced high level of luciferase reporter expression in cells transfected with empty plasmid, but luciferase expression was about 7 to 50-fold lower in cells expressing wild-type nsp1β and C96S, E28A/D31A, E41A/E43A, E68A/E71A mutants. In contrast, about 30-fold higher level of reporter signal was detected in cells expressing K130A/R134A mutant in comparison to that of wild-type nsp1β. We further determined whether these mutations had effect on nsp1β's ability to suppress IFN-dependent signaling pathway for the ISG expression. The panel of nsp1β mutants was analyzed using an ISRE promoter driven-luciferase reporter assay. Similar result was generated as that obtained in Fig. 3.2A, about 7 to 14-fold higher level of reporter signal was detected in cells expressing K130A/R134A mutant in comparison to those expressing wild-type nsp1β and C96S, E28A/D31A, E41A/E43A, E68A/E71A mutants (Fig. 3.2B). These results suggest that K130A and R134A mutations impaired IFN antagonist function of nsp1β.

To further confirm these results, we tested whether K130A/R134A mutations had effect on endogenous IFN-β mRNA expression. HEK-293T cells were transfected with the

empty plasmid, or the plasmid expressing wild-type nsp1β or K130A/R134A mutant, and then mock-infected or infected with SeV. At 16 hpi, intracellular RNA was extracted and the amount of IFN-β mRNA was measured by real-time RT-PCR. As shown in Fig. 3.3A, expression of wild-type nsp1β strongly inhibited the SeV-induced IFN-β mRNA accumulation. In contrast, there was about 3-fold increase of IFN-β mRNA expression in cells transfected with K130A/R134A mutant. This result indicates that K130A and R134A mutations impaired nsp1β's ability to suppress IFN-β mRNA expression. The K130 and R134 residues in nsp1β of type 1 PRRSV correspond to K124 and R128 in nsp1β of type 2 PRRSV. We repeated our experiment using nsp1β from a type 2 PRRSV strain, SD95-21. The result was consistent with that obtained from type 1 virus. The expression of wild-type nsp1β strongly suppressed the IFN-β mRNA expression (Fig. 3.3B) as well as IFN-β activation and signaling (Fig. 3.4), while increased levels of IFN-β mRNA (Fig. 3.3B) and luciferase reporter expression (Fig. 3.4) were observed in cells expressing K124A/R128A mutant.

**Mutations on amino acids K130(124) and R134(128) impaired nsp1β's ability to suppress "self-expression" and reporter gene expression *in vitro***

Western blot analysis confirmed the expression of nsp1β wild-type and mutants in luciferase assays (Fig. 3.2 and 3.4). Interestingly, the data consistently showed that mutations in K130(124) and R134(128) caused increased amount of nsp1β expression in comparison to that of wild-type nsp1β and other mutants, which suggested that nsp1β may suppress its "self-expression". To confirm this notion, we repeated luciferase assays and compared the cellular expression level of nsp1β with nsp1α, since nsp1α was also determined to be an interferon antagonist in previous studies (Beura *et al.*, 2010; Chen *et al.*, 2010; Song *et al.*, 2010). The HEK-293T cells were cotransfected with the reporter plasmid and equal amount of plasmid DNA expressing nsp1α or nsp1β. As we expected, the result showed that both nsp1α and nsp1β suppressed the expression of IFN-β promoter driven luciferase (Fig. 3.8A), and nsp1β had stronger inhibition on the gene expression under the control of ISRE promoter (Fig. 3.8B). Western blot analysis using anti-FLAG antibody detected higher amount of nsp1α protein, but only trace amount of nsp1β protein was detected in both luciferase assays. The data made us speculate that nsp1β may have general effect on cellular gene expression, including its "self-expression" *in vitro*. To test this possibility, we examined the effect of nsp1β on the reporter gene mRNA expression. The HEK-293T cells were cotransfected with a reporter plasmid (pRL-SV40) expressing *Renilla* luciferase reporter gene under the control of SV40 promoter, and the plasmid expressing type 1 wild-type nsp1β or K130A/R134A

mutant. The empty plasmid was used as a control. Intracellular RNA was extracted at 24 h post transfection, and the amount of mRNA was determined by real-time RT-PCR. In comparison to the *Renilla* luciferase mRNA expression level in cells transfected with empty plasmid, the wild-type nsp1β showed strong inhibition effect. However, the luciferase mRNA level was about 3-fold higher in cells expressing K130A/R134A mutant comparing to those in cells expressing wild-type nsp1β (Fig. 3.5A). In contrast, there was no apparent difference on the amounts of 28S and 18S rRNAs among different treatments (Fig. 3.5B). These data indicate that nsp1β specifically suppressed reporter gene mRNA expression and K130A/R134A mutations impaired this specific activity. Next, we determined the effect of nsp1β expression on the reporter protein production. In comparison to those cells expressing K130A/R134A mutant or transfected with empty plasmid, there was about 7 to 8-fold reduction on the amount of *Renilla* luciferase protein in cells expressing wild-type nsp1β (Fig. 3.5C). To further confirm this result, we cotransfected cells with a plasmid expressing another reporter gene, the enhanced green fluorescent protein (EGFP), and the plasmid expressing wild-type nsp1β or its mutant from both type 1 and type 2 viruses. Expression of EGFP was analyzed by fluorescence microscopy. As shown in Fig. 3.5E, in comparison to those cells cotransfected with empty plasmid, the expression of EGFP was strongly suppressed in cells expressing wild-type nsp1β. In contrast, higher levels of EGFP expression were observed in cells expressing K130A/R134A and K124A/R128A mutants. Western blot analysis using anti-nsp1β and anti-EGFP antibodies confirmed the expression of nsp1β and EGFP proteins (Fig. 3.5D and F). Due to the difference in sensitivity of different antibodies, we used anti-FLAG antibody to detect and compare the expression levels of different proteins. The result consistently showed that wild-type nsp1β expression resulted in lower levels of EGFP production, whereas 2- or 8-fold higher level of EGFP proteins were detected in cells cotransfected with the plasmid expressing nsp1β mutant from type 1 or type 2 PRRSV. Again, about 2- or 3-fold increased level of nsp1β protein was detected in cells expressing K130A/R134A or K124A/R128A mutant in comparison to those cells expressing wild-type nsp1β, indicating the important role of K130(124)/R134(128) residues involved in the nsp1β activities.

**Amino acids K130(124) and R134(128) locate on a highly conserved motif among PRRSV strains from both genotypes**

Based on the crystal structure of nsp1β from a type 2 PRRSV (Xue *et al.*, 2010), the K124 and R128 residues are exposed on the protein surface. We further searched the potential functional motif in this region and result showed that these two resides are located

on a potential B-cell epitope motif, G**K**YLQ**R**RLQ (Kolaskar & Tongaonkar, 1990). This motif has the highest surface accessibility value in comparison to the other regions of nsp1β (Fig. 3.1A; Emini *et al.*, 1985). Amino acid sequence alignment of nsp1β sequences from 212 PRRSV isolates available in GenBank revealed that the GKYLQRRLQ motif is highly conserved among all available PRRSV stains, including both type 1 and type 2 viruses (Fig. 3.1B), which suggests important role of GKYLQRRLQ motif in nsp1β function.

**Characterize recombinant viruses containing mutations in GKYLQRRLQ motif**

We further investigated whether specific mutations introduced into nsp1β region of the virus could improve innate immune responses in PRRSV-infected cells. Initially, two PRRSV nsp1β mutants were generated using reverse genetics (Fig. 3.6A), including vSD01-08-K130A/R134A (vSD01-08-mt) that contains K130A and R134A mutations in the nsp1β region of type 1 PRRSV SD01-08; and vSD95-21-K124A/R128A (vSD95-21-mt) that contains K124A and R128A mutations in the nsp1β region of type 2 PRRSV SD95-21. As a comparison, the wild-type viruses, vSD01-08 and vSD95-21 were also recovered from reverse genetics. Stability of those mutations introduced into the virus was determined by serial passaging each virus 10 times in MARC-145 cells, and sequence analysis showed that all targeted mutations were stably maintained in the virus. The growth property of these two mutants was compared with their wild-type parental viruses. Both mutants showed crippled growth phenotype in MARC-145 cells. The peak viral titer for vSD95-21-mt was $10^{5.4}$ FFU/ml, compared to the titer of $10^{6.3}$ FFU/ml for vSD95-21. The vSD01-08-mt appeared to be highly attenuated on its growth in cell culture (Fig. 3.6B). The virus titer remained around $10^2$ FFU/ml through all passages. Plaque assay result consistently showed that vSD95-21-mt developed smaller plaques than that of wild-type virus, while vSD01-08-mt barely produced plaques. In order to stimulate a measurable host IFN response, a high virus dose is required for the initial infection. Therefore, vSD95-21-mt was used in subsequent experiments for comparison of innate immune gene expression between cells infected with nsp1β mutant and wild-type virus (see below and data presented in Fig. 3.7).

The nsp1β encodes PCPβ protease that is responsible for proteolytic cleavage of the nsp1β/nsp2 site of pp1a and pp1ab polyproteins, a critical step in viral replication (Fang & Snijder, 2010). To investigate whether the crippled growth property of these mutants could be due to an effect on the function of PCPβ in replicase maturation, the nsp1β-2 region was expressed from both type 1 and type 2 PRRSV, designated as EU-nsp1β-2 and NA-nsp1β-2, respectively. Subsequently, K130A/R134A or K124A/R128A mutations were introduced into the nsp1β-2 region to generate EU-nsp1β-2-mt or NA-nsp1β-2-mt constructs. For a

comparison, PCPβ catalytic site mutant EU-nsp1β-2-C96S was also constructed. These constructs were analyzed in a recombinant vaccinia virus/T7 RNA polymerase expression system. The result showed that the C96S mutant prevented the cleavage of nsp1β/2 site as the nsp1β-2 proteins were detected as an uncleaved precursor form. In contrast, both K130A/R134A and K124A/R128A mutants being efficiently cleaved at the nsp1β/2 site, as individual nsp1β and nsp2 proteins were detected in the amount quite similar to those produced by the wild-type nsp1β-2 control (Fig. 3.9). The data indicate that the proteolytic function of PCPβ towards the nsp1β/2 site is not directly affected by mutation of K130(124) and R134(128), suggesting that the reduced growth rate (viral titer) of the vSD01-08-mt and vSD95-21-mt viruses may not directly caused by a basic defect in replicase polyprotein proteolysis, but instead may be due to an impaired ability to counteract cellular innate immune responses (see below).

**Expression of innate immune genes in nsp1β mutant-infected cells**

Since mutations introduced in GKYLQRRLQ motif reduced the nsp1β's ability to suppress IFN-β activity, we further determined whether these mutations could alter the effect of PRRSV on the innate immune response. Initially, we performed the IFN-β promoter-luciferase reporter assay using the full-length cDNA infectious clone of SD95-21 and its K124A/R128A mutant. HEK-293T cells were cotransfected with p125-Luc reporter plasmid and full-length cDNA of SD95-21 or K124A/R128A mutant. At 24 h post-transfection, cells were mock-infected or infected with SeV. After 16 h stimulation, cells were assayed for IFN-β activation. As shown in Fig. 3.7A, in comparison to that in empty plasmid vector-infected cells, the replication of wild-type virus significantly inhibited IFN-β promoter-dependent luciferase expression. The experiment was repeated three times and the result consistently showed that there was about a 2-fold increase of luciferase reporter level in cells transfected with full-length cDNA of K124A/R128A mutant comparing to that in cells transfected with full-length cDNA of parental virus. To further confirm this result, IFN-α expression was examined in vSD95-21-mt and vSD95-21 wild type virus-infected porcine alveolar macrophages. At 24 h post infection, culture supernatants were harvested and IFN-α expression level was quantified by a swine cytokine fluorescence microsphere immunoassay (FMIA). As shown in Fig. 3.7B, there was a 40-fold increase of IFN-α expression level in the vSD95-21-mt-infected cells, in comparison to that in the wild type virus-infected cells.

We further determined the effect of K124A and R128A mutations on the expression of ISG15 in mutant or wild type virus-infected MARC-145 cells. Initially, cells were mock-infected or infected with vSD95-21-mt or vSD95-21 wild type virus. At 18 hpi, cells were treated with

IFN-α to activate the expression of ISGs. Western blot analysis showed a 5-fold increase in the level of ISG15 protein production in vSD95-21-mt virus-infected cells, in comparison to those in wild type virus-infected cells (Fig. 3.7C). The expression level of nsp1β was also analyzed in western blot. Interestingly, in contrast to *in vitro* expression system, similar level of nsp1β protein expression was detected in vSD95-21-mt and vSD95-21 wild-type virus-infected cells.

## 3.4 Discussion

Previous studies from our laboratory and others identified PRRSV nsp1β as an interferon antagonist, in which nsp1β inhibited type I IFN activities in expression systems employing mainly reporter gene-based assays (Beura *et al.*, 2010; Chen *et al.*, 2010; Kim *et al.*, 2010; Patel *et al.*, 2010). It was suggested that the PRRSV nsp1β protein may act on the IFN-β production and signaling pathways, in which it could have a direct effect on the formation of the transcription enhanceosome on the IFN-β promoter in the nucleus as well as effect on the nuclear translocation of STAT1/STAT2 (Beura *et al.*, 2010; Chen *et al.*, 2010; Kim *et al.*, 2010; Patel *et al.*, 2010). The data generated from current study consistently showed that nsp1β inhibited reporter gene mRNA expression, resulting to a strong inhibition in reporter protein synthesis. Expression of nsp1β also suppressed Sendai virus-induced endogenous IFN-β mRNA accumulation and inhibited IFN-β protein synthesis. Another interesting phenomenon is that the level of nsp1β protein expression in nsp1β-transfected cells was lower in comparison to the expression level of another replicase protein, nsp1α, which also has ability to antagonize IFN function. Initially, we suspected that the nsp1β may have general effect on host gene expression, including its own RNA transcripts *in vitro*. However, it appeared not affect 28S and 18S rRNAs and β-actin expression. A similar observation was also reported for SARS-CoV nsp1 (Huang *et al.*, 2011; Kamitani *et al.*, 2009; Kamitani *et al.*, 2006; Narayanan *et al.*, 2008). Individual expression of SARS-CoV nsp1 resulted low expression level, which was due to its ability to promote cellular mRNA degradation, including its own RNA transcripts. However, during the infection, virus developed mechanism to prevent degradation of its own viral mRNAs, and the nsp1 protein only selectively cleaved cellular mRNAs with certain structures. We also noticed the difference in PRRSV nsp1β expression levels using different plasmid expression systems. When the PRRSV nsp1β expressed using p3xFLAG plasmid, which is under the control of CMV promoter, we detected lower level of nsp1β expression. In contrast, when nsp1β gene

was expressed under the control of a T7 RNA polymerase promoter and an internal ribosomal entry site, the wild-type nsp1β was expressed in a similar level as its mutant (Fig. 3.9), which could due to different mRNA structure in comparison to that expressed under the control of CMV promoter. Similar to that of SARS-CoV nsp1, in infected cells, PRRSV nsp1β did not appear to suppress the expression of its own mRNA (Fig. 3.7C), suggesting the virus evolves a mechanism to recognize its own mRNA structure in infected cells. The detailed mechanism of this activity is still unknown. PRRSV nsp1β may selectively suppress the expression of host cellular genes, including those involve in host innate immune responses. This leaves intact viral mRNA and host translational machineries for viral-specific protein synthesis. Therefore, besides promoting the cellular resources benefiting for its replication, PRRSV may also use nsp1β to block host innate immune responses to establish the infection.

In order to knock down the IFN antagonist function of nsp1β, we introduced a panel of site-specific mutations into the hydrophilic regions of the protein. The effect of G**K**YLQ**R**RLQ motif mutations on nsp1β's immune suppression function highlights the importance of this region in viral pathogenesis. Our results showed that double mutations introduced at K130(124) and R134(128) residues of G**K**YLQ**R**RLQ motif impaired the function of nsp1β on the suppression of IFN-β and reporter gene expression, as well as its "self-suppression" *in vitro*. The data suggest the association between the nsp1β's function on the suppression of IFN-β and its "self-suppression", since higher expression levels of the nsp1β-K130A/R134A and nsp1β-K124A/R128A mutant proteins result in reduced ability to suppression IFN activities. More importantly, amino acid sequence analysis showed that GKYLQRRLQ motif is conserved among all known PRRSV strains, implicating its critical role in viral replication and pathogenesis. Crystal structure analysis showed that this motif is exposed on the surface of PCPβ domain. However, the PCPβ proteinase cleavage function did not seem to be directly affected by K130(124) and R134(128) mutations in our *in vitro* proteinase cleavage assay (Fig. 3.9). We suspect that these mutations may affect the nsp1β's activity on primary targeting host mRNA and interaction with host cellular gene expression shut off factors. A detail mechanism of this effect needs to be elucidated in the future.

In an effort to reduce the innate immune suppression function of PRRSV, viable recombinant viruses containing mutations in G**K**YLQ**R**RLQ motif were generated, but these viruses showed certain level of impaired growth ability. The vSD95-21-K124A/R128A mutant replication caused a reduced ability to inhibit IFN-α, IFN-β and ISG15 expression in comparison to that of wild-type virus. These data further support the notion that PRRSV nsp1β is a key factor to suppress host innate immune response in PRRSV-infected cells. In

correlation with the result from *in vitro* PCPβ cleavage assay, the data suggest that impaired replication of nsp1β mutant may not be directly caused by an effect on PCPβ cleavage, but may rather be due to an impaired ability to suppress host innate immune gene expression. However, we cannot exclude the possibility that those mutations in G**K**YLQ**R**RLQ motif may affect other replicative functions of the PCPβ domain, which could have an indirect effect on viral replication.

The identification of viral elements responsible for innate immune evasion is fundamental for the development of a modified live PRRSV vaccine. Our mutagenesis study showed that modifying the key residues in G**K**YLQ**R**RLQ motif of nsp1β could attenuate the virus growth and improve the host innate immune responses. Since the G**K**YLQ**R**RLQ motif is highly conserved among PRRSV strains, the technology developed in this study would be easily adapted to other viral strains. Future studies are needed to test the ability of nsp1β mutants for induction of protective immune responses in animals.

## 3.5 References


**Allende, R., Lewis, T. L., Lu, Z., Rock, D. L., Kutish, G. F., Ali, A., Doster, A. R. & Osorio, F. A. (1999).** North American and European porcine reproductive and respiratory syndrome viruses differ in non-structural protein coding regions. *J Gen Virol* **80 ( Pt 2)**, 307-315.

**Basler, C. F., Wang, X., Muhlberger, E., Volchkov, V., Paragas, J., Klenk, H. D., Garcia-Sastre, A. & Palese, P. (2000).** The Ebola virus VP35 protein functions as a type I IFN antagonist. *Proc Natl Acad Sci U S A* **97**, 12289-12294.

**Beura, L. K., Sarkar, S. N., Kwon, B., Subramaniam, S., Jones, C., Pattnaik, A. K. & Osorio, F. A. (2010).** Porcine reproductive and respiratory syndrome virus nonstructural protein 1beta modulates host innate immune response by antagonizing IRF3 activation. *J Virol* **84**, 1574-1584.

**Chen, Z., Lawson, S., Sun, Z., Zhou, X., Guan, X., Christopher-Hennings, J., Nelson, E. A. & Fang, Y. (2010).** Identification of two auto-cleavage products of nonstructural protein 1 (nsp1) in porcine reproductive and respiratory syndrome virus infected cells: nsp1 function as interferon antagonist. *Virology* **398**, 87-97.

**Chen, Z., Li, Y. & Krug, R. M. (1999).** Influenza A virus NS1 protein targets poly(A)-binding protein II of the cellular 3'-end processing machinery. *EMBO J* **18**, 2273-2283.

**Emini, E. A., Hughes, J. V., Perlow, D. S. & Boger, J. (1985).** Induction of hepatitis A virus-neutralizing antibody by a virus-specific synthetic peptide. *J Virol* **55**, 836-839.

**Fang, Y., Rowland, R. R., Roof, M., Lunney, J. K., Christopher-Hennings, J. & Nelson, E. A. (2006).** A full-length cDNA infectious clone of North American type 1 porcine reproductive and respiratory syndrome virus: expression of green fluorescent protein in the Nsp2 region. *J Virol* **80**, 11447-11455.

**Fang, Y. & Snijder, E. J. (2010).** The PRRSV replicase: exploring the multifunctionality of an intriguing set of nonstructural proteins. *Virus Res* **154**, 61-76.

**Fang, Y., Treffers, E. E., Li, Y., Tas, A., Sun, Z., van der Meer, Y., de Ru, A. H., van Veelen, P. A., Atkins, J. F., Snijder, E. J. & Firth, A. E. (2012).** Efficient -2 frameshifting by mammalian ribosomes to synthesize an additional arterivirus protein. *Proc Natl Acad Sci U S A* **109**, E2920-2928.

**Foy, E., Li, K., Wang, C., Sumpter, R., Jr., Ikeda, M., Lemon, S. M. & Gale, M., Jr. (2003).** Regulation of interferon regulatory factor-3 by the hepatitis C virus serine protease. *Science* **300**, 1145-1148.

**Fuerst, T. R., Niles, E. G., Studier, F. W. & Moss, B. (1986).** Eukaryotic transient-expression system based on recombinant vaccinia virus that synthesizes bacteriophage T7 RNA polymerase. *Proc Natl Acad Sci U S A* **83**, 8122-8126.

**Gouet, P., Courcelle, E., Stuart, D. I. & Metoz, F. (1999).** ESPript: analysis of multiple sequence alignments in PostScript. *Bioinformatics* **15**, 305-308.

**Hopp, T. P. & Woods, K. R. (1981).** Prediction of protein antigenic determinants from amino acid sequences. *Proc Natl Acad Sci U S A* **78**, 3824-3828.

**Huang, C., Lokugamage, K. G., Rozovics, J. M., Narayanan, K., Semler, B. L. & Makino, S. (2011).** SARS coronavirus nsp1 protein induces template-dependent endonucleolytic cleavage of mRNAs: viral mRNAs are resistant to nsp1-induced RNA cleavage. *PLoS Pathog* **7**, e1002433.

**Kamitani, W., Huang, C., Narayanan, K., Lokugamage, K. G. & Makino, S. (2009).** A two-pronged strategy to suppress host protein synthesis by SARS coronavirus Nsp1 protein. *Nat Struct Mol Biol* **16**, 1134-1140.

**Kamitani, W., Narayanan, K., Huang, C., Lokugamage, K., Ikegami, T., Ito, N., Kubo, H. & Makino, S. (2006).** Severe acute respiratory syndrome coronavirus nsp1 protein suppresses host gene expression by promoting host mRNA degradation. *Proc Natl Acad Sci U S A* **103**, 12885-12890.

**Kim, O., Sun, Y., Lai, F. W., Song, C. & Yoo, D. (2010).** Modulation of type I interferon induction by porcine reproductive and respiratory syndrome virus and degradation of CREB-binding protein by non-structural protein 1 in MARC-145 and HeLa cells. *Virology* **402**, 315-326.

**Kolaskar, A. S. & Tongaonkar, P. C. (1990).** A semi-empirical method for prediction of antigenic determinants on protein antigens. *FEBS Lett* **276**, 172-174.

**Komatsu, T., Takeuchi, K., Yokoo, J. & Gotoh, B. (2004).** C and V proteins of Sendai virus target signaling pathways leading to IRF-3 activation for the negative regulation of interferon-beta production. *Virology* **325**, 137-148.

**Larkin, M. A., Blackshields, G., Brown, N. P., Chenna, R., McGettigan, P. A., McWilliam, H., Valentin, F., Wallace, I. M., Wilm, A., Lopez, R., Thompson, J. D., Gibson, T. J. & Higgins, D. G. (2007).** Clustal W and Clustal X version 2.0. *Bioinformatics* **23**, 2947-2948.

**Lawson, S. R., Li, Y., Patton, J. B., Langenhorst, R. J., Sun, Z., Jiang, Z., Christopher-Hennings, J., Nelson, E. A., Knudsen, D., Fang, Y. & Chang, K. O. (2012).** Interleukin-1beta expression by a recombinant porcine reproductive and respiratory syndrome virus. *Virus Res* **163**, 461-468.

**Le May, N., Dubaele, S., Proietti De Santis, L., Billecocq, A., Bouloy, M. & Egly, J. M. (2004).** TFIIH transcription factor, a target for the Rift Valley hemorrhagic fever virus. *Cell* **116**, 541-550.

**Li, Y., Tas, A., Snijder, E. J. & Fang, Y. (2012).** Identification of porcine reproductive and respiratory syndrome virus ORF1a-encoded non-structural proteins in virus-infected cells. *J Gen Virol* **93**, 829-839.

**Lokugamage, K. G., Narayanan, K., Huang, C. & Makino, S. (2012).** Severe Acute Respiratory Syndrome Coronavirus Protein nsp1 Is a Novel Eukaryotic Translation

Inhibitor That Represses Multiple Steps of Translation Initiation. *J Virol* **86**, 13598-13608.

**Miller, M. (2011).** PRRS price tag, $664 million. *Porknetwork http://www porknetwork com/pork-news/PRRS-price-tag-641-million–127963843 html*.

**Narayanan, K., Huang, C., Lokugamage, K., Kamitani, W., Ikegami, T., Tseng, C. T. & Makino, S. (2008).** Severe acute respiratory syndrome coronavirus nsp1 suppresses host gene expression, including that of type I interferon, in infected cells. *J Virol* **82**, 4471-4479.

**Nelsen, C. J., Murtaugh, M. P. & Faaberg, K. S. (1999).** Porcine reproductive and respiratory syndrome virus comparison: divergent evolution on two continents. *J Virol* **73**, 270-280.

**Patel, D., Nan, Y., Shen, M., Ritthipichai, K., Zhu, X. & Zhang, Y. J. (2010).** Porcine reproductive and respiratory syndrome virus inhibits type I interferon signaling by blocking STAT1/STAT2 nuclear translocation. *J Virol* **84**, 11045-11055.

**Ropp, S. L., Wees, C. E., Fang, Y., Nelson, E. A., Rossow, K. D., Bien, M., Arndt, B., Preszler, S., Steen, P., Christopher-Hennings, J., Collins, J. E., Benfield, D. A. & Faaberg, K. S. (2004).** Characterization of emerging European-like porcine reproductive and respiratory syndrome virus isolates in the United States. *J Virol* **78**, 3684-3703.

**Snijder, E. J. & Meulenberg, J. J. (1998).** The molecular biology of arteriviruses. *J Gen Virol* **79 ( Pt 5)**, 961-979.

**Snijder, E. J., Wassenaar, A. L. & Spaan, W. J. (1994).** Proteolytic processing of the replicase ORF1a protein of equine arteritis virus. *J Virol* **68**, 5755-5764.

**Song, C., Krell, P. & Yoo, D. (2010).** Nonstructural protein 1alpha subunit-based inhibition of NF-kappaB activation and suppression of interferon-beta production by porcine reproductive and respiratory syndrome virus. *Virology* **407**, 268-280.

**Sun, Z., Li, Y., Ransburgh, R., Snijder, E. J. & Fang, Y. (2012).** Nonstructural protein 2 of porcine reproductive and respiratory syndrome virus inhibits the antiviral function of interferon-stimulated gene 15. *J Virol* **86**, 3839-3850.

**Wang, X., Li, M., Zheng, H., Muster, T., Palese, P., Beg, A. A. & Garcia-Sastre, A. (2000).** Influenza A virus NS1 protein prevents activation of NF-kappaB and induction of alpha/beta interferon. *J Virol* **74**, 11566-11573.

**Weber, F., Kochs, G. & Haller, O. (2004).** Inverse interference: how viruses fight the interferon system. *Viral Immunol* **17**, 498-515.

**Xue, F., Sun, Y., Yan, L., Zhao, C., Chen, J., Bartlam, M., Li, X., Lou, Z. & Rao, Z. (2010).** The crystal structure of porcine reproductive and respiratory syndrome virus nonstructural protein Nsp1beta reveals a novel metal-dependent nuclease. *J Virol* **84**, 6461-6471.

**Yoneyama, M., Suhara, W., Fukuhara, Y., Sato, M., Ozato, K. & Fujita, T. (1996).** Autocrine amplification of type I interferon gene expression mediated by interferon stimulated gene factor 3 (ISGF3). *J Biochem* **120**, 160-169.

**Yoo, D., Song, C., Sun, Y., Du, Y., Kim, O. & Liu, H. C. (2010).** Modulation of host cell responses and evasion strategies for porcine reproductive and respiratory syndrome virus. Virus Res **154**, 48-60.

**Zeman, D., Neiger, R., Yaeger, M., Nelson, E., Benfield, D., Leslie-Steen, P., Thomson, J., Miskimins, D., Daly, R. & Minehart, M. (1993).** Laboratory investigation of PRRS virus infection in three swine herds. *J Vet Diagn Invest* **5**, 522-528.

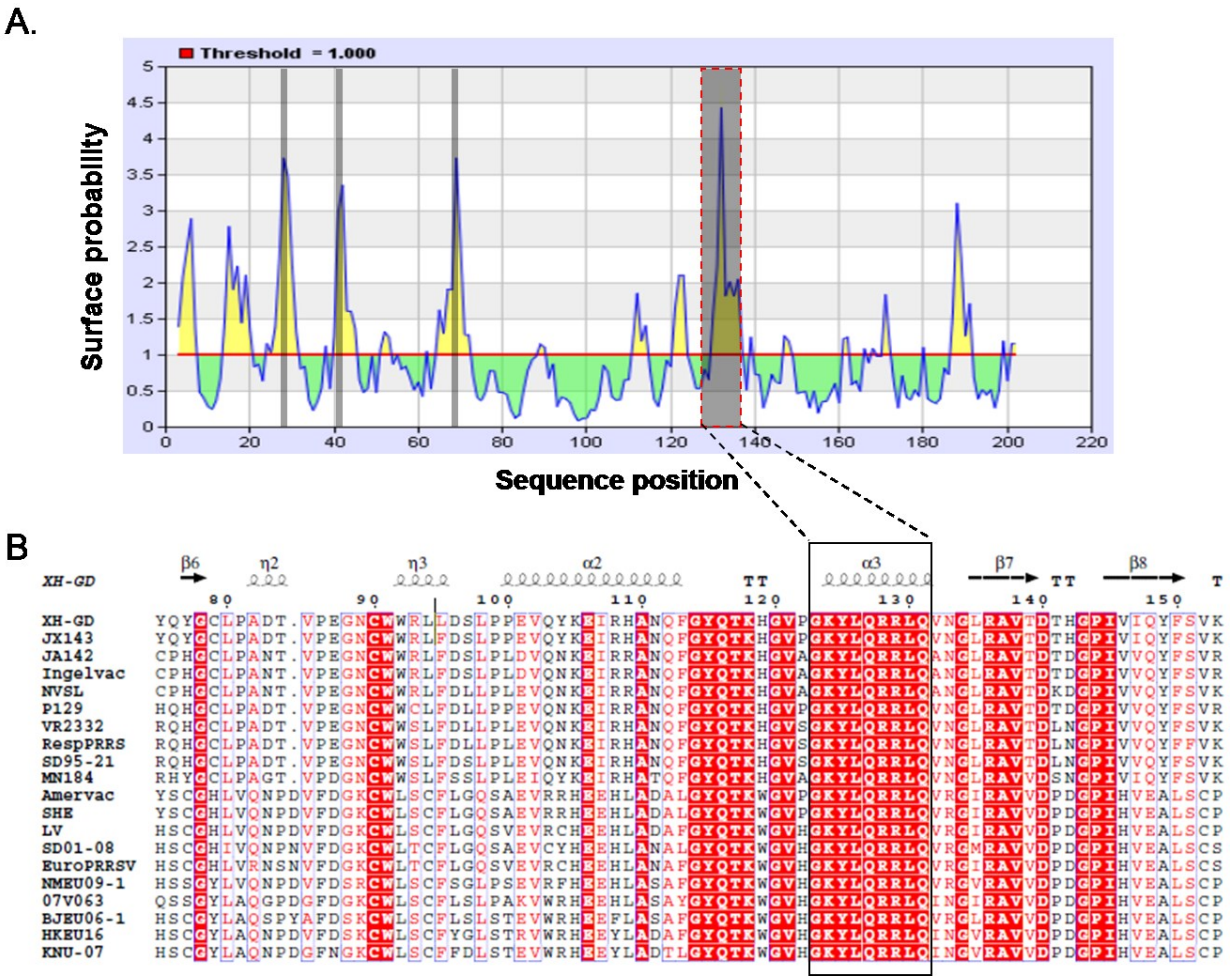


**Figure 3. 1 Surface accessibility prediction and sequence alignment of nsp1β.** (A) Emini surface accessibility prediction, four peaks highlighted with gray boxes shown the highest surface accessiblity values. (B) Amino acid sequence alignment of nsp1β from representative type 1 and type 2 PRRSV strains. The secondary-structure elements of PRRSV nsp1β are shown on the top of alignment based on the crystal structure of type 2 PRRSV XH-GD strain (Xue et al., 2010). The conserved motif, GKYLQRRLQ, is highlighted in black box. Amino acid numbers on the top refer to the residue position in nsp1β sequence of XH-GD strain. Sequences presented in the figure were from GenBank: GU737264 (07V063), GU067771 (Amervac PRRS), GU047344 (BJEU06-1), AY366525 (EuroPPRSV), EU076704 (HKEU16), FJ349261 (KNU-07), M96262 (LV; Lelystad Virus), GU047345 (NMEU09-1), DQ489311 (SD01-08), GQ461593 (SHE), EU624117 (XH-GD), EU708726 (JX143), AY424271 (JA142), DQ988080 (Ingelvac ATP), AF325691 (NVSL), AF494042 (P129), EF536003 (VR2332), EF488739 (MN184), AF066183.4 (RespPRRS MLV), KC469618 (SD95-21).

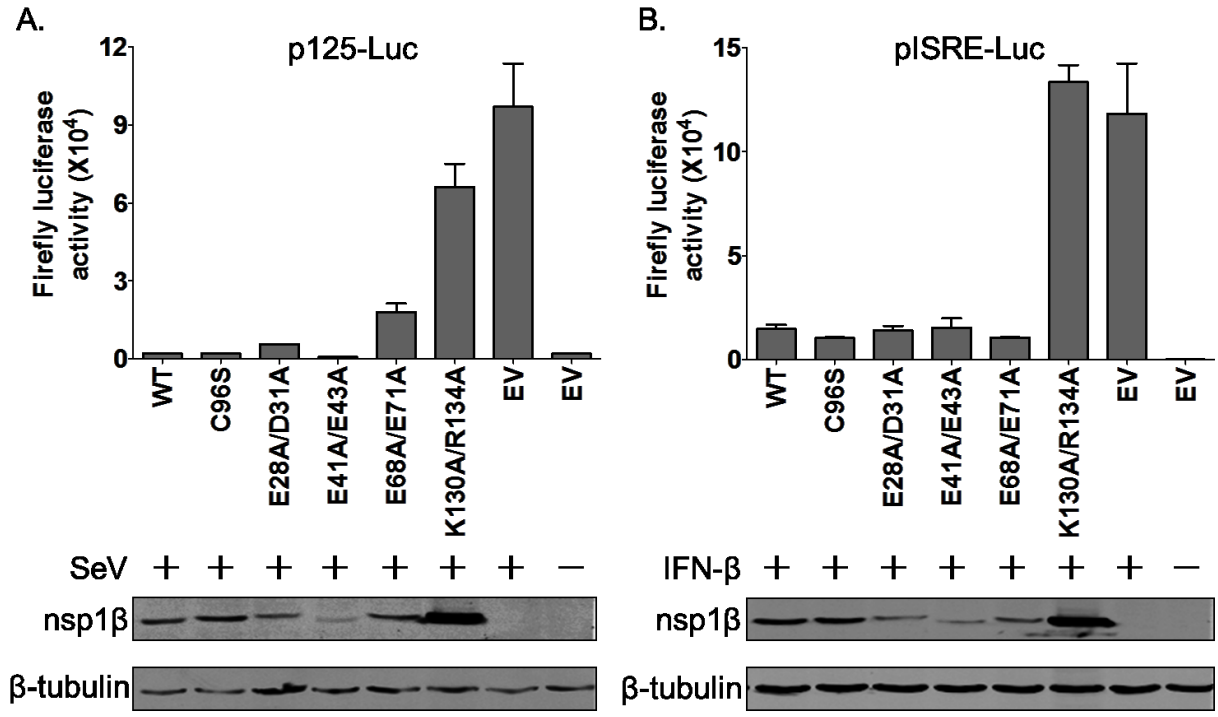


**Figure 3. 2 Effect of mutations on type 1 PRRSV nsp1β expression and its ability to inhibit IFN-β activation and signaling.** (A) HEK-293T cells were cotransfected with p125-Luc and a plasmid expressing FLAG-tagged nsp1β of PRRSV SD01-08 (WT) or its mutants. The empty plasmid vector (EV) was included as a control. At 20 h post transfection, cells were infected with SeV (100 HA units/ml) to stimulate the production of type I IFN. The luciferase activity was measured at 12-16 h post stimulation. (B) HEK-293T cells were cotransfected with pISRE-Luc and a plasmid expressing FLAG-tagged nsp1β (WT) or its mutants or empty vector (EV). Cells were treated with IFN-β (2000 IU/ml) for 16 h. The cells were harvested and measured for the firefly luciferase activity. The expression of nsp1β protein was analyzed by Western blot. Membranes were stained with anti-FLAG and anti-β tubulin monoclonal antibodies. Each experiment was repeated three times and a mean value was calculated. Error bars show standard deviations.

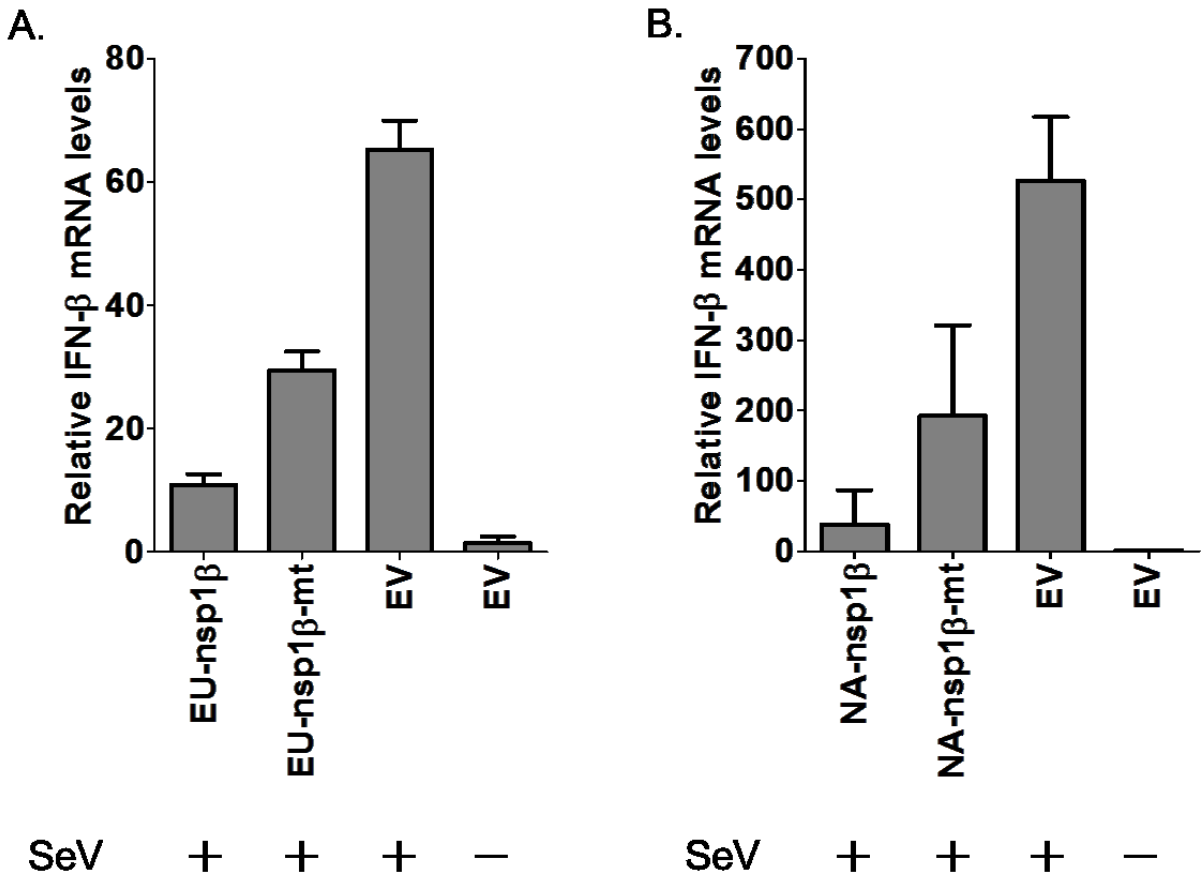


**Figure 3. 3 Effect of amino acids K130(124) and R134(128) mutations on the ability of nsp1β to suppress IFN-β mRNA expression.** (A) HEK-293T cells were transfected with a plasmid expressing type 1 PRRSV nsp1β (EU-nsp1β) or K130A/R134A mutant (EU-nsp1β-mt). (B) HEK-293T cells were transfected with a plasmid expressing type 2 PRRSV nsp1β (NA-nsp1β) or K124A/R128A (NA-nsp1β-mt). The empty plasmid vector (EV) was used as a control. Cells were mock-infected or infected with 100 HA units/ml SeV for 16 h. Cells were harvested and the level of IFN-β mRNA expression was measured by quantitative RT-PCR. The relative amount of IFN-β mRNAs was normalized to the expression level of endogenous 18S rRNA. Each experiment was repeated three times.

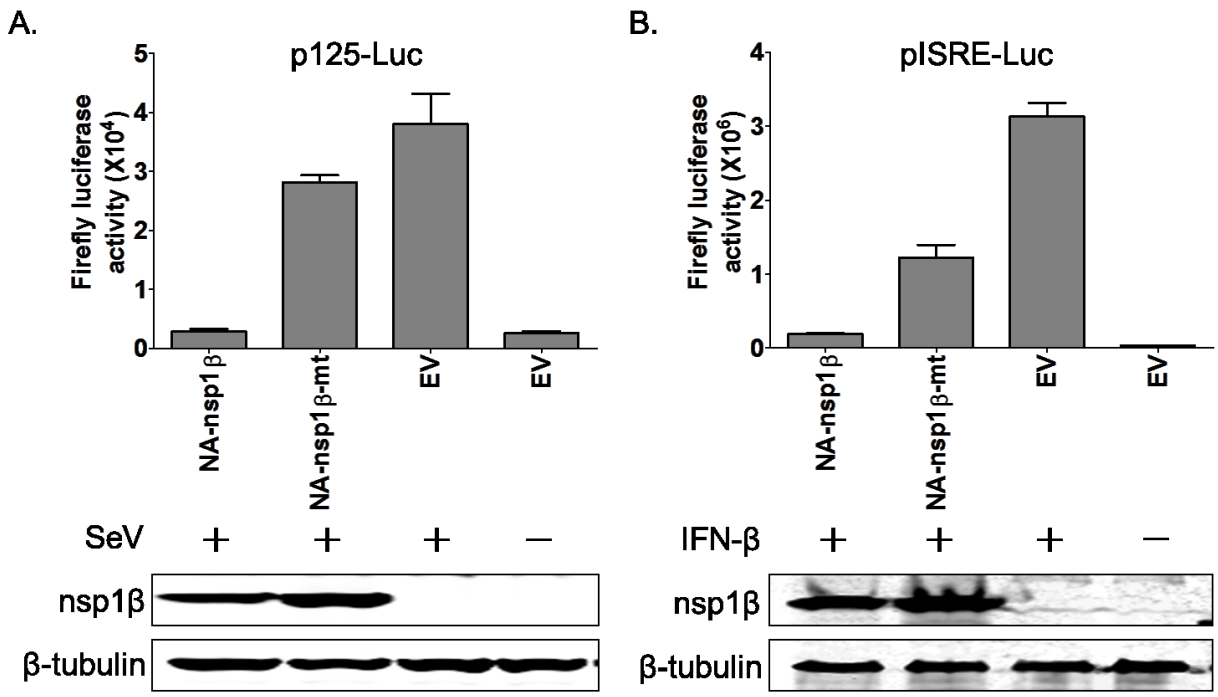


**Figure 3. 4 Effect of K124A/R128A mutations on type 2 PRRSV nsp1β expression and its ability to inhibit IFN-β activation and signaling.** (A) HEK-293T cells were cotransfected with p125-Luc and a plasmid expressing FLAG-tagged nsp1β of PRRSV SD95-21 (NA-nsp1β) or K124A/R128A mutant (NA-nsp1β-mt). The empty plasmid vector (EV) was included as a control. At 24 h post transfection, cells were infected with Sendai virus (SeV, 100 HA units/ml) to stimulate the type I IFN activation. The luciferase activity was measured at 12-16 h post stimulation. (B) HEK-293T cells were cotransfected with pISRE-Luc and a plasmid expressing FLAG-tagged nsp1β (NA-nsp1β) or K124A/R128A mutant (NA-nsp1β-mt) or empty vector (EV). Cells were treated with IFN-β (2000 IU/ml) for 16 h. Cells were harvested and measured for firefly luciferase activity. Each experiment was repeated three times. Standard deviations are shown as error bars. Western blot analysis was performed to evaluate the expression of nsp1β in both experiments using anti-FLAG mAbs. Membranes were also stained with anti-β tubulin antibody for loading control.

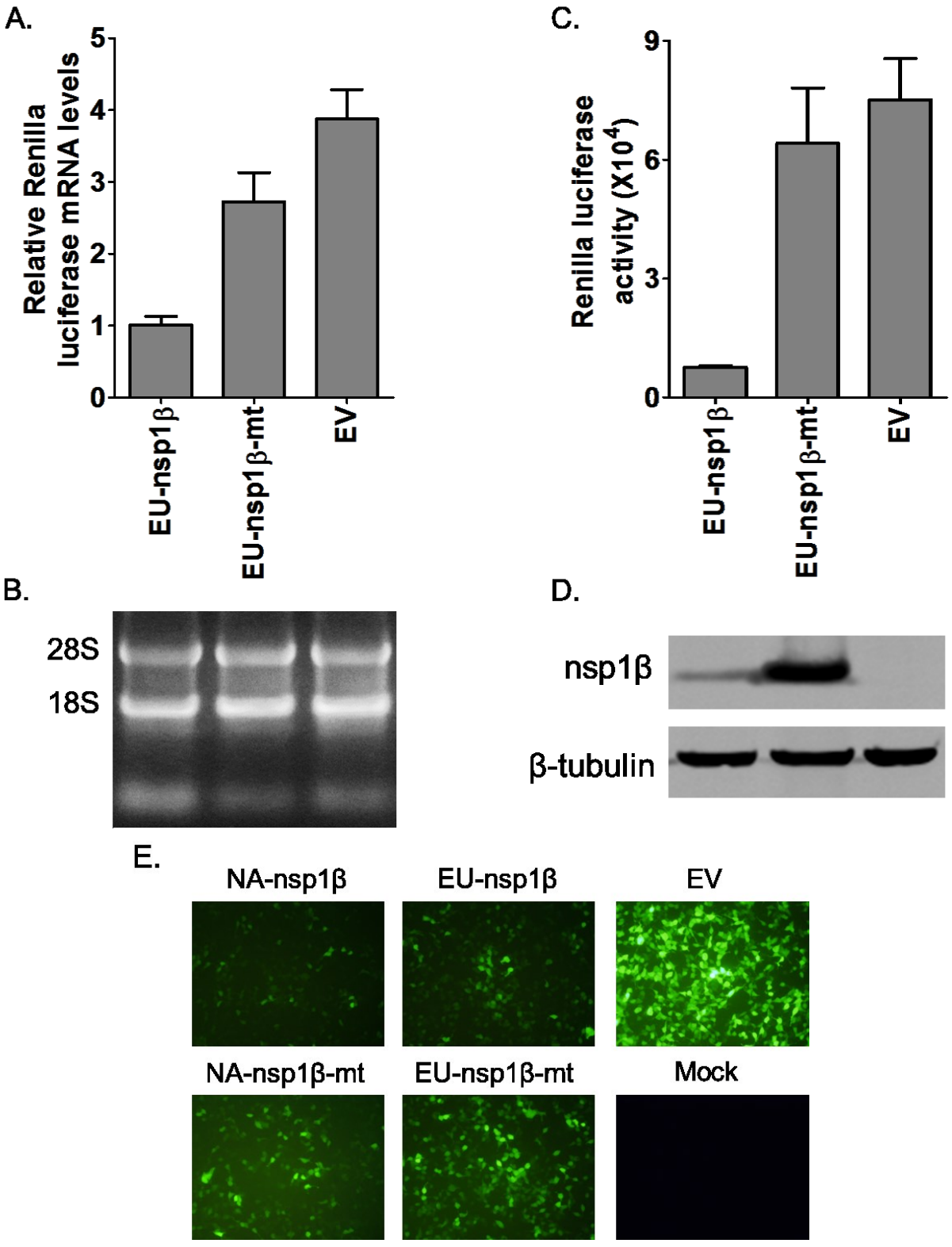
A.
Relative Renilla luciferase mRNA levels
0
1
2
3
4
5
EU-nsp1β
EU-nsp1β-mt
EV
C.
Renilla luciferase activity (X10^4)
0
3
6
9
EU-nsp1β
EU-nsp1β-mt
EV
B.
28S
18S
D.
nsp1β
β-tubulin
E.
NA-nsp1β
EU-nsp1β
EV
NA-nsp1β-mt
EU-nsp1β-mt
Mock

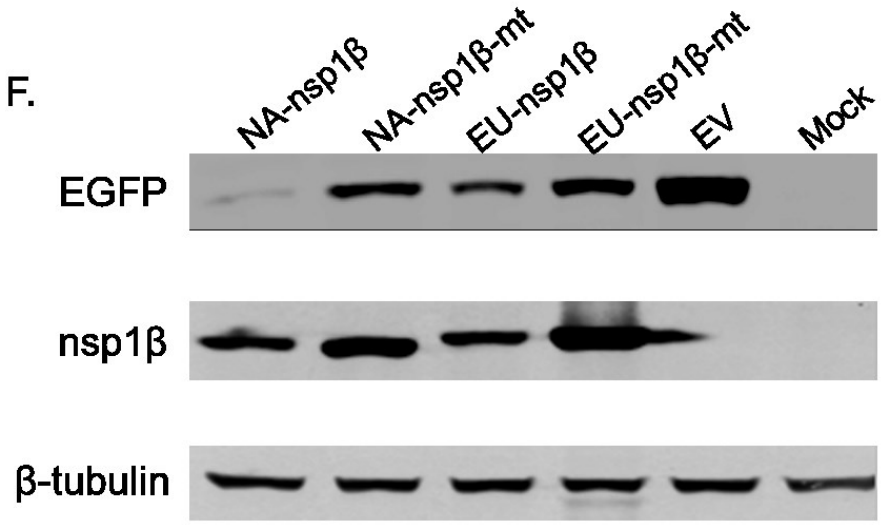


**Figure 3. 5 Effect of nsp1β on the expression of reporter genes.** (A-D) Effect of nsp1β on *Renilla* luciferase reporter gene expression. HEK-293T cells were cotransfected with the reporter plasmid pRL-SV40 and a plasmid expressing FLAG-tagged nsp1β (EU-nsp1β) or K130A/R134A mutant (EU-nsp1β-mt) or empty vector (EV). At 24 h post transfection, cells were harvested for RNA or protein quantification. (A) The amount of *Renilla* luciferase mRNAs was quantified by real-time PCR, and normalized to the expression level of endogenous 18S rRNA. (B) Ethidium Bromide Staining for detection of rRNA expression. (C) The *Renilla* luciferase activity measured by luciferase assay (Promega). Each experiment was repeated three times and the data are presented as mean values and standard deviations. (D) Western blot analysis for the expression of FLAG-tagged nsp1β and its mutant. (E-F) Effect of nsp1β on EGFP reporter gene expression. HEK-293T cells were cotransfected with the pEGFP-N1 and a plasmid expressing type 1 PRRSV nsp1β (EU-nsp1β) or K130A/R134A mutant (EU-nsp1β-mt), type 2 PRRSV nsp1β (NA-nsp1β) or K124A/R128A mutant (NA-nsp1β-mt). Empty plasmid vector (EV) was included as a control. (E) EGFP reporter gene expression was observed under fluorescence microscopy, and pictures were taken at 24 h post transfection. (F) Western blot analysis for detection the expression of EGFP and nsp1β. The membrane was stained with anti-FLAG and anti-EGFP mAbs. β-tubulin was detected as a loading control in all experiments.

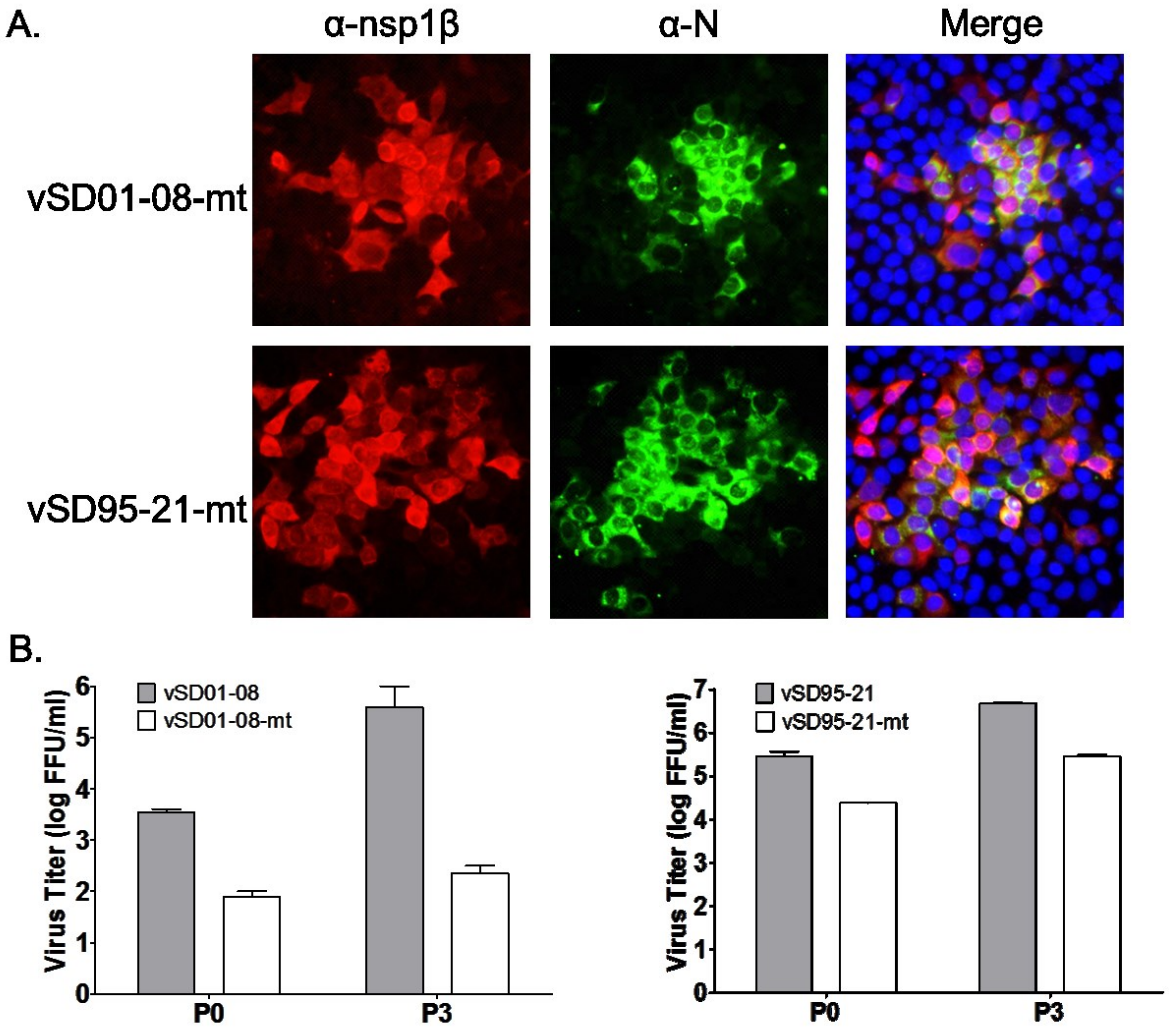


**Figure 3. 6 Recovery and growth characterization of vSD01-08-K130A/R134A (vSD01-08-mt) and vSD95-21-K124A/R128A (vSD95-21-mt) recombinant viruses.** (A) Recovery of recombinant viruses from cells transfected with full-length cDNA of wild-type viruses or nsp1β mutants. The fixed cells were first stained with a primary anti-nsp1β mAb at 37°C for 1 h. The Alexa Fluor 549-labeled goat anti-mouse antibody (Kirkegaard & Perry Laboratories) was used as a secondary antibody for detecting the expression of nsp1β. Nucleocapsid protein was detected by staining the cells with FITC-conjugated mAb SDOW17. Cell nucleus was stained with 4', 6-diamidino-2-phenylindole (DAPI, Molecular Probes). Images were obtained by fluorescence and phase-contrast microscopy using a 20X objective. (B) Virus titers of the parental and mutant viruses. P0: parental and recombinant viruses originally recovered from BHK-21 cells transfected with the full-length cDNA; P3: viruses passaged three times on MARC-145 cells.

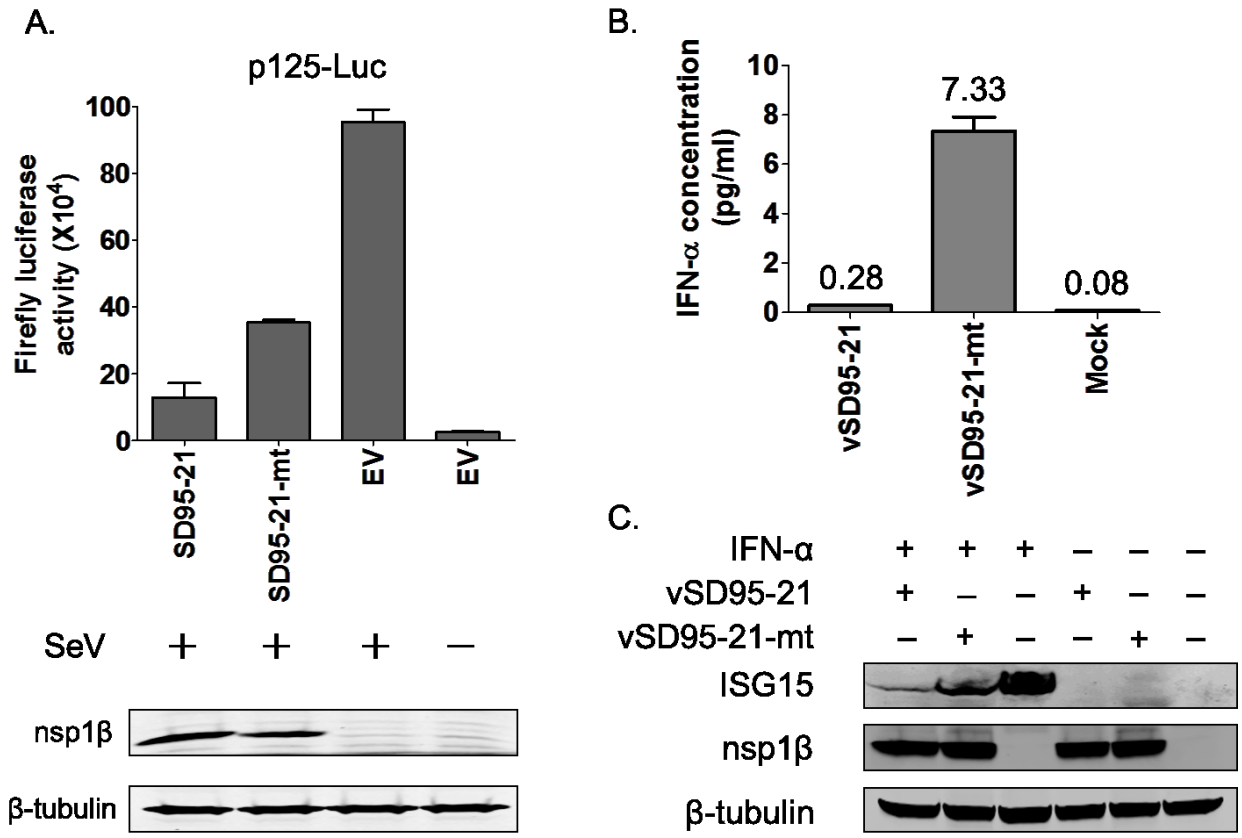


**Figure 3. 7 Effect of nsp1β K124/R128A mutations on the ability of PRRSV to inhibit IFN-β activation and signaling.** (A) HEK-293T cells were cotransfected with p125-Luc () and pCMV-SD95-21(SD95-21), p125-Luc and pCMV-SD95-21-K124/R128A (SD95-21-mt), or p125-Luc and empty plasmid vector (EV). At 24 h after transfection, cells were mock-infected or infected with 100 HA units/ml SeV to stimulate the production of type I IFN. Cells were harvested and luciferase activity was measured at 16 hpi. Western blot analysis was performed to detect nsp1β expression using anti-nsp1β mAb. (B) Swine macrophages were infected with 1 MOI of parental virus (vSD95-21), nsp1β K124A/R128A mutated virus (vSD95-21-mt), or mock-infected. At 24 hpi, culture supernatant was harvested for analyzing the IFN-α expression. Each experiment was repeated three times and the data are presented as mean values with standard deviations. (C) MARC-145 cells were infected with 0.1 MOI of vSD95-21, vSD95-21-mt, or mock-infected. At 18 hpi, cells were mock-treated or treated with 10000 IU/ml of IFN-α for 12 h. Cells were harvested and subjected to Western blot analysis. Membrane was probed with anti-ISG15 and anti-nsp1β mAbs for detecting the expression of ISG15 and nsp1β, and the β-tubulin expression was detected as a loading control.

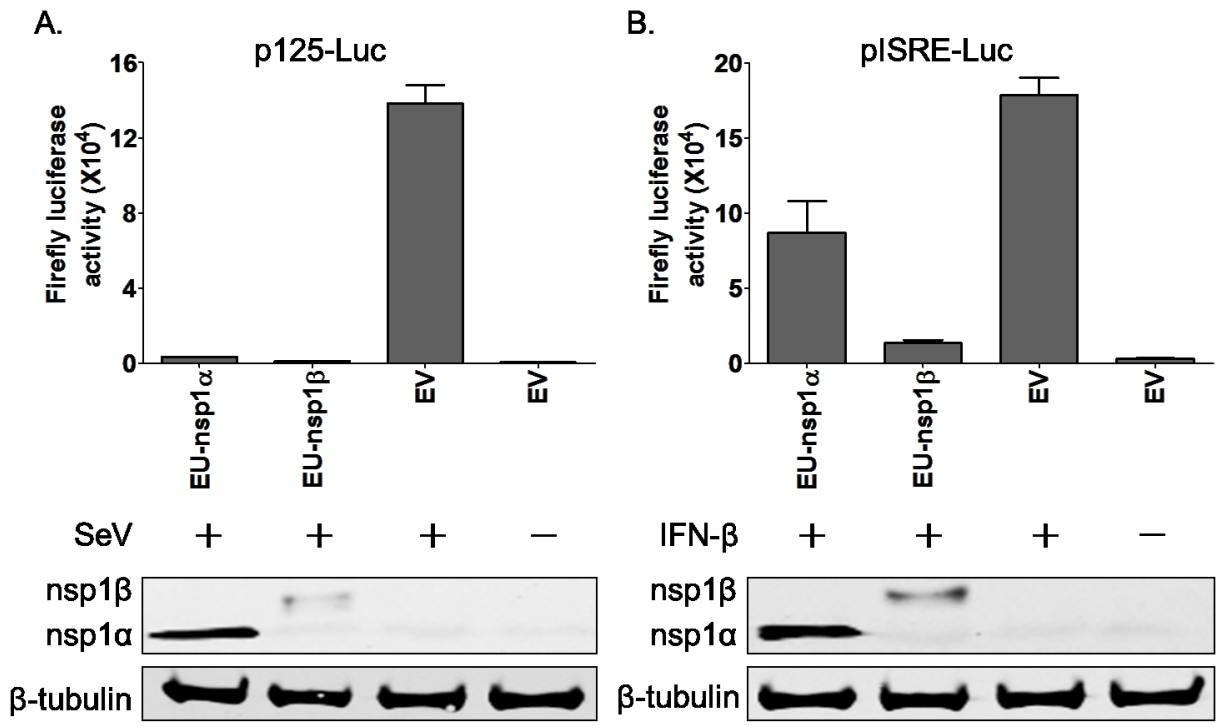


**Figure 3. 8 PRRSV nsp1α and nsp1β inhibit IFN-β expression and signaling.** HEK-293T cells were cotransfected with a plasmid expressing FLAG-tagged nsp1α (EU-nsp1α) or nsp1β (EU-nsp1β), and p125-Luc (A) or pISRE-Luc (B). The empty plasmid vector (EV) was used as a control. (A) Cells were mock-infected or infected with 100 HA units /ml SeV for 16 h; (B) Cells were mock-treated or treated with 2000 IU/ml IFN-β for 16 h. Cells were harvested and measured for firefly luciferase activity. Each experiment was repeated three times and a mean value was calculated. Error bars show the standard deviation of a mean value. Western blot analysis was performed to evaluate the expression of nsp1α, nsp1β and β-tubulin. Membranes were stained with anti-FLAG and anti-β tubulin mAbs.

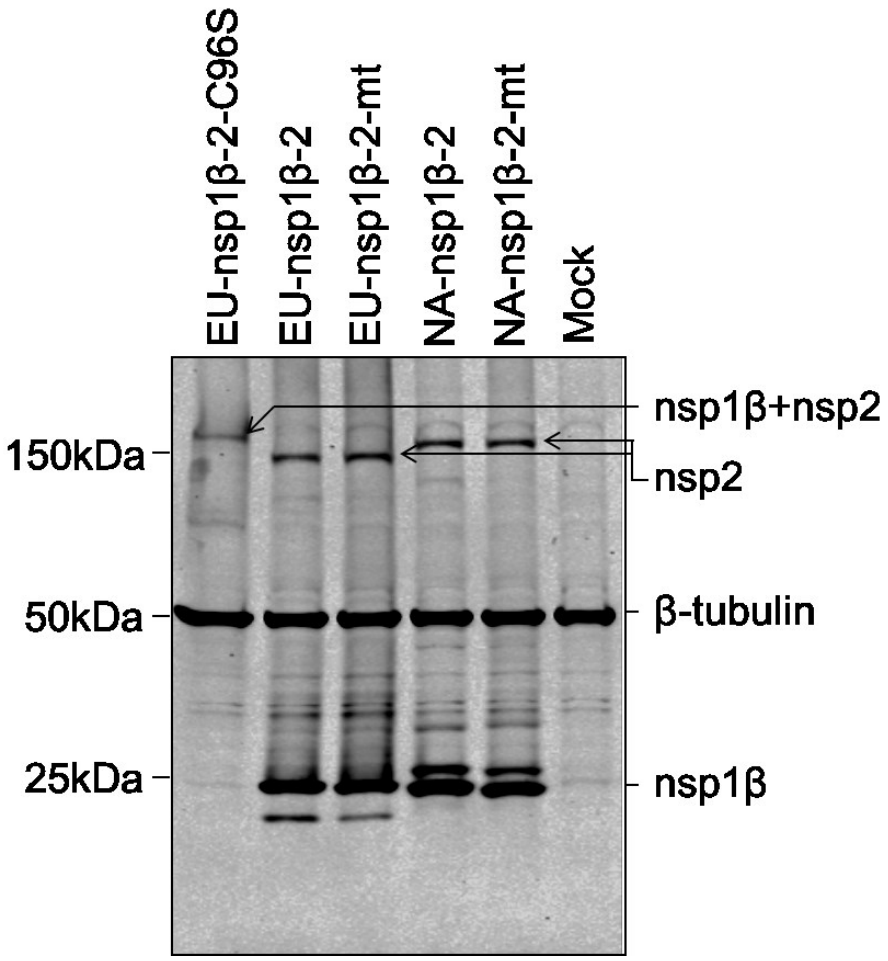


**Figure 3. 9 Effect of amino acids K130(124) and R134(128) mutations on the proteolytic cleavage activity of PCPβ.** HEK-293T cells were infected with the recombinant vaccinia virus at 10 MOI. After 1 hpi, cells were transfected with pL-EU-nsp1β-2-C96S, pL-EU-nsp1β-2, pL-EU-nsp1β-2-mt, pL-NA-nsp1β-2, or pL-NA-nsp1β-2-mt. The cells were harvested at 24 h post transfection and subjected to western blot analysis using mAbs specific to nsp1β and nsp2. The β-tubulin was detected as a loading control.

**Table 3. 1 List of constructs used in this study**

| Construct | Mutation | WT codon | Mutant codon | Virus strain |
|---|---|---|---|---|
| E28A/D31A | E-28→A | GAA | GCA | Type 1 |
| | D-31→A | GAC | GCC | |
| E41A/E43A | E-41→A | GAG | GCG | Type 1 |
| | E-43→A | GAA | GCA | |
| E68A/E71A | E-68→A | GAG | GCG | Type 1 |
| | E-71→A | GAG | GCG | |
| **K130A/R134A** | K-130→A | AAG | GCG | Type 1 |
| | R-134→A | CGC | GCC | |
| **K124A/R128A** | K-124→A | AAG | GCG | Type 2 |
| | R-128→A | CGG | GCG | |
| C96S | C-96→A | TGC | AGC | Type 1 |

# Chapter 4 - Transactivation of programmed ribosomal frameshifting by a viral protein

**Abstract:** Programmed –1 ribosomal frameshifting (–1 PRF) is a widely used translational mechanism facilitating the expression of two polypeptides from a single mRNA. Commonly, the ribosome interacts with an mRNA secondary structure that promotes –1 frameshifting on a homopolymeric slippery sequence. Recently, Fang *et al.* (2012) described an unusual –2 frameshifting (–2 PRF) signal directing efficient expression of a transframe protein (nsp2TF) of porcine reproductive and respiratory syndrome virus (PRRSV) from an alternative reading frame overlapping the viral replicase gene. Unusually, this arterivirus PRF signal lacks an obvious stimulatory RNA secondary structure, but as confirmed here, can also direct the occurrence of –1 PRF, yielding a third, truncated nsp2 variant named nsp2N. Remarkably, we now show that both –2 and –1 PRF are transactivated by a protein factor, specifically a PRRSV replicase subunit (nsp1β). Embedded in nsp1β's papain-like autoproteinase domain, we identified a highly conserved, putative RNA-binding motif that is critical for PRF transactivation. The minimal RNA sequence required for PRF was mapped within a 34-nucleotide region that includes the slippery sequence and a downstream conserved CCCANCUCC motif. Interaction of nsp1β with the PRF signal was demonstrated in pull-down assays. These studies demonstrate for the first time that a protein can function as a *trans*activator of ribosomal frameshifting. The newly-identified frameshifting determinants provide potential anti-viral targets for arterivirus disease control and prevention. Moreover, protein-induced *trans*activation of frameshifting may be a widely employed mechanism, potentially including previously undiscovered viral strategies to regulate viral gene expression and/or modulate host cell translation upon infection.

## 4.1 Introduction

Among the repertoire of mechanisms that viruses use to control or regulate their gene expression, non-canonical translation plays an important role, in particular for positive-strand RNA viruses whose genomic RNA serves a dual function as mRNA and genome [reviewed in (Firth & Brierley, 2012)]. A commonly used strategy is –1 programmed ribosomal frameshifting (–1 PRF), in which mRNA signals induce a significant proportion of translating ribosomes to change reading frame, with ribosomes slipping back (in the 5' direction) by one nucleotide (nt) into an overlapping open reading frame (ORF) before continuing translation,

generating a fusion protein composed of the products of both upstream and downstream ORFs [reviewed in (Atkins & Bjork, 2009; Brierley *et al.*, 2010; Firth & Brierley, 2012; Giedroc & Cornish, 2009)]. PRF was first described as the mechanism by which the Gag-Pol polyprotein of the retrovirus Rous sarcoma virus (RSV) is expressed from overlapping *gag* and *pol* ORFs (Jacks *et al.*, 1988a; Jacks & Varmus, 1985) and related signals have since been documented in many other viruses of medical, veterinary, and agricultural importance (Firth & Atkins, 2009; Jacks *et al.*, 1988b; Mador *et al.*, 1989; Nam *et al.*, 1993; Thiel *et al.*, 2003). PRF has also been increasingly recognized in cellular genes of both prokaryotes and eukaryotes as well as in other replicating elements, such as insertion sequences and transposons (Atkins & Gesteland, 2010).

Recently, we identified an unusual –2 programmed ribosomal frameshifting (–2 PRF) event that operates during the translation of the genome of porcine reproductive and respiratory syndrome virus (PRRSV), a member of the arterivirus family in the order *Nidovirales* (Fang *et al.*, 2012). PRRSV can be divided into distinct European (EU, type 1) and North American (NA, type 2) genotypes. The viral genome comprises a positive-sense RNA molecule, ~15 kb in length (Snijder *et al.*, 2013). As in other nidoviruses, its 5' proximal region contains two large replicase open reading frames [ORF1a and ORF1b; (Fang & Snijder, 2010)], with the ORF1b product being expressed as a fusion with the ORF1a product following –1 PRF in the short ORF1a/ORF1b overlap region (see Fig. 4.1). Four ORF1a-encoded proteinases (residing in nsp1α, nsp1β, nsp2, and nsp4) subsequently cleave the pp1a and pp1ab polyproteins into (at least) 14 different non-structural proteins (nsps; Fig. 4.1A). The recently identified –2 PRF signal is located several kilobases upstream of the ORF1a/ORF1b –1 PRF signal, and maps to the part of ORF1a that encodes nsp2. This large, multifunctional replicase subunit is involved in diverse steps of the arterivirus replicative cycle, including replicase polyprotein processing (Wassenaar *et al.*, 1997), the formation of replication structures (Knoops *et al.*, 2012; Snijder *et al.*, 2001), and innate immune evasion (Frias-Staheli *et al.*, 2007; Sun *et al.*, 2010; Sun *et al.*, 2012; van Kasteren *et al.*, 2013). At the PRRSV –2 PRF signal, a proportion of ribosomes back up two nucleotides, to generate a transframe fusion protein (nsp2TF) comprising the N-terminal two-thirds of nsp2 and the product encoded by a conserved alternative ORF (transframe; TF) in the –2 reading frame. Compared to full-length nsp2, the nsp2TF product is truncated, equipped with an alternative C-terminal transmembrane domain (Fig. 4.1A), and targeted to a different subcellular compartment (Fang *et al.*, 2012). Mutations preventing nsp2TF expression reduce PRRSV replication efficiency in cell culture 50- to 100-fold, highlighting the biological importance of

the frameshifting event and nsp2TF expression. The –2 PRF takes place at a highly conserved RG_GUU_UUU slippery sequence (R = G or A), and frameshifting is remarkably efficient [around 20% in virus-infected cells and up to 50% in expression systems; (Fang *et al.*, 2012)].

As depicted in Fig. 4.1B-C, the elements that promote PRF in PRRSV are quite distinct. The –1 PRF signal at the ORF1a/1b junction comprises a "slippery" sequence (generally U_UUA_AAC) where the ribosome changes frame, and a stimulatory RNA pseudoknot structure immediately downstream, an organization that is conserved throughout the *Nidovirales* order (Brierley *et al.*, 1989; den Boon *et al.*, 1991) and widely used in other viral –1 PRF mechanisms. It is thought that interaction of the translating ribosome with the pseudoknot confounds its RNA-unwinding activity (Qu *et al.*, 2011; Takyar *et al.*, 2005) and may induce tension in the mRNA that assists in the uncoupling of codon:anticodon interactions at the shift site (Lin *et al.*, 2012; Namy *et al.*, 2006; Plant & Dinman, 2005). In contrast, only a few cases of –2 PRF in mammalian cells have been documented thus far (Fang *et al.*, 2012; Lin *et al.*, 2012) and the elements involved are poorly understood. Our previous computer-based RNA folding analysis suggested that the RNA downstream of the slippery sequence (RG_GUU_UUU) used for –2 PRF in PRRSV is rather unstructured and does not fold into a structure compatible with canonical RNA-structure-stimulated PRF However, mutations within a conserved CCCANCUCC motif located 11 nt downstream of the shift site can reduce or inhibit frameshifting, consistent with the presence of a 3' stimulatory element of some form (Fang *et al.*, 2012). Remarkably, our previous study also provided indications for the occurrence of efficient –1 frameshifting at (or near) the same slippery sequence. Due to the presence of a translation termination codon in the –1 reading frame immediately following the slippery sequence, this would yield a truncated form of nsp2, termed nsp2N (Fig. 4.1A).

In this report, we identify PRRSV replicase subunit nsp1β as a transactivator of efficient –2 and –1 PRF at the same slippery sequence and provide evidence that its frameshift-stimulatory activity requires interaction with the viral mRNA. In support of this, a highly conserved putative RNA-binding motif (GKYLQRRLQ), integrated into the structure of nsp1β's papain-like autoproteinase domain, was found to be critical for the stimulation of frameshifting and for interacting with the RNA sequence of the PRRSV PRF signal. The minimal RNA sequence required to direct efficient PRF was mapped within a 34-nt region of the PRRSV nsp2-coding sequence that includes the shift site and the conserved CCCANCUCC motif. Our findings reveal an unusual non-canonical translation mechanism in which a viral protein functions as a transactivator of efficient –2 and –1 PRF. This study

advances our understanding of non-canonical translation, suggests that viruses may employ additional strategies to modulate viral and potentially host cell translation during infection, and has practical implications in biotechnology and the design of antiviral strategies.

## 4.2 Materials and methods

**Cells and viruses.** HEK-293T, RK-13, BHK-21, and MARC-145 cells were cultured as described previously (Fang *et al.*, 2006; Snijder *et al.*, 1994). The US type 1 PRRSV isolate SD01-08 (GenBank accession #DQ489311) and type 2 PRRSV isolate SD95–21 (GenBank accession #KC469618) were used in all experiments.

**Antibodies.** Antibodies recognizing PRRSV proteins (see also Fig. 4.9B for the nomenclature used in this paper), including mAb 22–28 (α-EU-nsp1β), mAb 123-128 (α-NA-nsp1β), mAb 36-19 (α-EU-PLP2), mAb 58-46 (α-EU-nsp2), mAb140-68 (α-NA-PLP2), mAb 148-43 (α-NA-nsp2), and a rabbit antiserum recognizing the C-terminal part of nsp2TF (α-EU-TF) were produced as described previously (Fang *et al.*, 2012). A rabbit antiserum (α-NA-TF) recognizing the C-terminal epitope (CFLKVGVKSAGDLV) of nsp2TF of type 2 PRRSV was generated by GenScript (Piscataway, NJ). For detection of FLAG-tagged proteins, an anti-FLAG mAb was obtained from Sigma® Life Science. Anti-β-tubulin and anti-dsRNA (J2-0601) mAbs were obtained from Lamda Biotech and English & Scientific Consulting, respectively.

**DNA constructs.** Except for the KO2 (Fig. 4.9) and pLnsp1βcc–2 (Fig. 4.11) mutants, for which synthetic DNA was used, all other constructs were made by using the Quick-Change site-directed mutagenesis kit (Stratagene) following the manufacturer's instruction and recombinant DNA techniques. Plasmids for expression of full-length or partial PRRSV ORF1a were constructed by RT-PCR amplification of corresponding regions from genomic RNA (nt 191-7702 nt of the SD95–21 genome; nt 222-7361 of the SD01-08 genome). The PCR product was digested with NcoI and NotI restriction enzymes and ligated into a pL1a backbone digested with the same enzymes. The design of pL1a was described previously (Fang *et al.*, 2012).

Plasmid pLnsp1βcc–2 was constructed by extensively mutating the SD01-08 PRRSV nsp1β-coding region with synonymous replacements (Fig. 4.11), while keeping the encoded amino acid sequence intact and avoiding rare codons. The modified sequence (nsp1βcc) was produced as a synthetic gene and fused back with the nsp2-coding region to generate the nsp1βcc–2 construct. To construct plasmids for the dual-luciferase assay, a 79-nt

oligonucleotide (3506 to 3584 nt of SD01-08 genome) containing the WT sequence or mutations (Fig. 4.11, IFC and KO2) at the PRF region was synthesized and cloned into the dual luciferase vector pDluc as described previously (Fixsen & Howard, 2010; Grentzmann *et al.*, 1998).

The plasmid expressing FLAG-tagged nsp1β (pFLAG-nsp1β) was generated by PCR amplification of the nsp1β-coding region (nt 762-1376 of the SD01-08 genome) and cloned into the plasmid vector p3xFLAG-CMV–24 (Sigma). Plasmids expressing EGFP-tagged PRF sequence (pR79WT-EGFP, pR79KO2-EGFP, and pR79CC2-EGFP) were generated by cloning the PRF region (nt 3506 to 3584 of SD01-08) into the plasmid vector pEGFP-N1 (Clontech).

**Reverse genetics.** Procedures for the construction of plasmids are provided in *SI Materials and Methods*. Methods for *in vitro* transcription, virus rescue from full-length cDNA clones, and virus titration were described previously (Fang *et al.*, 2006; Li *et al.*, 2013), (Fang *et al.*, 2012).

**Mass spectrometry.** Nsp2N was immunoprecipitated from SD95-21-M1–infected MARC-145 cell lysate using mAb α-NA-PLP2 and samples were separated on a 6% SDS-PAGE gel, which was fixed and stained with Coomassie Brilliant Blue G-250 (Bio-Rad). The band expected to contain nsp2N* (based on predicted protein size) was excised. Trypsin digestion and LC-MS/MS analysis were performed as described previously (van den Akker *et al.*, 2011). MS spectra were searched against a custom-made protein database containing the nsp2N* sequence. As positive control, a synthetic version of the identified frameshift peptide was made and analyzed by LC-MS/MS.

**Immunoassays.** To define the minimal sequence required for PRF, different regions of PRRSV ORF1a were transiently expressed in RK-13 cells or HEK-293T cells using truncated derivatives of expression plasmid pL1a and the recombinant vaccinia virus/T7 polymerase expression system (Snijder *et al.*, 1994). The expression of nsp1β and nsp2-related products was detected by immunoprecipitation and Western blot, as described previously (Fang *et al.*, 2012). To detect the expression of nsp1β and nsp2-related products in cells infected with SD95-21 WT and mutants, proteins were radioimmunoprecipitated with mAb α-NA-PLP2 or analyzed by Western blot using mAb α-NA-nsp1β, as described previously (Li *et al.*, 2013). Wild-type and mutant SD01-08 viruses were launched by transfecting *in vitro* transcribed full-length RNA into BHK-21 cells, and radioimmunoprecipitation was conducted to detect the expression of nsp1β and nsp2-related products.

**Dual luciferase assay.** Using FuGENE HD transfection reagent (Roche Molecular Biochemicals), HEK-293T cells were co-transfected with 0.2 μg of dual luciferase plasmid containing the PRRSV PRF sequence and 50 ng of pFLAG-nsp1β. At 24h post-transfection, cells were harvested and luciferase expression was measured using the Dual Luciferase Stop & Glo® Reporter Assay System (Promega) and a luminometer (Bethold). Frameshifting efficiencies were calculated from the ratio of firefly to *Renilla* luciferase activities, using the IFC control construct as the standard.

**Analysis of protein sequences and structure.** Sequence alignment of the PLP1β domain of PRRSV, LDV, and SHFV nsp1β and EAV nsp1 was performed using the MUSCLE algorithm in Geneious 6 (Biomatters Ltd, Auckland, NZ). Potential RNA-binding residues in nsp1β were identified using the program BindN (Wang & Brown, 2006). Images of the crystal structure of the PRRSV nsp1β dimer (PDB: 3MTV) (Xue *et al.*, 2010) were created using PyMOL (DeLano, 2002).

**Assays for detecting interactions between nsp1β and viral RNA.** Immunoprecipitation assays to detect RNA-binding proteins were performed using the Magna RIP™ kit (Millipore) and Ribo Trap kit (Medical & Biological Laboratories) following the manufacturer's instructions. The amount of target mRNA bound to nsp1β was determined by quantitative RT-PCR, and the presence of nsp1β in RNA-protein complexes was verified by Western blot.

**In vitro transcription and radioimmunoprecipitation analysis of SD01-08 WT and mutants.** Full length SD01-08-WT, KO2, or 1βKO RNA was transcribed from 1 ug of linearized plasmid DNA using the mMESSAGE mMACHINE T7 kit (Ambion) following the manufacturer's instructions. BHK-21 cells ($4x10^6$) were electroporated with 8 ug of in vitro transcribed RNA using program T-020 of the Amaxa Nucleofector and kit T (Lonza). Newly synthesized proteins were labeled from 16.5 to 18.5 hours post transfection in cysteine- and methionine-free medium containing 200 μCi/ml [$^{35}$]S-methionine and [$^{35}$]S-cysteine (Perkin-Elmer). Cell lysis and immunoprecipitation analysis were performed as described previously (Snijder *et al.*, 1994). The mAbs α-EU-nsp1β and α-EU-nsp2 were used to immunoprecipitate nsp1β and nsp2/nsp2TF/nsp2N, and precipitated proteins were separated on a 12% SDS-PAGE gel. Protein bands were visualized using phosphorimaging and a Typhoon Variable Mode Imager (GE Healthcare). Image analysis was performed with the ImageQuant TL software (GE Healthcare).

**Pulse-chase analysis of nsp1β expression by SD01-08 WT and mutants KO2 and 1βKO.** Following electroporation with in vitro transcribed SD01-08 WT, KO2, or 1βKO RNA, $0.3x10^6$ BHK-21 cells were labeled at 16.5h post transfection for 15' in cysteine- and

methionine-free medium containing 500 μCi/ml [$^{35}$]S-methionine and [$^{35}$]S-cysteine (Perkin-Elmer). After removal of the label medium, cells were either lysed immediately or chased for 1h in the presence of an excess of unlabeled methionine and cysteine. Immunoprecipitation was performed as described previously (Snijder *et al.*, 1994) with mAb α-EU-nsp1β. Precipitated proteins were separated on a 12% SDS-PAGE gel and phosphorimaging was performed as described above.

**Immunofluorescence microscopy of transfected BHK-21 cells.** Following electroporation with in vitro transcribed SD01-08 WT, KO2, or 1βKO RNA, 0.15x10$^6$ BHK-21 cells were seeded on glass coverslips. At 18 h post transfection, cells were fixed in 3% para-formaldehyde in PBS. Cells were double-labeled with a mAb recognizing dsRNA and Hoechst 33342 to stain nuclear DNA.

**RNA isolation, denaturing formaldehyde gel electrophoreses and in gel hybridization.** BHK cells (0.75x106) were electroporated with in vitro transcribed RNA of SD01-08 WT, KO2, and 1βKO. At 18 h post transfection, cells were lysed in 20 mM Tris-HCl (pH 7.4), 100 mM LiCl, 2 mM EDTA, 5 mM DTT, 5% (w/v) lithium dodecyl sulfate, and 100 μg/ml proteinase K. Total RNA was extracted and separated on a denaturing formaldehyde gel. Positive-stranded viral RNA was visualized by gel drying and hybridization with a 32P-labeled oligonucleotide probe (PRRSV-hyb1 5'-TCGCCCTAATTGAATAGGTG-3') that is complementary to the 3' end of the viral genome and therefore recognizes all viral mRNAs. 18S ribosomal RNA was used as a loading control and was detected with probe 5'-ATGCCCCCGGCCGTCCCTCT-3'. Hybridized gels were analyzed by phosphorimaging as described above. Correction for loading variations was performed using the amount of 18S RNA in the same lane. The sum of the signal for all viral mRNAs in each lane was used to calculate the relative abundance of each individual mRNA.

**RNA-binding protein immunoprecipitation and RNA pull-down assay.** RNA-binding protein immunoprecipitation was performed using a Magna RIP™ kit (Millipore) according to the manufacturer's instruction. Briefly, HEK 293T cells seeded in 10-cm petri dishes were co-transfected with plasmids expressing the RNA bait (R79WT-EGFP, R79KO2-EGFP, R79CC2-EGFP, or pEGFP; 8ug) and the nsp1β bait (nsp1β-WT, nsp1β-KO, or pFLAG; 2 μg). At 24 h post transfection, cell lysates were prepared for co-immunoprecipitation. FLAG-tagged nsp1β was immunoprecipitated using an α-FLAG mAb, and co-precipitating target RNA was quantified by qRT-PCR using TaqMan® Gene Expression Assay kit (Life technologies) targeting the EGFP RNA sequence. The expression of nsp1β in all co-transfected samples was determined by Western blot analysis using an nsp1β-specific mAb.

Ribo Trap kit (MBL International Corporation) was used to further confirm the interaction between nsp1β and the 79-nt RNA sequence from the PRRSV PRF region. The R79WT, R79KO2, or R79CC2 RNA was labeled with 5-bromo-U and in vitro synthesized using the MEGAscript® T7 Kit (Life technologies). The 5-bromo-U-labeled RNA transcripts were bound to magnetic beads conjugated with anti-BrU mAb. Subsequently, these magnetic beads were incubated with lysates of HEK 293T cell expressing FLAG-tagged 1βKO or WT of nsp1β. The amount of nsp1β pulled-down with the RNA bait was determined by western blot analysis using an nsp1β-specific mAb.

## 4.3 Results

**Alternative –2 and –1 PRF at the same PRRSV slippery sequence.**

Previously (Fang *et al.*, 2012), we demonstrated expression of the PRRSV TF ORF (Fig. 4.1A) using a rabbit antiserum raised against the epitope on the C-terminus of the polypeptide it encodes. Subsequently, the frameshift product was immunopurified from infected cells and mass spectrometry (MS) was employed to identify both the site (RG_GUU_UUU) and direction (–2, rather than +1) of ribosomal frameshifting. In both PRRSV-infected cells and an ORF1a expression system, and using distantly related type 1 and type 2 PRRSV isolates, the same studies revealed an additional nsp2-related product (nsp2N) with a size consistent with –1 PRF occurring at the same site [estimated efficiency ~7%; (Fang *et al.*, 2012)]. However, a stop codon is present in the –1 frame immediately downstream of the RG_GUU_UUU slippery sequence (Fig. 4.1A) and consequently, if nsp2N were derived from –1 frameshifting, it would lack a unique C-terminal sequence that could be used to discriminate it from a product derived through the internal proteolytic cleavage of full-length nsp2. In an attempt to confirm the occurrence of –1 PRF by IP-MS, we sought to extend the potential –1 frameshift product with a unique C-terminal signature. In a full-length cDNA clone of the previously used PRRSV isolate SD01-08 [a type 1 virus; (Fang *et al.*, 2006)], the –1 frame stop codon (UGA) was replaced by a tryptophan codon (UGG), extending the –1 frame by an additional 87 codons (Fig. 4.9, SD01-08-M1). However, this point mutation unavoidably also introduced amino acid substitutions in the overlapping 0 and –2 frames encoding nsp2 and nsp2TF (Glu→Gly and Lys→Glu, respectively), and perhaps as a consequence, the resulting recombinant virus was severely crippled (titer reduced to $10^3$ FFU/ml), preventing us from immunopurifying sufficient nsp2N for reliable MS analysis. We, therefore, reverted to a type 2 PRRSV isolate [SD95-21; (Li *et al.*, 2013)]

and introduced the same A to G mutation, which in this case extended the –1 ORF by 23 additional codons to generate mutant SD95-21-M1 (Fig. 4.9). Fortunately, despite carrying Asp→Gly and Thr→Ala mutations in the nsp2 and nsp2TF products respectively, this recombinant virus replicated to much higher titers ($10^{6.2}$ FFU/ml) and the C-terminally extended nsp2N product (nsp2N*) could be immunopurified from infected MARC-145 cells. A gel slice containing the nsp2N* band was analyzed by LC/MS/MS and a QVFWPR tryptic peptide that spanned the frameshift site and is compatible with −1 PRF at the RG_GUU_UUU sequence was identified (Fig. 4.10). To verify correct identification of this peptide, a synthetic version was subjected to the same LC/MS/MS analysis. The tandem mass spectrum of this synthetic peptide was found to be identical to that of the peptide derived from the nsp2N*-containing gel slice (Fig. 4.10D), confirming that nsp2N is indeed translated via −1 PRF at the RG_GUU_UUU slippery sequence, which is, therefore, able to direct both −1 and −2 PRF.

**PRRSV nsp1β is required for efficient −1 and −2 frameshifting in the nsp2-coding region.**

Previously we demonstrated that translation of the complete PRRSV ORF1a sequence is sufficient to allow efficient –2 PRF (Fang *et al.*, 2012). To define the minimal sequence requirements for –2/–1 PRF in PRRSV isolate SD01-08, we focused our attention on the N-terminal half of ORF1a (the nsp1α-nsp3 region) and generated a panel of truncated ORF1a constructs (Fig. 4.2A) for expression in the recombinant vaccinia virus/T7 RNA polymerase system (Fuerst *et al.*, 1986). Following radiolabeling of proteins synthesized in transfected cells, expression of nsp2, nsp2TF, and nsp2N was analyzed by immunoprecipitation using monoclonal antibody (mAb) α-EU-nsp2 and rabbit antiserum α-EU-TF, recognizing all three nsp2-related products and the unique C-terminal epitope of nsp2TF, respectively (see Fig. 4.9B for a summary of antibody nomenclature and epitopes recognized). As shown in Fig. 4.2B, constructs lacking the nsp1α- and/or nsp3-coding region still efficiently expressed nsp2TF and nsp2N. In contrast, constructs lacking the nsp1β-coding region expressed nsp2 but only trace amounts of nsp2TF or nsp2N were detected. This indicates that nsp1β, or the RNA sequence encoding nsp1β, is required for efficient –2/–1 PRF at the RG_GUU_UUU slippery sequence in the nsp2-coding region, located some 2.5 kb downstream of the nsp1β-coding region.

Extending this further, separate plasmids expressing nsp2 (pLnsp2) and a FLAG epitope-tagged nsp1β (pFLAG-nsp1β) were co-transfected into HEK 293T cells. In this system, nsp2TF and nsp2N were again produced (Fig. 4.2C), indicating that nsp1β can

stimulate –2/–1 PRF *in trans* (i.e. outside the setting of the regular replicase polyprotein). To test whether this effect was mediated by the nsp1β protein rather than the nsp1β-coding RNA sequence, a drastically altered version of the nsp1β-nsp2 expression vector (pLnsp1β-2) was produced in which almost every codon of the nsp1β-coding sequence was mutated synonymously, while avoiding rare codons (mutant pLnsp1βcc-2; Fig. 4.11). This pLnsp1βcc-2 construct expresses an unaltered nsp1β protein, but the nucleotide sequence encoding it is changed to such an extent that we would expect to have disrupted any primary sequence or RNA secondary structure elements that might be involved in –2 PRF (for example, an element having a long-range interaction with the PRF region in the nsp2-coding sequence). Immunoprecipitation and Western blot analysis revealed that nsp2TF and nsp2N were expressed with equal efficiency in cells transfected with pLnsp1βcc-2 and wild-type pLnsp1β-2 (Fig. 4.2D), indicating that PRF stimulation involves the nsp1β protein itself rather than an RNA signal in the nsp1β-coding sequence.

**Minimal RNA sequence requirements for –2/–1 PRF.**

We next set out to define the minimal RNA sequences in the nsp2-coding region that are required for efficient –2/–1 PRF. To this end, we prepared a reporter gene construct in which PRRSV RNA sequences from the PRF-inducing region were placed between two luciferase genes [pDluc (Fixsen & Howard, 2010; Grentzmann *et al.*, 1998); Fig. 4.3A]. Whereas the ORF1a frame of the PRRSV insert was placed in-frame with the upstream (*Renilla*) luciferase gene, the downstream (firefly) luciferase was in the –2 frame and thus its expression depended on the occurrence of –2 frameshifting. Also –1 PRF could be monitored, since the native stop codon in the –1 frame was retained and –1 PRF would, therefore, yield a polypeptide slightly shorter than the product resulting from translation termination in the zero reading frame. As controls, an in-frame control (IFC) construct was also prepared in which the two luciferase genes were aligned in the same frame by inserting two nucleotides (CU) immediately downstream of the slippery sequence. A previously described PRF knockout construct [KO2; Fig. 4.9; (Fang *et al.*, 2012)] containing point mutations within the slippery sequence and downstream C-rich region was also included in the analysis.

Initially, a 79-nt region spanning 5 nt upstream of the slippery sequence to 66-nt downstream (including the conserved CCCANCUCC motif) was cloned between the two luciferase genes (construct pDluc-WT). Frameshifting efficiencies were determined by comparing the ratio of enzymatic activities of firefly and *Renilla* luciferase in parallel HEK293T cell cultures transfected with individual pDluc constructs with or without co-transfection of the plasmid expressing nsp1β. As shown in Fig. 4.3B, in comparison to the

IFC control, the wild-type PRRSV –2 PRF efficiency was ~38%, and this high-level of –2 PRF was only observed in cells co-transfected with the nsp1β-expressing plasmid; in the absence of the *trans*activator, only low levels of –2 PRF (<5%) were observed. As expected, frameshifting was not observed in cells transfected with pDluc-KO2. Western blot analysis of transfected cell lysates revealed that both efficient –2 PRF and efficient –1 PRF could be observed with pDluc-WT provided that an nsp1β expression plasmid was co-transfected (Fig. 4.3C). These data indicated that the 79-nt PRRSV sequence included in pDluc-WT contains all *cis*-acting sequences required for efficient –2/–1 PRF, and that, as documented above, both types of frameshift depend on the presence of nsp1β. In the absence of this *trans*activator, only low levels of PRF were observed.

To further investigate the key RNA sequences required for PRF, in-frame deletions were introduced into pDluc-WT, starting from the 3' end of the PRRSV insert. As shown in Fig. 4.3C, an initial deletion that reduced the PRRSV sequence downstream of the shift site to 45 nt (pDluc-45) led to a small reduction in –2 PRF (about 2-fold), albeit with a concurrent increase in –1 PRF. Subsequent deletions had no further effect until part of the conserved CCCANCUCC motif was removed (Fig. 4.3C; compare pDluc-21 and pDluc-15). In pDluc-15, which lacked the second half (CUCC) of the conserved motif, the capacity for *trans*activation of PRF by nsp1β was lost. These data provided further support for a role of the C-rich motif in PRF, and allowed us to define the functional PRRSV –2/–1 PRF cassette as a 34-nt region containing the slippery sequence and the 3' C-rich motif.

**Identification of a conserved nsp1β motif that is critical for PRF *trans*activation.**

The nsp1α-nsp1β region has previously been implicated in a variety of processes in the arterivirus replicative cycle, including replicase polyprotein processing (den Boon *et al.*, 1995), transcriptional control (Nedialkova *et al.*, 2010; Tijms *et al.*, 2001), and innate immune evasion (Chen *et al.*, 2010; Li *et al.*, 2013). An analysis of nsp1β sequence conservation (Fig. 4.4A), together with the published crystal structure of nsp1β from a type 2 PRRSV isolate [(Xue *et al.*, 2010); Fig. 4.4B-C], pointed towards a previously identified conserved sequence motif as a potential RNA interaction domain. This sequence, GKYLQRRLQ in both type 1 and type 2 PRRSV, forms one of three alpha-helices [labeled α4 in (Xue *et al.*, 2010)] in the region between the active site Cys and His residues of the papain-like proteinase domain (PLP1β) that constitutes the C-terminal two-thirds of nsp1β. Interestingly, compared to the active site of the PLP1β proteinase, helix α4 maps to the other side of the molecule and, in the available crystal structure, the three conserved basic residues of the GKYLQRRLQ motif are exposed on the nsp1β surface. Moreover, in the nsp1β

homodimer that was the basis for structural studies, the α4 helices of both monomers map to the same side of the dimer and may form a continuous surface across the protein that binds nucleic acid (Fig. 4.4C; see Discussion).

In a recent study (Li *et al.*, 2013), the GKYLQRRLQ motif was targeted by site-directed mutagenesis and the Lys and the first Arg of the motif were replaced with Ala (mutant 1βKO, Fig. 4.9). For both PRRSV genotypes, the replication of the 1βKO mutant in MARC-145 cells was found to be seriously crippled. The fact that we had observed similar defects in mutants in which the –2/–1 PRF signal had been inactivated, or in which the expression of a functional nsp2TF was prevented (Fang *et al.*, 2012), prompted us to investigate whether this KR→AA double mutation affected nsp2TF/nsp2N expression. Strikingly, upon expression of nsp1β-nsp2 from either PRRSV genotype carrying these nsp1β mutations, nsp2TF could not be detected; only trace amount of nsp2N was detected in type 2 PRRSV mutant (Fig. 4.5). These data indicate that the GKYLQRRLQ motif plays a key role in PRF activation.

To investigate nsp1β *trans*activation of PRF in the context of PRRSV infection, we analyzed nsp2 expression using the 1βKO mutant of both PRRSV genotypes. As controls, we included the corresponding KO2 mutants, which carry mutations within the slippery sequence and C-rich region that eliminate frameshifting [Fig. 4.9 (Fang *et al.*, 2012)]. Using reverse genetics, KO2 and 1βKO mutant viruses were recovered from full-length infectious clones of the two PRRSV genotypes. Both mutants replicated poorly in MARC-145 cells, but for the type 2 PRRSV isolate (SD95-21), they produced titers ($10^{5.1}$ and $10^{5.3}$ FFU/ml for KO2 and 1βKO, respectively) that sufficed for the subsequent experiments of infection, metabolic labeling and radioimmunoprecipitation analysis. As expected (Fig. 4.6A), the expression of nsp2, nsp2TF, and nsp2N was detected in SD95-21-WT-infected cells, whereas only nsp2 was recovered from cells infected with either SD95-21-KO2 or SD95-21-1βKO, while their nsp1β was expressed at a level similar to that observed with the wild-type (WT) virus.

Unfortunately, the 1βKO mutant of the PRRSV type 1 isolate (SD01-08) yielded very low titers in MARC-145 cells ($10^2$ FFU/ml). Considering the number of viral functions and properties potentially affected by nsp1β mutations (see Discussion), we therefore performed a so-called 'first-cycle analysis' of the phenotypes of SD01-08 WT, KO2, and 1βKO. The three viruses were launched by transfecting *in vitro* transcribed full-length RNA into BHK-21 cells, which support replication of transfected PRRSV RNA but cannot be infected by the progeny virus released from the transfected cells, due to the lack of the appropriate receptor(s) on their surface (Meulenberg *et al.*, 1998). Moreover, BHK-21 cells have a defect in interferon

production (Clarke & Spier, 1983), thus minimizing the (potential) impact of host innate responses on the comparison of viral replication phenotypes. Following metabolic labeling of protein synthesis in transfected cells, a radioimmunoprecipitation analysis revealed that SD01-08-1βKO produced large amounts of nsp2, whereas the production of nsp2TF was greatly reduced and nsp2N was not detected (Fig. 4.6B). As previously established, SD01-08-KO2 produced only nsp2, while SD01-08-WT produced all three nsp2 variants. Equal expression of nsp1β in WT-, KO2-, and 1βKO-transfected cells was confirmed by immunoprecipitation with an nsp1β-specific mAb. We also investigated whether the mutations in 1βKO affected the activity of the PLP1β protease or the (potential) involvement of nsp1β in the control of viral subgenomic mRNA synthesis. While the total amount of nsp1β and viral RNA was somewhat reduced in 1βKO-transfected cells, cleavage of the site between nsp1β and nsp2 and subgenomic mRNA production (Fig. 4.12B-C), were not affected by the mutations in the GKYLQRRLQ motif, nor did they affect nsp1β stability (Fig. 4.12D). Finally, we included a double-transfection of BHK-21 cells with KO2 and 1βKO full-length RNA (Fig. 4.6B) and demonstrated complementation between the two PRF-negative mutants leading to reactivation of nsp2TF/nsp2N expression. As expected, the wild-type nsp1β expressed by mutant KO2 was able to *trans*activate -2/-1 PRF on the wild-type ORF signal in the 1βKO genome, again confirming that the GKYLQRRLQ motif plays a critical role in the PRF stimulatory activity of nsp1β in PRRSV-infected cells.

**PRRSV nsp1β interacts with the RNA signals that direct –2/–1 PRF.**

To test the hypothesis that nsp1β, and specifically its GKYLQRRLQ motif, interacts with the PRRSV RNA sequences that direct –2/–1 PRF, we developed an RNA-binding protein immunoprecipitation assay. To produce an RNA target, we engineered plasmid pR79WT-EGFP yielding an RNA in which a 79-nt PRRSV SD01-08 RNA sequence (Fig. 4.3A) containing the shift site and conserved CCCAUCUCC motif was fused to the enhanced green fluorescent protein (EGFP) open reading frame (Fig. 4.7A). The latter served as a target for quantitative RT-PCR (qRT-PCR) amplification of target RNA bound to nsp1β. As controls, we included plasmids pR79KO2-EGFP and pR79CC2-EGFP, containing combinations of point mutations in the shift site and/or CCCAUCUCC motif that were previously demonstrated to completely inactivate PRF [Fig. 4.9; (Fang *et al.*, 2012)]. To express the nsp1β bait, we used constructs pFLAG-nsp1β-WT and pFLAG-nsp1β-KO, producing wild-type and mutant (K130A/R134A) nsp1β, respectively, each fused to an N-terminal triple FLAG tag. The empty vectors pFLAG and pEGFP were included as negative controls.

Following co-transfection of vectors expressing RNA target and nsp1β into 293T cells, cell lysates were prepared. Western blot and qRT-PCR analysis (Fig. 4.7B) were first used to determine the expression levels of nsp1β bait and target RNA, respectively, and confirmed the presence of similar amounts of both molecules in all co-transfection samples. Subsequently, we immunoprecipitated FLAG-nsp1β using an anti-FLAG mAb and analyzed these samples for co-immunoprecipitation of target RNA using the same qRT-PCR method, while verifying successful immunoprecipitation of nsp1β with a specific mAb (Fig. 4.7C). A strong and specific RNA co-immunoprecipitation signal was detected only in samples from cells co-transfected with pFLAG-nsp1β-WT and pR79WT-EGFP. In contrast, when mutant 1βKO carrying the K130A/R134A double mutation in the GKYLQRRLQ motif was used, only very low levels of target RNA were pulled down, suggesting that the K130A/R134A mutations impaired the interaction of nsp1β with PRRSV RNA. Only background signal was detected when using a negative control mouse IgG for immunoprecipitation, or when expressing the pFLAG empty vector control, demonstrating specificity for nsp1β. When the PRRSV PRF-specific sequences in the RNA target were mutated (R79KO2-EGFP or R79CC2-EGFP) or the pEGFP empty vector control was used, only trace amounts of RNA (6% or less of the R79WT-EGFP signal) could be captured, thus demonstrating that co-immunoprecipitation of the target RNA strongly depends on the presence of the CCCAUCUCC motif.

To further corroborate the interaction between nsp1β and the 79-nt RNA sequence from the PRF region, we employed a complementary assay [RiboTrap system; (Beach & Keene, 2008)] in which RNA transcripts were labeled with 5-bromo-uridine, facilitating their immunopurification using a 5-bromo-U-specific mAb, and subsequent analysis of immunoprecipitates for the presence of proteins binding to the RNA bait. Using PCR amplicons containing T7 promoter and 79-nt PRRSV RNA sequence (R79WT, R79KO2, or R79CC2) as template, 5-bromo-U-labeled RNA transcripts were produced *in vitro* and incubated with lysates of 293T cells transfected with the plasmid expressing 1βKO or wild-type nsp1β. Following immunoprecipitation with the 5-bromo-U-specific mAb, samples were analyzed for the presence of nsp1β using SDS-PAGE and Western blot analysis (Fig. 4.8). A strong and specific nsp1β signal was detected only when the R79WT bait was incubated with cell lysates containing nsp1β-WT. When using lysates containing 1βKO of nsp1β, only a very small fraction of the available protein was bound to the RNA. Likewise, only trace amounts of wild-type nsp1β were pulled down when 5-bromo-U-labeled R79KO2 or R79CC2 RNA was used as bait. These data are consistent with those obtained in the RNA-binding protein

immunoprecipitation assay presented in Fig. 4.7 and further support a key role for the GKYLQRRLQ motif in the specific *trans*activation of the PRRSV –2/–1 PRF by nsp1β.

## 4.4 Discussion

In this paper, we report the remarkable discovery that efficient ribosomal frameshifting in the expression of the PRRSV nsp2TF and nsp2N proteins requires the viral nsp1β protein as a *trans*activator. Protein-stimulated PRF is unprecedented. It has been reported that cellular annexin A2 may interact with the –1 PRF signal of the coronavirus infectious bronchitis virus, but its role appears to be to down-regulate frameshifting through destabilization of the stimulatory pseudoknot (Kwak *et al.*, 2011), and no specific frameshift-stimulatory protein factors have been identified to date. While down-regulation of eukaryotic translation release factor levels can lead to a low-level stimulation of –1 PRF (Kobayashi *et al.*, 2010; Park *et al.*, 2009), this is a poorly-characterized phenomenon, likely to be a rather non-specific effect brought about by changes in translation rates (Gendron *et al.*, 2008). It is known that –1 PRF at the human immunodeficiency virus type 1 slippery sequence can be promoted by replacing the natural stimulatory RNA with a combination of the iron-responsive element (IRE) RNA and its cognate binding partner (the IRE-binding protein), but this is a highly artificial experimental system and the stimulation of –1 PRF is very weak (Kollmus *et al.*, 1996).

Exactly how nsp1β stimulates frameshifting remains to be determined. Based on the RNA binding experiments, we propose that the region 3' of the PRRSV PRF slippery sequence acts to recruit nsp1β, or an nsp1β-containing protein complex, which modulates ribosome function to promote frameshifting. Our evidence to date supports the view that nsp1β binds directly to the C-rich region, since point mutations within this region strongly reduce RNA binding (Fig. 4.7). However, we cannot rule out the involvement of other factors, for example, poly C-binding proteins [PCBPs; (Makeyev *et al.*, 2005)], which are known to interact with C-rich regions. Moreover, certain PCBPs have been reported to bind to PRRSV nsp1β in pull-down assays (Beura *et al.*, 2011). As the C-rich region is located only 11 nt downstream of the slippery sequence, this would likely place bound nsp1β, or an nsp1β-containing complex, in close proximity to a ribosome decoding the slippery sequence, permitting interactions that may lead to frameshifting. While this model is speculative, there is growing evidence that proteins can modulate the elongation step of protein synthesis. The fragile X mental retardation protein reversibly stalls ribosomes on its target mRNAs (Darnell

*et al.*, 2011) and the HIF-1α mRNA-associated cytoplasmic polyadenylation element binding protein 2 binds eEF2 and slows elongation (Chen & Huang, 2012). Conceivable routes through which bound proteins could modulate ribosomal function include induction of ribosomal pausing by acting as a roadblock, recruitment of, or localized depletion of translation factors, and direct interaction with a ribosomal component(s). It may be significant that nsp1β was reported to interact with rpS14 (Beura *et al.*, 2011), a protein immediately adjacent to rpS3 of the ribosomal helicase (Ben-Shem *et al.*, 2011), and PCBP1, which is known to interact with RACK1, a ribosome-associated protein located close to the mRNA entry channel (Nahar-Gohad *et al.*, 2013). These features are consistent with a role for nsp1β in modulating the ribosomal helicase, the suspected target for the stimulatory RNA sequences of canonical –1 PRF signals.

An interesting aspect of this PRRSV PRF signal is that both –2 and –1 frameshifting events are promoted. Tandem slippage of ribosome-bound tRNAs on RG_GUU_UUU would allow complete A-site re-pairing in both –1 and –2 frames (tRNA anticodon:mRNA codon pairing in 0-frame is 3'-AAG-5' : 5'-UUU-3'; single $tRNA^{Phe}$ isoacceptor AAG), but especially for –2 PRF, P-site re-pairing appears to be compromised [at least at the 2nd and 3rd positions (lower case), 3'-Cai-5' : 5'-Ggg-3'; i is inosine]. Some tolerance for P-site mis-pairing has been noted at certain viral –1 PRF signals, but usually, these are associated with single mis-matches in the anticodon:codon interaction (Brierley *et al.*, 1992; Firth & Brierley, 2012). It may be that in the particular context of a –2 PRF, stable P-site re-pairing is not required, reminiscent of the unusual "single-tRNA" slippage events seen in prokaryotic systems with slippery sequences ending in AAG, where P-site re-pairing does not appear to be present (Mejlhede *et al.*, 1999; Napthine *et al.*, 2003). In a recent study on RNA secondary structure-stimulated –1 and –2 PRF on a GU_UUU_UUA slippery sequence (Lin *et al.*, 2012), it was noted that the length of the spacer between slippery sequence and secondary structure affected the relative utilisation of –1 or –2 PRF modes, perhaps a reflection of differences in mRNA tension arising as the ribosomal helicase unwinds the secondary structure, with increased tension forcing the ribosome into the –2 rather than the –1 frame. Interestingly, the relative levels of the PRRSV –2 and –1 PRF products were seen to change as the length of the PRRSV region 3' of the slippery sequence was shortened from 67 to 45 nt (Fig. 4.3C), although the sum total of PRF was similar. This may hint at the involvement of additional factors, or some subtle effect on the positioning of a bound protein (or complex), that can influence frameshift magnitude, although it remains to be determined whether this is linked to mRNA tension.

Analysis of the published structure of nsp1β from a type 2 PRRSV isolate provides insights into the mechanism of how the protein may interact with viral RNA. The PLP1β domain of nsp1β adopts a papain-like fold consisting of three α-helices that pack against a β-sheet of 4 antiparallel strands (Xue *et al.*, 2010) (Fig. 4.4B). One of the helices (helix α4 in the overall nsp1β structure) contains a conserved GKYLQRRLQ motif that we now show plays a critical role in the *trans*activation of frameshifting. The crystal structure of nsp1β suggests that the protein exists as a homodimer (Xue *et al.*, 2010) and, interestingly, helix α4 of both nsp1β monomers resides on the same side of the dimer, which may generate a continuous, positively charged surface that could bind a long single- or double-stranded RNA molecule (Fig. 4.4C). The involvement of an α-helix in RNA binding is consistent with the observation that nucleoproteins of many RNA viruses encapsidate the viral genome using domains of α-helical structure (Albertini *et al.*, 2006; Ruigrok *et al.*, 2011). Thus, it is plausible that the GKYLQRRLQ motif of helix α4 directly binds viral RNA, although we cannot exclude the possibility that this helix may be a binding site for a cellular protein that in turn could bind to the PRF signal in the viral RNA.

Except for equine arteritis virus (EAV), the –2 PRF mechanism seems to be conserved in all currently known arteriviruses as judged by the presence of a TF ORF overlapping ORF1a and a conserved slippery sequence and downstream C-rich region (Fang *et al.*, 2012). In PRRSV and lactate dehydrogenase elevating virus (LDV) –1 PRF can occur, but in contrast the RG_GUC_UCU shift site in some of the recently identified simian haemorraghic fever virus (SHFV)-like viruses (Lauck *et al.*, 2013) would preclude –1 PRF while still allowing –2 PRF. It is expected that such PRF events in LDV and SHFV would also be controlled by nsp1β, and indeed the *trans*activating motif in nsp1β was found to be largely conserved in these viruses (Fig. 4.4A). Possibly, the nsp1β component of the frameshift mechanism, which is encoded several kilobases upstream of the PRF site, evolved secondarily, for example to enhance the efficiency of nsp2TF/nsp2N expression, since in the absence of nsp1β low levels of PRF could still be observed (Fig. 4.2A). Amino acid sequence comparisons reveal that the GKYLQRRLQ motif-containing helix is highly conserved in the PLP1β domains of PRRSV, SHFV, and LDV, but the motif is lacking in EAV. For the latter virus, the three helices of the PLP1β domain are predicted to be present, but with an insertion of three amino acids in the EAV equivalent of the α4 helix compared to the other arteriviruses. The nsp2-encoding region of EAV lacks an equivalent of the (overlapping) TF ORF and produces a substantially smaller nsp2. Assuming the TF ORF was lost at some point

during the evolution of the EAV lineage, changes in this helix may have been tolerated when it was no longer required to stimulate PRF *in trans*. Although an alternative evolutionary scenario (*i.e.* a common ancestor of PRRSV, SHFV, and LDV independently acquiring a TF ORF) cannot be excluded, loss of the requirement to *trans*activate PRF may also explain a second remarkable difference between the nsp1 region of EAV and other arteriviruses: the inactivation of the proteolytic activity of the PLP1α proteinase, resulting in the synthesis of a single nsp1 protein rather than nsp1α and nsp1β (den Boon *et al.*, 1995; Snijder *et al.*, 1992). In particular, the N-terminal zinc finger of nsp1 (EAV) or nsp1α (PRRSV) has been implicated in the control of viral subgenomic mRNA synthesis (Kroese *et al.*, 2008; Nedialkova *et al.*, 2010; Sun *et al.*, 2009; Tijms *et al.*, 2007), a function that may not be compatible with a role in PRF *trans*activation, thus requiring the internal cleavage of nsp1 by PLP1α in arteriviruses that employ nsp1β-mediated *trans*activation of TF ORF expression.

The capacity of nsp1β to stimulate both –1 and –2 PRF suggests that protein transactivation could be employed more widely in the induction of programmed frameshifting events in diverse systems. With regards to arteriviruses, it is possible that nsp1β might also modulate translation of host cell mRNAs containing appropriate signals. A cursory search of porcine mRNAs revealed hundreds of –1 and/or –2 frameshift-compatible shift sites followed by C-rich motifs at an appropriate spacing, though no site that is exactly identical to the PRRSV minimal PRF cassette (8-nt shift site plus the downstream 21 nt). Whether and to what extent frameshifting occurs at such sites remains to be investigated. While the occurrence of nsp1β-responsive frameshift signals in host mRNAs would presumably be spurious, the overall effect may perturb cellular gene expression, thus adding an extra dimension to virus-host interactions.

When screening PRRSV nonstructural proteins for their capacity to suppress type I IFN expression, both nsp1β and nsp2 were found to possess such activities (Beura *et al.*, 2011; Chen *et al.*, 2010; Li *et al.*, 2013; Sun *et al.*, 2010; van Kasteren *et al.*, 2013). In reporter gene-based assays, nsp1β had the strongest potential to inhibit IFN-β promoter activity and could also inhibit downstream IFN-induced signaling pathways for expression of IFN-stimulated genes (ISGs), including ISG15 (Beura *et al.*, 2011; Chen *et al.*, 2010; Kim *et al.*, 2010; Li *et al.*, 2013; Patel *et al.*, 2010). On the other hand, the PLP2 activity of nsp2 is able to disrupt innate immune signalling by removing ubiquitin (Ub) and Ub-like modifiers from host cell substrates, exhibiting a general deubiquitinating (DUB) activity towards cellular ubiquitin conjugates and also cleaving the ubiquitin homolog ISG15 (Frias-Staheli *et al.*, 2007; Sun *et al.*, 2010; Sun *et al.*, 2012; van Kasteren *et al.*, 2013). As documented here,

nsp1β *trans*activates both nsp2TF and nsp2N expression, resulting in the synthesis of three nsp2-related proteins (nsp2, nsp2TF, and nsp2N) that have the N-terminal PLP2-DUB domain in common. Thus, it remains to be established to which extent nsp1β directly modulates the innate immune response or does so by stimulating the expression of nsp2TF and nsp2N. Furthermore, nsp1β may affect the immune response through modulation of host cell mRNA translation. The identification of viral/host elements responsible for innate immune evasion is fundamental for the development of modified live virus vaccines. As illustrated by our reverse genetics studies, mutagenesis of key residues in nsp1β and the PRF site could attenuate virus growth and improve host innate immune responses (Fang *et al.*, 2012; Li *et al.*, 2013). Since the GKYLQRRLQ motif and PRF site are highly conserved, technologies developed in this study may have broad application in the field.

## 4.5 References


**Albertini, A. A., Wernimont, A. K., Muziol, T., Ravelli, R. B., Clapier, C. R., Schoehn, G., Weissenhorn, W. & Ruigrok, R. W. (2006).** Crystal structure of the rabies virus nucleoprotein-RNA complex. *Science* **313**, 360-363.

**Atkins, J. F. & Bjork, G. R. (2009).** A gripping tale of ribosomal frameshifting: extragenic suppressors of frameshift mutations spotlight P-site realignment. *Microbiol Mol Biol Rev* **73**, 178-210.

**Atkins, J. J. F. & Gesteland, R. F. (2010).** *Recoding: expansion of decoding rules enriches gene expression*: Springer.

**Beach, D. L. & Keene, J. D. (2008).** Ribotrap : targeted purification of RNA-specific RNPs from cell lysates through immunoaffinity precipitation to identify regulatory proteins and RNAs. *Methods Mol Biol* **419**, 69-91.

**Ben-Shem, A., Garreau de Loubresse, N., Melnikov, S., Jenner, L., Yusupova, G. & Yusupov, M. (2011).** The structure of the eukaryotic ribosome at 3.0 A resolution. *Science* **334**, 1524-1529.

**Beura, L. K., Dinh, P. X., Osorio, F. A. & Pattnaik, A. K. (2011).** Cellular poly(c) binding proteins 1 and 2 interact with porcine reproductive and respiratory syndrome virus nonstructural protein 1beta and support viral replication. *J Virol* **85**, 12939-12949.

**Brierley, I., Digard, P. & Inglis, S. C. (1989).** Characterization of an efficient coronavirus ribosomal frameshifting signal: requirement for an RNA pseudoknot. *Cell* **57**, 537-547.

**Brierley, I., Gilbert, R. J. & Pennell, S. (2010).** Pseudoknot-Dependent Programmed—1 Ribosomal Frameshifting: Structures, Mechanisms and Models. In *Recoding: Expansion of Decoding Rules Enriches Gene Expression*, pp. 149-174: Springer.

**Brierley, I., Jenner, A. J. & Inglis, S. C. (1992).** Mutational analysis of the "slippery-sequence" component of a coronavirus ribosomal frameshifting signal. *J Mol Biol* **227**, 463-479.

**Chen, P. J. & Huang, Y. S. (2012).** CPEB2-eEF2 interaction impedes HIF-1alpha RNA translation. *EMBO J* **31**, 959-971.

**Chen, Z., Lawson, S., Sun, Z., Zhou, X., Guan, X., Christopher-Hennings, J., Nelson, E. A. & Fang, Y. (2010).** Identification of two auto-cleavage products of nonstructural

protein 1 (nsp1) in porcine reproductive and respiratory syndrome virus infected cells: nsp1 function as interferon antagonist. *Virology* **398**, 87-97.

**Clarke, J. B. & Spier, R. E. (1983).** An investigation into causes of resistance of a cloned line of BHK cells to a strain of foot-and-mouth disease virus. *Vet Microbiol* **8**, 259-270.

**Darnell, J. C., Van Driesche, S. J., Zhang, C., Hung, K. Y., Mele, A., Fraser, C. E., Stone, E. F., Chen, C., Fak, J. J., Chi, S. W., Licatalosi, D. D., Richter, J. D. & Darnell, R. B. (2011).** FMRP stalls ribosomal translocation on mRNAs linked to synaptic function and autism. *Cell* **146**, 247-261.

**DeLano, W. L. (2002).** The PyMOL molecular graphics system.

**den Boon, J. A., Faaberg, K. S., Meulenberg, J. J., Wassenaar, A. L., Plagemann, P. G., Gorbalenya, A. E. & Snijder, E. J. (1995).** Processing and evolution of the N-terminal region of the arterivirus replicase ORF1a protein: identification of two papainlike cysteine proteases. *J Virol* **69**, 4500-4505.

**den Boon, J. A., Snijder, E. J., Chirnside, E. D., de Vries, A. A., Horzinek, M. C. & Spaan, W. J. (1991).** Equine arteritis virus is not a togavirus but belongs to the coronaviruslike superfamily. *J Virol* **65**, 2910-2920.

**Fang, Y., Rowland, R. R., Roof, M., Lunney, J. K., Christopher-Hennings, J. & Nelson, E. A. (2006).** A full-length cDNA infectious clone of North American type 1 porcine reproductive and respiratory syndrome virus: expression of green fluorescent protein in the Nsp2 region. *J Virol* **80**, 11447-11455.

**Fang, Y. & Snijder, E. J. (2010).** The PRRSV replicase: exploring the multifunctionality of an intriguing set of nonstructural proteins. *Virus Res* **154**, 61-76.

**Fang, Y., Treffers, E. E., Li, Y., Tas, A., Sun, Z., van der Meer, Y., de Ru, A. H., van Veelen, P. A., Atkins, J. F., Snijder, E. J. & Firth, A. E. (2012).** Efficient -2 frameshifting by mammalian ribosomes to synthesize an additional arterivirus protein. *Proc Natl Acad Sci U S A* **109**, E2920-2928.

**Firth, A. E. & Atkins, J. F. (2009).** A conserved predicted pseudoknot in the NS2A-encoding sequence of West Nile and Japanese encephalitis flaviviruses suggests NS1' may derive from ribosomal frameshifting. *Virol J* **6**, 14.

**Firth, A. E. & Brierley, I. (2012).** Non-canonical translation in RNA viruses. *J Gen Virol* **93**, 1385-1409.

**Fixsen, S. M. & Howard, M. T. (2010).** Processive selenocysteine incorporation during synthesis of eukaryotic selenoproteins. *J Mol Biol* **399**, 385-396.

**Frias-Staheli, N., Giannakopoulos, N. V., Kikkert, M., Taylor, S. L., Bridgen, A., Paragas, J., Richt, J. A., Rowland, R. R., Schmaljohn, C. S., Lenschow, D. J., Snijder, E. J., Garcia-Sastre, A. & Virgin, H. W. t. (2007).** Ovarian tumor domain-containing viral proteases evade ubiquitin- and ISG15-dependent innate immune responses. *Cell Host Microbe* **2**, 404-416.

**Fuerst, T. R., Niles, E. G., Studier, F. W. & Moss, B. (1986).** Eukaryotic transient-expression system based on recombinant vaccinia virus that synthesizes bacteriophage T7 RNA polymerase. *Proc Natl Acad Sci U S A* **83**, 8122-8126.

**Gendron, K., Charbonneau, J., Dulude, D., Heveker, N., Ferbeyre, G. & Brakier-Gingras, L. (2008).** The presence of the TAR RNA structure alters the programmed -1 ribosomal frameshift efficiency of the human immunodeficiency virus type 1 (HIV-1) by modifying the rate of translation initiation. *Nucleic Acids Res* **36**, 30-40.

**Giedroc, D. P. & Cornish, P. V. (2009).** Frameshifting RNA pseudoknots: structure and mechanism. *Virus Res* **139**, 193-208.

**Grentzmann, G., Ingram, J. A., Kelly, P. J., Gesteland, R. F. & Atkins, J. F. (1998).** A dual-luciferase reporter system for studying recoding signals. *RNA* **4**, 479-486.

**Jacks, T., Madhani, H. D., Masiarz, F. R. & Varmus, H. E. (1988a).** Signals for ribosomal frameshifting in the Rous sarcoma virus gag-pol region. *Cell* **55**, 447-458.

**Jacks, T., Power, M. D., Masiarz, F. R., Luciw, P. A., Barr, P. J. & Varmus, H. E. (1988b).** Characterization of ribosomal frameshifting in HIV-1 gag-pol expression. *Nature* **331**, 280-283.

**Jacks, T. & Varmus, H. E. (1985).** Expression of the Rous sarcoma virus pol gene by ribosomal frameshifting. *Science* **230**, 1237-1242.

**Kim, O., Sun, Y., Lai, F. W., Song, C. & Yoo, D. (2010).** Modulation of type I interferon induction by porcine reproductive and respiratory syndrome virus and degradation of CREB-binding protein by non-structural protein 1 in MARC-145 and HeLa cells. *Virology* **402**, 315-326.

**Knoops, K., Barcena, M., Limpens, R. W., Koster, A. J., Mommaas, A. M. & Snijder, E. J. (2012).** Ultrastructural characterization of arterivirus replication structures: reshaping the endoplasmic reticulum to accommodate viral RNA synthesis. *J Virol* **86**, 2474-2487.

**Kobayashi, Y., Zhuang, J., Peltz, S. & Dougherty, J. (2010).** Identification of a cellular factor that modulates HIV-1 programmed ribosomal frameshifting. *J Biol Chem* **285**, 19776-19784.

**Kollmus, H., Hentze, M. W. & Hauser, H. (1996).** Regulated ribosomal frameshifting by an RNA-protein interaction. *RNA* **2**, 316-323.

**Kroese, M. V., Zevenhoven-Dobbe, J. C., Bos-de Ruijter, J. N., Peeters, B. P., Meulenberg, J. J., Cornelissen, L. A. & Snijder, E. J. (2008).** The nsp1alpha and nsp1 papain-like autoproteinases are essential for porcine reproductive and respiratory syndrome virus RNA synthesis. *J Gen Virol* **89**, 494-499.

**Kwak, H., Park, M. W. & Jeong, S. (2011).** Annexin A2 binds RNA and reduces the frameshifting efficiency of infectious bronchitis virus. *PLoS One* **6**, e24067.

**Lauck, M., Sibley, S. D., Hyeroba, D., Tumukunde, A., Weny, G., Chapman, C. A., Ting, N., Switzer, W. M., Kuhn, J. H., Friedrich, T. C., O'Connor, D. H. & Goldberg, T. L. (2013).** Exceptional simian hemorrhagic fever virus diversity in a wild African primate community. *J Virol* **87**, 688-691.

**Li, Y., Zhu, L., Lawson, S. R. & Fang, Y. (2013).** Targeted mutations in a highly conserved motif of the nsp1beta protein impair the interferon antagonizing activity of porcine reproductive and respiratory syndrome virus. *J Gen Virol* **94**, 1972-1983.

**Lin, Z., Gilbert, R. J. & Brierley, I. (2012).** Spacer-length dependence of programmed -1 or -2 ribosomal frameshifting on a U6A heptamer supports a role for messenger RNA (mRNA) tension in frameshifting. *Nucleic Acids Res* **40**, 8674-8689.

**Mador, N., Panet, A. & Honigman, A. (1989).** Translation of gag, pro, and pol gene products of human T-cell leukemia virus type 2. *J Virol* **63**, 2400-2404.

**Makeyev, A. V., Kim, C. B., Ruddle, F. H., Enkhmandakh, B., Erdenechimeg, L. & Bayarsaihan, D. (2005).** HnRNP A3 genes and pseudogenes in the vertebrate genomes. *J Exp Zool A Comp Exp Biol* **303**, 259-271.

**Mejlhede, N., Atkins, J. F. & Neuhard, J. (1999).** Ribosomal -1 frameshifting during decoding of Bacillus subtilis cdd occurs at the sequence CGA AAG. *J Bacteriol* **181**, 2930-2937.

**Meulenberg, J. J., van Nieuwstadt, A. P., van Essen-Zandbergen, A., Bos-de Ruijter, J. N., Langeveld, J. P. & Meloen, R. H. (1998).** Localization and fine mapping of antigenic sites on the nucleocapsid protein N of porcine reproductive and respiratory syndrome virus with monoclonal antibodies. *Virology* **252**, 106-114.

**Nahar-Gohad, P., Sultan, H., Esteban, Y., Stabile, A. & Ko, J. L. (2013).** RACK1 identified as the PCBP1-interacting protein with a novel functional role on the regulation of human MOR gene expression. *J Neurochem* **124**, 466-477.

**Nam, S. H., Copeland, T. D., Hatanaka, M. & Oroszlan, S. (1993).** Characterization of ribosomal frameshifting for expression of pol gene products of human T-cell leukemia virus type I. *J Virol* **67**, 196-203.

**Namy, O., Moran, S. J., Stuart, D. I., Gilbert, R. J. & Brierley, I. (2006).** A mechanical explanation of RNA pseudoknot function in programmed ribosomal frameshifting. *Nature* **441**, 244-247.

**Napthine, S., Vidakovic, M., Girnary, R., Namy, O. & Brierley, I. (2003).** Prokaryotic-style frameshifting in a plant translation system: conservation of an unusual single-tRNA slippage event. *EMBO J* **22**, 3941-3950.

**Nedialkova, D. D., Gorbalenya, A. E. & Snijder, E. J. (2010).** Arterivirus Nsp1 modulates the accumulation of minus-strand templates to control the relative abundance of viral mRNAs. *PLoS Pathog* **6**, e1000772.

**Park, H. J., Park, S. J., Oh, D. B., Lee, S. & Kim, Y. G. (2009).** Increased -1 ribosomal frameshifting efficiency by yeast prion-like phenotype [PSI+]. *FEBS Lett* **583**, 665-669.

**Patel, D., Nan, Y., Shen, M., Ritthipichai, K., Zhu, X. & Zhang, Y. J. (2010).** Porcine reproductive and respiratory syndrome virus inhibits type I interferon signaling by blocking STAT1/STAT2 nuclear translocation. *J Virol* **84**, 11045-11055.

**Plant, E. P. & Dinman, J. D. (2005).** Torsional restraint: a new twist on frameshifting pseudoknots. *Nucleic Acids Res* **33**, 1825-1833.

**Qu, X., Wen, J. D., Lancaster, L., Noller, H. F., Bustamante, C. & Tinoco, I., Jr. (2011).** The ribosome uses two active mechanisms to unwind messenger RNA during translation. *Nature* **475**, 118-121.

**Ruigrok, R. W., Crepin, T. & Kolakofsky, D. (2011).** Nucleoproteins and nucleocapsids of negative-strand RNA viruses. *Curr Opin Microbiol* **14**, 504-510.

**Snijder, E. J., Kikkert, M. & Fang, Y. (2013).** Arterivirus molecular biology and pathogenesis. *J Gen Virol* **94**, 2141-2163.

**Snijder, E. J., van Tol, H., Roos, N. & Pedersen, K. W. (2001).** Non-structural proteins 2 and 3 interact to modify host cell membranes during the formation of the arterivirus replication complex. *J Gen Virol* **82**, 985-994.

**Snijder, E. J., Wassenaar, A. L. & Spaan, W. J. (1992).** The 5' end of the equine arteritis virus replicase gene encodes a papainlike cysteine protease. *J Virol* **66**, 7040-7048.

**Snijder, E. J., Wassenaar, A. L. & Spaan, W. J. (1994).** Proteolytic processing of the replicase ORF1a protein of equine arteritis virus. *J Virol* **68**, 5755-5764.

**Sun, Y., Xue, F., Guo, Y., Ma, M., Hao, N., Zhang, X. C., Lou, Z., Li, X. & Rao, Z. (2009).** Crystal structure of porcine reproductive and respiratory syndrome virus leader protease Nsp1alpha. *J Virol* **83**, 10931-10940.

**Sun, Z., Chen, Z., Lawson, S. R. & Fang, Y. (2010).** The cysteine protease domain of porcine reproductive and respiratory syndrome virus nonstructural protein 2 possesses deubiquitinating and interferon antagonism functions. *J Virol* **84**, 7832-7846.

**Sun, Z., Li, Y., Ransburgh, R., Snijder, E. J. & Fang, Y. (2012).** Nonstructural protein 2 of porcine reproductive and respiratory syndrome virus inhibits the antiviral function of interferon-stimulated gene 15. *J Virol* **86**, 3839-3850.

**Takyar, S., Hickerson, R. P. & Noller, H. F. (2005).** mRNA helicase activity of the ribosome. *Cell* **120**, 49-58.

**Thiel, V., Ivanov, K. A., Putics, A., Hertzig, T., Schelle, B., Bayer, S., Weissbrich, B., Snijder, E. J., Rabenau, H., Doerr, H. W., Gorbalenya, A. E. & Ziebuhr, J.**

**(2003).** Mechanisms and enzymes involved in SARS coronavirus genome expression. *J Gen Virol* **84**, 2305-2315.

**Tijms, M. A., Nedialkova, D. D., Zevenhoven-Dobbe, J. C., Gorbalenya, A. E. & Snijder, E. J. (2007).** Arterivirus subgenomic mRNA synthesis and virion biogenesis depend on the multifunctional nsp1 autoprotease. *J Virol* **81**, 10496-10505.

**Tijms, M. A., van Dinten, L. C., Gorbalenya, A. E. & Snijder, E. J. (2001).** A zinc finger-containing papain-like protease couples subgenomic mRNA synthesis to genome translation in a positive-stranded RNA virus. *Proc Natl Acad Sci U S A* **98**, 1889-1894.

**van den Akker, J., VanBavel, E., van Geel, R., Matlung, H. L., Guvenc Tuna, B., Janssen, G. M., van Veelen, P. A., Boelens, W. C., De Mey, J. G. & Bakker, E. N. (2011).** The redox state of transglutaminase 2 controls arterial remodeling. *PLoS One* **6**, e23067.

**van Kasteren, P. B., Bailey-Elkin, B. A., James, T. W., Ninaber, D. K., Beugeling, C., Khajehpour, M., Snijder, E. J., Mark, B. L. & Kikkert, M. (2013).** Deubiquitinase function of arterivirus papain-like protease 2 suppresses the innate immune response in infected host cells. *Proc Natl Acad Sci U S A* **110**, E838-847.

**Wang, L. & Brown, S. J. (2006).** BindN: a web-based tool for efficient prediction of DNA and RNA binding sites in amino acid sequences. *Nucleic Acids Res* **34**, W243-248.

**Wassenaar, A. L., Spaan, W. J., Gorbalenya, A. E. & Snijder, E. J. (1997).** Alternative proteolytic processing of the arterivirus replicase ORF1a polyprotein: evidence that NSP2 acts as a cofactor for the NSP4 serine protease. *J Virol* **71**, 9313-9322.

**Xue, F., Sun, Y., Yan, L., Zhao, C., Chen, J., Bartlam, M., Li, X., Lou, Z. & Rao, Z. (2010).** The crystal structure of porcine reproductive and respiratory syndrome virus nonstructural protein Nsp1beta reveals a novel metal-dependent nuclease. *J Virol* **84**, 6461-6471.

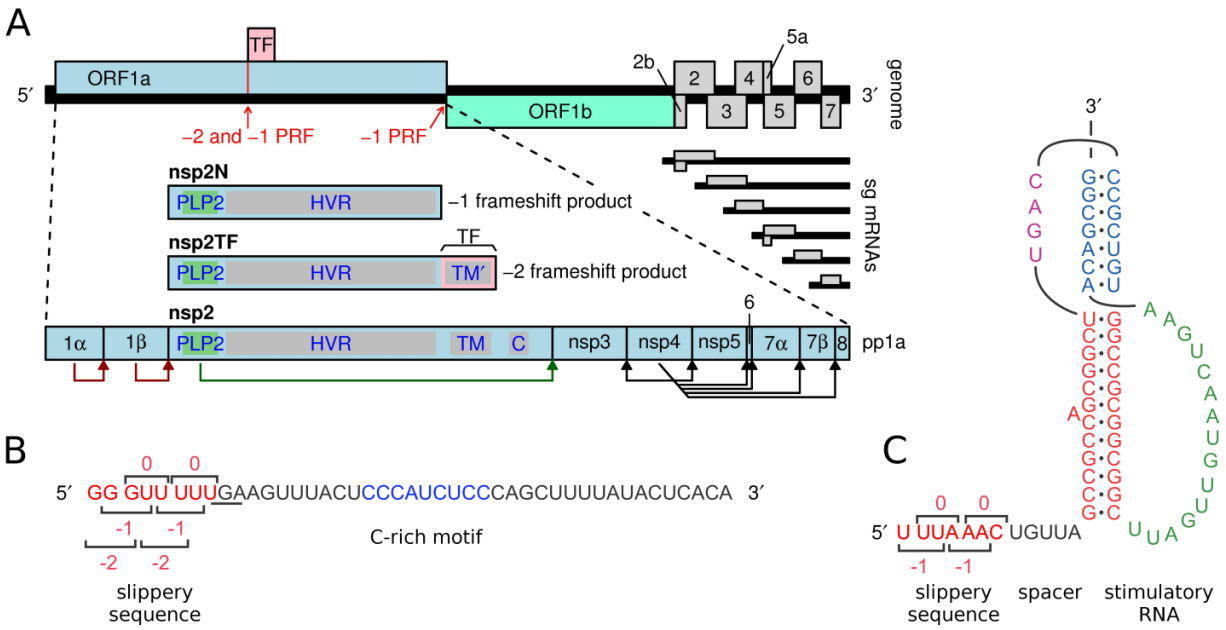


**Figure 4. 1 PRRSV genome organization and location of ribosomal frameshifting signals.** (*A*) Overview of the ~15-kb PRRSV genome. The long 5′ ORFs 1a and 1b encode nonstructural polyproteins, and at least eight shorter 3′ ORFs (2a-7) encode structural proteins. The 3′ ORFs are translated from a nested set of subgenomic mRNAs, two of which are bicistronic. ORF1a and ORF1b are translated from the genomic RNA, with translation of ORF1b depending on −1 PRF at the end of ORF1a. The TF ORF overlaps the central ORF1a region in the −2 reading frame and is accessed via −2 PRF (13). A –1 frameshift at the same site generates the nsp2N product (see text). The vertical red line indicates the location of the RG_GUU_UUU shift site (R = A or G, in different arteriviruses). Domains in nsp2/nsp2TF: PLP2, papain-like proteinase; HVR, hypervariable region; TM/TM′, (putative) transmembrane domains; C, Cys-rich domain. (*B*) Sequence of the SD01-08 RNA in the region of the −2/−1 PRF signal, with the slippery sequence (red) and C-rich motif (blue) highlighted. The −1 reading frame stop codon is underlined and codons for each of the reading frames are indicated. (*C*) Features of the canonical −1 PRF signal present in the PRRSV ORF1a/ORF1b overlap region. The stimulatory RNA pseudoknot is composed of two stems connected by single-stranded loops.

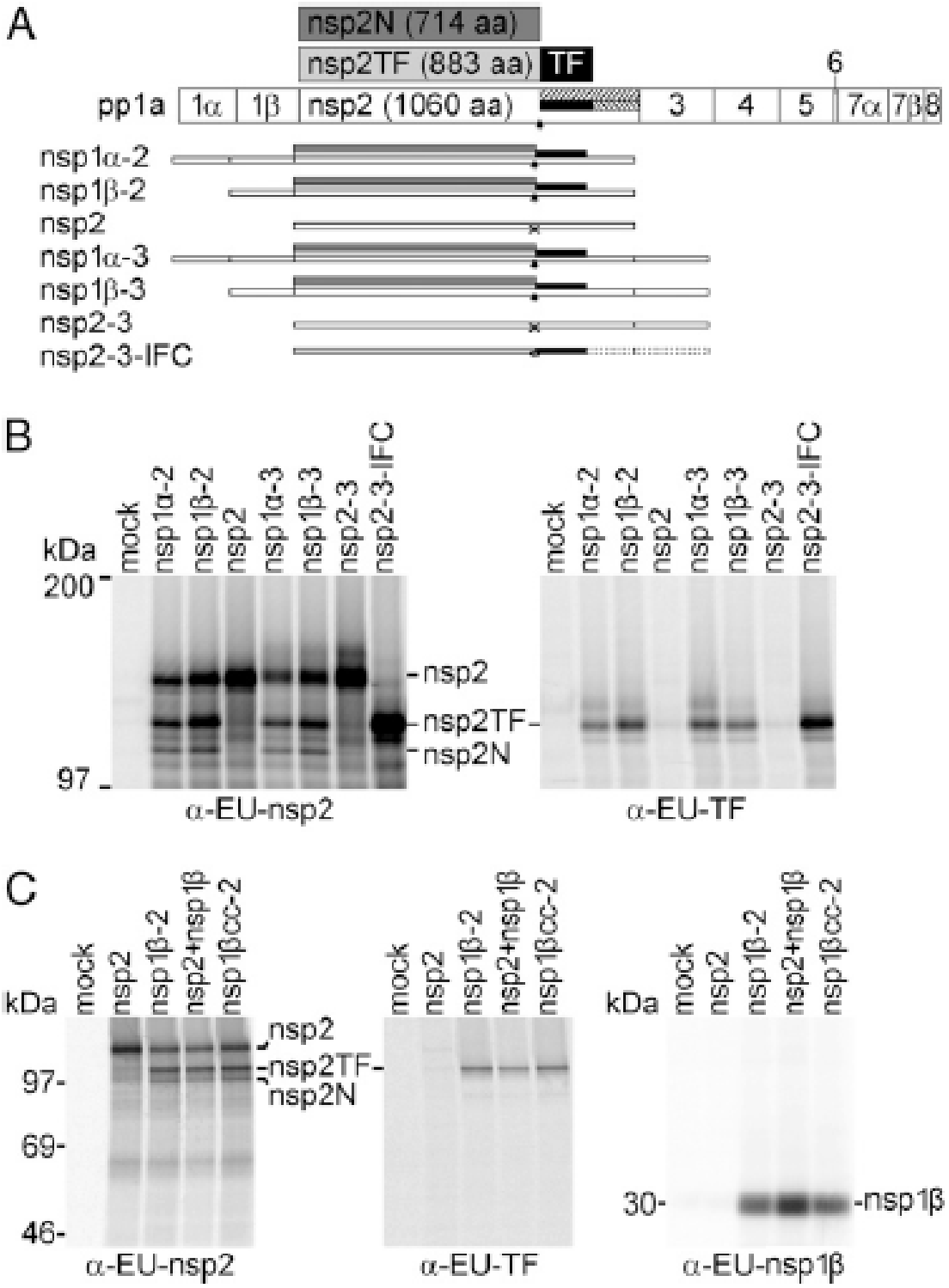
A
nsp2N (714 aa)
nsp2TF (883 aa)
TF
6
pp1a
1α
1β
nsp2 (1060 aa)
3
4
5
7α
7β
8
nsp1α-2
nsp1β-2
nsp2
nsp1α-3
nsp1β-3
nsp2-3
nsp2-3-IFC
B
kDa
mock
nsp1α-2
nsp1β-2
nsp2
nsp1α-3
nsp1β-3
nsp2-3
nsp2-3-IFC
200
97
nsp2
nsp2TF
nsp2N
α-EU-nsp2
α-EU-TF
C
kDa
mock
nsp2
nsp1β-2
nsp2+nsp1β
nsp1βα-2
97-
69-
46-
nsp2
nsp2TF
nsp2N
α-EU-nsp2
α-EU-TF
30-
nsp1β
α-EU-nsp1β

**Figure 4. 2 PRRSV nsp1β transactivates –2/–1 PRF.** (*A*) Schematic representation of expression vectors encoding different combinations of replicase subunits from the nsp1α-nsp3 region of type 1 PRRSV (isolate SD01-08), which were expressed as single nsps or self-cleaving multi-nsp polyproteins. PRRSV pp1a and its processing scheme are shown at the top and the proteins expressed from different constructs are shown in grey, whereas the polypeptide encoded by the TF ORF is indicated in black. The nsp2-3-IFC control (13) is an in-frame construct that expresses nsp2TF only. (B) Expression of different protein combinations (A) using the recombinant vaccinia virus/T7 RNA polymerase expression system and RK-13 cells, revealing that nsp1β expression is required for efficient –2/–1 PRF. After metabolic labeling, expression products were immunoprecipitated with the antibodies indicated below each panel; mAb α-EU-nsp2 recognizes the common N-terminal domain of nsp2, nsp2TF, and nsp2N, while α-EU-TF recognizes the C-terminal domain of nsp2TF. Immunoprecipitated (IP) proteins were separated by SDS-PAGE and visualized by autoradiography. (*C*) Analysis of −2/−1 PRF transactivation by nsp1β using the recombinant vaccinia virus–T7 RNA polymerase expression system as described for B. RK-13 cells were transfected with plasmid DNAs expressing nsp2, nsp1β-2, nsp2+nsp1β (from separate plasmids), or nsp1βcc-2, with the latter containing an nsp1β-coding sequence in which the large majority of codons had been synonymously mutated (Fig. 4.11). Expression products were immunoprecipitated using specific antibodies indicated at the bottom of each panel and visualized by SDS/PAGE and autoradiography.

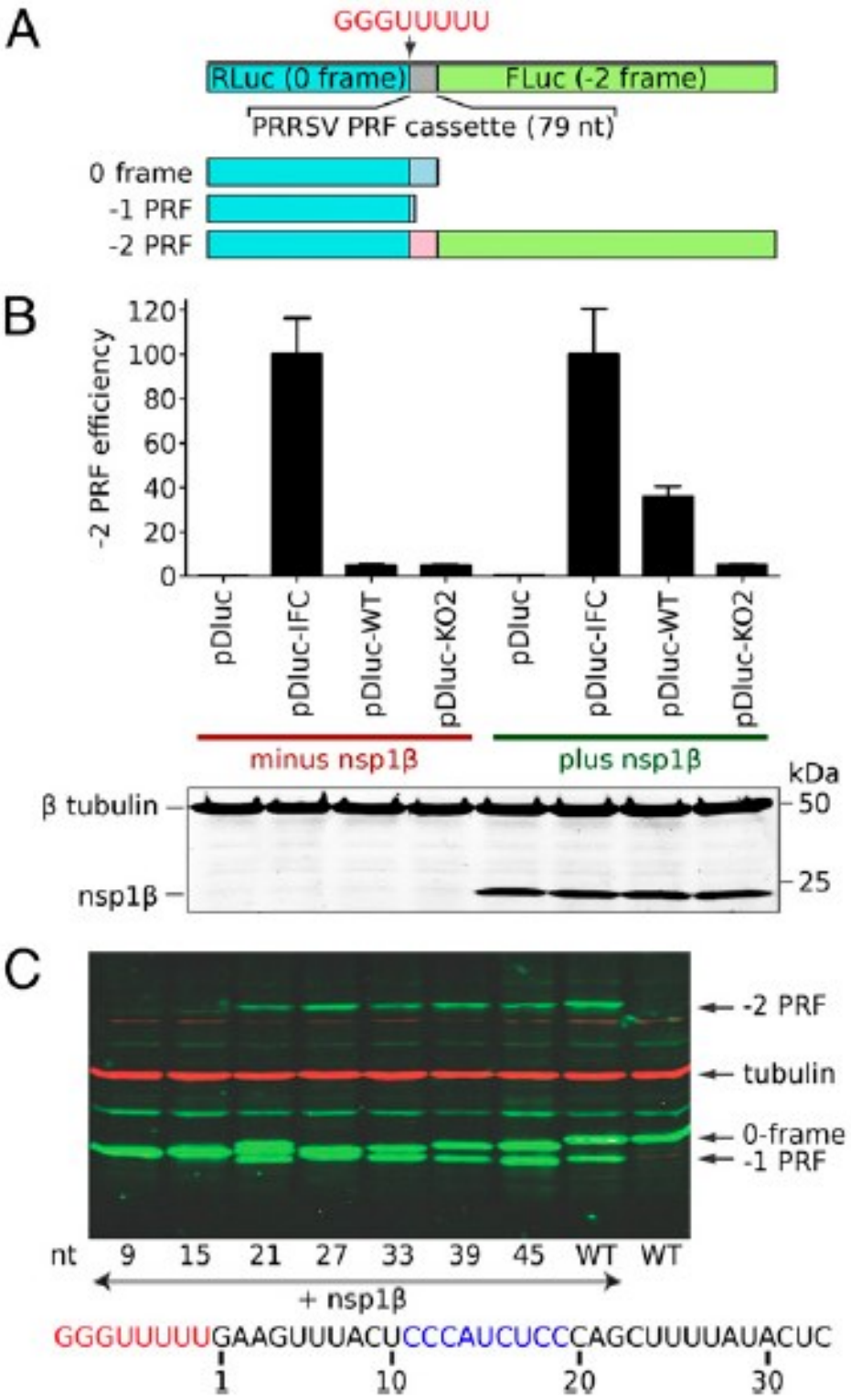
A
GGGUUUUU
RLuc (0 frame)
FLuc (-2 frame)
PRRSV PRF cassette (79 nt)
0 frame
-1 PRF
-2 PRF
B
-2 PRF efficiency
120
100
80
60
40
20
0
pDluc
pDluc-IFC
pDluc-WT
pDluc-KO2
pDluc
pDluc-IFC
pDluc-WT
pDluc-KO2
minus nsp1β
plus nsp1β
kDa
β tubulin
nsp1β
50
25
C
-2 PRF
tubulin
0-frame
-1 PRF
nt 9 15 21 27 33 39 45 WT WT
+ nsp1β
GGGUUUUUGAAGUUUACUCCCAUCUCCCAGCUUUUAUACUC
1 10 20 30

**Figure 4. 3 Delineation of RNA elements required for PRRSV –2/–1 PRF.** (*A*) Schematic representation of the pDluc dual luciferase construct. The GG_GUU_UUU shift site, 5 upstream nucleotides and 66 downstream nucleotides (79 nt in total) were inserted between the *Renilla* and firefly luciferases genes such that –2 PRF is required for firefly luciferase expression. (*B*) Dual luciferase reporter assay showing that efficient –2 PRF depends on co-expression of nsp1β. For type1 PRRSV (isolate SD01-08), nsp1β was co-expressed with dual luciferase constructs containing a WT or –2 PRF knock out (KO2) frameshift signal. Mutant KO2 [Fig. 4.9; (Fang *et al.*, 2012)] contains point mutations within both slippery sequence and downstream C-rich motif. The –2 PRF efficiencies were calculated by comparing the ratio of firefly and *Renilla* luciferase activities, using the in-frame control mutant (IFC, Fig. 4.9A) as a reference. Error bars represent the standard deviation of three independent experiments, in which each construct was transfected in duplicate. The bottom panel shows a Western blot analysis confirming equal expression of nsp1β and equal loading (β tubulin). (*C*) Delineation of the minimal RNA sequence requirements for efficient –2/–1 PRF. Starting from a construct containing the 66 nt downstream of the slippery sequence, a series of 3' truncations was engineered in pDluc. Upon co-expression with nsp1β, cell lysates were analyzed by Western blot, using an antibody recognizing the common *Renilla* luciferase part of all pDluc translation products (see panel A). The number below each lane represents the remaining PRRSV-specific RNA sequence downstream of the slippery sequence, of which 21 nt were sufficient for efficient –2/–1 PRF in this assay.

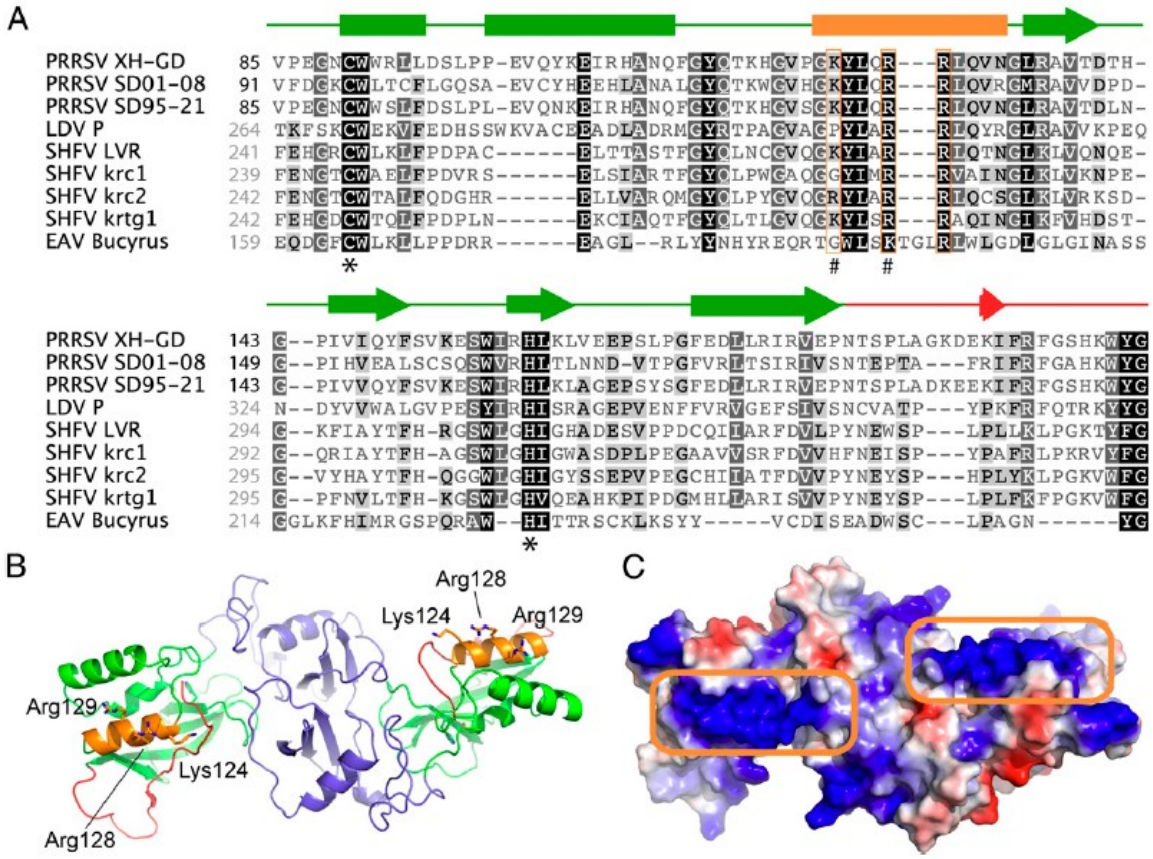
A
PRRSV XH-GD 85 VPEGNCWWRLLDSLPP-EVQYKEIRHANQFGYCTKHGVPGKYLQR---RLQVNGLRAVTDTH-
PRRSV SD01-08 91 VFDGKCWLTCFLGQSA-EVCYHEEHLANAILGYCTKWGVHGKYLQR---RLQVRGMRAVVDPD-
PRRSV SD95-21 85 VPEGNCWWSLFDSLPL-EVQNKEIRHANQFGYCTKHGVSGKYLQR---RLQVNGLRAVTDLN-
LDV P 264 TKFSKCWEKVFEDHSSWKVACEEADLADRMGYRTPACVAGPYLAR---RLQYRGLRAVVKPEQ
SHFV LVR 241 FEHGRCWLKLFPDPAC------ELTTASTFGYCLNCGVQGKYIAR---RLQTNGLKLVQNQE-
SHFV krc1 239 FENGTCWAELFPDVRS------ELSIARTFGYCLPWGAQGGYIMR---RVAINGLKLVKNPE-
SHFV krc2 242 FENGTCWTALFQDGHR------ELLVARQMGYCLPYGVQGRYLAR---RLQCSGLKLVRKSD-
SHFV krtg1 242 FEHGDCWTQLFPDPLN------EKCIAQTFGYCLTLGVQGKYLSR---RAQINGIKFVHDST-
EAV Bucyrus 159 EQDGFCWLKLLPPDRR------EAGL--RLYYNHYREQRTGWLSKTGLRLWLGDLGLGINASS
PRRSV XH-GD 143 G--PIVIQYFSVKESWIRHILKLVEEPSLPGFEDLLRIRVEPNTSPLAGKDEKIFRFGSHKWYG
PRRSV SD01-08 149 G--PIHVEALSCSQSWVRHLTLNND-VTPGFVRLTSIRIVSNTEPTA---FRIFRFGAHKWYG
PRRSV SD95-21 143 G--PIVVQYFSVKESWIRHLKLAGEPSYSGFEDLLRIRVEPNTSPLADKEEKIFRFGSHKWYG
LDV P 324 N--DYVVWALGVPESYIRHISRAGEPVENFFVRVGEFSIVSNCVATP---YPKFRFQTRKYYG
SHFV LVR 294 G--KFIAYTFH-RGSWIGHIGHADESVPPDCQILARFDVLPYNEWSP---LPLLKLPGKTYFG
SHFV krc1 292 G--QRIAYTFH-AGSWIGHIGWASDPLPEGAAVVSRFDVVHFNEISP---YPAFRLPKRVYFG
SHFV krc2 295 G--VYHAYTFH-QGGWIGHIGYSSEPVPEGCHILATFDVVPYNEYSP---HPLYKLPGKVWFG
SHFV krtg1 295 G--PFNVLTFH-KGSWIGHVQEAHKPIPDGMHLEARISVVPYNEYSP---LPLFKFPGKVWFG
EAV Bucyrus 214 GGLKFHIMRGSPQRAW--HITTRSCKLKSYY-----VCDISEADWSC---LPAGN------YG
B
Arg128
Lys124
Arg129
Arg129
Lys124
Arg128
C

**Figure 4. 4 PRRSV nsp1β sequence and structure.** *(A)* Amino acid sequence alignment of the PLP1β domains from selected arterivirus nsp1β proteins. Secondary structure elements [based on the published crystal structure from type 2 PRRSV isolate XH-GD; (Xue *et al.*, 2010)] are shown above the alignment and are color-matched to the nsp1β structure in panel B. Conserved basic residues in PLP1β helix α4 are boxed in orange; #, residues mutated in mutant 1βKO (see text for details); *, PLP1β active site residues. PRRSV sequences are numbered (black) from the nsp1α/nsp1β cleavage site, whereas all other sequences are numbered (grey) starting from the N-terminus of the pp1a polyprotein. EAV, equine arteritis virus; LDV, lactate dehydrogenase elevating virus; SHFV, simian hemorrhagic fever virus; names of specific isolates used are indicated. Genbank accession numbers of sequences used: EU624117 (PRRSV XH-GD), DQ489311 (PRRSV SD01-08), KC469618 (PRRSV SD95-21), NC_001639 (LDV P), NC_003092 (SHFV LVR), HQ845737 (SHFV krc1), HQ845738 (SHFV krc2), JX473847 (SHFV krtg1), NC_002532 (EAV Bucyrus). (*B*) Cartoon representation of the crystal structure of the nsp1β dimer from a type 2 PRRSV isolate [PRRSV XH-GD; PDB entry 3MTV; (Xue *et al.*, 2010)]. For both monomers, the N-terminal domain is colored purple, whereas the PLP1β domain and the C-terminal extension (leading up to the nsp1β/nsp2 site cleaved by PLP1β) are colored green and red, respectively. Helix α4 of PLP1β, containing the conserved GKYLQRRLQ motif, is colored orange with basic residues represented as sticks. (*C*) Electrostatic surface representation of the nsp1β dimer showing the positively charged (blue) patches on helix α4 of PLP1β (boxed in orange) created by the basic residues of the GKYLQRRLQ motif. Both patches reside on the same side of the structure, potentially allowing for RNA to bind across the entire dimer surface.

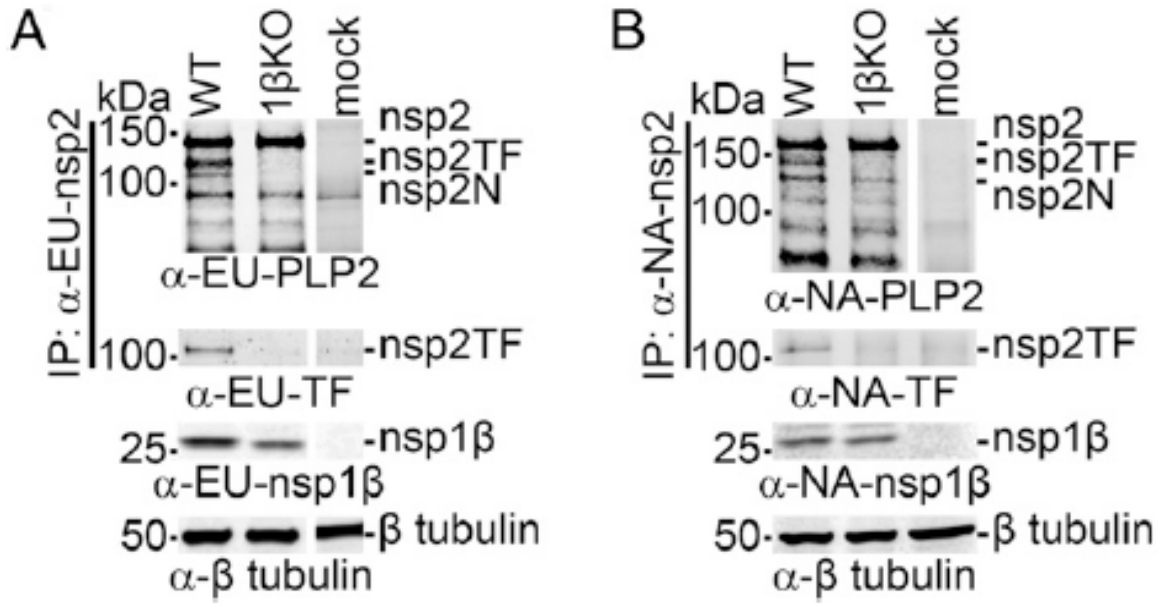


**Figure 4. 5 A conserved motif in PRRSV PLP1β is critical for transactivation of –2/–1 PRF in an expression system.** The recombinant vaccinia virus/T7 RNA polymerase expression system and HEK 293T cells were used to express WT and 1βKO mutant nsp1β-nsp2 polyproteins from *(A)* type 1 and *(B)* type 2 PRRSV. The 1βKO mutant carried a double Ala substitution of basic residues in the highly conserved GKYLQRRLQ motif of nsp1β (see also Fig. 4.4 and 4.9). Expression products were immunoprecipitated with mAbs recognizing the common N-terminal domain of the nsp2-related products. Following SDS-PAGE, they were identified in Western blot analysis using antibodies recognizing the common nsp2 domain, the C-terminus of nsp2TF, or nsp1β. A tubulin antiserum was used for a loading control.

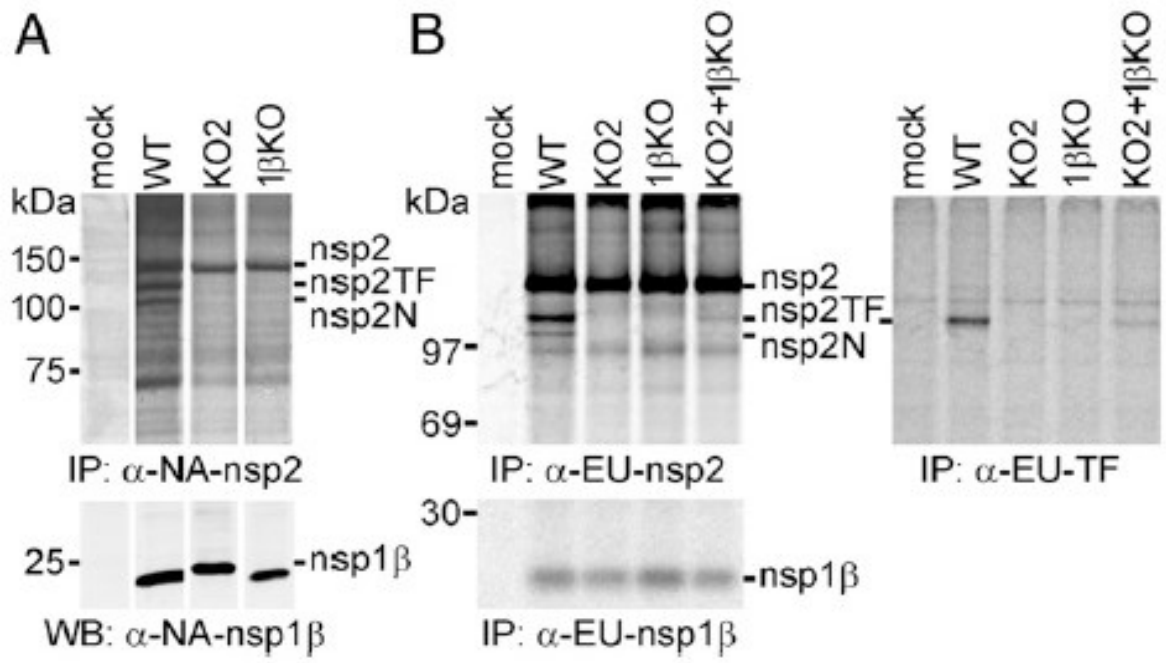


**Figure 4. 6 A conserved motif in PRRSV PLP1β is critical for transactivation of –2/–1 PRF in infected cells.** (*A*) Analysis of nsp2-related products in MARC-145 cells infected with WT type 2 PRRSV (isolate SD95-21) or mutants KO2 and 1βKO. Mutant KO2 (Fig. 4.9) contained PRF-inactivating point mutations in both slippery sequence and downstream C-rich motif, whereas 1βKO carried a double Ala substitution of basic residues in the highly conserved GKYLQRRLQ motif of nsp1β. Following metabolic labeling, proteins were immunoprecipitated using mAb α-NA-nsp2 and visualized by SDS-PAGE and autoradiography. The expression of nsp1β was monitored by Western blot analysis. (*B*) BHK-21 cells were transfected with *in vitro* transcribed full-length RNA of WT, KO2 or 1βKO PRRSV SD01-08 (type 1) or were double-transfected with equal amounts of KO2 and 1βKO RNA to demonstrate complementation between these two virus mutants. Following metabolic labeling, viral proteins were immunoprecipitated using specific mAbs that recognize a common nsp2 domain (α-EU-nsp2 panel), the polypeptide encoded by the TF ORF (α-EU-TF panel), or nsp1β (α-EU-nsp1β panel). Protein products were visualized using SDS-PAGE and autoradiography.

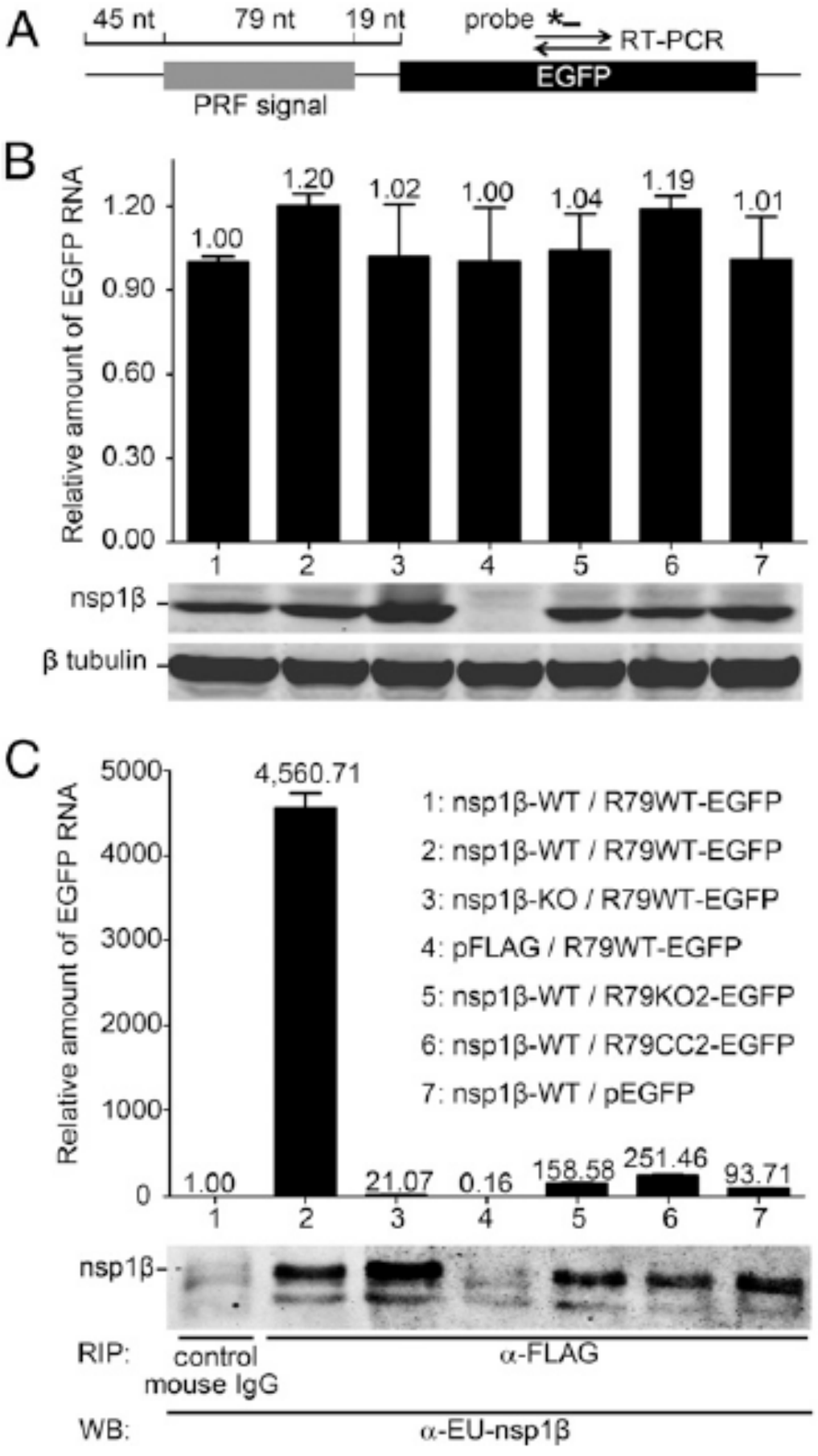
A
45 nt
79 nt
19 nt
probe
RT-PCR
EGFP
PRF signal
B
Relative amount of EGFP RNA
1.20
0.90
0.60
0.30
0.00
1.00
1.20
1.02
1.00
1.04
1.19
1.01
1
2
3
4
5
6
7
nsp1β
β tubulin
C
Relative amount of EGFP RNA
5000
4000
3000
2000
1000
0
4,560.71
1.00
21.07
0.16
158.58
251.46
93.71
1: nsp1β-WT / R79WT-EGFP
2: nsp1β-WT / R79WT-EGFP
3: nsp1β-KO / R79WT-EGFP
4: pFLAG / R79WT-EGFP
5: nsp1β-WT / R79KO2-EGFP
6: nsp1β-WT / R79CC2-EGFP
7: nsp1β-WT / pEGFP
nsp1β
RIP:
control mouse IgG
α-FLAG
WB:
α-EU-nsp1β

**Figure 4. 7 An RNA carrying the PRRSV –2/–1 PRF signal co-immunoprecipitates with nsp1β.** A protein-RNA interaction assay was designed based on co-immunoprecipitation of nsp1β and RNA transcripts containing 79-nt of type1 PRRSV sequence, including the –2/–1 PRF signal. (A) Schematic representation of the target RNA in which a WT 79-nt PRF signal (R79WT-EGFP), or its mutant KO2 or CC2 derivatives (see Fig. 4.9A), was fused to the EGFP sequence. The latter served as a target for qRT-PCR amplification (primer set and TaqMan probe indicated), which was used to quantify the amount of RNA target bound to nsp1β. (B-C) HEK-293T cells were co-transfected with a plasmid expressing WT or 1βKO FLAG-tagged nsp1β and a plasmid expressing a WT or mutant target RNA. Empty vectors (pFLAG and pEGFP) were included as negative controls. (*B*) Detection of input levels of nsp1β bait and RNA target in cell lysates prior to the co-immunoprecipitation assay. Quantitative qRT-PCR was used to determine the levels of WT or mutant R79-EGFP mRNA in transfected cells (top panel). Western blot analysis was used to monitor the input of 1βKO or WT nsp1β bait (middle panel) and to verify the use of equal amounts of cell lysate (β-tubulin control; bottom panel). Lane numbers are explained in panel B. (*C*) Following FLAG-nsp1β immunoprecipitation, the amount of co-precipitating target RNA was determined by qRT-PCR (see panel A). Western blot analysis using a mAb α-EU-nsp1β was used to monitor the amount of immunoprecipitated nsp1β. A legend explaining the co-transfected plasmids for each lane number is given on the right side of the panel.

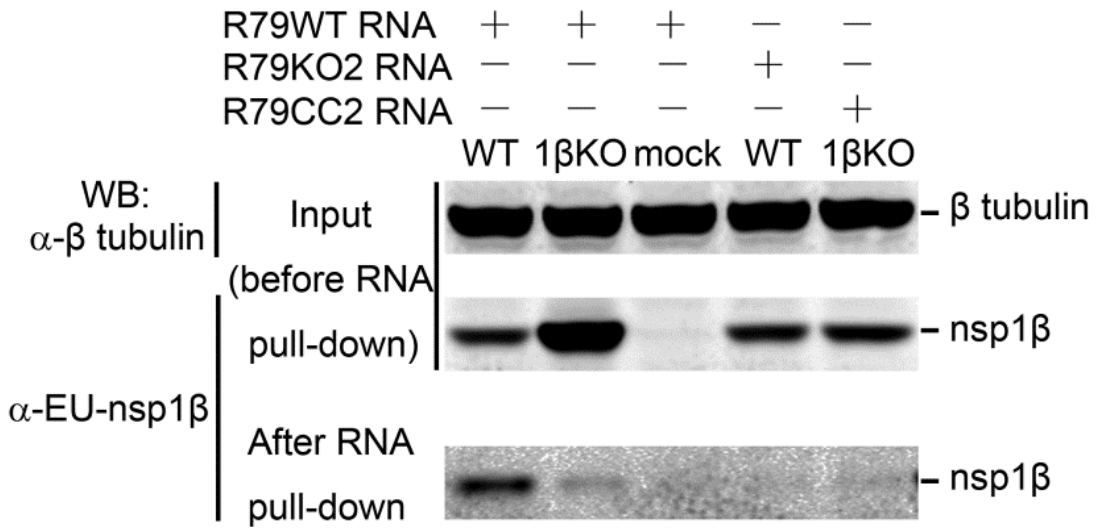


**Figure 4. 8 PRRSV nsp1β can be pulled-down using an RNA carrying the –2/–1 PRF signal.** Cell lysates from 1βKO or WT nsp1β-expressing HEK-293T cells were incubated with *in vitro* produced BrU-labeled RNA transcripts containing WT or mutant (KO2 or CC2, Fig. 4.9) versions of a 79-nt sequence from the –2/–1 PRF region of type 1 PRRSV (isolate SD01-08). RNA-protein complexes were immunoprecipitated with an anti-BrU antibody and subjected to Western blot analysis using an nsp1β-specific mAb. The amount of β-tubulin in the initial samples was monitored to verify equal loading.

A

PRRSV SD01-08 (EU, type 1)

```
 WT   3507-ACA UGG GUU UUU   GAA GUU UAC UCC CAU CUC CCA GCU UUU AUA CUC ACA
IFC   3507-ACA UGG GUG UUCUU GAA GUU UAC UCC CAU CUC CCA GCU UUU AUA CUC ACA
CC2   3507-ACA UGG GUU UUU   GAA GUU UAC AGA AAU AUG GCA GCU UUU AUA CUC ACA
 M1   3507-ACA UGG GUU UUU   GGA GUU UAC UCC CAU CUC CCA GCU UUU AUA CUC ACA
KO2   3507-ACA UGG GUA UUC   GAA GUU UAU AGU CAU UUG CCA GCU UUU AUA CUG ACA

1βKO  K130A/R134A in nsp1β
```

PRRSV SD95-21 (NA, type 2)

```
 WT   3878-CGU CAG GUU UUU   GAC CUC GUC UCC CAU CUC CCU GUU UUC UUC UCA CGC
 M1   3878-CGU CAG GUU UUU   GGC CUC GUC UCC CAU CUC CCU GUU UUC UUC UCA CGC
KO2   3878-CGU CAG GUA UUC   GAC CUA GUG AGU CAU UUG CCU GUU UUC UUC UCA CGC

1βKO  K124A/R128A in nsp1β
```

B

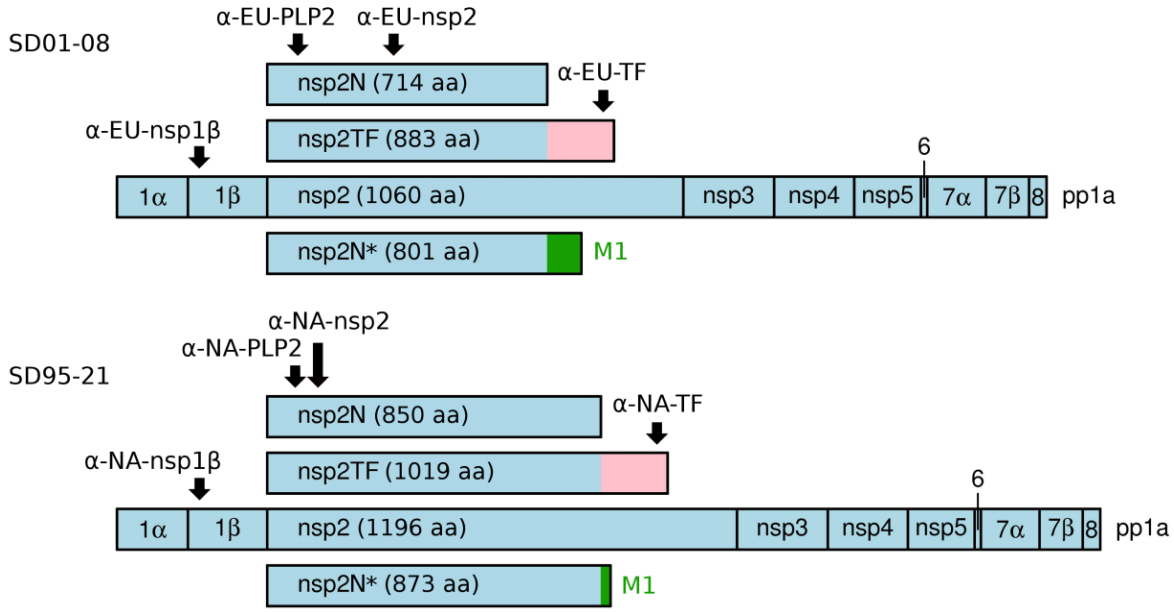

**Figure 4. 9 Overview of mutants and antibodies used in this study.** (*A*) List of WT and mutant sequences of the PRRSV PRF region (GGUUUUU shift site and conserved CCCANCUCC motif indicated with orange and magenta boxes, respectively). Mutated nucleotides are highlighted in cyan. Coordinates of starting nucleotides refer to PRRSV sequences DQ489311 (type 1 PRRSV) and KC469618 (type 2 PRRSV). IFC, in-frame control; CC2, disrupted CCCANCUCC motif; M1, mutated −1 frame termination codon to C-terminally extend nsp2N; KO2, knockout mutant 2 (premature –2 frame termination codon and disrupted frameshift cassette); 1βKO, knockout mutant 3 (double mutation introduced into the nsp1β GKYLQRRLQ motif). (*B*) Sizes of nsp2-related polypeptides described in this study and location of epitopes recognized by the PRRSV-specific antibodies in the nsp1β-2 region. Nsp2N* refers to the C-terminally extended version of nsp2N that is produced by mutant M1, due to removal of the stop codon (see panel A). Origin and original name of each antibody are provided in the Materials and Methods section. Sizes (in aa) for nsp2-related products are shown for GenBank sequences DQ489311 (SD01-08, PRRSV type 1) and KC469618 (SD95-21, PRRSV type 2).

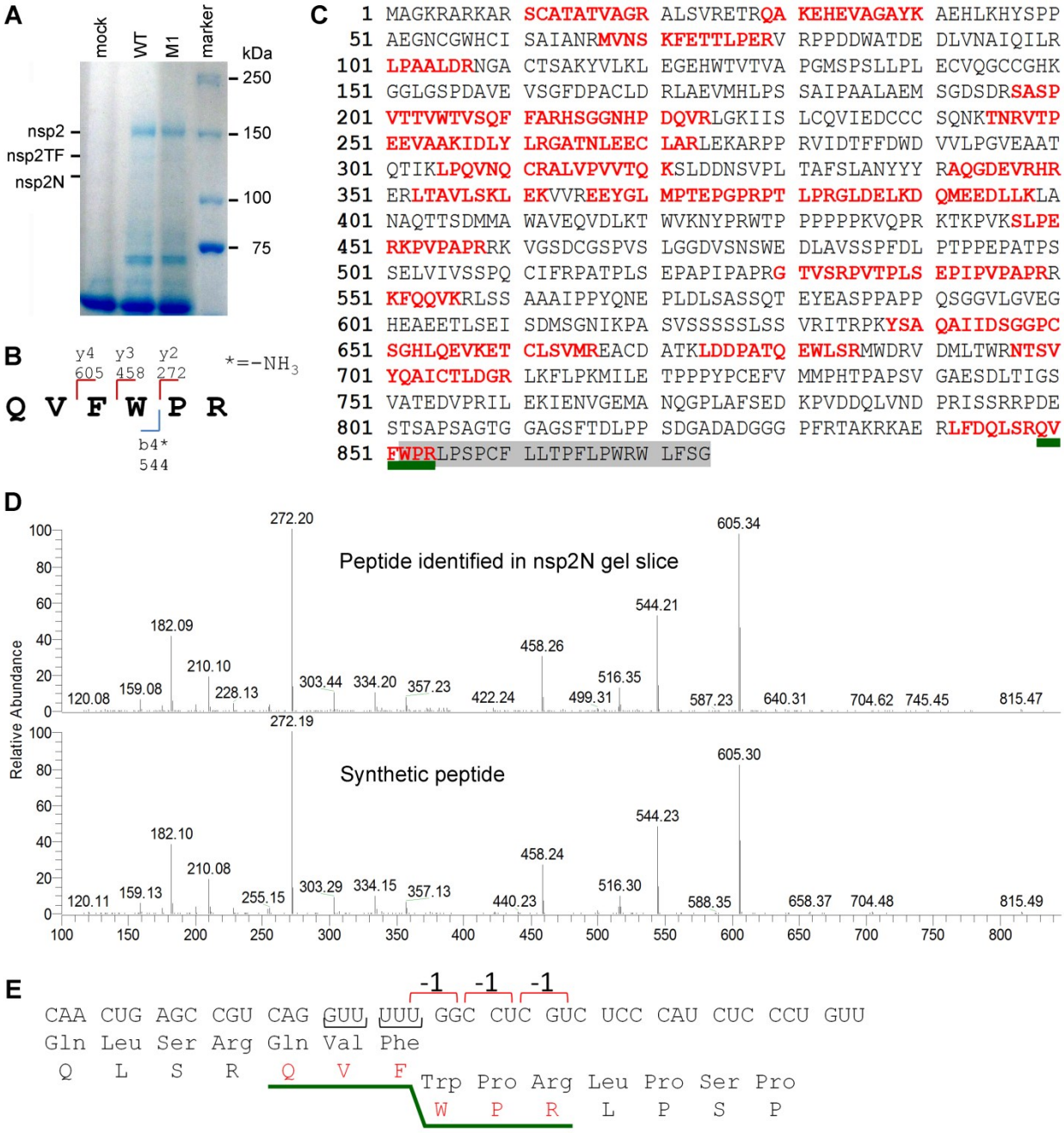
A
mock
WT
M1
marker
kDa
250
150
100
75
nsp2
nsp2TF
nsp2N
B
y4 y3 y2
605 458 272
*=-NH3
Q V F W P R
b4*
544
C
1 MAGKRARKAR SCATATVAGR ALSVRETRQA KEHEVAGAYK AEHLKHYSPP
51 AEGNCGWHCI SAIANRMVNS KFETTLPERV RPPDDWATDE DLVNAIQILR
101 LPAALDRNGA CTSAKYVLKL EGEHWTVTVA PGMSPSLLPL ECVQGCCGHK
151 GGLGSPDAVE VSGFDPACLD RLAEVMHLPS SAIPAALAEM SGDSDRSASP
201 VTTVWTVSQF FARHSGGNHP DQVRLGKIIS LCQVIEDCCC SQNKTNRVTP
251 EEVAAKIDLY LRGATNLEEC LARLEKARPP RVIDTFFDWD VVLPGVEAAT
301 QTIKLPQVNQ CRALVPVVTQ KSLDDNSVPL TAFSLANYYY RAQGDEVRHR
351 ERLTAVLSKL EKVVREEYGL MPTEPGPRPT LPRGLDELKD QMEEDLLKLA
401 NAQTTSDMMA WAVEQVDLKT WVKNYPRWTP PPPPPKVQPR KTKPVKSLPE
451 RKPVPAPRRK VGSDCGSPVS LGGDVSNSWE DLAVSSPFDL PTPPEPATPS
501 SELVIVSSPQ CIFRPATPLS EPAPIPAPRG TVSRPVTPLS EPIPVPAPRR
551 KFQQVKRLSS AAAIPPYQNE PLDLSASSQT EYEASPPAPP QSGGVLGVEG
601 HEAEETLSEI SDMSGNIKPA SVSSSSSLSS VRITRPKYSA QAIIDSGGPC
651 SGHLQEVKET CLSVMREACD ATKLDDPATQ EWLSRMWDRV DMLTWRNTSV
701 YQAICTLDGR LKFLPKMILE TPPPYPCEFV MMPHTPAPSV GAESDLTIGS
751 VATEDVPRIL EKIENVGEMA NQGPLAFSED KPVDDQLVND PRISSRRPDE
801 STSAPSAGTG GAGSFTDLPP SDGADADGGG PFRTAKRKAE RLFDQLSRQV
851 FWPRLPSPCF LLTPFLPWRW LFSG
D
Peptide identified in nsp2N gel slice
Synthetic peptide
Relative Abundance
272.20
605.34
544.21
182.09
458.26
210.10
516.35
120.08
159.08
228.13
303.44
334.20
357.23
422.24
499.31
587.23
640.31
704.62
745.45
815.47
272.19
605.30
544.23
182.10
458.24
210.08
516.30
120.11
159.13
255.15
303.29
334.15
357.13
440.23
588.35
658.37
704.48
815.49
E
-1 -1 -1
CAA CUG AGC CGU CAG GUU UUU GGC CUC GUC UCC CAU CUC CCU GUU
Gln Leu Ser Arg Gln Val Phe
Q L S R Q V F Trp Pro Arg Leu Pro Ser Pro
W P R L P S P

**Figure 4. 10 Mass spectrometric analysis of nsp2N* (a C-terminally extended version of nsp2N) purified from cells infected with mutant SD95-21-M1.** (*A*) PRRSV-infected or mock-infected MARC-145 cell lysates were immunoprecipitated with nsp2-specific α-NA-PLP2. Immunoprecipitated proteins were separated by SDS-PAGE and stained with Coomassie Blue. The positions of nsp2, nsp2TF, and nsp2N are indicated. (*B*) Fragmentation spectrum of the –1 frameshift-specific peptide QVFWPR. (*C*) Complete amino acid sequence of nsp2N* comprising nsp2N and a 23-amino-acid C-terminal extension (highlighted in gray). Peptides identified by mass spectrometry are depicted in red. The peptide spanning the –1 frameshift site is underlined in green. (*D*) Peptide sequence of the nsp2N* –1 frameshift-specific peptide. The fragment ions that were identified in the LC-MS/MS analysis of the gel slice are indicated. (*E*) Nucleotide sequence and -1 PRF-directed translation of nsp2N* at the frameshift site.

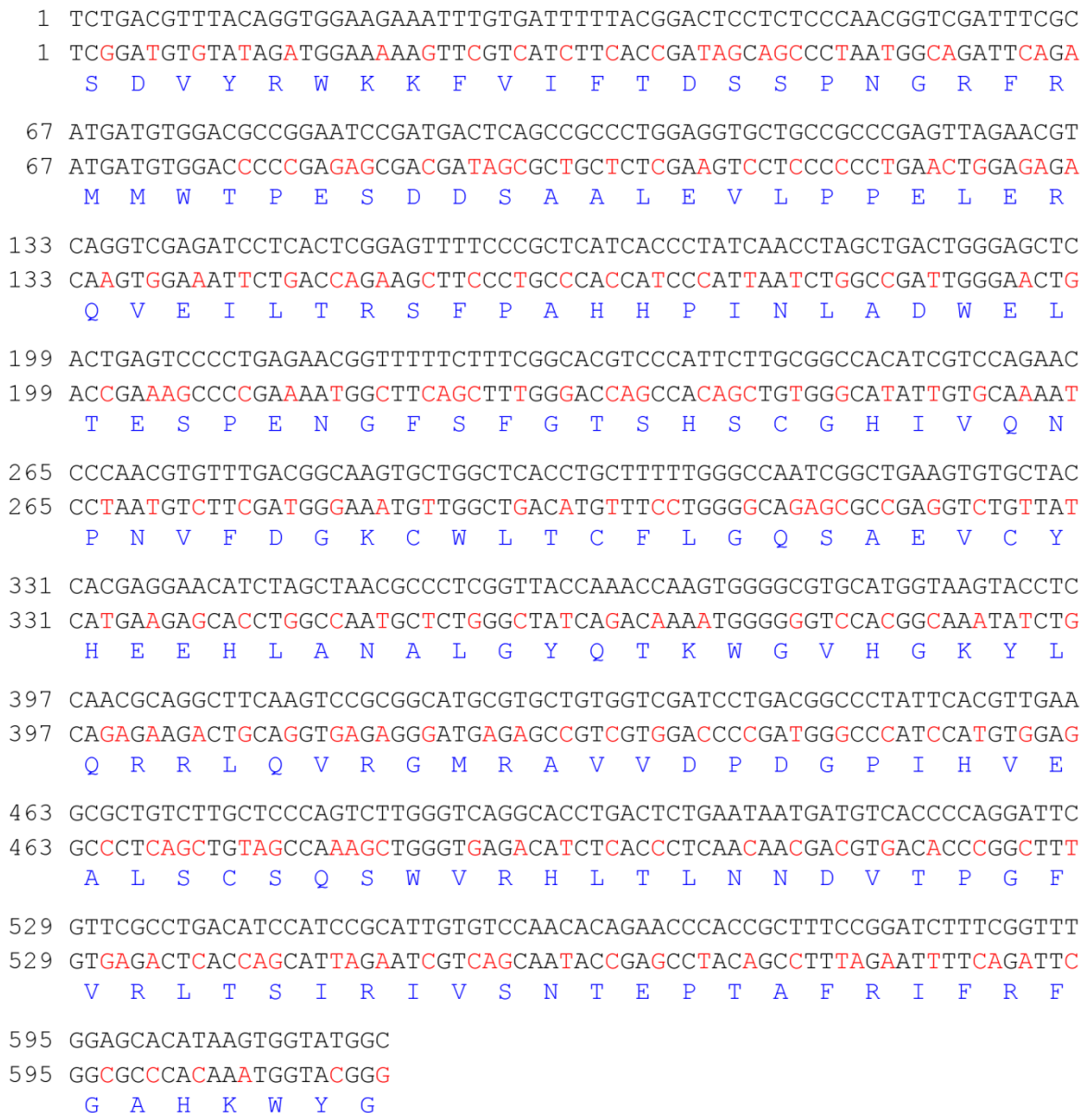


**Figure 4. 11 Nucleotide sequences of the WT and synonymously mutated nsp1β-coding region.** For each block, the top, middle, and bottom line gives the wild type nsp1β-coding sequence (black), the synonymously mutated sequence (mutations present in pLnsp1βcc-nsp2 given in red), and the (unchanged) translation into amino acids (blue).

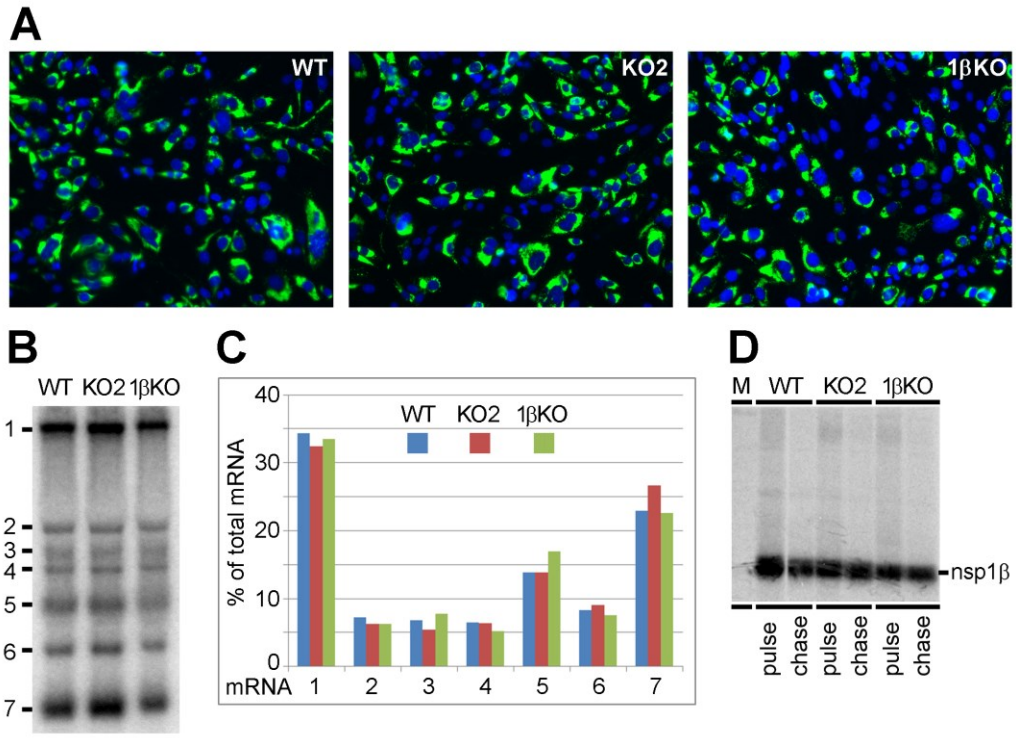


**Figure 4. 12 First-cycle analysis of RNA synthesis and nsp1β stability of WT and mutant (KO2/1βKO) SD01-08 virus in BHK-21 cells.** (*A*) IF microscopy analysis of transfection rate in BHK-21 cells electroporated with *in vitro* transcribed full-length PRRSV RNA. Transfected cells were double labeled with a mAb specific for viral dsRNA (green) and Hoechst 33342 (blue) for staining of DNA in cell nuclei. *(B, C)* Gel hybridization analysis and quantification of PRRSV-specific mRNA accumulation in cells transfected with mutants KO2 and 1βKO or a WT control. (*B*) Total intracellular RNA was isolated at 18 h post-transfection and resolved by denaturing formaldehyde agarose gel electrophoresis. PRRSV-specific mRNAs were detected by hybridization of the dried gel with a $^{32}$P-labelled probe complementary to the 3'-end of the viral genome and subsequent phosphorimaging. The positions of the PRRSV genome (RNA1) and the six sg mRNAs (RNA2 to RNA7) are indicated. (*C*) The volume of the bands corresponding to each of the viral mRNAs was quantified by phosphorimaging and adjusted for the control 18S ribosomal RNA band in the same lane. The sum of the signals for all viral mRNA bands in each lane was used to calculate the relative abundance of each individual mRNA. (*D*) Pulse-chase analysis of nsp1β expression. BHK-21 cells were transfected with RNA transcribed from WT or mutants of PRRSV full-length cDNA clones. At 16.5 h post transfection, protein synthesis was labeled for 15 min and chased for 1h. Cells were lysed and, following immunoprecipitation with mAb α-EU-nsp1β, the production and turn-over of nsp1β were analyzed using SDS-PAGE and autoradiography.

# Chapter 5 - Attenuation of porcine reproductive and respiratory syndrome virus by inactivating expression of ribosomal frameshifting products: implication for the rational design of vaccines

**Abstract:** The ribosomal frameshift products of PRRSV, nsp2TF and nsp2N, are novel proteins recently identified. In this study, they were determined to have ability to interfere with cellular protein ubiquitination (Ub) and ISGylation activities that associated with innate immune suppression function of the virus. Three recombinant viruses (KO1, KO2 and 1βKO), generated by partially or completely inactivation of nsp2TF/nsp2N expression, displayed impaired de-Ub and de-ISGylation ability and induced higher levels of IFN-α and ISG15 expression in infected cells. When tested in our nursery pig model, these mutants showed reduced level of viremia compared to wild-type (WT) virus. After challenge, mutant virus-immunized pigs demonstrated improved protection with reduced lung lesion and viral load in lung and tonsil tissues, in comparison to pigs immunized with WT virus. Taken together, the results suggest that nsp2TF and nsp2N may have important functions in modulation of host immune response, and nsp2TF-deficient viruses are attenuated *in vivo*.

## 5.1 Introduction

The innate immune response provides the first line of defense against pathogen intruders. It is essential for the initial control of infection and allows time for the establishment of an adaptive immune response. The type I interferon (IFN) system is a key component of the innate immune response (reviewed by (Haller & Weber, 2007; Randall & Goodbourn, 2008; Samuel, 2001)). Initially, the pathogen-associated molecular pattern in double stranded RNA (dsRNA) is recognized by host cell receptors to activate protein signaling cascades, which results in the activation of type I IFN production and signaling. In the signaling pathways, critical signaling proteins are dynamically modulated by protein posttranslational modifications. Among various posttranslational modifiers, ubiquitin (Ub) and Ub-like proteins, such as ISG15, are key molecules for orchestrating the appropriate innate immune responses. Both Ub conjugation (ubiquitination) and ISG15 conjugation (ISGylation) to substrate proteins follow a similar process, and together with other

posttranslational modifications (phosphorylation, acetylation, SUMOylation), they fine-tune the strength and duration of the innate immune responses.

As a counteraction to cellular antiviral effects, some viruses express proteins to suppress innate immune responses (reviewed in (Randall & Goodbourn, 2008; Versteeg & Garcia-Sastre, 2010)). Previous studies showed that porcine reproductive and respiratory syndrome virus (PRRSV) encodes multiple proteins to suppress type 1 IFN response (reviewed in (Fang & Snijder, 2010)). PRRSV is an enveloped, positive-stranded RNA virus, which belongs to the order *Nidovirales,* family *Arteriviridae*, a family which also includes equine arteritis virus (EAV), mouse lactate dehydrogenase-elevating virus (LDV), and simian hemorrhagic fever virus (SHFV) (reviewed in (Snijder *et al.*, 2013)). Its genome is about 15kb in length and contains at least eleven open reading frames. The replicase-associated genes, ORF1a and ORF1b, are situated at the 5' end and represent nearly 75% of the viral genome. ORF1a and ORF1b encode two long nonstructural polyproteins, pp1a and pp1ab, with expression of the latter depending on a -1 programmed ribosomal frameshift in the ORF1a/ORF1b overlap region. Following their synthesis from the genomic mRNA template, the pp1a and pp1ab replicase polyproteins are processed into at least 14 functional nonstructural proteins (nsps) by a complex proteolytic cascade that is directed by four proteinase domains encoded in ORF1a - two papain-like cysteine proteases (PLPα and PLPβ) located in nsp1α and nsp1β, a cysteine protease (PLP2) domain located in the N-terminal region of nsp2, and a serine protease (SP) located in nsp4. PLPα autocleaves between nsp1α/1β, PLPβ autocleaves between nsp1β/2, and PLP2 cleaves between nsp2/3, thus mediating rapid release of nsp1α, nsp1β and nsp2 from the polyprotein (Fang & Snijder, 2010). In previous studies, nsp1α, nsp1β and nsp2 (PLP2) were identified to be innate immune antagonists (Beura et al., 2010; Chen et al., 2010; Kim et al., 2010; Li et al., 2013; Sun et al., 2010; Sun et al., 2012)**.**

Recently, a new ORF (TF) was discovered overlapping a central region of ORF1a in the –2/+1 reading frame (Fang et al., 2012). TF is translated via a novel –2 programmed ribosomal frameshifting (PRF) mechanism to produce a novel transframe fusion protein comprising the N-terminal approximately two thirds of nsp2 followed by a unique C-terminal domain that is specified by the novel TF ORF (Fang et al., 2012). The same frameshift site also induces efficient -1 PRF to yield a third, truncated nsp2 variant named nsp2N. Remarkably, our recent study showed that both –2 and –1 PRF are transactivated by a PRRSV replicase subunit, nsp1β. Embedded in PLP1β, a highly conserved, putative RNA-

binding motif was identified to be critical for PRF transactivation at the TF frameshift site (Li et al., 2014).

The newly identified nsp2TF and nsp2N proteins add to the complexity of potential functions encoded in the nsp2 region of the viral genome, and this region has been previously explored for genetically modified live virus (MLV) vaccine development (reviewed in (Fang & Snijder, 2010)). More importantly, nsp2, nsp2TF and nsp2N share the N-terminal PLP2 domain. In previous studies, PLP2 was determined to be able to disrupt innate immune signaling by removing Ub and Ub-like modifiers from host cellular proteins. PLP2 was found to exhibit general de-Ub activity towards cellular Ub conjugates and also showed deISGylation activity to remove the IFN-induced Ub homologue ISG15 (Frias-Staheli et al., 2007; Sun et al., 2010; Sun et al., 2012). The biological significance of these activities was supported by the ability of PLP2 to inhibit type I IFN activation and antagonize the antiviral effect of ISG15 (Sun *et al.*, 2012; van Kasteren *et al.*, 2012). In this study, we analyzed the de-Ub and deISGylation function of nsp2TF and nsp2N. A panel of nsp2TF/nsp2N deficient recombinant viruses was constructed by mutating the key RNA and protein sites required for -1/-2 PRF. Their potential application as candidate MLV vaccines was assessed in a PRRSV challenge piglet model.

## 5.2 Materials and Methods

**Virus and Cells:** The US type 2 PRRSV isolate SD95-21 (GenBank accession no. KC469618) and its nsp2TF-deficient mutants were used in all experiments. BHK-21 cells were used for initial transfection and recovery of recombinant virus. MARC-145 cells were used for recombinant virus rescue and subsequent experiments. These cells were maintained in Eagle's minimum essential medium (Invitrogen) supplemented with 10% heat-inactivated fetal bovine serum and antibiotics at $37^0$C with 5% $CO_2$. Porcine alveolar macrophages were obtained by lung lavage of 6-week-old PRRSV-naıve piglets using a method described previously (Zeman et al., 1993). The Sendai virus (SeV) Cantell strain was grown in embryonated chicken eggs. Virus titer was determined by hemagglutination assay using chicken red blood cells as described previously (Yonemitsu and Kaneda, 1999).

**Luciferase reporter assay:** HEK-293T cells were transfected with 0.5 μg plasmid DNA of p125-luc (a luciferase reporter plasmid containing IFN-β promoter) or pISRE-luc (a luciferase reporter plasmid containing ISRE promoter), 20 ng plasmid DNA of pRL-SV40, and 0.5μg of plasmid DNA expressing nsp2, nsp2TF, nsp2N, PLP2 or empty vector (EV).

Transfection was conducted using FuGENE HD reagent (Promega) following the manufacturer's instructions. At 24 h post transfection, cells were stimulated by SeV at 100 HA unit per ml for 16 hours. Cells were harvested and subjected to a reporter gene assay using a dual luciferase reporter system (Promega) according to the manufacturer's instructions. Firefly or Renilla luciferase activity was measured in FLUOstar Omega (BMG Labtech). Cell lysates were also subjected to SDS-PAGE and Western blot analysis using mAb 140-68 specific to PLP2 domain of nsp2-related proteins.

**Ubiquitination assay:** HEK-293T cells were transfected with plasmid DNAs of pcDNA3.1-HA-Ub (0.5 μg) expressing HA-tagged ubiquitin and pCMV-SD95-21 (2 μg) containing the full-length cDNA clone of type 2 PRRSV SD95-21 or nsp2TF-deficient mutant KO1, KO2, or 1βKO. Transfection was conducted using FuGENE HD reagent (Promega) following the manufacturer's instruction. At 48 h post-transfection, cells were harvested for Western blot analysis. The mAb HA.11 clone 16B12 (Covance, Inc.) was used to detect the expression of HA-tagged proteins. The expression of PRRSV nsp1β was detected by mAb 123-128 as described previously (Li et al., 2012), and mAb anti-β tubulin (Applied Biological Materials, Inc.) was used to detect β-tubulin expression.

**ISG15 conjugation (ISGylation) assay:** MARC-145 cells were infected with PRRSV SD95-21 WT or nsp2TF-deficient mutants, KO1, KO2, or 1βKO. At 18 h post-infection, cells were stimulated with IFN-α at 1000 IU/ml. The cell monolayer was lysed in Laemmli sample buffer for Western blot analysis at 16 h post-stimulation. For the detection of ISG15 expression, the nitrocellulose membrane was probed with mAb F-9 or rabbit polyclonal antibody H-150 (both from Santa Cruz Biotechnology, Santa Cruz, CA). The expression of PRRSV nsp1β was detected by mAb 123-128 as described previously (Li et al., 2012), and mAb anti-β tubulin (Applied Biological Materials, Inc.) was used to detect β-tubulin expression.

**Radioimmunoprecipitation analysis:** MARC-145 cells were infected with 0.01 MOI of viruses. Newly synthesized proteins were labeled from 24 to 26 hours post transfection in cysteine- and methionine-free medium containing 500 μCi/ml [$^{35}$]S-methionine and [$^{35}$]S-cysteine (Perkin-Elmer). Cell lysis and immunoprecipitation analysis were performed as described previously (Li et al., 2014). The mAb 140-68 (anti-PLP2) was used to immunoprecipitate nsp2/nsp2TF/nsp2N, and precipitated proteins were separated on a 6% SDS-PAGE gel. Protein bands were visualized using phosphorimaging and a Typhoon Variable Mode Imager (GE Healthcare).

**In vitro growth characterization of recombinant viruses in cell culture:** Growth kinetics of the recombinant and parental viruses were examined by infecting MARC-145 cells with viruses at a multiplicity of infection (MOI) of 0.01. Infected cells were collected at 0, 12, 24, 36, 48, 60 and 72 hours post infection (hpi), and viral titers were determined by immunofluorescent assay (IFA) on MARC-145 cells and quantified as fluorescent focus units (FFU)/ml.

**Animals and challenge groups:** A total of forty-five 4-week-old, PRRSV-naıve pigs obtained from a certified PRRSV-negative herd were divided randomly into 6 groups and housed separately in the animal isolation facility. Nsp2TF-deficient mutants or WT viruses (2 ml, $1x10^5$ $TCID_{50}$/ml) were used to immunize pigs. After a four-day acclimation period, pigs from group3-6 (n = 8) were inoculated intramuscularly with parental virus (group 3) and mutant virus of KO1 (group 4), KO2 (group 5), 1βKO (group 6). Group 1 (n=5) and group 2 (n=8) pigs were mock-infected with cell culture medium. At 10 days post-infection (dpi), three pigs from group 2-6 were euthanized for assessment of gross pathology following acute infection. At 28 dpi, the rest of pigs (n=5) in group 2-6 were challenged intranasally with the WT virus, SD95-21 (2 ml, $1x10^6$ $TCID_{50}$/ml). The group 1 pigs were kept as mock-infected negative control. Pigs were euthanized at 13 days post challenge (dpc).

**Blood and tissue sampling and lung pathology:** Blood samples were obtained from all pigs on days 0, 3, 7, 14, 21, 28, 31, 35, 41 days post-infection. Gross lung lesions were evaluated using a previously developed system (Halbur et al., 1995) based on the approximate volume that each lobe contributes to the entire lung: the left and right apical lobes, the left and right cardiac lobes, and the intermediate lobe each contribute 10% of the total lung volume, and the left and right caudal lobes each contribute 25%. These scores were then used to calculate the total lung lesion score based on the relative percentage contributions of each lobe. Blood and lung tissue samples were collected at the time of euthanasia. For tissue sampling, a representative tissue was collected from each lobe of the lung.

**Full-length genome sequencing:** At 21 dpi, WT and mutant viruses were isolated by 2-fold titration of serum samples on Marc-145 cells. After 3-4 days incubation, the culture supernatant was harvested, and cells were fixed for detection of virus using IFA. Viral RNA was extracted from the harvested culture supernatant using a QIAamp viral RNA kit (Qiagen) following the manufacturer's instruction. To remove DNA contamination, viral RNAs were further processed with DNA-free RNA kit™ (Zymo Research) following the manufacturer's instruction. Next generation sequencing was performed to determine viral full-length genome at Genomic core facility of Purdue University.

**Quantification of viral load**: For the detection of viral RNA and quantification of viral load, serum and tissue samples were examined using a Tetracore VetAlert PRRS quantitative RT-PCR kit (Tetracore, MD) following the manufacturer's instruction.

**Fluorescence microsphere immunoassay (FMIA) detection of IFN-α expression:** Porcine alveolar macrophages were infected with 1 MOI of WT virus or nsp2TF-deficient mutants. At 48 hpi, culture supernatant was harvested for analyzing the IFN-α expression using a cytokine FMIA as described previously ((Lawson *et al.*, 2010). The quantity of IFN-α was determined using mean fluorescent intensity (MFI) values, and the result was compared with the mean values from mock-infected control cells.

**Statistical analysis***:* Statistical analysis was performed using GraphPad InStat version 5.0 (GraphPad Software). Comparison was performed by unpaired t test to determine the statistical significance. Differences between groups of pigs at different times post-inoculation were considered statistically significant at $P<0.05$ for all analyses.

## 5.3 Results

**Nsp2TF and nsp2N expression affect cellular protein ubiquitination and ISGylation**

Initially, we examined the innate immune suppression ability of nsp2TF and nsp2N using an IFN-β promoter-luciferase reporter assay. Each of these protein-encoding regions (Fig. 5.1A) was cloned into a eukaryotic expression vector, p3xFLAG. As controls, the empty plasmid vector (EV) and a plasmid expressing the PLP2 domain region were included in the analysis. Protein expression from these plasmids was confirmed by Western blot analysis (Fig. 5.1B). As expected, PLP2 strongly suppressed expression of the luciferase reporter gene driven by the IFN-β promoter. Compared to full-length nsp2 and nsp2TF, nsp2N showed greater inhibition of luciferase reporter gene expression (Fig. 5.1C). We further evaluated the effect of these proteins on the expression of downstream type I IFN signaling pathway. Luciferase reporter assay was performed using the pISRE-luc reporter plasmid that expresses firefly luciferase under the control of the interferon-stimulated response element (ISRE) promoter. Again, PLP2 strongly suppressed expression of the luciferase reporter gene driven by the ISRE promoter. Compared to full-length nsp2, nsp2TF and nsp2N had a stronger suppressive effect on luciferase reporter gene expression (Fig. 5.1D). Next, we compared the effect of full-length nsp2, nsp2TF and nsp2N expression on host cellular protein ubiquitination. HEK-293T cells were transfected with a plasmid expressing HA-tagged ubiquitin and the plasmid expressing full-length nsp2, nsp2N or nsp2TF. Again, the plasmid

expressing nsp2-PLP2 and the empty p3xFLAG plasmid were used as controls. As shown in Fig. 5.2A, expression of all four PLP2-containing products resulted in a decreased level of ubiquitin-conjugated proteins. In comparison to nsp2, both nsp2TF and nsp2N had the greater effect on ubiquitin conjugation. Subsequently, we analyzed the effect of nsp2N and nsp2TF expression on host cellular protein ISGylation. ISG15 conjugates were generated by transfecting HEK-293T cells with plasmids that express ISG15 and E1, E2, and E3 enzymes. Cells were co-transfected with plasmids expressing each of the individual nsp2-related products. Co-expression of either nsp2TF or nsp2N resulted in a clear decrease in the level of ISGylated proteins (Fig. 5.2B). Taken together, these data confirmed that individually expressed nsp2TF or nsp2N has the ability to interfere with cellular protein ubiquitination and ISGylation processes.

**Effect of inactivating nsp2TF expression on the ability of PRRSV to suppress host cellular innate immune responses**

To determine whether the de-Ub and de-ISGylation effect induced by nsp2TF and nsp2N in the *in vitro* expression system is consistent with that in the context of viral infection, we further analyzed nsp2TF-deficient mutants. Previously, a panel of recombinant viruses that partially or completely knocked out nsp2TF/nsp2N expression was constructed (Fang *et al.*, 2012; Li *et al.*, 2014; Li *et al.*, 2013). In this study, three type 2 PRRSV mutants were analyzed (Fig. 5.3A), including vSD95-21-KO1 (KO1), vSD95-21-KO2 (KO2) and vSD95-21-nsp1βKO (1βKO). KO1 makes a truncated nsp2TF protein that lacks the C-terminal region encoded by the 3' end of the TF ORF (indicated by red arrow in Fig.3B), but the expression of nsp2 and nsp2N is not affected. KO2 contains mutations that disrupt the frameshift site and the downstream frameshift-stimulatory CCCANCUCC motif. These mutations were intended to knock out the frameshift signal completely so that only nsp2 is expressed. The 1βKO mutant contains mutations in nsp1β, in which the Lys and the first Arg of a GKYLQRRLQ motif in nsp1β were replaced with Ala. This mutant was designed to inactivate the PRF-transactivation function of nsp1β to inhibit frameshifting, so that again only nsp2 would be expressed (Li et al., 2014). None of the mutations in KO1 and KO2 affect the nsp2 amino acid sequence. As shown in Fig. 5.3B, the expression of nsp2 appears not to be affected by the mutations in each individual recombinant virus. Growth kinetics analysis (Fig. 5.3C) showed that all three mutants grew to a similar viral titer in MARC-145 cells. They reached peak viral titer ($10^{5.06}$-$10^{5.27}$ FFU/ml) 12-24 h later than wild-type (WT) virus, with peak titers about 20 to 40-fold lower than the peak viral titer of WT virus ($10^{6.6}$FFU/ml), indicating that these nsp2TF-deficient mutants had reduced growth ability in cell culture.

To determine whether knock out of nsp2TF/nsp2N expression could alter the virus ability to interfere with cellular ubiquitination and ISGylation process, we performed de-Ub and de-ISGylation assays. HEK-293T cells were co-transfected with a plasmid expressing HA-tagged ubiquitin and a plasmid containing full-length cDNA of WT PRRSV or its mutants. The empty plasmid vector was used as a control. As shown in Fig. 5.4A, transfection with WT PRRSV resulted in decreased expression levels of ubiquitin-conjugated proteins, while the nsp2TF-deficient mutants displayed an impaired ability to interfere with cellular protein ubiquitination. Next, we tested the de-ISGylation ability of these nsp2TF-deficient mutants. The result of the ISGylation assay is shown in Fig. 5.4B. A clear decrease in the level of ISGylated proteins was observed in cells infected with WT virus, demonstrating the ability of WT virus to counteract the ISGylation of cellular proteins. In contrast, all three mutants, KO1, KO2 and 1βKO, had almost lost their ability to interfere with ISGylation (Fig. 5.4B), even though the knockout of nsp2TF/nsp2N expression did not appear to affect the expression level of nsp2 (Fig. 5.3B).

As indicated previously, the biological significance of de-Ub and deISGylation activities is to disrupt innate immune signaling and suppress IFN activation (reviewed in (Fang & Snijder, 2010; Snijder *et al.*, 2013)). Thus, IFN-α expression was examined in porcine alveolar macrophages infected with nsp2TF-deficient mutant or WT viruses. Cells were infected with equal MOI of KO1, KO2, 1βKO, and WT viruses. At 48 h post-infection, culture supernatants were harvested and IFN-α expression level was quantified by a swine cytokine fluorescence microsphere immunoassay (FMIA). Compared to WT virus, each of the three mutants showed an increased level of IFN-α induction (Fig. 5.5A). KO2 and 1βKO had significantly impaired ability to inhibit IFN-α activation, with 1.7 and 2.1-fold increased IFN-α expression, respectively, while KO1 induced a slightly higher level of IFN-α production. Subsequently, we analyzed the effect of nsp2TF knockout on the expression of ISG product. When virus-infected Marc-145 cells were stimulated by IFN-α, the type 1 IFN signaling pathway was activated. Compare to WT virus-infected cells, we observed a 0.9-fold increase of ISG15 expression in KO1-infected cells, and 2.3-fold and 1.3-fold higher ISG15 expression in KO2 and 1βKO-infected cells, respectively (Fig. 5.5B).

**Nsp2TF-deficient mutants are attenuated in vivo**

To assess the potential application of nsp2TF-deficient mutants in vaccine development, we performed *in vivo* characterization of these mutants in a nursery pig model. WT virus was included as a control. Six groups of pigs were used. Group 3-6 pigs were infected with $2x10^5$ FFU of WT virus (group 3), KO1 (group 4), KO2 (group 5) or 1βKO

(group 6). Group 1 and 2 pigs kept uninfected. To determine whether these nsp2TF-deficient mutants replicated *in vivo*, serum samples collected at 7–28 days post-infection (dpi) were used for virus isolation on MARC-145 cells. Viruses were recovered from the serum samples of pigs from groups 3–6 collected at 7, 14 and 21 dpi, indicating active replication of the mutant viruses in pigs. To confirm the stability of the mutations, full-length genome sequencing was performed using viruses isolated from serum samples collected at 21 dpi. The results confirmed that the viruses recovered from pigs infected with the KO1, KO2 or 1βKO mutants retained the corresponding mutations in the ORF1a region.

The duration and peak amount of viremia was quantified by real-time qRT-PCR (Fig. 5.6). At 3 and 7 dpi, pigs infected with any of the three nsp2TF-deficient mutant viruses had significantly lower viral load than those pigs infected with WT virus (Fig. 5.6A and 6B). At 14, 21 and 28 dpi, the viral loads in all three groups of mutant-infected pigs were lower than in WT-infected pigs, although at these time-points the differences were not statistically significant. The 1βKO group of pigs consistently showed a lower mean viral load than the other groups of pigs during the 0-28 dpi time course (Fig. 5.6A). Clinical symptoms were monitoring during the first 10 dpi. None of the infected animals developed fever, cough or other clinical signs. At 10 dpi, lung pathology during the acute infection was assessed with three pigs from each of the group 2-6 pigs. Gross lung lesions were absent in mutant virus-infected pigs, and mild lesions (5-6%) were observed in two of the WT virus-infected pigs (data not shown). These results indicate that the mutant viruses were attenuated *in vivo* and they were safe for administration to piglets.

**Nsp2TF-deficient mutants induced protection in pigs against homologous virus challenge**

To investigate whether these nsp2TF-deficient mutants are capable of inducing protection against PRRSV challenge, group 2-6 pigs were challenged with $2x10^6$ FFU of WT virus at 28 dpi. In comparison to group 2 pigs (negative control/challenged: NC group in Fig. 5.6 & 7), viral load in serum was significantly lower in all immunized pigs at 3 and 7 days post challenge (dpc; Fig. 5.6C). At necropsy (13 dpc), the mean scores of lung lesions in immunized pigs (WT, KO1, KO2, and 1βKO) were lower than those in the group 2 pigs (Fig. 5.7A). Significant differences were observed for the KO1 and KO2 groups of pigs in comparison to the group 2 pigs. The protection (based on lung pathology) appeared to be more effective in the pigs immunized with the nsp2TF-deficient mutants. In comparison to the mean lung lesion score of 25.6 for the WT group of pigs, the lesion score was 53% reduced in the KO1 group of pigs, 70 % reduced in the KO2 group of pigs and 38% reduced

in the 1βKO group of pigs. Results from real time RT-PCR confirmed that there was a 0.4-1.4 log reduced mean viral load in lung tissues from pigs immunized with the nsp2TF-deficient mutants in comparison to that from pigs infected with WT virus (Fig. 5.7B). Since tonsil is another main tissue site harboring PRRSV, we further measured the viral load in tonsils and the result was consistent with that from lung tissues. In comparison to WT group pigs, the mean viral load in tonsils showed a 1.3-1.5 log reduction in KO1 and KO2 group pigs, while mean viral load in tonsils from 1βKO pigs showed a 0.8 log reduction (Fig. 5.7C).

## 5.4 Discussion

Since its emergence, PRRSV has caused tremendous economic loss and it has been estimated to cost at least $600 million annually in the US swine industry alone (Miller, 2011). The difficulties encountered in the development of a broadly effective PRRS vaccine emphasize our incomplete understanding of the viral biology and PRRS immunology. PRRSV infection appears to elicit poor innate immune responses. This initial suppression of the innate immune response, leading to the delayed induction of protective cellular and humoral immunity, provides a window of time allowing PRRSV to replicate, shed and transmit to other contact naïve animals. Therefore, one of the key steps in new PRRS vaccine construction is to identify and alter the viral proteins/genetic elements involved in antagonizing host innate immune response.

Previous studies determined the PRRSV PLP2 domain as a major innate immune antagonist (Frias-Staheli et al., 2007; Sun et al., 2010; Sun et al., 2012; van Kasteren et al., 2012). The recently identified nsp2TF and nsp2N proteins share the PLP2 domain with nsp2, which raised the question on which of the three proteins actually function as innate immune antagonist(s). In this study, we compared the ability of the full-length nsp2, nsp2TF and nsp2N proteins to suppress the host innate immune response. They were first analyzed in an *in vitro* expression system and the result showed that nsp2TF and nsp2N both have the capacity to de-conjugate ubiquitin and ISG15 from host cellular proteins at a level apparently higher than that of nsp2. To exclude the possibility that the observed effects may be (partially) due to more general consequences of cytotoxicity caused by protein over-expression, we further analyzed recombinant viruses in which nsp2TF/nsp2N expression was partially or completely knocked out. The results were consistent with those obtained from the *in vitro* expression system, in which all three mutants showed impaired de-Ub and deISGylation ability. To determine whether impaired de-Ub and deISGylation ability could subsequently

alter the ability of the virus to antagonize Ub- and ISG15-dependent innate immune responses, we analyzed IFN-α and ISG15 expression in porcine alveolar macrophages and Marc-145 cells infected with mutant viruses. The mutant viruses had a reduced ability to inhibit IFN-α and ISG15 expression in comparison to WT virus, which further indicated that nsp2TF/nsp2N are involved in the modulation of the innate immune response. The 1βKO mutant had the highest reduction in its ability to inhibit IFN-α and ISG15 expression. This result is expected, since mutations in 1βKO were introduced in nsp1β, which is also an innate antagonist. In previous studies, we have demonstrated that the K124A/R128A mutations in nsp1β not only knocked out the expression of nsp2TF and nsp2N (Li et al., 2014), but also affected the innate immune suppression function of nsp1β (Li et al., 2013). It remains to be established to what extent nsp1β directly modulates the innate immune response or does so by stimulating the expression of nsp2TF and nsp2N. The mutations introduced in KO1 appeared to have less effect on the ability of the virus to suppress cellular IFN-α and ISG15 expression. This could be explained that the KO1 mutations only C-terminally truncated the nsp2TF protein but do not inhibit frameshifting or the expression of nsp2N and the truncated nsp2TF, both still containing the PLP2 domain. In PRRSV-infected cells, nsp2TF was found to be targeted to a different location from full-length nsp2, *i.e.* the exocytic pathway rather than the modified ER membranes where nsp2 is located and associated with viral RNA synthesis (Fang et al., 2012). Our results showed that all three mutants had reduced de-Ub and de-ISGylation ability, even though knock out of the expression of nsp2TF (and nsp2N in KO2 and nsp1βKO) still permitted the expression of similar levels of nsp2 as that of WT virus (Fig. 5.2B). These data made us speculate that nsp2TF and/or nsp2N, rather than nsp2, might be the protein(s) mainly involved in the suppression of the host innate immune response. It could be possible that nsp2TF/nsp2N localizes to the specific cellular compartment(s) (locations) to antagonize the host innate immune response, whereas nsp2 localizes to the ER as a membrane-anchored protein for the formation of the replication complex. It also worth noting that, while the TF region of nsp2TF contains predicted TM domains (Fang et al., 2012), nsp2N lacks both nsp2TF and nsp2 C-terminal TM domains, and could be a secretory protein possessing unique function(s). The mechanistic aspects of the role of PRRSV nsp2TF and nsp2N in counteracting host innate immune response need to be further studied.

The identification of viral elements responsible for immune evasion is fundamental for the development of modified live virus (MLV) vaccines. Previous studies demonstrated that recombinant viruses generated with targeted mutations (deletions) in genes encoding for

immune antagonists are excellent candidates for MLV vaccines (Kochs et al., 2007; Richt et al., 2006; Steel et al., 2009; Valarcher et al., 2003). For example, the influenza virus NS1 protein is a strong innate immune antagonist. Recombinant viruses with truncated NS1 proteins are attenuated in animals and provide protection against wild-type virus challenge (reviewed in (Richt & Garcia-Sastre, 2009)). In our study, we successfully knocked out the expression of two potential innate immune antagonists, nsp2TF and nsp2N, and viable recombinant viruses were generated. We further used a nursery pig model to assess the feasibility of applying these TF-deficient mutants in vaccine development. The result demonstrated that all three mutants were attenuated in pigs. No clinical symptoms and adverse side effects were observed in these mutant virus-infected pigs. Viable mutant viruses could be isolated from serum of infected pigs at 21 dpi, indicating active viral replication in the host. Further genomic sequencing results confirmed the stability of the mutations introduced in the nsp1β or nsp2 regions. In comparison to the WT virus, all three mutants showed a lower level of viral load in serum (3-28 dpi) and no apparent lung lesions were observed in mutant virus-infected pigs following the acute phase of infection (10 dpi). The 1βKO-infected pigs had the lowest viral load in serum (3-28 dpi). This correlates well with the result from the *in vitro* cellular immune analysis. As discussed above, the 1βKO mutations not only knocked out the expression of nsp2TF and nsp2N, but also affected the innate immune suppression function of nsp1β. After challenge, vaccinated pigs showed a significant level of protection from a WT virus challenge, as evidenced by the significant reduction of gross lung lesions and a 1-3 log reduction of the viral load in serum at 3 and 7 dpc. Although the viral load in serum had similar levels in all vaccinated pigs, lower levels of mean viral load in lung and tonsil tissues were observed in pigs vaccinated with mutant viruses, which is correlated with the lower lung lesion scores, demonstrating the improved level of protection generated by these TF-deficient mutants.

The KO2 mutant appears to induce the best protection in animals. It was expected that KO2 would generate better protection than KO1. As discussed above, in comparison to KO1, the KO2 mutant had a stronger effect on the ability of the virus to interfere with cellular protein ubiquitination and ISGylation, and subsequently induced higher IFN-α and ISG15 expression in cultured cells. Initially, we suspected that 1βKO mutant would induce the best protection, but the data from the animal challenge study seemed to contradict our results in cultured cells. To explain this discrepancy, one should take into account that the KO2 mutant replicated much better than the 1βKO mutant in animals. During 0-21 dpi, KO2 reached a serum viral RNA load of $10^{5.0}$-$10^{6.0}$ copies / ml in infected pigs, whereas 1βKO constantly

showed the lowest viral RNA load of $10^{4.0}$-$10^{4.5}$ copies / ml in serum. Thus, even if KO2 viruses have a lower intrinsic IFN inducing potential than 1βKO viruses, the higher replication capacity of the former viruses in animals could eventually result in a comparably stronger stimulation of the IFN system *in vivo*. This phenomenon provides an insight into future study of the role of viral proteins in host immunity and has implications for vaccine development. So far, most of the studies in this area have drawn conclusions using data generated from *in vitro* expression systems and cultured cells. However, these require extensive follow-up experiments to test in animals to confirm whether specific mutations and deletions in certain viral genomic regions alter the IFN and cytokine responses *in vivo* and provide protection in challenged animals.

In conclusion, we determined that nsp2TF and nsp2N are potential innate immune antagonists. Recombinant viruses in which expression of these frameshift products was inhibited were attenuated and provided improved protection in vivo. Since the nsp1β motif involved in frameshift stimulation, and the ribosomal frameshift site are highly conserved, technologies developed in this study could have a broad application in the field.

## 5.4 References


**Beura, L. K., Sarkar, S. N., Kwon, B., Subramaniam, S., Jones, C., Pattnaik, A. K. & Osorio, F. A. (2010).** Porcine reproductive and respiratory syndrome virus nonstructural protein 1beta modulates host innate immune response by antagonizing IRF3 activation. *J Virol* **84**, 1574-1584.

**Chen, Z., Lawson, S., Sun, Z., Zhou, X., Guan, X., Christopher-Hennings, J., Nelson, E. A. & Fang, Y. (2010).** Identification of two auto-cleavage products of nonstructural protein 1 (nsp1) in porcine reproductive and respiratory syndrome virus infected cells: nsp1 function as interferon antagonist. *Virology* **398**, 87-97.

**Fang, Y. & Snijder, E. J. (2010).** The PRRSV replicase: exploring the multifunctionality of an intriguing set of nonstructural proteins. *Virus Res* **154**, 61-76.

**Fang, Y., Treffers, E. E., Li, Y., Tas, A., Sun, Z., van der Meer, Y., de Ru, A. H., van Veelen, P. A., Atkins, J. F., Snijder, E. J. & Firth, A. E. (2012).** Efficient -2 frameshifting by mammalian ribosomes to synthesize an additional arterivirus protein. *Proc Natl Acad Sci U S A* **109**, E2920-2928.

**Frias-Staheli, N., Giannakopoulos, N. V., Kikkert, M., Taylor, S. L., Bridgen, A., Paragas, J., Richt, J. A., Rowland, R. R., Schmaljohn, C. S., Lenschow, D. J., Snijder, E. J., Garcia-Sastre, A. & Virgin, H. W. t. (2007).** Ovarian tumor domain-containing viral proteases evade ubiquitin- and ISG15-dependent innate immune responses. *Cell Host Microbe* **2**, 404-416.

**Halbur, P. G., Paul, P. S., Frey, M. L., Landgraf, J., Eernisse, K., Meng, X. J., Lum, M. A., Andrews, J. J. & Rathje, J. A. (1995).** Comparison of the pathogenicity of two US porcine reproductive and respiratory syndrome virus isolates with that of the Lelystad virus. *Vet Pathol* **32**, 648-660.

**Haller, O. & Weber, F. (2007).** Pathogenic viruses: smart manipulators of the interferon system. *Curr Top Microbiol Immunol* **316**, 315-334.

**Kim, O., Sun, Y., Lai, F. W., Song, C. & Yoo, D. (2010).** Modulation of type I interferon induction by porcine reproductive and respiratory syndrome virus and degradation of CREB-binding protein by non-structural protein 1 in MARC-145 and HeLa cells. *Virology* **402**, 315-326.

**Kochs, G., Koerner, I., Thiel, L., Kothlow, S., Kaspers, B., Ruggli, N., Summerfield, A., Pavlovic, J., Stech, J. & Staeheli, P. (2007).** Properties of H7N7 influenza A virus strain SC35M lacking interferon antagonist NS1 in mice and chickens. *J Gen Virol* **88**, 1403-1409.

**Lawson, S., Lunney, J., Zuckermann, F., Osorio, F., Nelson, E., Welbon, C., Clement, T., Fang, Y., Wong, S., Kulas, K. & Christopher-Hennings, J. (2010).** Development of an 8-plex Luminex assay to detect swine cytokines for vaccine development: assessment of immunity after porcine reproductive and respiratory syndrome virus (PRRSV) vaccination. *Vaccine* **28**, 5356-5364.

**Li, Y., Tas, A., Snijder, E. J. & Fang, Y. (2012).** Identification of porcine reproductive and respiratory syndrome virus ORF1a-encoded non-structural proteins in virus-infected cells. *J Gen Virol* **93**, 829-839.

**Li, Y., Treffers, E. E., Napthine, S., Tas, A., Zhu, L., Sun, Z., Bell, S., Mark, B. L., van Veelen, P. A., van Hemert, M. J., Firth, A. E., Brierley, I., Snijder, E. J. & Fang, Y. (2014).** Transactivation of programmed ribosomal frameshifting by a viral protein. *Proc Natl Acad Sci U S A* **111**, E2172-2181.

**Li, Y., Zhu, L., Lawson, S. R. & Fang, Y. (2013).** Targeted mutations in a highly conserved motif of the nsp1beta protein impair the interferon antagonizing activity of porcine reproductive and respiratory syndrome virus. *J Gen Virol* **94**, 1972-1983.

**Miller, M. (2011).** PRRS price tag, $664 million. *Porknetwork http://wwwporknetworkcom/pork-news/127963843html*.

**Randall, R. E. & Goodbourn, S. (2008).** Interferons and viruses: an interplay between induction, signalling, antiviral responses and virus countermeasures. *J Gen Virol* **89**, 1-47.

**Richt, J. A. & Garcia-Sastre, A. (2009).** Attenuated influenza virus vaccines with modified NS1 proteins. *Curr Top Microbiol Immunol* **333**, 177-195.

**Richt, J. A., Lekcharoensuk, P., Lager, K. M., Vincent, A. L., Loiacono, C. M., Janke, B. H., Wu, W. H., Yoon, K. J., Webby, R. J., Solorzano, A. & Garcia-Sastre, A. (2006).** Vaccination of pigs against swine influenza viruses by using an NS1-truncated modified live-virus vaccine. *J Virol* **80**, 11009-11018.

**Samuel, C. E. (2001).** Antiviral actions of interferons. *Clin Microbiol Rev* **14**, 778-809, table of contents.

**Snijder, E. J., Kikkert, M. & Fang, Y. (2013).** Arterivirus molecular biology and pathogenesis. *J Gen Virol* **94**, 2141-2163.

**Steel, J., Lowen, A. C., Pena, L., Angel, M., Solorzano, A., Albrecht, R., Perez, D. R., Garcia-Sastre, A. & Palese, P. (2009).** Live attenuated influenza viruses containing NS1 truncations as vaccine candidates against H5N1 highly pathogenic avian influenza. *J Virol* **83**, 1742-1753.

**Sun, Z., Chen, Z., Lawson, S. R. & Fang, Y. (2010).** The cysteine protease domain of porcine reproductive and respiratory syndrome virus nonstructural protein 2 possesses deubiquitinating and interferon antagonism functions. *J Virol* **84**, 7832-7846.

**Sun, Z., Li, Y., Ransburgh, R., Snijder, E. J. & Fang, Y. (2012).** Nonstructural protein 2 of porcine reproductive and respiratory syndrome virus inhibits the antiviral function of interferon-stimulated gene 15. *J Virol* **86**, 3839-3850.

**Valarcher, J. F., Furze, J., Wyld, S., Cook, R., Conzelmann, K. K. & Taylor, G. (2003).** Role of alpha/beta interferons in the attenuation and immunogenicity of recombinant bovine respiratory syncytial viruses lacking NS proteins. *J Virol* **77**, 8426-8439.

**van Kasteren, P. B., Beugeling, C., Ninaber, D. K., Frias-Staheli, N., van Boheemen, S., Garcia-Sastre, A., Snijder, E. J. & Kikkert, M. (2012).** Arterivirus and nairovirus ovarian tumor domain-containing Deubiquitinases target activated RIG-I to control innate immune signaling. *J Virol* **86**, 773-785.

**Versteeg, G. A. & Garcia-Sastre, A. (2010).** Viral tricks to grid-lock the type I interferon system. *Curr Opin Microbiol* **13**, 508-516.

**Zeman, D., Neiger, R., Yaeger, M., Nelson, E., Benfield, D., Leslie-Steen, P., Thomson, J., Miskimins, D., Daly, R. & Minehart, M. (1993).** Laboratory investigation of PRRS virus infection in three swine herds. *J Vet Diagn Invest* **5**, 522-528.

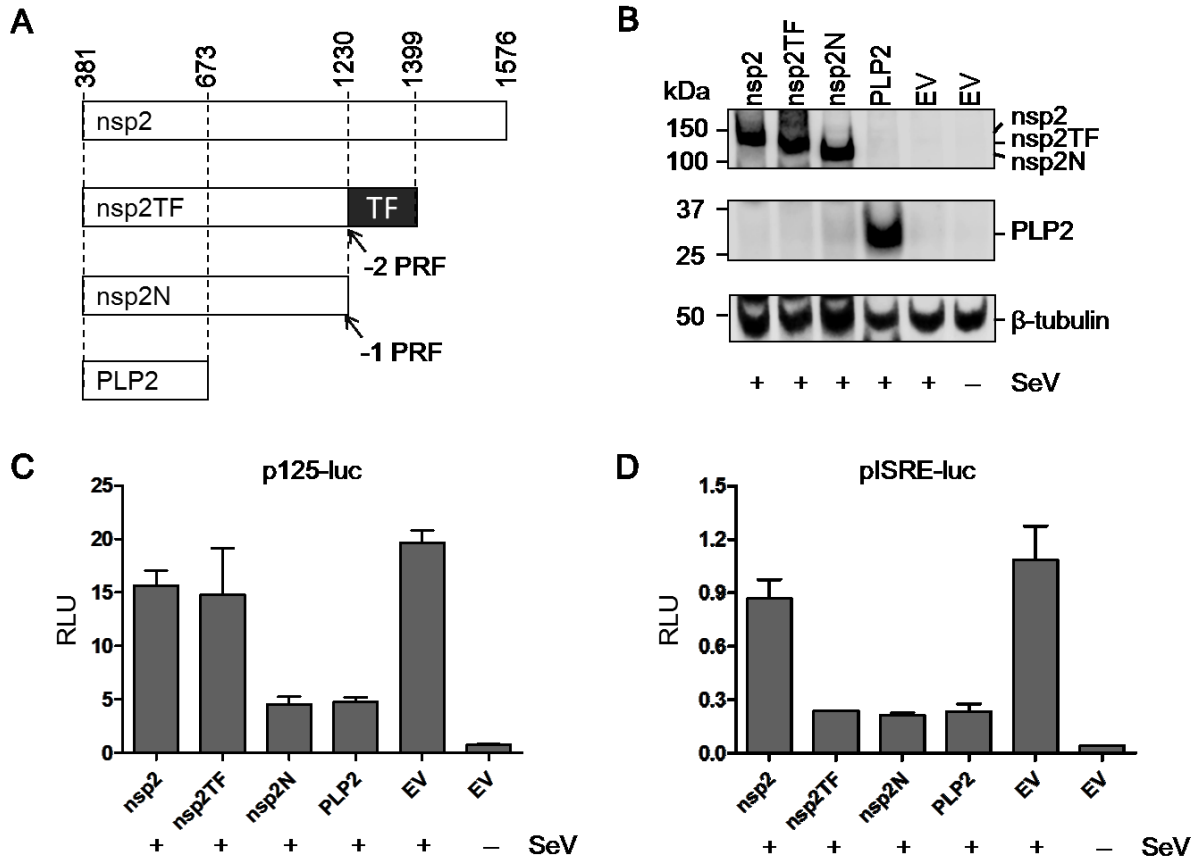


**Figure 5. 1 Effect of full-length nsp2, nsp2TF and nsp2N expression on IFN-β synthesis and signaling, host cellular protein ubiquitination and ISGylation.** (A) A schematic diagram of the viral genomic regions cloned for the expression of nsp2-related proteins. Numbers refer to amino acid number of ORF1a in PRRSV strain SD95-21 (GenBank accession no. KC469618). (B) Western blot analysis of the expression of nsp2-related proteins in HEK-293T cells. The membrane was stained with anti-PLP2 mAb. β-tubulin was used as a loading control. (C) IFN-β promoter luciferase reporter assay to determine the effect of nsp2-related proteins on IFN-β induction. HEK-293T cells were transfected with a plasmid that expresses a nsp2-related protein, or p3xFLAG empty vector (EV), along with the reporter plasmid p125-Luc and *Renilla* luciferase expression plasmid pRL-SV40. (D) ISRE promoter luciferase reporter assay to evaluate the effect of nsp2-related proteins on the type 1 IFN signaling pathway. In experiments for both (B) and (D), cells were stimulated with Sendai virus at 24 h post-transfection. Luciferase activity was measured at 16 h post-stimulation. Relative luciferase activity is defined as the ratio of firefly luciferase reporter activity to *Renilla* luciferase activity. Each data point represents a mean value from three experiments. Error bars show standard deviations of the normalized data.

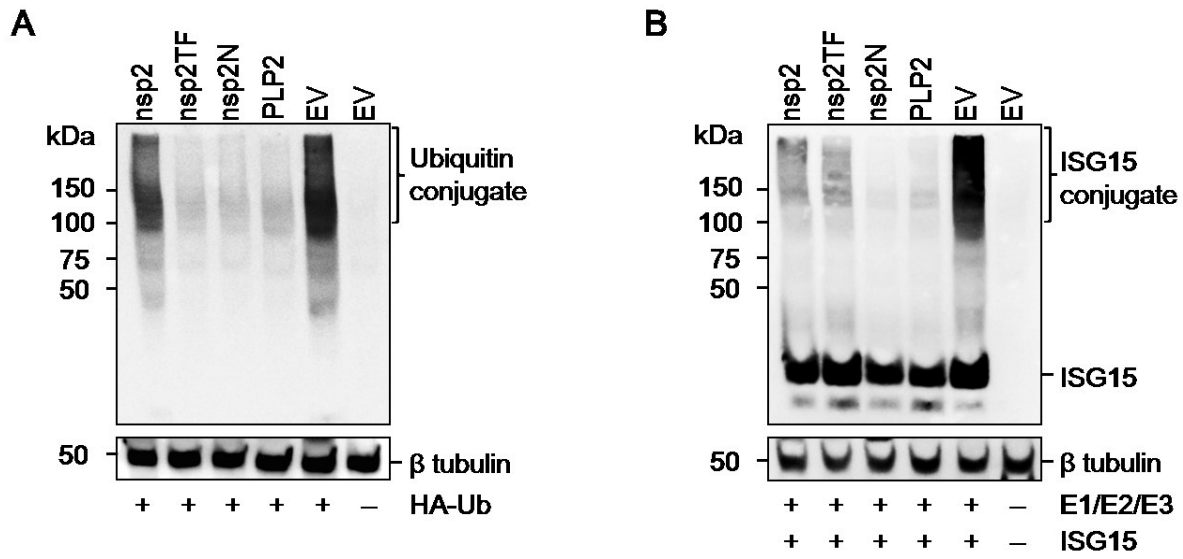


**Figure 5. 2 Effect of full-length nsp2, nsp2TF and nsp2N expression on host cellular protein ubiquitination and ISGylation.** (A) HEK-293T cells were cotransfected with a plasmid expressing HA-tagged ubiquitin and a plasmid expressing nsp2, nsp2TF, nsp2N, PLP2 or the p3xFLAG empty vector (EV). Cells were lysed at 48 h post-transfection and analyzed by Western blotting using anti-HA mAb. (B) Plasmids expressing conjugation enzymes E1/E2/E3 and ISG15 were cotransfected with a plasmid expressing nsp2, nsp2TF, nsp2N, PLP2 or the p3xFLAG empty vector (EV) control in HEK-293T cells. At 48 h post-transfection, cells were harvested for Western blot analysis. Free or conjugated form of ISG15 was detected by mouse anti-FLAG monoclonal antibody.

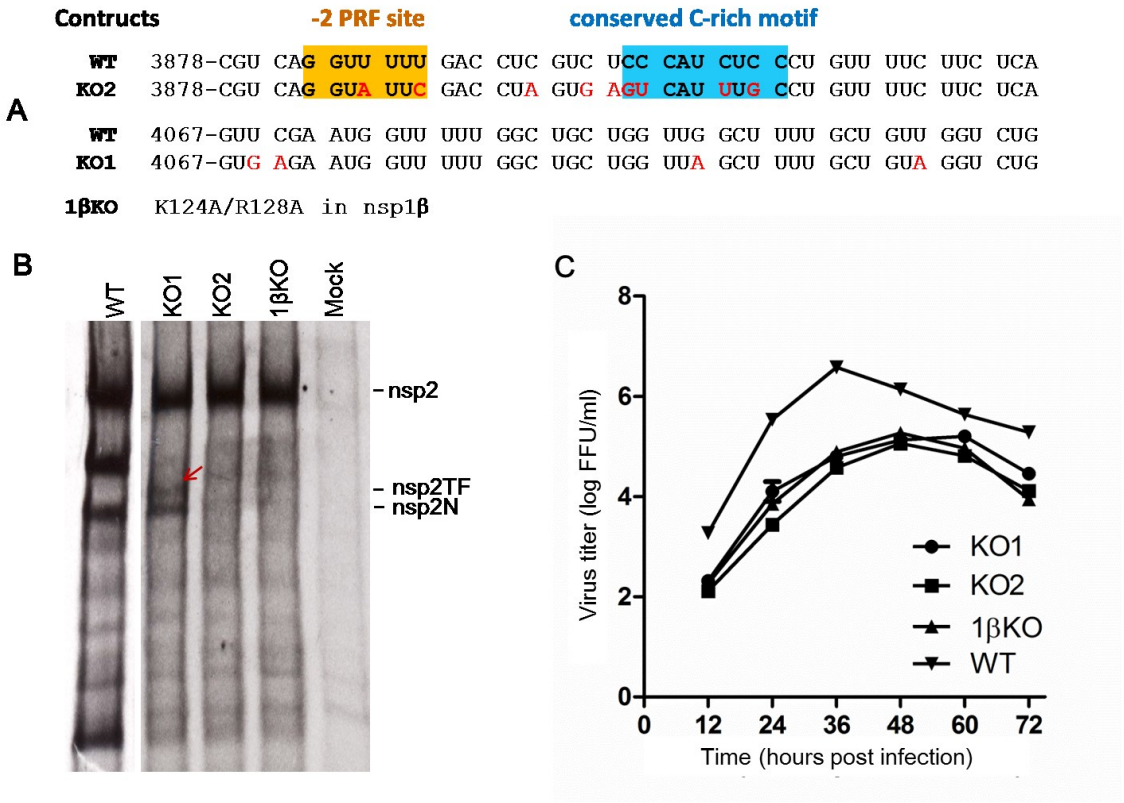


**Figure 5. 3 In vitro characterization of nsp2TF-deficient recombinant viruses.** (A) List of WT and mutant sequences of recombinant viruses. The GGUUUUU frameshift site and the conserved downstream CCCANCUCC frameshift stimulatory motif are indicated with orange and cyan boxes, respectively. Mutated nucleotides are colored in red. Numbers of starting nucleotides refer to the PRRSV SD95-21 sequence (GenBank accession no. KC469618); KO1, knockout mutant 1 (premature termination codons in the TF ORF); KO2, knockout mutant 2 (disrupted frameshift cassette); 1βKO, nsp1β knockout mutant (double mutation introduced into the nsp1β GKYLQRRLQ motif). (B) Analysis of nsp2-related products in cells infected with WT or nsp2TF-deficient mutants. MARC-145 cells were infected with WT or nsp2TF-deficient mutants, or were mock-infected. Following metabolic labeling with $^{35}$S-Met/Cys, proteins were immunoprecipitated with anti-PLP2 mAb and precipitated products were analyzed by SDS-PAGE and autoradiography. Size markers and nsp2-related products are indicated at the side of each panel. The red arrow points to the C-terminally truncated nsp2TF produced by the KO1 mutant. (C) Growth kinetics of WT virus or nsp2TF-deficient mutants. MARC-145 cells were infected in parallel at an MOI of 0.01 with parental or recombinant viruses. At 12, 24, 36, 48, 60 and 72 h post-infection, cells were harvested and virus titers were determined by an immunofluorescence assay with MARC-145 cells. The results are mean values from three replications of the experiment, and viral titers are expressed as numbers of fluorescence focus units per milliliter (FFU/ml).

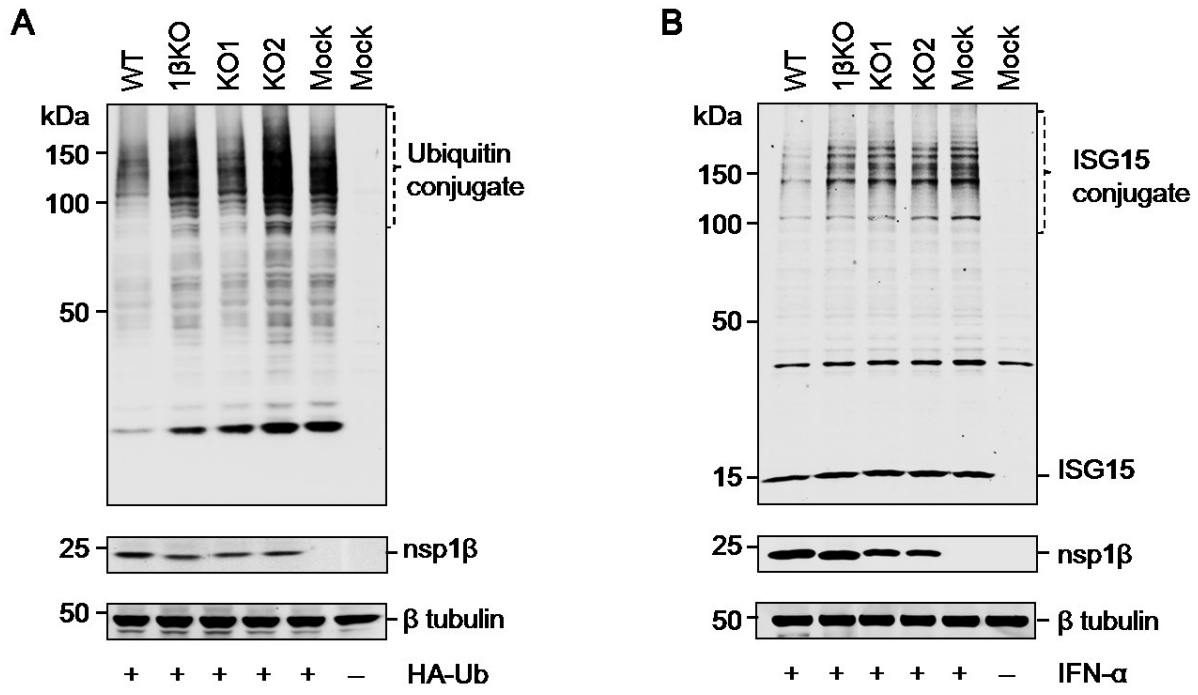


**Figure 5. 4 Effect of inactivating nsp2TF expression on the de-ubiquitination and de-ISGylation ability of PRRSV.** (A) Comparison of de-ubiquitination ability of WT virus and nsp2TF-deficient mutants in transfected cells. HEK-293T cells were transfected with a plasmid expressing HA-tagged ubiquitin and the plasmid pCMV-SD95-21 containing the full-length cDNA clone of PRRSV SD95-21 or nsp2TF-deficient mutants, KO1, KO2, or 1βKO. The expression of ubiquitin-conjugated proteins was analyzed by Western blot using mAb that recognizes HA-tagged ubiquitin. (B) Comparison of de-ISGylation ability of WT virus and nsp2TF-deficient mutants in infected cells. MARC-145 cells were infected with PRRSV SD95-21 WT or nsp2TF-deficient mutants, KO1, KO2, or 1βKO. At 18 h post-infection, cells were stimulated with IFN-α at 1000 IU/ml. The expression of free ISG15 or ISG15-conjugated cellular proteins was detected by Western blot using anti-ISG15 rabbit polyclonal antibody. The expression of PRRSV nsp1β was detected by a specific mAb, and β-tubulin expression was detected as a loading control.

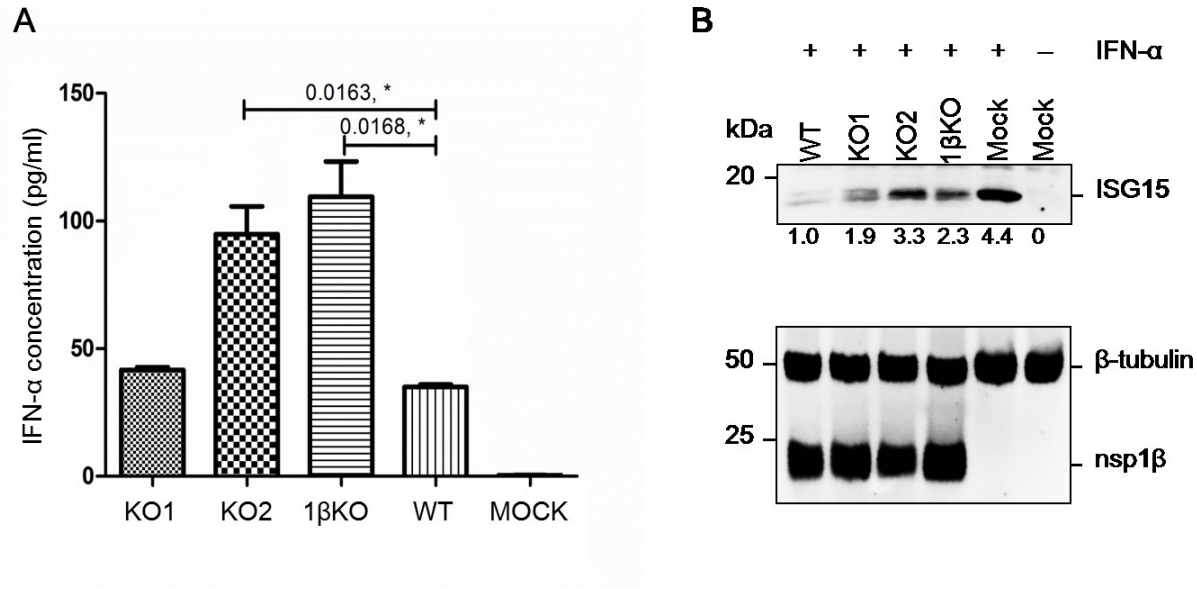


**Figure 5. 5 Effect of inactivating nsp2TF expression on the ability of PRRSV to inhibit IFN-β activation and signaling.** (A) Swine macrophages were infected with WT virus or nsp2TF-deficient mutants, or were mock infected. At 24 h post infection, cell-culture supernatant was harvested for the quantification of IFN-α expression. Each experiment was repeated three times, and results are shown as mean value ± standard deviation. (B) MARC-145 cells were infected with WT virus or nsp2TF-deficient mutants, or were mock infected. At 18 h post infection, cells were mock-treated or treated with 10,000 IU IFN-α/ml for 12 h. Cells were harvested and subjected to Western blot analysis using anti-ISG15 and anti-nsp1β mAbs to detect the expression of ISG15 and nsp1β. The expression of β-tubulin was detected as a loading control. Numbers shown on the bottom of the upper panel indicate the fold changes in the ISG15 expression level compared with that in cells infected with WT virus.

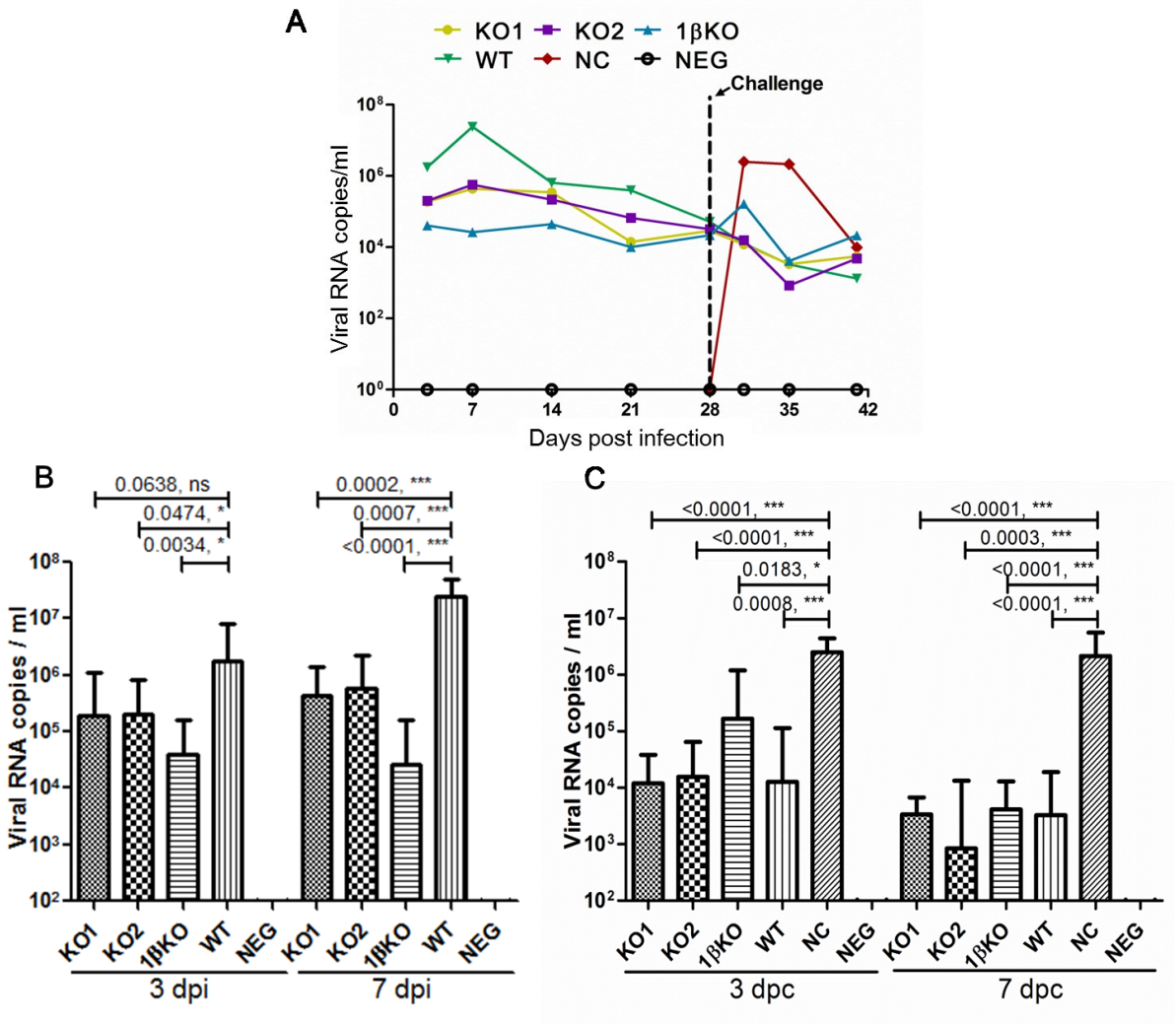


**Figure 5. 6 Viral-RNA load in serum samples from pigs infected with WT virus or nsp2TF-deficient mutants.** Viral-RNA load was quantified by real-time RT-PCR, and the result was interpreted as RNA copy numbers per ml. (A) Mean viral-RNA load in serum from each group of pigs through the time course of study. Dotted line indicates the time point (28 dpi) for challenge. (B) Comparison of viral load in serum among different treatment groups of pigs at 3 and 7 days post infection; and (C) Comparison of viral load in serum among different treatment groups of pigs at 3 and 7 days post challenge. Significant differences of mean viral-RNA loads are indicated with asterisks (*, $p < 0.05$, ***, $p < 0.001$); ns: no significant difference; KO1, group of pigs infected with KO1 mutant; KO2, group of pigs infected with KO2 mutant; 1βKO, group of pigs infected with 1βKO mutant; WT, group of pigs infected with WT virus; NC, uninfected pigs but challenged with WT virus; NEG, negative control group of pigs.

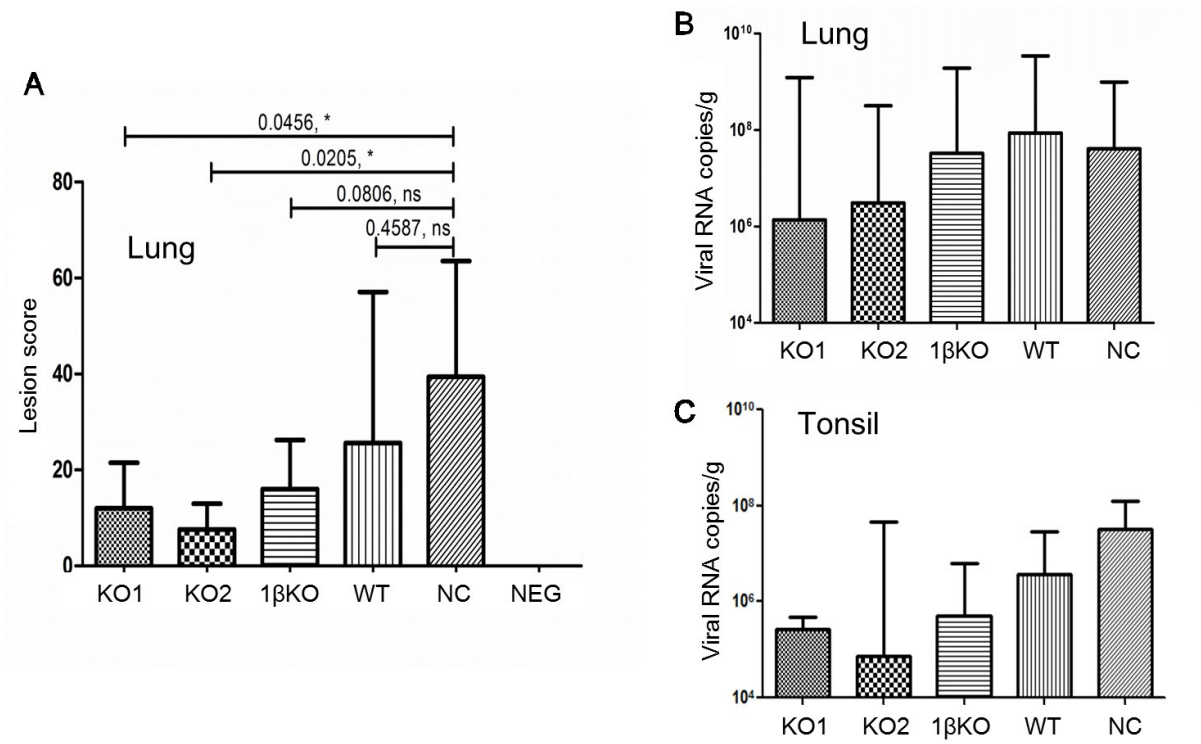


**Figure 5. 7 Comparison of gross lung lesion and viral RNA load in lung and tonsil tissues among different groups of pigs after challenged with wild type virus.** (A) The lung lesion score is assigned based on the evaluation of percent pneumonia in each lobe and then added up for the entire lung. Data points are presented as the mean values of gross lung lesion scores. Significant differences of mean gross lung lesion are indicated with asterisks (*, $p < 0.05$); ns: no significant difference. (B &C) Viral RNA load in lung and tonsil tissues was quantified by real-time RT-PCR, and the result was interpreted as RNA copy numbers per gram of tissue sample. (B) Mean viral RNA load in lungs from each group of pigs at 13 days post challenge. (C) Mean viral RNA load in tonsils from each group of pigs at 13 days post challenge. KO1, group of pigs infected with KO1 mutant; KO2, group of pigs infected with KO2 mutant; 1βKO, group of pigs infected with 1βKO mutant; WT, group of pigs infected with WT virus; NC, uninfected pigs but challenged with WT virus; NEG, negative control group of pigs.

# Chapter 6 – Conclusion and future prospects

Since its emergence in the mid 1980's, PRRSV became the most devastating and economically important pathogen to challenge the global swine industry. During the past two decades, a great amount of information has been obtained on PRRSV structural proteins. However, the structure and function of PRRSV nsps is largely undetermined. In this dissertation, we mainly focus on the studies designed to identify ORF1a-encoded nsps in PRRSV-infected cells, dissect the function of nsp1β and nsp2 related proteins, and explore their potential application in the development of improved vaccine candidates.

Based on comparative sequence analysis, PRRSV ORF1a-encoded replicase polyproteins is predicted to produce at least ten nsps, named as nsp1-8, with nsp1 and nsp7 being cleaved internally yielding nsp1α/β and nsp7α/β. In chapter 2, we developed a panel of monoclonal antibodies and polyclonal antibodies against PRRSV ORF1a-encoded nsps to verify previous predictions. Using these antibodies, we detected individual cleavage products in PRRSV-infected Marc-145 cells, including nsp1α, nsp1β, nsp2, nsp4, nsp7α, nsp7β and nsp8 by multiple immunoassays. As early as 6 h post-infection, most nsps could be detected by immunofluorescence microscopy, suggesting this antibody panel could be useful for early detection of PRRSV infection. At the early stages of infection, all of the detected nsps co-localized in the perinuclear region of the cell, where the *de novo*-synthesized viral RNA was recognized by *in situ* labelling. In addition, consistent with previous studies of replicase polyprotein processing in EAV, several long-lived processing intermediates (nsp3–4, nsp5–7, nsp5–8 and nsp3–8) were identified by western blot and immunoprecipitation. Thus, this PRRSV antibody panel developed in this project will be an important toolbox for further structure-function studies of PRRSV nsps.

Previous studies on the virus-host interaction have demonstrated that PRRSV nsp1β is an IFN antagonist with a strong inhibitory effect on type I IFN induction and signaling pathways. In chapter 3, we were trying to remove the IFN antagonism function of PRRSV nsp1β. Unexpectedly, the data from this study showed that overexpression of nsp1β exhibited strong inhibition effect on reporter gene expression at both transcriptional and translational level. More interestingly, the self-expression level of nsp1β was inhibited, but β-action expression level appeared to be unaffected. A similar observation has been reported for SARS-CoV nsp1, and the mechanism is that SARS-CoV nsp1 promotes cellular mRNA degradation. Based on the data generated in this study, we speculate that PRRSV nsp1β may

inhibit the expression of selected host cellular genes, like genes involved in host innate immune response. Future studies are needed to elucidate the basic mechanism of nsp1β involves in modulation of cellular gene expression. By mutagenesis analysis, double mutations at the K130(124) and R134(128) residues within a highly conserve motif (GKYLQRRLQ) was identified to impair nsp1β's function on the suppression of IFN-β and reporter gene expression, as well as its self-suppression effect. Using reverse genetics, the recombinant viruses containing the double mutations were generated. In addition to attenuated growth behavior in Marc-145 cells, the vSD95-21-K124A/R128A mutant (1βKO) showed reduced ability to inhibit IFN-α, IFN-β and ISG15 expression *in vitro,* in comparison with that of the wild type virus. These results suggest the 1βKO mutant could be used as a modified live PRRSV vaccine. The *in vivo* growth phenotype and immunogenicity of this mutant virus was further evaluated in the nursery pig disease model in chapter 4.

Previously, we discovered an unusual -2/-1 PRF signal in PRRSV nsp2 coding-region, which is utilized to translate additional viral proteins, nsp2TF and nsp2N. However, the detailed mechanism of this -2/-1 PRF is still unknown. In chapter 4, we found that nsp1β-coding region is required for efficiently expression of nsp2TF and nsp2N by mapping the minimal viral protein sequence requirements of -2/-1 PRF. Our data indicate that expression of nsp1β *in trans* can stimulate -2/-1 PRF in the nsp2-coding region. That transactivator function of nsp1β protein is supported by that the altered version of nsp1β with coding sequence mutated synonymously maintained the transactivating activity. At the same time, the minimal RNA sequences in the nsp2-coding region were determined, in which a 34-nt region containing the slippery sequence and the conserved 3' C-rich motif was defined as minimal RNA sequence required for the functional PRRSV −2/−1 PRF. In addition, it is noteworthy that the conserved nsp1β motif identified in chapter 3 is also critical for PRF transactivation, which further supports that nsp1β functions as a transactivator. The interaction between nsp1β protein and -2/-1 PRF signal was further confirmed with RNA binding assays, however, the underlying mechanism is largely unknown. Clearly, more studies are needed to extensively address the in depth mechanisms of -2/-1 PRF in arteriviruses.

Previous studies identified the PRRSV PLP2 domain as an innate immune antagonist. The newly identified PRRSV nsp2TF and nsp2N proteins share the PLP2 domain with nsp2, which raised the question on which of the three proteins actually function as innate immune antagonist(s). In chapter 5, the study was focused on characterizing the ability of these three

proteins to inhibit the host innate immune response. Our data indicates that nsp2TF and nsp2N both have ability to suppress type I IFN induction and signaling. In comparison with full-length nsp2, nsp2TF and nsp2N proteins show stronger ability to de-conjugate ubiquitin and ISG15 from host cellular proteins. By introducing mutations at the -2/-1 PRF signal region, we further rescued the recombinant viruses (KO1 and KO2) with partially or completely knocked out of nsp2TF/nsp2N expression. We further performed *in vitro* and *in vivo* characterization of three recombinant viruses, KO1, KO2 and 1βKO (1βKO was constructed in chapter 3, in which expression of nsp2TF and nsp2N was completely knocked out). Consistent with the data generated from *in vitro* expression system, all recombinant viruses showed impaired de-Ub and de-ISGylation ability. All three mutant viruses have a reduced capacity to inhibit IFNα and ISG15 expression in virus-infected porcine alveolar macrophages and Marc-145 cells. The nursery pig disease model was used to determine the attenuation phenotype and immunogenicity of the mutant viruses. In comparison with the wild type virus, all three mutants showed a lower level of viral load in serum (3-28 dpi) and no apparent lung lesions were observed in mutant virus-infected pigs following the acute phase of infection (10 dpi). Additionally, the KO2 mutant appears to induce the best protection in animals. All the data presented here suggest that nsp2TF and nsp2N are potential innate immune antagonists, and knock-out (down) the expression of these proteins could be a new strategy for the development of improved vaccine candidates.

Given the importance of nsps in viral replication and virus-host interaction, the replicase genes have attracted increasing attention during the past decade. However, current information of PRRSV nsps encoded by ORF1a and ORF1ab may be just the tip of the iceberg. Clearly, there are more questions raised in this dissertation, including: What are the authentic proteolytic cleavage sites in PRRSV polyproteins (pp1a and pp1ab)? Does PRRSV utilize two alternative processing pathways (major and minor pathways) for pp1a processing like EAV? What is the function of the processing intermediates identified in virus-infected cells? Does PRRSV nsp1β suppress the expression a group of cellular genes? What are the genes? What the mechanism of nsp1β's suppression effect on gene expression? How does nsp1β transactivate the unusual -2/-1 PRF? Could nsp1β cause ribosomal frameshifting event in the cellular gene containing similar -2 PRF signal? What is the detailed functional difference of three nsp2-related proteins? Answering these questions will be future research directions.

# Publisher's Permission for Reproducing Published Materials

**Chapter 2** related:
http://vir.sgmjournals.org/content/93/Pt_4/829.full.pdf+html?sid=d80fb5a2-14cd-4163-9d87-9d674afdab65

**Chapter 3** related: http://vir.sgmjournals.org/content/94/Pt_9/1972.full.pdf+html

## JGV – Permission and Reprints

**Authors requesting permission to reuse their own content**

The Copyright Transfer Agreement/Licence to Publish signed by authors of papers published in JGV explicitly grants the authors permission to reuse their own content **without seeking further permission**, provided that the original source of the material is credited appropriately. Some other publishers may ask authors to provide evidence that they have permission to reuse their own content previously published in JGV; in that case, authors should contact the JGV Editorial Office (jgv.permission@sgm.ac.uk).

**Chapter 4** related: http://www.pnas.org/content/111/21/E2172.full.pdf+html?with-ds=yes

## PNAS Rights and Permissions

**PNAS authors need not obtain permission for the following cases:** (1) to use their original figures or tables in their future works; (2) to make copies of their papers for their own personal use, including classroom use, or for the personal use of colleagues, provided those copies are not for sale and are not distributed in a systematic way; (3) **to include their papers as part of their dissertations;** or (4) to use all or part of their articles in printed compilations of their own works. Citation of the original source must be included and copies must include the applicable copyright notice of the original report.